Norwegian University of Life Sciences
Faculty of Chemistry, Biotechnology and Food Science

Philosophiae Doctor (PhD)
Thesis 2023:22

The site-2-protease RseP as a novel antimicrobial target

RseP, en posisjon-2-protease, som et nytt antimikrobielt angrepspunkt

Sofie Sagvaag Kristensen

The site-2-protease RseP as a novel antimicrobial target

RseP, en posisjon-2-protease, som et nytt antimikrobielt angrepspunkt

Philosophiae Doctor (PhD) Thesis

Sofie Sagvaag Kristensen

Norwegian University of Life Sciences
Faculty of Chemistry, Biotechnology and Food Science

Ås 2023

Thesis number 2023:22
ISSN 1894-6402
ISBN 978-82-575-2052-6

Table of contents

Acknowledgements

The work presented in this thesis was carried out in the Laboratory of Microbial Gene Technology (LMG) and in the Protein Engineering and Proteomics (PEP) group at the Faculty for Chemistry, Biotechnology, and Food Science (KBM) at the Norwegian University of Life Sciences (NMBU), Ås, Norway, from 2019 to 2023. The work was founded by the Norwegian Research Council (NRF) as part of the project "Enterococcal RseP as a target for new diagnostics and antibiotics" (Project number: 275190).

Firstly, I would like to express my gratitude to my main supervisor Dzung B. Diep, who sadly passed away in December 2022. Thank you for guidance, your witty comments and for giving me the opportunity to work on this exciting project. I would also like to thank my co-supervisors Geir Mathiesen, Morten Kjos and Jens Preben Morth. A special thanks to Morten and Geir. Morten, thank you for taking on the role as co-supervisor over the last couple of months and for your valuable perspective on this work. To Geir, thank you for always being enthusiastic and curious about the experiments performed, for your encouragement and valuable insights. Your support and guidance have been invaluable.

Furthermore, I would like to thank all co-authors for their valuable contribution to the papers presented in this thesis. A special thanks to Thomas F. Oftedal and Christian Kranjec. Thank you for inspiring discussions and for always celebrating LMG achievements.

I would also like to express my gratitude to Kamilla Wiull. Thank you for all your help in the lab, your valuable insights and encouragement. Most of all, thank you for being an exceptional friend. To all members of LMG and PEP, thank you for providing a fun, interesting, and supporting working environment.

To my family and friends, thank you for your continuous support and encouragement. Paal, thank you for your unconditional love and support, I am forever grateful.

Sofie Sagvaag Kristensen

Ås, February 2023

Summary

The discovery and development of antibiotics have revolutionized modern medicine. Today, several decades after the first patients were treated with antibiotics, bacterial infections are again becoming increasingly difficult to treat. The rapid appearance of antibiotic resistant bacteria has caused antibiotic agents to lose their efficacy, posing a serious threat to human health. To combat antibiotic resistant bacteria, novel treatment options are needed. Bacteriocins are small, antimicrobial peptides produced by bacteria to inhibit growth of other bacteria in competition for nutrients and/or habitats. Most notably, several bacteriocins show potent activity against multiple prominent human pathogens, highlighting their potential as novel antimicrobial agents. One such bacteriocin is enterocin K (EntK1), a member of the LsbB family of bacteriocins, exhibits particularly potent activity against vancomycin resistant enterococci. The antimicrobial activity of EntK1 depends on interaction with an intramembrane protease of the site-2-protease (S2P) family known as RseP. While EntK1 and other bacteriocins hold significant potential as novel antimicrobials, their clinical applications have so far been limited. Understanding the mechanisms of action and molecular details underlying target recognition and binding are essential steps toward developing bacteriocins as novel antimicrobial agents. This thesis aimed to investigate the molecular mechanism underlying EntK1 recognition and interaction with RseP, as well as explore the potential of the LsbB family as a basis for engineering novel bacteriocins.

Paper I comprehensively reviews the role of S2P in bacteria. The S2P family is highly conserved among Gram-positive and Gram-negative bacteria and play an essential role in physiology and virulence in multiple prominent human pathogens. Notably, S2P have been implied in virulence in multiple human pathogens, including *Staphylococcus aureus*, *Pseudomonas aeruginosa*, *Mycobacterium tuberculosis* and *Enterococcus faecalis*. The prominent role of S2P highlights the potential of S2P as novel antimicrobial targets.

Paper II describes the design of a novel hybrid bacteriocin Hybrid 1 (H1), consisting of the N-terminal region of EntK1 and the C-terminal region of enterocin EJ97 (EntEJ97). H1 targets RseP and exhibits a distinct inhibition spectrum compared to the parental bacteriocins. Importantly, H1 showed superior antimicrobial activity against the human

pathogen *Staphylococcus haemolyticus* and contributed to complete eradication of *S. haemolyticus* biofilm. Taken together, the results presented in paper II demonstrate that members of the LsbB family can be engineered to enhance potency and/or alter the activity spectrum.

Paper III describes a mutational analysis of *Enterococcus faecium* RseP. To identify regions involved in EntK1 sensitivity and binding, conserved motifs related to substrate binding and catalysis were targeted. Mutational effects were assessed by investigating EntK1 sensitivity and binding using the naturally EntK1-resistant *Lactiplantibacillus plantarum* as a host for expressing several variants of RseP. The mutational analysis revealed that EntK1 depends on interactions with the extracellular PDZ domain and the third transmembrane helix, particularly the residue Asn359, for its antimicrobial activity. The results from paper III provided valuable insights into mechanisms underlying EntK1:RseP interaction. However, increased structural characterization of *E. faecium* RseP would further contribute to our understanding of EntK1:RseP interaction and mode of action of this bacteriocin.

Paper IV describes the pSIP system and *L. plantarum* as a novel platform for production and purification of integral membrane proteins. Integral membrane proteins, such as RseP, are notoriously difficult to express and purify. Structural characterization often requires large amount of protein, thus establishing a reliable protocol for purification of stable RseP with high purity is an important milestone in the efforts of structural characterization. Paper IV thus describes an efficient protocol for production and purification of integral membrane proteins using the pSIP-system and *L. plantarum*. The protocol does not only lay the foundation for further structural and biochemical characterization of *E. faecium* RseP but may serve as a platform for production and purification of other membrane proteins.

Taken together, the work presented in this thesis (i) highlights the key role of S2P in prominent human pathogens and the potential of S2P as antimicrobial targets (Paper I), (ii) show that bacteriocins of the LbsB family can be engineered to improve potency and altered activity spectrum (Paper II), (iii) provide detailed insight into the EntK1:RseP interaction (paper III), and (iv) establishes an expression and purification platform needed for structural characterization of RseP (Paper IV).

Sammendrag

Oppdagelsen og utviklingen av antibiotika er et av de største fremskrittene i medisinsk historie. I dag, flere tiår etter de første pasientene ble behandlet med antibiotika, er bakterielle infeksjonssykdommer igjen blitt et økende problem. Stadig flere bakterier blir motstandsdyktige (resistente) mot antibiotika, som fører til at flere typer antibiotika mister sin effekt. Utvikling av nye behandlingsmetoder mot antibiotikaresistente bakterier er derfor avgjørende. Bakteriosiner er små antimikrobielle peptider som produseres av bakterier for å hemme veksten av andre, konkurrerende bakterier i kampen om habitat og næring. Flere bakteriosiner har vist seg å effektivt hemme veksten av flere ulike patogene bakterier. Enterocin K1 (EntK1) er medlem av bakteriosinfamilien LsbB, og er spesielt effektiv mot vancomycinresistente enterokokker. Den antimikrobielle aktiviteten til EntK1 avhenger av interaksjonen med RseP på målcellens overflate. RseP er et transmembranprotein tilhørende proteinfamilien kalt posisjon-2-protease (S2P). Selv om EntK1 og andre bakteriosiner viser god effekt mot flere humane patogen, har så langt få bakteriosiner blitt tatt i bruk i klinisk sammenheng. Et viktig steg i utviklingen av bakteriosiner som nye, mulige behandlingsmetoder, er en økt forståelse av hvordan bakteriosinene gjenkjenner og binder til målproteinet. Denne avhandlingen hadde derfor som mål å undersøke de molekylære mekanismene involvert i EntK1:RseP interaksjonen, samt vurdere potensialet til medlemmer av LsbB familien som et utgangspunkt for design av nye bakteriosiner.

Artikkel I gir en detaljert sammenfatting av rollen til S2P i bakterier. S2P finnes i både Gram-positive og Gram-negative bakterier og spiller en viktig rolle for bakteriens evne til å respondere på endringer i miljøet og til å etablere infeksjon. S2P har vist seg å være viktig for etablering av infeksjon for en rekke patogene bakterier, blant annet *Staphylococcus aureus*, *Pseudomonas aeruginosa*, *Mycobacterium tuberculosis* og *Enterococcus faecalis*. S2P viktige rolle i infeksjon fremhever S2P som et nytt, mulig antimikrobielt angrepspunkt.

Artikkel II beskriver konstruksjonen av et nytt bakteriosin kalt Hybrid 1 (H1). H1 består av den C-terminalen-delen av EntK1 og den N-terminale delen av enterocin EJ97 (EntEJ97). Den antimikrobielle aktiviteten til H1 er avhengig av binding til RseP på mottakercellens

overflate. Sammenlignet med EntK1 og EntEJ97, som også binder til RseP, har H1 et unikt inhiberingsspektrum. H1 er spesielt aktiv mot *Staphylococcus haemolyticus* og bidro sammen med to andre bakteriosiner til å fullstendig hemming av biofilm dannelse. Resultatene presentert i Artikkel II viser at det er mulig å modifisere medlemmer av LsbB familien slik at de antimikrobielle egenskapene forbedres.

Artikkel III beskriver en mutasjonsanalyse av RseP fra *Enterococcus faecium*. For å undersøke hvilke områder av RseP som er involvert i EntK1:RseP interaksjonen, ble det introdusert mutasjoner i områder som i tidligere studier er vist viktig for substrat interaksjon. Effekten av de ulike mutasjonene ble evaluert ved å benytte *Lactiplantibacillus plantarum*, som er resistent mot EntK1, som en vert for uttrykk av ulike varianter av RseP i kombinasjon med bindings- og sensitivitets analyser. Resultatene fra Artikkel III viser at et område kalt PDZ domenet og aminosyre 359 i den tredje transmembranheliksen er viktig for den antimikrobielle aktiviteten til EntK1. Økt kunnskap om strukturen til RseP vil gi dypere innsikt i interaksjonen mellom EntK1 og RseP.

Artikkel IV beskriver hvordan pSIP systemet og *L. plantarum* kan benyttes i produksjon og rensing av transmembranproteiner. Transmembranproteiner, slik som RseP, er svært krevende å rense. For å gjennomføre karakterisering av proteiners tredimensjonale struktur kreves det store mengder, rent protein. Derfor er etableringen av en effektiv protokoll for produksjon og rensing av RseP er den første milepælen på vei mot strukturell karakterisering av RseP. Artikkel IV beskriver en effektiv protokoll for rensing av transmembranproteiner ved bruk av pSIP-systemet og *L. plantarum*. Denne protokollen legger grunnlaget for videre biokjemiske og strukturelle studier av RseP, men vil også kunne benyttes for produksjon og rensing av andre transmembranproteiner.

Til sammen viser resultatene i denne avhandlingen: (i) S2P spiller en viktig rolle i bakterier og kan være nye antimikrobielle angrepspunkt (Artikkel 1), (ii) enkle modifikasjoner kan forbedre og/eller endre den antimikrobielle aktiviteten til medlemmer av LsbB familien (Artikkel II), (iii) gir økt forståelse av interaksjonen mellom EntK1 og RseP (Artikkel III), og (iv) etablerer en ny protokoll for produksjon og rensing av membranproteinet RseP (Artikkel IV).

Abbreviations

CBS	Cystathionine-β-synthase
CD	Circular dichroism
Cryo-EM	Cryogenic electron microscopy
ER	Endoplasmic reticulum
Enterocin EJ97	EntEJ97
Enterocin K1	EntK1
Enterocin Q	EntQ
GarKS	Garvicin KS
GRAS	Generally recognized as safe
H1	Hybrid 1
I-CLiPs	Intramembrane cleaving protease
IMP	Intramembrane proteases
Insig	Insulin-induced gene protein
Man-PTS	Mannose phosphotransferase transport system
MREβ-loop	Membrane-reentrant β-loop
MP1	Micrococcin P1
NICE	Nisin-controlled expression system
OMPs	Outer membrane proteins
PCT	PDZ-C terminal region
RIP	Regulated intramembrane proteolysis
RiPPs	Ribosomally synthesized and post-translationally modified peptides
RseP	Regulator of sigma E protease
SCAP	SREBP cleaving activating protein
S1P	Site-1-protease
S2P	Site-2-protease
SpoIVFB	Stage IV sporulation protein FB

SREBP	Sterol regulatory element binding protein
TM	Transmembrane segment
UppP	Undercaprenyl pyrophosphate phosphatase
VISA	Intermediate vancomycin resistant phenotype
VRE	Vancomycin-resistant enterococci

List of papers

Paper I **The Role of Site-2-Proteases in Bacteria: A review on physiology, virulence, and therapeutic potential.** Sofie S. Kristensen, Dzung B. Diep, Morten Kjos and Geir Mathiesen. *Manuscript.*

Paper II **A bacteriocin-based treatment option for *Staphylococcus haemolyticus* biofilms.** Christian Kranjec*, Sofie S. Kristensen*, Karolina T. Bartkiewicz, Mikkel Brønner, Jorunn P. Cavanagh, Aparna Srikantam, Geir Mathiesen and Dzung B. Diep. (2021). Sci Rep. 2021 Jul 6;11(1):13909. doi: 10.1038/s41598-021-93158-z.

Paper III **The extracellular domain of site-2-metalloprotease RseP is important for sensitivity to bacteriocin EntK1.** Sofie S. Kristensen*, Thomas F. Oftedal*, Åsmund K. Røhr, Vincent G. H. Eijsink, Geir Mathiesen and Dzung B. Diep. (2022). J Biol Chem. 2022 Oct 14;298(11):102593. doi: 10.1016/j.jbc.2022.102593.

Paper IV **A novel platform for production and purification of integral membrane proteins using *Lactiplantibacillus plantarum* as expression host**

Sofie S. Kristensen, Suzana Siebenhaar, Dzung B. Diep, J. Preben Morth and Geir Mathiesen. *Manuscript.*

*These authors contributed equally to the respective papers

Other publications by the author

Broad-spectrum in vitro activity of macrophage infectivity potentiator inhibitors against Gram-negative bacteria and Leishmania major.

Iwasaki, Jua; D. Lorimer, Donald; Vivoli-Vega, Mirella; Kibble, Emily A.; Peacock, Christopher S.; Abendroth, Jan; Mayclin, Stephen J.; Dranow, David M.; Pierce, Phillip G.; Fox, III, David; Lewis, Maria; Bzdyl, Nicole M.; Kristensen, Sofie S.; Inglis, Timothy J.J; Kahler, Charlene M.; Bond, Charles S.; Hasenkopf, Anja; Seufert, Florian; Schmitz, Jens; Marshall, Laura E.; Scott, Andrew E.; Norville, Isobel H.; Myler, Peter J.; Holzgrabe, Ulrike; Harmer, Nicholas J.; Sarkar-Tyson, Mitali. (2022) J. Antimicrob. Chemother. March 4; 77(6). Doi: 10.1093/jac/dkac065

1. Introduction

The discovery and development of antibiotics has provided an effective tool to combat bacterial infections, and forms the foundation of several medical advancements, including surgery, and chemotherapy. Unfortunately, increased dependence on antibiotics has been accompanied by a rapid appearance of antibiotic resistance (1). Today, antibiotic-resistant bacteria are an increasing public health concern worldwide and resistant bacterial infections are becoming increasingly challenging to treat. In 2019, the global burden associated with antimicrobial resistant infections were estimated to 4.95 million deaths, placing antibiotic resistant bacteria in the top three leading causes of mortality (2).

Managing antibiotic resistance is a complex issue, however three basic principles for addressing antibiotic resistance should be recognized. First, curtailing antibiotic consumption is needed. Although antimicrobial resistance genes are naturally present in the environment, the selection of antimicrobial resistance is primarily driven by overconsumption and excessive use in agriculture (1, 3). According to the O'Neill report on antimicrobial resistance, several measures should be implemented to reduce the misuse of antibiotics, including: (i) adopting antibiotic stewardship programs to improve the rational use of antibiotics, (ii) improved prescription practices and diagnostic tools, thereby limiting unnecessary and/or incorrect administration of antibiotics; and (iii), improved infection control (i.e., improved hygiene, vaccination, sanitation facilities), thereby preventing transmission of bacterial infections and thus limiting the need for antibiotics (4). In the context of agriculture, several countries have implemented bans on routine use of antibiotics in farmed animals, however; due to the increasing demand for animal protein for human consumption, the use of antibiotics in the agricultural section is predicted to significantly increase in the years to come (5, 6).

Second, the report suggests that mechanisms driving resistance development should be more investigated and global resistance development should be monitored (4). By exploring the molecular mechanism underlying development of antimicrobial resistance, long-term persistence and clonal spread, methods can be developed to counter these effects (3, 7). Lastly, there is an urgent need for the development of novel treatment options. Novel

sources for antibiotics (i.e., bioprospecting) and alternative strategies to target multi-resistant bacteria (i.e., anti-virulence targets, antimicrobial peptides, vaccines) are currently being explored (7). In the context of developing novel antimicrobials, antimicrobial peptides known as bacteriocins are receiving increased scientific interest. In the following section, general aspects of bacteriocins, their mode of action, and potential as an alternative to conventional antibiotics will be discussed.

1.1 Bacteriocins

1.1.1 General aspects of bacteriocins: Biosynthesis and classification

Bacteriocins are small, antimicrobial peptides produced by bacteria in order to kill or inhibit other bacteria in competition for nutrients or habitats. In contrast to antibiotic peptides, such the glycopeptides vancomycin and teicoplanin, bacteriocins are ribosomally produced (8-10). Most bacteriocins have a narrow inhibition spectrum, commonly targeting species closely related to the producer strain; however, bacteriocins with a broader inhibition spectrum have been identified (10-13). It can be presumed that most bacterial genera produce one or more bacteriocins, however lactic acid bacteria have received particular attention as bacteriocin producers due to their generally recognized as safe (GRAS) status (14, 15).

Bacteriocins comprise a highly heterogenous group of peptides, for which various classification systems have been proposed (9, 11, 14). Moreover, these classification systems have been adapted several times to accommodate new insights into the structures and modes of action of bacteriocins, as well as to include the plethora of novel bacteriocins continuously being discovered. Most commonly, bacteriocins are divided into two classes (Table 1) (9, 11, 14). Class I contains bacteriocins with post-translational modifications, thus belonging to the family of ribosomally synthesized and post-translationally modified peptides (RiPPs). Based on the comprehensive nomenclature developed for RiPPs, class I bacteriocins are subdivided into several subclasses (Table 1) (16).

Table 1 | Classification of selected bacteriocins

Class I - post-translationally modified peptides (RiPPs)			
Subclass*	**Key features**	**Example(s)**	**Proposed target**
Lantibiotics	Contains lanthionine and β-methyl lanthionine	Nisin, Lacticin 3147, Plantaricin C	Lipid II
Sactibiotics	Contains sulfur to alpha-carbon linkage	Thuricin CD	Unknown
Circular	N-to-C cyclized peptides	Garvicin ML	Maltose ABC transporter
Thiopeptides	Macrocyclic peptides.	Micrococcin P1	Unknown
Siderophore peptides	Contain a siderophore mimicking domain attached to the C-terminal region	Microcin E492	Man-PTS
Class II – unmodified peptides			
Subclass	**Key features**	**Example(s)**	**Suggested target**
II-A	Single peptides, pediocin-like bacteriocins containing the YGNGV consensus sequence	Pediocin PA-1	Man-PTS
		Sakacin P	Unknown
II-B	Two-peptide bacteriocins	Lactococcin G	UppP (undecaprenlyl diphosphatase)
		Plantaricin EF	CorC (Mg/Co efflux pump)
		Plantaricin JK	APC amino acid transporter
II-C	Synthesized without an N-terminal leader peptide	LsbB, EntK1, EntEj97, EntQ	RseP
II-D	Single peptide, lacking the pediocin-like consensus sequence	Lactococcin A	Man-PTS
		Microcin V	SdaC (serine uptake protein)

*Class I is further subdivided, including the subgroups Linardins, Glycocins, LAPs, Bottromycin, Cynabatcin, Lasso peptides and Nucleotid peptides, for which members are not discussed in this thesis.

Class II consists of unmodified peptides, which are further divided into four subclasses (Table 1) (14). Class II-A bacteriocins comprise the pediocin-like bacteriocins, which harbor a conserved N-terminal YGNGV consensus motif, known as the pediocin box (17). Class II-B consists of two-peptide bacteriocins, whose activity requires the presence of two individual peptides (18). Class II-C are linear, leaderless bacteriocins, which are produced without an N-terminal leader sequence (19). Lastly, Class II-D consists of linear bacteriocins lacking the characteristic pediocin-box, often referred to as non-pediocin-like bacteriocins (14).

Most bacteriocins are synthesized as inactive precursor peptides, with an N-terminal leader peptide attached to a core peptide (16, 20). The N-terminal leader peptide is removed during translocation of the bacteriocin across the membrane by ABC or Sec-dependent transporters (16, 20-22). The N-terminal leader peptides are necessary for this export and to render the intracellular bacteriocin inactive, thus protecting the producer strain from the antimicrobial activity of the bacteriocin. In addition, the leader peptides serve as a recognition site for enzymes involved in the post-translational modifications in the case of class I bacteriocins (16, 23, 24).

Interestingly, some bacteriocins, such as LsbB of the class II-C, are synthesized without a leader peptide (19, 25). While the mechanism of how these leaderless bacteriocins are secreted out of the cell is somewhat unknown, genes encoding ABC transporters are often located in the proximity of the structural bacteriocin genes for several leaderless bacteriocins (19, 25, 26). Notably, the lack of a leader sequence also results in the leaderless bacteriocins being produced in its active form. The mechanisms underlying self-protection are largely unknown.

Genes required for bacteriocin production and export are typically arranged in operons together with genes conferring self-immunity, thereby protecting the producer strain from the active bacteriocin (14, 19). Immunity is generally conferred by dedicated immunity proteins and/or efflux pumps (27-29). While putative immunity proteins are known for most bacteriocins, the mechanism conferring immunity often remains elusive. This is also the case for leaderless bacteriocins of class II-C, where putative immunity may be particularly critical to avoid self-killing prior to export (19). Self-immunity is best

characterized by the class I lantibiotic nisin, for which a dual mechanism of immunity has been described; in the producer cell, a designated ABC transporter exports the bacteriocins out of the cell, while, on the extracellular side, the immunity protein NisI interacts with nisin, thus preventing interaction between nisin and the bacteriocin target lipid II (27). Another partially characterized immunity mechanism is that of the class II-A bacteriocins, in which the dedicated immunity protein binds to the target receptor and thereby inhibits the antimicrobial action of the peptides (28, 29).

Expression of the genes in bacteriocin-operons is commonly inducible and tightly regulated by quorum-sensing based two/three-component systems (9, 30, 31). The inducible and controlled regulation of the genes involved in bacteriocin synthesis has been exploited to develop efficient expression systems. This includes the nisin-controlled expression system (NICE) and the pSIP-expression vectors, which are the most commonly used expression systems in lactic acid bacteria (30, 32). The NICE and the pSIP expression system are based on the regulatory elements in the nisin and sakacin P operons, respectively (31, 33, 34). The pSIP-system has been extensively used in the work presented in this thesis and is an essential tool used in papers II-VI.

1.1.2 Applications of bacteriocins

Bacteriocins have been investigated with respect to their antimicrobial activity in agriculture, the food industry, and for applications in human- and animal-health (11). Most notably, bacteriocins are known as potent food preservatives, with several commercially available bacteriocin-based products (11, 35). While bacteriocins predominantly have been investigated with respect to food safety, these antimicrobial peptides are now receiving increased interest as promising alternatives and/or complements to antibiotics (10, 11). In this section, the potential of bacteriocins as a viable alternative to antibiotics will be highlighted.

As reviewed by Cotter and colleagues, bacteriocins exhibit several desirable properties with respect to therapeutic applications (10). Most notably, bacteriocins are highly potent

against prominent human pathogens. The potency of bacteriocins have been demonstrated both *in vitro* and *in vivo* including considerable activity against several human pathogens, such as *Enterococcus faecium*, *Staphylococcus aureus*, and *Clostridioides difficile* (12, 36-41). Intriguingly, several bacteriocins show a mode of action which is different from traditional antibiotics, ensuring activity against both antibiotic sensitive pathogens and their antibiotic resistant counterparts. Indeed, some bacteriocins exhibit potent activity against vancomycin-resistant enterococci (VRE) and methicillin-resistant *S. aureus* (36, 37, 39, 42, 43). Moreover, the effectiveness of individual bacteriocins can be enhanced through combinatory treatments with other bacteriocins and/or conventional antibiotics – a strategy which, in many cases, also reduces resistance development (38-40, 44-47).

Another advantage of bacteriocins is the presumed non-toxic effect on mammalian cells (10, 11). Indeed, many bacteriocins are produced by lactic acid bacteria with a GRAS status and have been consumed for centuries in fermented food and dairy products (14). Nonetheless, some bacteriocins, such as microcin E492, have shown cytotoxicity in certain human cell lines (11, 48), indicating that bacteriocin might not be completely harmless and highlighting the need to investigate this effect for every single bacteriocin.

As mentioned above, bacteriocins generally have a narrow inhibition spectrum, often only targeting closely related species. A narrow inhibition spectrum is normally desirable, as it limit adverse effect on the commensal microbiota. For example, studies have shown that the narrow spectrum class I bacteriocin thuricin CD is equally effective as antibiotics to treat *C. difficile*-associated diarrhea, without affecting the commensal gut microbiota (12, 49). Similarly, intragastrical administration pediocin PA-1 have limited effect on the balance of commensal bacteria in the gastrointestinal tract (50). While a narrow inhibition spectrum may limit off-target effects of bacteriocins, their use requires precise diagnostics and the identification of the infection causing agent prior to use. This precludes the use of bacteriocins when treating an infection with an unknown origin. Nonetheless, the precise and potent activity of selected bacteriocins against human pathogens highlights the therapeutic potential of these antimicrobial peptides.

Lastly, most bacteriocins can readily be engineered or synthetically produced to enhance pharmacological and/or physiochemical properties, including specificity, stability,

efficiency and target range (51-56). Bacteriocins are gene-encoded, and most have relatively simple structures, making manipulation and optimization of properties and production by genetic engineering a relatively easy and low-cost option.

Despite the promising qualities, the use of bacteriocins in therapeutic applications is so far limited. Several challenges hamper the clinical use of bacteriocins, including low solubility and sensitivity towards proteases, which complicates the mode of delivery (10, 11).

1.1.3 Receptors and docking molecules on target cells

Bacteriocins exert their antimicrobial activity through one of three mechanisms: (i) targeting the cell envelope via specific receptor molecules, (ii) targeting intracellular processes (i.e., gene expression and protein production), or through (iii) unspecific electrostatic interactions with the cell envelope (i.e., phospholipids, teichoic acids, and lipopolysaccharides) (10, 11, 57-60). In the context of developing novel antimicrobials, bacteriocins targeting specific receptors in the cell membrane are particularly interesting, as they: (a) ease the mode of delivery compared to intracellular targets, (b) attacks the bacterial cell in a way conceptually different from conventional antibiotics, and as (c) a detailed understanding of bacteriocin:receptor interaction may aid rational design of novel and improved antimicrobial peptides. Consequently, bacteriocins targeting specific receptor molecules in the cell envelope will be discussed in the following section.

Several bacteriocins depend on cell-envelope associated receptors for their antimicrobial activity, with nisin using lipid II as a receptor being the earliest example (Figure 1). Lipid II is an essential precursor for the synthesis of peptidoglycan, the main component of the bacterial cell wall. The lipid II molecule consists of a MurNAc-GlcNac disaccharide with a pentapeptide covalently linked to a pyrophosphorylated lipid tail (61). The MurNAc-GlcNac pentapeptide is synthesized intracellularly and serves as the basic building block for peptidoglycan, while the lipid tail aids the transport of the pentapeptide building block across the cytosolic membrane (61). The essential role of lipid II in peptidoglycan synthesis makes it an excellent antimicrobial target. Indeed, several class I lantibiotics, including

nisin, lacticin 3147 and plantaricin C (Table 1), and several antibiotics, such as the clinically relevant glycopeptide vancomycin, depend on lipid II for their antimicrobial activity (61-64).

The structure of the nisin-lipid II complex shows that the N-terminal lanthionine ring of nisin forms a cage-like structure surrounding the pyrophosphate of lipid II (65). By binding lipid II, nisin exhibits antimicrobial activity through two distinct mechanisms of action: (i) The N-terminal of nisin II sequesters lipid II, thereby inhibiting peptidoglycan synthesis, while (ii) the C-terminal is inserted in the membrane, creating a stable pore complex (61, 65, 66). This dual mechanism of action makes nisin a highly potent antimicrobial agent. Importantly, the mechanism of lipid II binding and inhibition by nisin is different from that of vancomycin, which binds to D-Ala-D-Ala in the pentapeptide of lipid II, resulting in blockage of peptidoglycan synthesis (61, 65, 67, 68). This difference in recognition sites allows nisin to retain activity against *vanA*-type resistant *Enterococcus*, suggesting that modifications of the D-Ala-D-Ala motif of lipid II do not provide resistance towards lipid II-targeting bacteriocins (39). However, it should be noted that *S. aureus* with an intermediate vancomycin resistant phenotype (VISA), also shows increased resistance to nisin and lacticin 3147 compared to their vancomycin-susceptible counterparts (39). This is because the resistance to vancomycin in VISAs most often results from reduced access to lipid II due to increased impermeability of the cell wall, not modifications of lipid II itself.

Another common target receptor for bacteriocins is the mannose phosphotransferase transport system (man-PTS) (29, 69-72) (Figure 1). Man-PTS is a transmembrane sugar-transporting system consisting of cytoplasmic phosphotransferase proteins (Enzyme I and Hpr) and a species-dependent, sugar-specific enzyme II complex (IIA, IIB, IIC and IID) (73). Most, if not all, pediocin-like bacteriocins (class II-A), as well as class II-D bacteriocin garvieacin Q, ubericin K, bacteriocin SJ and lactococcin A, and the class I siderophore peptide microcin E492, depend on man-PTS for their antimicrobial activity (13, 29, 69, 70, 74, 75).

The membrane components of man-PST, IIC and IID, have been shown to be essential for bacteriocin sensitivity, while the intracellular IIA and IIB are redundant for sensitivity (29, 75). Recently, the structure of several pediocin-like bacteriocins in complex with man-PTS

has been studied in detail using cryogenic electron microscopy (Cryo-EM) (28, 76), confirming the importance for IIC and IID in bacteriocin sensitivity. The structural studies indicate that the N-terminal region of pediocin-like bacteriocins initially interacts with the extracellular surface of the man-PTS core domain, while the C-terminal half penetrates the membrane domains to alter the protein, prying the core domain and the V-motif open, thereby creating a pore (28, 76). A similar mechanism has been proposed for microcin E492, a pore-forming bacteriocin targeting Gram-negative bacteria (77), suggesting a common mode of action for bacteriocins targeting man-PTS. Several other sugar phosphotransferase systems, like glucose-PTS and cellobiose-PTS, have been linked to bacteriocin sensitivity, however, their role as a receptor has not yet been confirmed (78-81).

Whole genome sequencing of bacteriocin resistant mutants have been a valid first approach in identifying potential bacteriocin receptors in several studies (58). For example, in a study by Kjos and colleagues, genome sequencing of mutants resistant to lactococcin G were shown to harbor mutations within or near the *uppP* gene, which encoded an undecaprenyl pyrophosphate phosphatase (UppP) (82). Importantly, heterologous expression of *uppP* in *Streptococcus pneumonia* renders the lactococcin G resistant host sensitive to the bacteriocin, confirming the role of UppP as a bacteriocin receptor (82). Using a similar approach, the site-2-protease (S2P) RseP were identified as essential for the antimicrobial activity of the class II-C LsbB bacteriocin family (Table 1) (37, 57). In addition to complementation of the resistant mutants, heterologous expression of *rseP* renders naturally insensitive strains sensitive to LsbB (57). Notably, a physical interaction between LsbB lactococcal RseP has been demonstrated using a GTS-pulldown assay, confirming the role of RseP:LsbB interaction in LsbB sensitivity (83). The LsbB family and RseP will be further discussed in section 1.1.4.

Lastly, in a study by Gabrielsen and colleagues, genome sequencing of mutants with reduced sensitivity towards garvicin ML was shown to harbor a deletion in genes encoding maltose ABC transporters. Complementation of the deletion mutants with the maltose ABC transporter, restored wild-type levels of sensitivity, indicating that an intact sugar transporter was needed for bacteriocin sensitivity (84). In contrast to lipid II, man-PTS and

RseP, a physical interaction between the Maltose ABC transporter and UppP, and their respective target bacteriocins, has not yet been shown experimentally. Thus, it is not fully established whether these proteins function as target receptors *per* se or whether their involvement in the bacteriocin mechanism of action is more indirect.

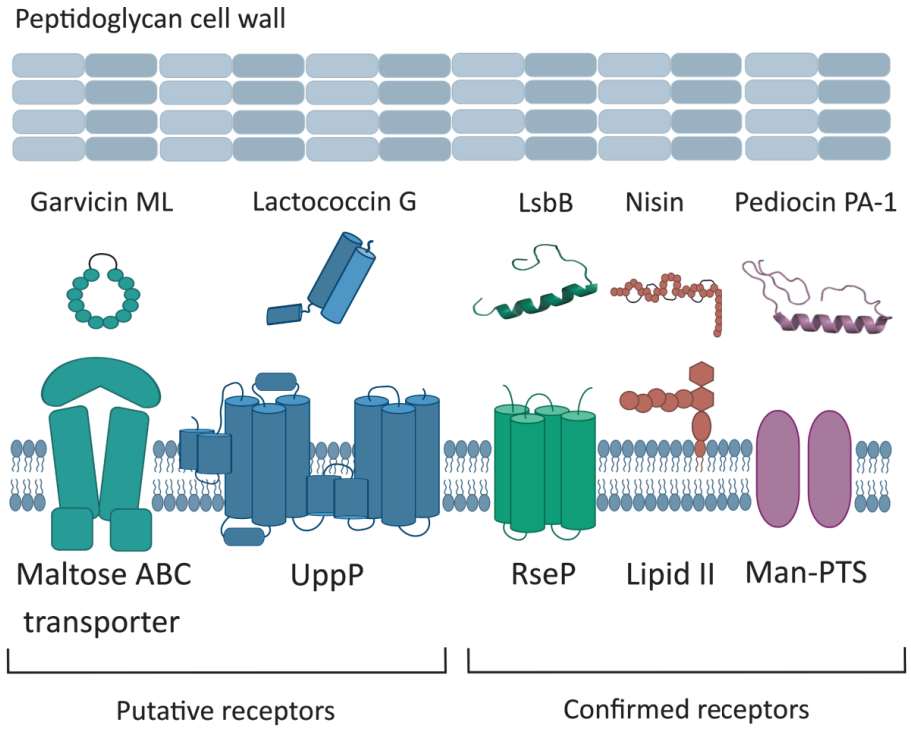

Figure 1| Selected bacteriocins targeting the cell envelope of Gram-positive bacteria via specific receptors. Maltose ABC transporter and UppP are suggested to act as a receptor for the bacteriocins garvicin ML and lactococcin G, respectively. The site-2-protease RseP, the peptidoglycan precursor Lipid II and the sugar transporter Man-PTS act as receptors for the LsbB family, nisin, and pediocin PA-1, respectively. A physical interaction has been confirmed between the latter three receptors and their respective bacteriocins.

Sequencing of resistant mutants have further shown that a serine transporter (SdaC), a magnesium/cobalt efflux pump (CorC) and amino acid transporter of the APC superfamily, is needed for the sensitivity of microcin V, plantaricin EF and plantaricin JK, respectively (85-88). Although the mechanism of action has not been determined for these bacteriocins, these results indicate that bacteriocins may use a range of different target receptors and that many bacteriocin receptors remains to be identified.

The mechanism of action and nature of the target receptor also have impact on the development of resistance to bacteriocins. While changes in surface properties of the bacterial cell may alter bacteriocin-sensitivity, specific receptor-related mechanisms have also been observed (9). Indeed, resistance to class II-A bacteriocins has been linked to reduced expression of the target receptor man-PTS (89, 90). Combinations of bacteriocin and other antimicrobials with different mechanisms of action have shown to efficiently reduce resistance development (38, 40, 44, 47).

1.1.4 The LsbB bacteriocin family and RseP

A subgroup of the leaderless, class II-C bacteriocins, known as the LsbB family, depends on the site-2-metalloprotease RseP for their antimicrobial activity (37, 57, 91). The family presently consists of four naturally produced bacteriocins with similar sequences: LsbB, enterocin Q (EntQ), enterocin K1 (EntK1) and enterocin EJ97 (EntEJ97) (Figure 2) (91). LsbB, the founding member of the family, is produced by *Lactococcus. lactis*, while the remaining members, EntQ, EntK1 and EntEJ97, are produced by various enterococcal strains (25, 37, 92, 93). All members of the LsbB family are short (30-44 amino acids), leaderless bacteriocins with cationic and amphiphilic nature. NMR-based structural analysis of EntK1 and LsbB indicates an α-helix in the N-terminal half, while the C-terminal region is largely unstructured (37, 91) (Figure 2A). The hallmark of the LsbB family is the conserved C-terminal motif, KxxxGxxPWE, also known as the LsbB-like motif (Figure 2B) (91).

Despite high structure and sequence similarity (Figure 2), the inhibition spectrum among the LsbB bacteriocin family differs greatly. While LsbB exhibits a narrow inhibition spectrum, exclusively targeting *L. lactis*, the inhibition spectrum of EntK1, EntEJ97 and EntQ is broader, including potent activity against the human pathogens *E. faecium* and *Enterococcus faecalis* (36, 37, 92).

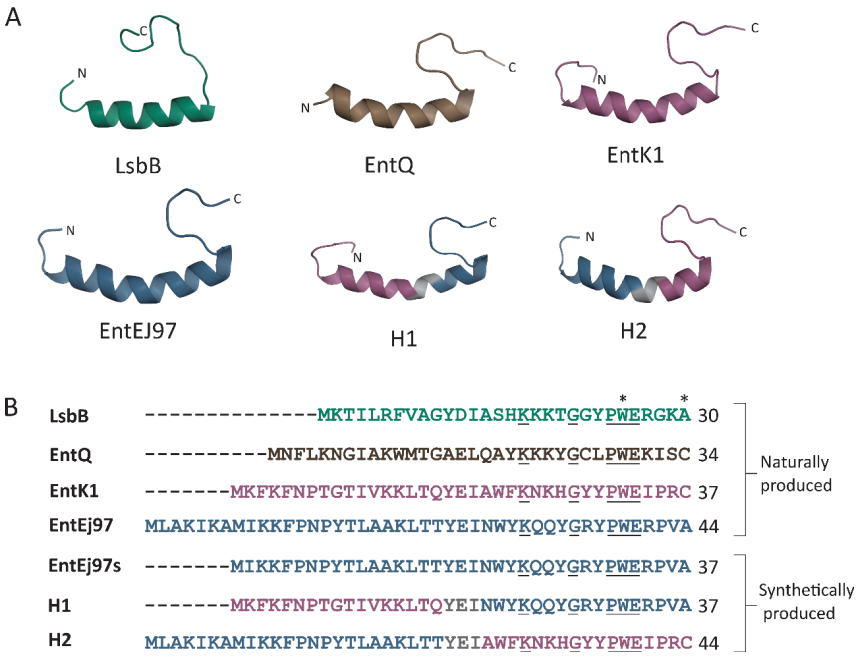

Figure 2| The LsbB bacteriocin family. A) Structural comparison of the members of the LsbB bacteriocin family. LsbB (PDB: 2MLV) and EntK1 (PDB: 5L82) are depicted by NMR structure, while the structure of EntQ, EntEJ97, Hybrid 1 and Hybrid 2 was predicted using Phyre2. The predicted models of EntEJ97, Hybrid 1 and Hybrid 2 were highly confident (97.4-99.5 %) and with coverage of 73-95 %. The confidence of the predicted EntQ structure is 49.4 %. B) Alignment of the amino acid sequences of the members of the LsbB bacteriocin family. Asterisk (*) indicates amino acids of LsbB, which are crucial for LsbB activity. The consensus sequence of the LsbB-like motif (KxxxGxxPWE) is underscored. For the hybrid bacteriocins Hybrid 1 and Hybrid 2, regions derived from EntK1 and EntEJ97 are indicated in purple and blue, respectively.

It has previously been shown that the antimicrobial activity of LsbB, EntK1 and EntEJ97 depends on binding to an intramembrane protease known as RseP (37, 57, 91). In a study by Miljkovic and colleagues, the construction of hybrid-RseP receptors, i.e., RseP proteins containing a combination of regions from sensitive and non-sensitive strains, indicated that the third putative transmembrane domain of *L. lactis* RseP is needed for LsbB interaction (83). Amino acid substitutions further pin-pointed the amino acids Tyr356 as crucial for LsbB sensitivity, as a substitution at this position converted a resistant strain into an LsbB-sensitive strain (83). Amino acids in the vicinity of Tyr356, including Ala353, were also suggested as important for LsbB sensitivity, although single substitutions at these positions had a less striking effect compared to position 356 (83).

For the bacteriocin itself, the C-terminal region has been proposed as important for LsbB:RseP interaction. In a competition assay, truncated LsbB having only the last eight C-terminal residues blocked the activity of the full-length peptide when added in excess (91). Thus, the authors proposed that the C-terminal region of LsbB was needed for RseP-interaction, while the N-terminal region was suggested to be responsible for the antimicrobial activity of the peptide. In efforts to identify specific amino acids involved in LsbB:RseP interaction, Ovchinnikov and colleagues performed several amino acid substitutions in the C-terminal region of LsbB. The W25A substitution abolished antimicrobial activity, while the other mutations (Y23A, P24A, E26A, R27A, and K29A) retained activity and blocking ability, although with variable strength (91). Interestingly, the Trp25 is highly conserved among the members of the LsbB family as part of the so-called LsbB-motif (Figure 2). Additionally, deletion of Ala30, the final C-terminal amino acid, resulted in reduced antimicrobial activity (37, 83).

In the context of developing novel antimicrobial agents, the LsbB family members EntK1 and EntEJ97 show significant potential due to their potent activity against vancomycin resistant enterococci (VRE) (36, 37). Although considered commensal, *E. faecalis* and *E. faecium* have emerged as important healthcare-associated pathogens in the past few decades, causing a variety of infections such as urinary tract infections and bacteremia (94). Two main characteristics have contributed to the rise of enterococci as nosocomial pathogens. First, the *Enterococcus* genus is highly resilient, allowing survival in harsh

environments such as hospitals and other healthcare facilities (94, 95). Second, enterococci efficiently attain antimicrobial resistance and displays a variety of mechanisms for both intrinsic and acquired resistance, making treatment options limited (94, 95). The therapeutic potential of EntK1 and EntEJ97 in the treatment of enterococcal infections has recently been explored. Notably, the bacteriocins are resilient to autoclavation, and retain most of their antimicrobial activity in blood (36). Furthermore, incubation of the bacteriocin in blood did not result in hemolysis, suggesting that EntK1 and EntEJ97 may be a viable option for the treatment of systemic VRE infections (36).

While the antimicrobial potential of EntK1 and EntEJ97 is evident, it should be noted that resistant colonies have been observed following high exposure to these bacteriocins under laboratory conditions (36, 37). Notably, phenotypic analyses of enterococcal *rseP* mutants with developed resistance to EntEJ97 and EntK1, demonstrated that these strains have reduced fitness; they showed a 6-8-fold increase in lysozyme susceptibility, reduced tolerance to heat and a significant reduction in desiccation tolerance (36, 37). Indeed, as discussed in detail in paper I, RseP is suggested to regulate stress response through activation of the sigma factor σ^V in *E. faecalis.* Δ*rseP* or Δ*sigV* in *E. faecalis* lead to reduced survival in response to multiple stressors, including heat, acid, and ethanol (96, 97). Notably, Δ*rseP* and/or Δ*sigV* were attenuated in murine urinary tract infection and systemic infection models, highlighting the role of RseP in enterococcal virulence. Thus, as the RseP mediated activation of σ^V is crucial for enterococcal cells, resistance to EntK1 and EntEJ97 seems to come at a high price for the bacterial cells.

1.2 Intramembrane proteases and regulated intramembrane proteolysis

Intramembrane proteases (IMP), also known as intramembrane cleaving proteases (I-CLiPs), constitute a unique class of membrane-bound proteases that hydrolyze peptide bonds within the cell membrane. IMPs can be divided into four distinct families based on their catalytic mechanism: the site-2-proteases (S2P; zinc metalloproteases), the

presenilin/signaling peptide peptidase (aspartyl proteases), the rhomboid proteases (serine proteases) and Rec1 (glutamyl proteases) (98-101). By the virtue of being membrane embedded proteases, the biochemical environment of IMP differs greatly compared with that of their soluble counterparts. Most notably, the water-excluding environment of the lipid bilayer has puzzled scientists, as proteases generally rely on water molecules to initiate the nucleophilic attack on the peptide bond of their substrate during proteolysis (102). Additionally, the substrates cleaved by IMP are also somewhat unusual. Commonly, substrates of IMP exhibit an α-helical shape, a conformation which makes the amide bond inaccessible to the nucleophilic attack due to steric hindrance by the amino acid sidechains (102, 103). Thus, IMP must not only create a water-accommodating environment needed for hydrolysis within the lipid bilayer, but also unwind the substrates to make the amide bonds accessible for the nucleophilic attack (102). Structural determination of prototypic members of all four families have confirmed the membrane-embedded location of the catalytic active site (104-108). While the structural features vary within an IMP class, all members are proposed to contain a hydrophilic cavity or channel, delivering water from either side of the membrane to the active site (104-108). Several substrate gating models have been proposed for substrate regulation by IMP, however these models vary among the members of this class of proteins (98, 104, 108).

While intriguing simply from a biochemical perspective, IMP are receiving increasing scientific interest due to their vital role in regulated intramembrane proteolysis (RIP) (99, 101, 109). In the most general terms, RIP can be described as a highly conserved signaling mechanisms in which an IMP cleave a membrane-bound substrate, thereby liberating an effector domain from the membrane (Figure 3A). RIP-mediated signaling regulates a diverse array of cellular processes, of which many have been implied in human health and disease. Notably, the conceptualization of RIP arose following the molecular characterization of the transcriptional regulation of cholesterol metabolism, which in mammals is depended on RIP-mediated maturation of the membrane-bound transcriptional regulator SREBP (Sterol regulatory element binding protein) (110-112). When cholesterol is depleted, the SREBP precursor is sequentially processed by the serine protease Site-1-protease (S1P, previously known as MBTPS1) and the S2P (previously

known as MBTPS2), resulting in activation of genes needed for cholesterol synthesis (Figure 3B) (110, 111, 113, 114). This process also has an interesting dynamic in the cell. When cholesterol is abundant, SREBP is kept in the endoplasmic reticulum (ER) in a complex with SCAP (SREBP cleaving activating protein) and Insig (insulin-induced protein (114-118). Cholesterol depletion results in SCAP disassociating from Insig, followed by the SREBP:SCAP complex being translocated to the Golgi membrane (114-118). This subcellular compartmentalization ensures that the RIP-mediated activation of genes involved in cholesterol synthesis is strictly regulated and only occurs when needed. Inactivation of S2P has been linked to several human diseases, including several skin-and bone disorders such as osteogenesis imperfecta ("brittle bone disease") (119, 120).

Human S2P (*Hs*S2P) is the founding member of the S2P family, and the first identified IMP (110). Shortly following the discovery of *Hs*S2P, mutational analysis identified *Escherichia coli* RseP (*Ec*RseP; regulator of sigma E protease) and *Bacillus subtilis* SpoIVFB (Stage IV sporulation protein FB) as site-2-proteases (121-123), thereby expanding the concept of RIP signaling to the bacterial world. In the following section, the vital role of S2P-mediated RIP signaling in bacteria will be discussed.

1.2.1 The role of S2P and regulated intramembrane proteolysis in bacteria

As reviewed in detail in paper I and by others, S2P-mediated RIP signaling regulates a vast range of critical cellular processes in bacteria (99, 124). This includes, but is not limited to, stress response in *E. coli*, sporulation in *B. subtilis*, iron acquisition in *Pseudomonas* spp. and cell polarization in *Caulobacter crescentus* (121, 122, 125-131). Notably, S2P-mediated RIP signaling has also been implicated in virulence characteristics of several important human pathogens, such as toxin production in *Vibrio cholera*, lysozyme resistance in *E. faecalis* and cell-wall composition and persistence of *Mycobacterium tuberculosis* (96, 132-134). The evident role of S2P in bacterial pathogenicity highlights the potential of S2P as novel antimicrobial targets (see paper I for more details on the role of S2P-mediated RIP in the physiology and virulence in bacteria).

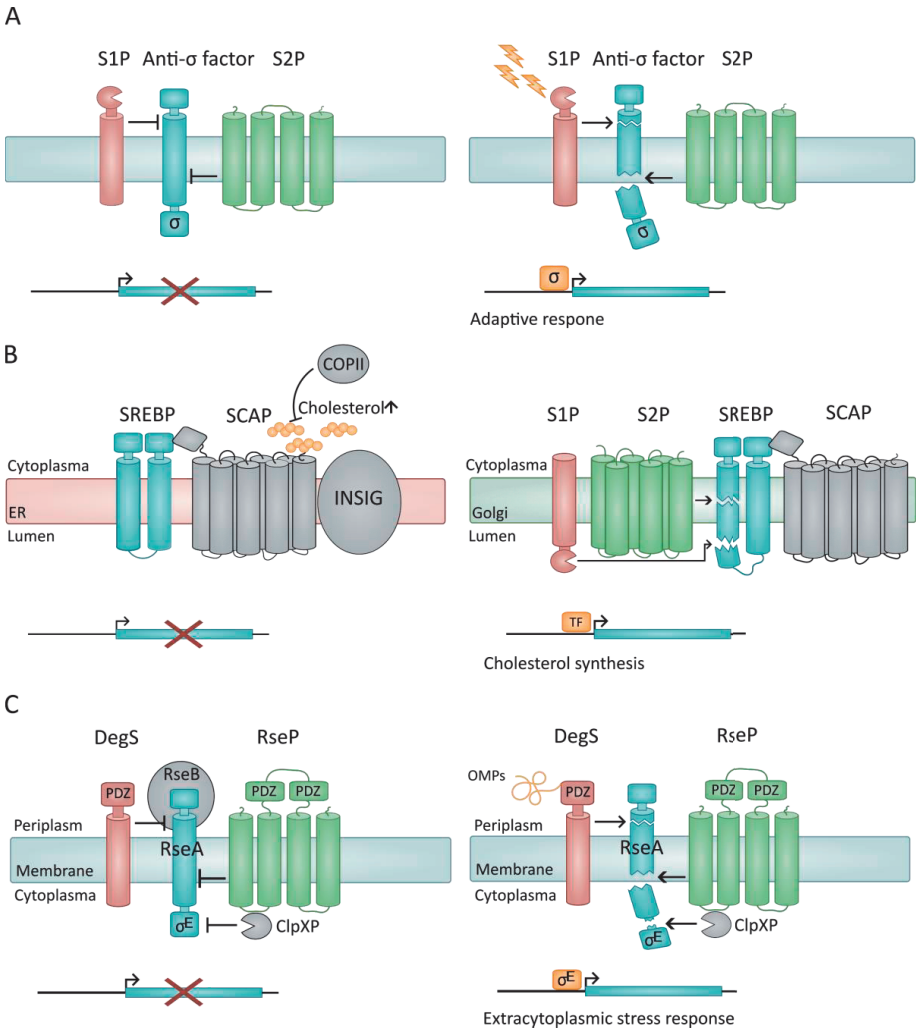

Figure 3| S2P-mediated RIP signaling. A) The general site-2-protease (S2P)-mediated RIP paradigm. In the absence of environmental cues, the membrane-bound anti-sigma factor inhibits σ-factor activity by sequestering the σ-factor to the membrane (left panel). When environmental stimuli are detected, a site-protease (S1P) and a S2P sequential degrade the anti-sigma factor, releasing the σ-factor from the membrane. B) S2P-mediated activation of cholesterol synthesis in mammals. When cholesterol is abundant, SREBP is kept in the endoplasmic reticulum (ER) in complex with SCAP and Insig. Cholesterol inhibits the COPII mediated translocation to the Golgi membrane (left panel). When

cholesterol is depleted, SCAP:SREBP is translocated to the Golgi where SREBP is sequentially depredated by S1P and S2P (rigth panel). This releases the transcription factor domain of SREBP, which activated genes involved in cholesterol synthesis. C) S2P-mediated activation of the extracytoplasmic stress response in *E. coli*. The PDZ domain of the S1P DegS recognizes unfolded outer membrane proteins (OMPs). This recognition initiates the site-1-cleavage of the anti-sigma-factor RseA. The S2P RseP subsequently cleaves RseA, releasing σ^E which is maturated further by ClpXP in the cytosol. σ^E activated genes involved in the adaptive stress response. In all panels: The suggested stimuli signal is shown in yellow, the substrate in blue, presumed S1P in red, S2P in green, substrates in active form in yellow, and additional components in grey. This figure is adapted from Figure 1 and 2, paper I.

Although regulating a diverse array of cellular processes, S2P-mediated RIP signaling normally adheres to the same general paradigm (103, 135) (Figure 3A). First, a site-1-protease cleaves a membrane-bound substrate in response to specific stimuli (site-1-cleavage). This primary cleavage triggers a S2P to cleave the membrane-bound substrate within lipid bilayer (site-2-cleavage). Most commonly, the membrane-bound substrate is an anti-sigma factor, which negatively regulates the activity of the sigma factor by sequestering it to the membrane. The sequential degradation of the anti-sigma factor by the site-1-protease and the S2P, releases the sigma factor from the membrane, subsequently resulting in an adaptive response (Figure 3A). S2P-mediated RIP signaling is found among both Gram-negative and Gram-positive bacteria, with variations of this paradigm continuing to emerge as the role of S2P in different species are explored (see paper I for more details).

Based on phylogenetic analysis, the S2P family can further be divided into four subgroups (136) (Figure 4). HsS2P, *Ec*RseP and the enterococcal RseP, belongs to the largest subgroup, group I, which is characterized by a variable number of PDZ domains (IPR001478, structural domain commonly found in signaling proteins). The second largest subgroup, group III, contains a cystathionine-β-synthase (CBS) domain (IPR000644, structural domain found in a variety of proteins), but no PDZ domain. SpoIVFB, the S2P of *B. subtilis,* resides within group III. The two remaining subgroups (II and IV) lacks any additional domains, however, none of these putative proteases have been extensively characterized (136). To date, the structure of only three members of the S2P family has been determined:

The group I members *Ec*RseP (PDB: 7W6X) and RseP of *Kangiella koreensis* (*Kk*RseP; PDB:7W6Y, YW6Z) and *Mj*S2P (PDB:3B4R), the S2P homolog from the thermophilic archaea *Methanocaldococcus jannaschii*, which belongs to group III (104, 137).

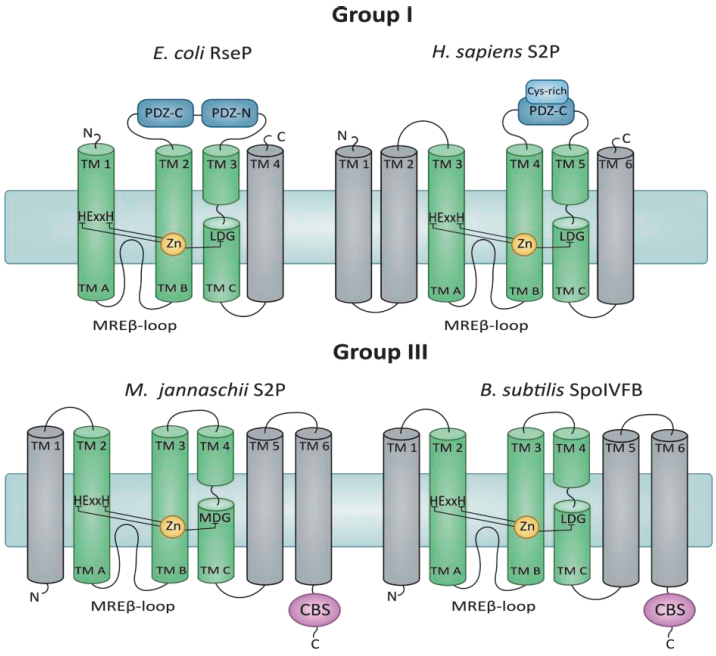

Figure 4| Group I and group III of the S2P family. Phylogenetic analysis has divided the S2P family into four subgroups. Group I contains one or more PDZ domains (indicated in blue). *E. coli* RseP and the human S2P are members of this subgroup. Group III contains an CBS domain (indicated in purple). The S2P of *M. jannaschii* and SpoIVFB from *B. subtilis* are members of this subgroup. The catalytic region (TM A-C, green) consists of the conserved zinc-coordinating motifs HExxH (TM A) and LDG (TM C). Additionally, all members contain a conserved MREβ-loop partially embedded in the membrane between TM A and TM B.

While members of the S2P differ in membrane topology, size and extramembrane domains, this family of proteases shares some common key features. The hallmark of the S2P family is the catalytic core region, observed among all four subgroups (Figure 4) (104, 122, 136, 138). The catalytic core region consists of three transmembrane segments (TM; TM A-C in Figure 4), with the conserved zinc-binding motif HExxH and the zinc-coordinating

aspartate residue of the LDG motif, located in TM A and TM C, respectively (104, 136). During catalysis, the conserved glutamate residue of the HExxH motif is suggested to activate a zinc-bound water molecule, thereby initiating the nucleophilic attack on the peptide bond. As seen for soluble metalloproteases, mutations in the conserved residues of the catalytic motif (HExxH, LDG) significantly reduce the protease activity of S2P homologs in multiple species (104, 121, 128, 139, 140).

In addition to the catalytic core region, several conserved motifs are suggested to be involved in S2P substrate recognition and processing. The following section will discuss S2P regulation and substrate processing, focusing on the S2P of *E. coli, Ec*RseP. *Ec*RseP is the best characterized member of the S2P family, and *Ec*RseP-mediated degradation of the anti-sigma factor RseA serves as a blueprint for RIP-mediated signaling in bacteria (128). Notably, enterococcal S2P, which functions as a receptor for bacteriocins of the LsbB family (section 1.1.4), belongs to the same subgroup as *Ec*RseP (group I) and contains several of the conserved motifs suggested to be important for *Ec*RseP:substrate interaction.

1.2.2 *E. coli* RseP and RIP-mediated regulation of the extracytoplasmic stress response

*Ec*RseP, previously known as YaeL, is one of the most extensively characterized members of the S2P family. *Ec*RseP was first identified as a key regulator of the σ^E-dependent extracytoplasmic stress response (Figure 3C) (123, 128, 141). In the absence of stress, σ^E is held inactive by RseA, a transmembrane anti-sigma factor (142, 143). Under stressful conditions compromising the cell wall (e.g., heat, acid, antibiotics), misfolded outer membrane proteins (OMPs) accumulate in the periplasm. The C-terminal residues of unfolded OMPs directly interacts with the PDZ-domain of the inner membrane protease DegS (144). DegS, the site-1-protease of this RIP signaling cascade, subsequently cleaves the periplasmic region of RseA (site-1-cleavage) (128, 145). *Ec*RseP then cleaves RseA within the membrane (site-2-cleavage), thereby releasing the C-terminal region of RseA from the membrane into the cell (128, 141, 146). RseA is further processed in the cytosol by ATP-dependent proteases such as ClpXP to form the mature σ^E, which subsequently

activates genes involved in the stress response (147). A similar S2P-mediated stress response has been observed in other bacteria, including *B. subtilis* and *P. aeruginosa* (148-151).

*Ec*RseP mediated degradation of RseA is regulated at multiple levels to ensure that σ^E activation is strictly stress dependent. Most notably, *Ec*RseP fails to efficiently cleave RseA prior to stress-induced, site-1 cleavage by DegS (152). Additionally, DegS depends on the inactivation of RseB, a periplasmic protein which binds to the C-terminal region of RseA (Figure 3C) (142, 143). RseB has been demonstrated to suppress DegS dependent cleavage of RseA, likely by binding to and thus blocking the DegS cleavage site (153, 154). Accumulation of OMPs and lipopolysaccharides is suggested to relieve the RseB-mediated RseA inhibition (155-157). In this sense, RseB and DegS serve as joint gatekeepers for the extracytoplasmic stress response, ensuring that site-1-cleavage, and thus site-2-cleavage, is strictly stress-dependent.

This requirement for substrate priming (i.e., primary substrate processing by a site-1-protease) appears to be a common feature of S2P-mediated RIP signaling (98, 100, 124). In the case of *Ec*RseP, the PDZ-tandem, located between TM2 and TM3 in the periplasm, has been proposed to act as a size-exclusion filter, preventing interaction with substrates with bulky periplasmic domains, such as full-length RseA (158) (Figure 3C). According to this model, the DegS cleaved RseA, which is no longer associated with RseB and has lost most of its periplasmic domain, can pass through the PDZ filter and access the *Ec*RseP activity site, while the full-length RseA cannot. Experimental data suggest that this is indeed the case. The PDZ-tandem of *Ec*RseP was first implied in negative regulation of substrate cleavage following results from mutational analysis, demonstrating that disruption of the PDZ domains cause degradation of RseA in a site-1-independent manner (159-161). Structural studies have provided additional evidence for this idea, indicating that the PDZ tandem forms a pocket-like space facing the catalytic center (137, 158). Indeed, the positioning of the PDZ tandem is suggested to sterically hinder access of substrates with a bulky periplasmic domain to the catalytic active site, thereby preventing undesirable S2P cleavage under non-stress conditions. Substrate discrimination by PDZ-mediated size-

exclusion has also been suggested as a regulatory mechanism for RasP, the S2P of *B. subtilis* (162).

In addition to the PDZ tandem, several conserved regions of *Ec*RseP have been suggested to have a role in substrate recognition and cleavage. This includes: (i) conserved residues near the LDG catalytic motif in TM3, in this work, referred to as the extended LDG motif (NxxxxNxxPxPxLDG), (ii) the membrane-reentrant β-loop (MREβ-loop), which is partially embedded in the membrane between TM1 and TM2, and (iii) the PDZ-C terminal region (PCT), consisting of two helices located adjacent to the C-terminal PDZ domain (Figure 4) (163-166). The extended LDG motif and the MREβ-loop are conserved among members of group I and group III, while the two helices of the PTC region is partially conserved among members of group I (122, 136, 165, 167). Mutational analysis of the extended LDG motif in *Ec*RseP and SpoIVFB, the S2P homolog of *B. subtilis*, resulted in reduced substrate binding and cleavage (122, 139, 164, 167, 168). *Ec*RseP and SpoIVFB are assigned to group I and group III, respectively, suggesting that the involvement of the extended LDG motif may be conserved among S2P from different subgroups. Likewise, cross-linking analysis indicated that residues of MREβ-loop of both SpoIVFB and *Ec*RseP are necessary for substrate interaction (164, 167). Lastly, *in vivo* photo-cross-linking experiments implied a direct interaction with the PTC region and the DegS-cleaved form of RseA (165).

Based on the mutational analysis of conserved motifs presented above, and the recently resolved crystal structure of *Ec*RseP, a model involving three-step mechanism has been proposed for substrate discrimination and accommodation by *Ec*RseP (137). (i) The PDZ-tandem works as a size exclusion filter by sterically hindering entry of bulky substrates, such as full-length RseA, to the active site. (ii) The PDZ-tandem, PCT and TM4 collectively act as gate, with conformational changes resulting in the substrate gaining entry into the active site (137). Gating mechanisms have also been suggested to regulate substrate entry in other IMP, including *Mj*S2P (104, 106). (iii) Lastly, interactions with the MREβ-loop is suggested to extend the transmembrane segment of the substrate, thereby making the peptides-bond of the α-helix accessible for the nucleophilic attack (137, 164). Similarly, several soluble metalloproteinases have β-strands in close proximity to their active site, which is suggested to bind the substrate in extended conformation (169, 170).

2. The purpose of this study and outline of the thesis

Antibiotic resistance is a global concern, yet limited novel treatments are available to combat multidrug-resistant bacteria. In this context, bacteriocins are receiving increased scientific interest. Most notably, several bacteriocins show strong activity against multidrug resistant pathogens, highlighting their potential as novel antimicrobial agents.

The bacteriocin EntK1 is one example of a bacteriocin with high activity against human pathogens. EntK1 is particularly potent against *E. faecium*, including vancomycin-resistant isolates, which are an increasing problem in nosocomial infections. EntK1 belongs to the LsbB family of bacteriocins. These bacteriocins are short peptides, synthesized without an N-terminal leader sequence and post-translational modifications. Together, these qualities make the LsbB family an ideal starting point for bioengineering to improve potency or target range of the bacteriocins.

The antimicrobial activity of EntK1 and other members of the LsbB family depends on interaction with RseP, an integral membrane protein of the S2P family. RseP is conserved in multiple species, yet the potency of EntK1 varies considerably. To further develop EntK1 as a novel treatment option in bacterial infections, an increased understanding of the mechanism underlying bacteriocin sensitivity is essential. A detailed understanding of the interaction between EntK1 and RseP might provide a powerful basis for guided construction of novel bacteriocins and may contribute to establish RseP as a novel drug target.

The aim of the work presented in this thesis was to use LsbB family bacteriocins as a basis for engineering novel bacteriocins with improved functions and to characterize the mechanism of action of these bacteriocins by defining the structures and sequences involved in the interaction between bacteriocins and RseP.

RseP is an intramembrane protease belonging to the S2P family. S2P proteases are conserved in all kingdoms of life and regulate a vast array of cellular processes through RIP-mediated signaling. **Paper I** reviews the role of S2P in bacteria and discuss their potential as therapeutic targets. S2P are highly conserved among bacteria and play an essential role

in physiology and virulence in multiple human pathogens. This includes alginate production in *Pseudomonas aeruginosa*, persistence, cell-envelope composition in *M. tuberculosis*, and lysozyme resistance in *E. faecalis*. The prominent role of S2P in multiple human pathogens highlights the potential of RseP as an antimicrobial target. However, so far only a limited number of inhibitors have been shown to target these proteins. Several challenges hamper the development of novel RseP-inhibitors, including potential adverse interaction between host S2P and the inhibitor, and lack of detailed structural and biochemical knowledge of S2P.

Paper II of this thesis describes the design of a novel hybrid bacteriocin, hybrid 1 (H1). H1 was constructed by combining the N-terminal region of EntK1 with the C-terminal region EntEJ97. Like the parental bacteriocins, H1 depends on the membrane-bound protease RseP for its antimicrobial activity. However, the inhibition spectrum of the hybrid bacteriocin differs greatly from the inhibition spectra of the parental bacteriocins. Most notably, H1 showed superior antimicrobial activity towards *Staphylococcus haemolyticus* - an important nosocomial pathogen. In a bacteriocin-based three-component formulation, H1 contributed to completely eradicating *S. haemolyticus* biofilms *in vitro*, highlighting the potential of these bacteriocins as a possible treatment option for pathogenic bacteria. The construction of H1 confirms that the LsbB family can be easily engineered to improve both potency and alter the activity spectrum. A detailed understanding of how these bacteriocins interact with RseP would further aid the rational design of novel bacteriocins.

Paper III describes a mutational analysis of *E. faecium* RseP to identify regions of the protein involved in bacteriocin interaction and sensitivity. Mutational effects were assessed by studying EntK1 binding and sensitivity using minimal inhibition concentration (MIC_{50}) assays and flow cytometry-based binding assays, as well as structural techniques and AI-based structure prediction by AlphaFold. The mutational analysis revealed that the extracellular PDZ domain and the extended LDG domain of *E. faecium* RseP are key determinants for EntK1 sensitivity. These regions are highly conserved in several RseP homologs, suggesting that bacteriocins could potentially target RseP in multiple species.

When the work presented in this thesis was initiated, no crystal structures of RseP homologs containing a PDZ domain was reported. Purification and structural

determination of RseP from *E. faecium* was therefore a subgoal of this work. **Paper IV** describes the utilization of *L. plantarum* and the pSIP-expression system as a novel platform for large-scale production of membrane proteins. Various technical challenges impede structural characterization of membrane proteins, with obtaining sufficient amounts of pure and homogeneous protein generally being a major bottleneck. *E. coli* is undoubtedly the most used expression host for recombinant expression of membrane proteins; however, many membrane proteins fail to fold correctly using *E. coli*, resulting in unwanted inclusion bodies. Our investigations show that, RseP from *E. faecium* has been challenging to express in *E. coli*, prompting investigations of alternative expression systems. In paper IV, RseP derived from *E. faecium* was expressed and successfully purified using the bacteriocin-based pSIP expression system in *L. plantarum*.

3. Main results and discussion

In recent years, bacteriocins have received increased scientific interest as alternative and/or complements to conventional antibiotics (10, 11). When the work presented in this thesis was initiated, the leaderless bacteriocin EntK1, belonging to the LsbB family of bacteriocins, was recently discovered and showed significant potential as novel antimicrobial, due to its potent activity against vancomycin-resistant enterococcal strains (37). Most notably, EntK1, alongside other members of the LsbB family, depend on binding to a membrane-bound S2P for their antimicrobial activity (37, 57, 91). As comprehensively reviewed in Paper I and elsewhere, bacterial S2P are regarded as excellent antimicrobial targets due to their vital role in physiology and virulence in multiple human pathogens (99, 124). While EntK1 depends on enterococcal RseP for its antimicrobial activity (37), little is known about how EntK1 interacts with RseP or how this interaction eventually leads to cell death.

3.1 Engineered bacteriocins and their potential as novel antimicrobials

Bacteriocins hold significant potential for applications in human and animal health (see section 1.1.2 for more details). A key feature of bacteriocins is that they are highly amenable to be engineered. Indeed, several bacteriocins have been engineered, genetically or by *de novo* synthesis, to confer enhanced activity or stability (51-56). As outlined in section 1.1.5, the LsbB family consists of sequence-related bacteriocins with a simple structure and no post-translational modifications, making these bacteriocins an ideal starting point for designing novel antimicrobial peptides (Figure 2) (25, 37, 92).

Paper II describes the design of the novel hybrid bacteriocin H1. This bacteriocin was synthetically constructed by combining the N-terminal region of EntK1 with the C-terminal region of EntEJ97 (Figure 2). Despite high sequence similarity and similar mode of action (i.e., targeting RseP), members of the LsbB family exhibit distinct inhibition spectra. The

bacteriocin LsbB exhibits a very narrow inhibition spectrum, with activity only against *L. lactis*, while the inhibition spectra of EntK1 and EntEJ97 are broader, targeting several species of enterococci, lactococci and staphylococci, and importantly have a potent activity against *E. faecium* and *E. faecalis* (36, 37, 92). Mutational analysis suggests that the C-terminal region of the LsbB family bacteriocins play a critical role in initial docking to RseP (83, 91), and we therefore rationalized that combinations of C- and N-terminal regions from different bacteriocins could lead to bacteriocins with different spectra and potencies.

To define the inhibition spectrum of the novel bacteriocin, H1 and the parental bacteriocins were initially screened against a panel of 50 bacterial species across different genera (Paper II; Table S1). The inhibition spectrum of H1 was largely similar to the inhibition spectrum of EntEJ97, from which the C-terminal region of the hybrid bacteriocin is derived. The most notable difference was that H1 showed unique and potent activity against *Streptococcus uberis* and *Streptococcus thermophilus* and enhanced activity against the nosocomial pathogens *Staphylococcus epidermidis* and *S. haemolyticus*, compared to the parental bacteriocins (Paper II; Table S1).

To further explore the antimicrobial potential of H1, the engineered hybrid bacteriocin was evaluated against an additional 27 clinical and commensal *S. haemolyticus* strains (Paper II; Table 1, Table S2). Notably, H1 exhibited enhanced activity (i.e., larger inhibition zones) for 74 % of the strains tested in an initial a spot-on-lawn analysis compared to the parental bacteriocins EntK1 and EntEJ97. The minimal inhibition concentration (MIC_{50}) ranged between 0.1-0.78 µg/ml (Paper II; Table S2), highlighting the potency of the novel hybrid bacteriocin against *S. haemolyticus*. For *S. epidermidis*, only a single strain was evaluated in Paper II. Following publication of paper II, H1 was screened against six additional *S. epidermidis* strains in a spot-on-lawn assay. Notably, H1 showed overall low activity (i.e., unclear zones), suggesting that the potent activity against *S. epidermis* (Paper II; Table S1) is strain specific (data not published).

Despite the promising activity against *S. haemolyticus,* the antimicrobial potential of H1 is hampered by resistance development. Indeed, resistant colonies emerged within 24 hours of exposure to the bacteriocin (Paper II; Table 1, Figure 2). As discussed in section 1.1.4, combinatory treatment are a common approach to curtail resistance development. In paper

II, we exploited the synergy between H1 and the bacteriocins micrococcin P1 (MP1) and garvicin KS (GarKS) in a three-component combinatory treatment (Paper II; Figure 3-4, Table S3). MP1 is a class I thiopeptide targeting the protein synthesis machinery, while GarKS is a newly discovered class II three-peptide bacteriocin with an unknown mode of action (171-173). We hypothesized that by combining bacteriocins with different modes of action, the development of resistance would be effectively reduced. Indeed, the three-component combination (HGM) showed a significant reduction in MIC values for planktonic cells after a 48-hour exposure compared to H1 alone, indicating reduced resistance development (Paper II; Figure 3). Notably, the three-component combination completely eradicated *S. haemolyticus* biofilm formation *in vitro* (Paper II; Figure 4), highlighting the potential of these bacteriocins as a treatment option for *S. haemolyticus* infections. Bacteriocins have previously been successfully used in combination with conventional antibiotics, resulting in enhanced antimicrobial activity and reduced resistance development for several human pathogens (38, 40, 44, 45, 174). However, the combination presented in paper II (H1/GarKS/MP1) is an example of a bacteriocin-based and antibiotic-free combinatory treatment that targets the biofilm of a human pathogen.

Resistance to bacteriocins is commonly caused by alterations and/or disruption of the antimicrobial target (57, 72, 82, 175, 176). Indeed, disruptive mutations in *rseP* have been observed among EntK1 and EntEJ97 resistant isolates (36, 37). Heterologous expression of *S. haemolyticus* RseP in the naturally H1-resistant *L. plantarum* confirmed that *S. haemolyticus rseP* is needed for the antimicrobial activity of H1 (Paper II; Table 2, Figure S1). Thus, it was surprising to note that among 14 randomly selected H1 resistant isolates, only two contained mutations within *rseP*. To gain deeper insights into H1 resistance development in *S. haemolyticus*, whole genome sequencing was conducted on five additional H1-resistant mutants and their corresponding H1-sensitive wild-type (Paper II; Table 3). Interestingly, four of the five mutants sequenced contained mutations within the *ecsAB* genes, encoding the ATP-binding cassette (ABC) transporter Ecs (177). As discussed in paper I, it has been suggested that *E. faecium* RseP contributes to the sequentially degradation of lipoprotein signal peptides to form mature pheromones, which are subsequently transported out of the cell by an ABC transporter (178) (Paper I; Figure 2E).

While the role of RseP in *S. haemolyticus* is unknown, the mutations observed in Ecs in H1 resistant mutants suggest a molecular link between RseP and the ABC transporter also in this species.

Taken together, the results presented in paper II clearly demonstrate that the members of the LsbB family can be engineered to improve potency and alter activity spectrum. Moreover, H1 did not only exhibit superior antimicrobial activity against *S. haemolyticus* compared to the parental bacteriocins, but also contributed to complete eradication of *S. haemolyticus* biofilms. This highlights the potential of bacteriocin engineering in the development of novel treatment options against human pathogens.

It should be noted that a second hybrid bacteriocin with an inverse order of H1 (i.e., N-terminal region of EntEJ97 and C-terminal region of EntK1) designated Hybrid 2 (Figure 2), showed overall poor activity in an initial screen (data not shown). Additionally, hybrid bacteriocins consisting of LsbB and EntK1 have also been constructed. However, using the same panel of indicator species as in Paper II, an improved or differential activity spectrum has not been observed (unpublished data obtained from colleagues). A detailed understanding of how these bacteriocins interact with RseP would further aid the rational design of novel bacteriocins and improve the success rate for engineering bacteriocins with improved potency.

3.2 Identification of RseP regions involved in bacteriocin sensitivity and binding

Paper II established that the members of the LsbB-bacteriocin family can be engineered to improve potency and alter the activity spectrum. Members of the LsbB family depend on binding to RseP for their antimicrobial activity (37, 57, 91); however, in which manner the bacteriocins recognize and bind RseP and how the interaction eventually leads to cell death remains elusive.

Paper II describes a mutational analysis of RseP derived from EntK1-sensitive *E. faecium* to identify regions involved in bacteriocin binding and sensitivity. As discussed in paper I, S2P

cleaves a wide range of substrates. Indeed, *E. coli* RseP cleaves the anti-sigma factors RseA and FecR, while also proposedly contributing to quality control of the cytoplasmic membrane by degrading various signal peptides (128, 140, 179). Similarly, RseP of *E. faecalis* is suggested to cleave the anti-sigma factor RsiV and various lipoproteins (96, 180, 181), highlighting the promiscuity of these proteases. The known substrates of S2P family share no apparent sequence homology; however, the small size and amphiphilic helical nature of the substrates appears to be a common feature (103, 146, 163). Considering the small size and helical structure of EntK1 (37), it is plausible that EntK1 interacts with *E. faecium* RseP in a similar manner as the native substrate. Thus, in paper III, the role of conserved S2P region known to be essential for substrate recognition and processing was evaluated in the context of EntK1 sensitivity and binding.

As seen in paper II, the pSIP system can be efficiently used to express heterologous *rseP* in *L. plantarum* (Paper II; Table 2, Figure S1). While *L. plantarum* contains a *rseP* ortholog on the chromosome, this bacterium is insensitive to EntK1. *L. plantarum* harboring the empty vector and cells overexpressing *L. plantarum* RseP remained insensitive to EntK1, while overexpression of enterococcal *rseP* conferred EntK1-senstivity (Paper III; Table 1). Consistent with these results, *L. plantarum* expressing plasmid encoded *Efm*RseP showed a strong fluorescent signal following exposure to fluorescently tagged EntK1, while no fluorescent signal was detected for *L. plantarum* harboring the empty vector or overexpressing *L. plantarum* RseP (Paper III; Figure 2 & 3). This suggests that *L. plantarum* is a suitable host for heterologous expression of *Efm*RseP and that this system may be further used to identify regions of RseP involved in EntK1 binding and sensitivity.

The hallmark of the S2P family is the conserved catalytic motifs (HExxH and LDG) located in the transmembrane segments of the protease (Figure 4). To explore the role of the proteolytic activity in the context of EntK1 sensitivity, all conserved residues of the catalytic active site were substituted with alanine (Paper III; Figure 1). Single substitutions of the conserved active site (EfmH18A, EfmE19A, EfmH22A, and EfmD372A) only resulted in a minor increase in MIC_{50} and EntK1 binding. A triple mutant, containing alanine in all conserved positions of the HExxH motif (AAxxA), showed a significant increase in MIC_{50} as well as reduced binding abilities (Paper III; Table 3). However, the triple mutant remained

more than 8-fold more sensitive to EntK1 than *L. plantarum* harboring the empty vector (Paper III; Table 3). Taken together, this indicates that the catalytic activity of *Efm*RseP is not essential for the antimicrobial activity of EntK1.

Several additional regions have been suggested to be involved in S2P substrate recognition (i.e., MRE-β loop, GxG motif, LDG motif) (163, 164, 166-168) (Paper III; Figure 4). However, site-directed mutagenesis of these conserved sequence motifs, or even deletion of such motifs, did not abolish bacteriocin sensitivity, with one exception. Strikingly, the single alanine substitution of Asn359 of the extended LDG motif abolished EntK1-senstivity and binding (Paper III; Table 3, Figure 1 & 3). Importantly, the mutant remained sensitive to EntEJ97. As discussed above, EntEJ97 targets RseP but exhibits a differential inhibition spectrum compared to EntK1 (Paper II; Table S1). N359A showed a significant increase in EntEJ97 sensitivity compared to L. plantarum harboring the empty vector, suggesting that the lack of EntK1-sensitivity is not caused by failure to produce the mutated RseP (Paper III; Figure S2). This was further confirmed by western blot analysis, which indicated that N359A accumulates at levels comparable to EfmRseP when induced (Paper III; Figure S4). Notably, a circular dichroism (CD) analysis of purified N359A was performed following the publication of Paper III. The CD-analysis suggested that the secondary structure of the mutant was comparable to that observed for the purified wild-type *Efm*RseP (unpublished data). Taken together, this indicates that the alanine substitution did not drastically alter protein structure nor expression levels, confirming that the loss of the asparagine side chain at position 359 alone is responsible for the observed abolition of EntK1 sensitivity and binding. Furthermore, it is interesting to note that Asn389 in *Ec*RseP, which corresponds to Asn359 in *Efm*RseP, also plays a key role in substrate recognition. Mutational analysis of Asn389 has been shown to reduce the substrate binding and processing by *Ec*RseP (137, 163).

Even though the effect of the single Asn359 substitution is striking, it is interesting to note that the extended LDG motif, including Asn359, is highly conserved among EntK1-sensitive and naturally EntK1-resistant species (Paper III; Figure 1). This indicates that yet other regions of RseP may be involved in bacteriocin binding and sensitivity. To further map the region of RseP involved in EntK1 sensitivity and binding, several hybrid RseP proteins, i.e.,

RseP proteins containing a combination of regions from EntK1-insensitive *L. plantarum* and the EntK1-sensitive *E. faecium*, were constructed (Paper III; Figure S3). Construction of hybrid proteins is not a novel approach for mapping regions involved in bacteriocin sensitivity. Indeed, Kjos and colleagues identified the extracellular loop of man-PST component IIC as important for sensitivity to class II-A bacteriocins by constructing man-PTS chimeras consisting of regions from the sensitive *Listeria monocytogenes* and the non-sensitive *L. lactis* (75). Recently, structural analysis of pediocin-like bacteriocin in complex with man-PST confirmed the importance of IIC in bacteriocin interaction (28, 76). Similarly, the C-terminal region of RseP has been implied in LsbB-sensitivity following construction of hybrid proteins containing regions of RseP from LsbB-sensitive and LsbB-resistant lactococcal strains (83).

Four of the 11 constructed hybrid-RseP proteins conferred EntK1-senstivity to the naturally EntK1-insensitive *L. plantarum*. Importantly, 10 of the 11 RseP hybrids, conferred sensitivity to EntEJ97, thereby suggesting proper expression and folding of the hybrid RseP (Paper III; Figure S2). All sensitive hybrids contained parts of the enterococcal PDZ-domain. Notably, the three hybrids exhibiting the lowest MIC_{50} values (Hyb4, Hyb10, and Hyb11) contained the full PDZ domain from *E. faecium*, highlighting the importance of this domain in EntK1:RseP interaction (Paper III; Table 3, Figure S3). PDZ domain-containing proteins are found in several signaling pathways and are commonly important for interaction with the C-terminal sequence of proteins or peptides (144, 182, 183). Indeed, the PDZ domain of S2P have previously been implied in substrate binding and recognition (158, 160, 162). Similarly, the results presented in paper III indicates that the PDZ domain of *Efm*RseP is the defining region of bacteriocin binding and sensitivity.

To better understand the role and positioning of the conserved motifs in RseP, the three-dimensional structure of *Efm*RseP was predicted using the artificial intelligence-based structure prediction tool AlphaFold (184) (Paper III; Figure 4). The predicted structure indicated that the *Efm*RseP PDZ domain forms a pocket-like structure facing the catalytic center, with Asn359 protruding towards the PDZ domain. Taken together with the experimental data presented in paper III, it is tempting to speculate that EntK1 initially

interacts with the *Efm*RseP PDZ domain resulting in subsequent interaction with core residues such as Asn359.

During the finalization of paper III, AlphaFold-Multimer was published (185). AlphaFold-Multimer is an extension of AlphaFold 2, optimized for prediction of protein complexes. In line with experimental data presented in paper III, predictions of the EntK1:*Efm*RseP complex using AlphaFold multimer indicated that interaction between EntK1 and RseP primarily involve the PDZ domain and the third transmembrane helix (Figure 5A-B). Strikingly, the C-terminus of EntK1 makes multiple close contacts (< 3 Å) with Asn359, the amino acid experimentally shown to be essential for EntK1 binding and sensitivity (Figure 5A-B; Paper III; Table 3, Figure 3). Interestingly, when predicting the complex between EntEJ97 and *Efm*RseP, Asn359 shows no direct contact with the bacteriocin (Figure 5C). This difference in interaction may explain why the N359A mutant remained sensitive towards EntEJ97, while sensitivity towards EntK1 was lost. Mutational analysis of lactococcal RseP and LsbB has suggested the third transmembrane helix of RseP, with Tyr356 in particular, and Trp25 of LsbB, as important for LsbB:RseP interaction (83, 91). In line with these experimental data, AlphaFold predicts interactions between Tyr356 of RseP and the N-terminal region of the bacteriocin, while the PWE (including Trp25) motif closely interacts with the PDZ domain of lactococcal RseP (Figure 5D). This highlights that Alphafold, in combination with experimental data, may be a valuable tool when assaying bacteriocin:receptor interactions.

While these observations are intriguing, it should be strongly emphasized that the structures of these complexes are highly speculative. Most residues of RseP in complex with EntK1 exhibited a high confidence score with AlphaFold-Multimer (pLDDT > 90), however residues of EntK1 were ranked poorly (pLDDT < 50). Confidence scores below 50 may indicate disorder, suggesting that EntK1 may be unstructured in physiological condition or only structured as part of a complex. Thus, these structural predictions should be interpreted with caution.

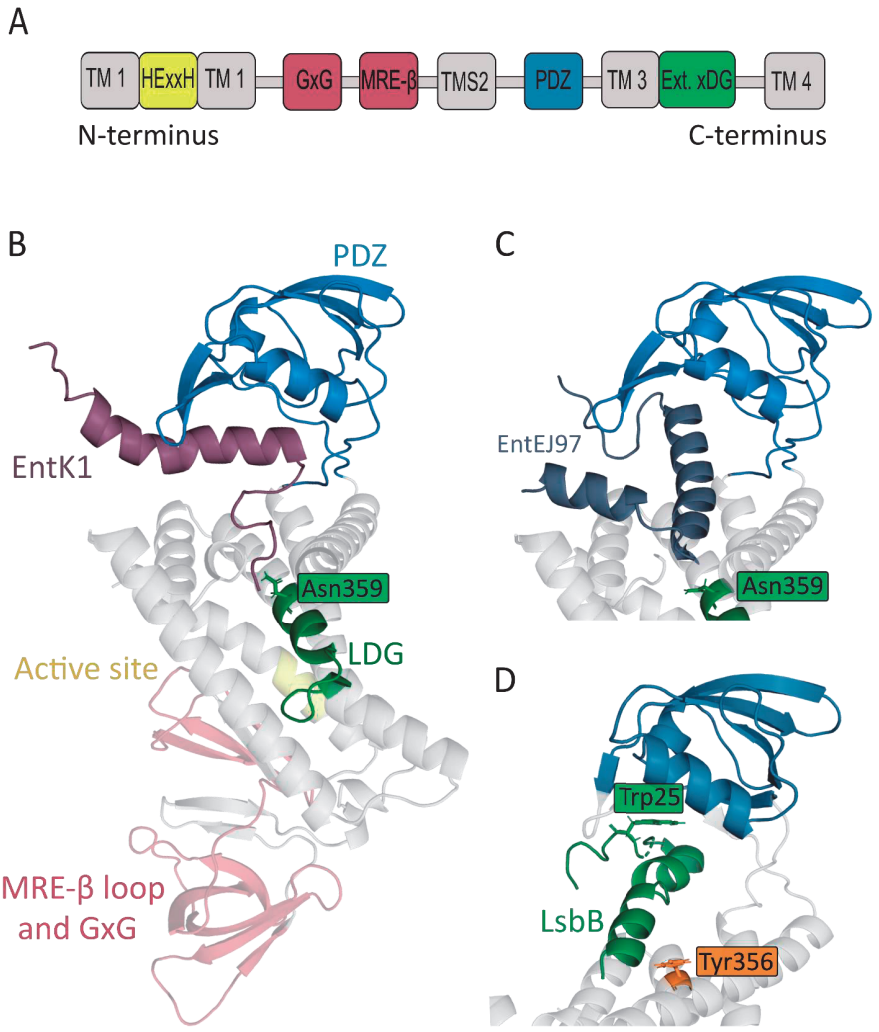

Figure 5 | Predicted structure of *Efm*RseP. A) Shematic overview of the conserved S2P-motifs found in *Efm*RseP. B) Predicted complex of *Efm*RseP:EntK1 with conserved S2P-motifs highlighted. The PDZ domain is indicated in blue, the extended LDG motif in green, the HExxH motif in yellow and the region encompassing the MREβ-loop and the GxG motif is indicated in red. C) Predicted complex of *Efm*RseP:EntEJ97. D) Predicted complex between RseP from *L. lactis* and LsbB. Tyr356 of the third transmembrane helix is indicated in orange. Amino acids experimentally determined as important for bacteriocin senstivity is highligthed in all panels. All structural prediction of complexes was performed using Alphafold Multimer.

Collectively, the experimental data presented in paper III demonstrates that interactions with the RseP PDZ domain and Asn359 are needed for the antimicrobial activity of EntK1. While the results from paper III provide valuable knowledge on the EntK1:RseP interaction, increased structural characterization of *Efm*RseP would likely contribute to our understanding of EntK1:RseP interaction and possibly also provide insight into the mode of action of these bacteriocins. Structural determination of *Efm*RseP alone or in complex with EntK1 may provide a powerful basis for guided construction for new and improved bacteriocins, and further contribute to establishing RseP as a drug target.

3.3 Structural characterization of RseP: Challenges and opportunities

Structural characterization can greatly impact the understanding of protein function as well as contribute to rational design of novel inhibitors. In the context of bacteriocins, structural characterization of pediocin-like bacteriocin in complex with man-PTS has contributed to an increased understanding of the mode of action and immunity of this class of bacteriocins (see section 1.1.1 and 1.1.3 for more details) (28, 76). Thus, structural characterization of RseP alone, or in complex with EntK1, may provide important insights into the mode of action of these bacteriocins, as well as provide a powerful basis for construction of novel bacteriocins.

Despite their evident role in multiple cellular processes, atomic structures of membrane proteins are greatly underrepresented in the Protein Data Bank (186, 187). Indeed, within the S2P family only three proteins have been structurally characterized: *Mj*S2P (PDB: 3B4R), *Kk*RseP (PDB: 7W6Y,7W6Z) and *Ec*RseP (PDB:7W6X) (104, 137). It should be noted that the *Mj*S2P structure only represent the core region of the protein (residues 1-224), as the full-length protein (residues 1-399) was found to be highly susceptible to degradation following purification (104). *Efm*RseP and *Ec*RseP/*Kk*RseP belong to the same S2P subgroup (Group I); however, while *Efm*RseP is predicted to contain a single PDZ-domain, *Kk*RseP and *Ec*RseP contain a PDZ-tandem (137). The results presented in Paper III indicated that the PDZ domain is the defining region of bacteriocin binding and sensitivity. Thus, if modeling the EntK1:RseP interaction based on a RseP structure with a PDZ tandem,

the potential interaction would likely be very different from the EntK1:RseP interaction responsible for the antimicrobial activity seen against VRE. Therefore, structural characterization of *Efm*RseP is still desirable to fully understand EntK1 binding and mode of action.

Several challenges hamper the structural characterization of membrane proteins, with obtaining sufficient amounts of pure and soluble protein being the first major bottleneck. *E. coli* is the most commonly used heterologous protein expression system (Paper IV; Figure 1). However, when expressed in *E. coli,* membrane proteins frequently (i) have a toxic effect on the host, (ii) have poor stability and (iii) form insoluble inclusion bodies (188, 189). Thus, development of an expression and purification protocol resulting in pure and stable RseP is a necessary milestone in the efforts of structural characterization of RseP.

Paper IV describes the use of the pSIP expression system and the Gram-positive *L. plantarum* as a novel platform for production and purification of RseP. Intracellular protein expression is well established in *L. plantarum* (32, 190-192), however; Paper IV is the first description of production and purification of a membrane protein using this platform. Initially, the protein production of five RseP orthologs where screened, with RseP from *E. faecium* exhibiting the highest expression levels (Paper IV; Figure 3A). Orthologue screening is a common approach for increasing protein production, as minor differences in length and/or the amino acid sequence may effect expression and solubility. Indeed, prior to resolving the *Mj*S2P structure, 40 bacterial and archaebacterial orthologs were screened (104), while Imaizumi and colleagues examined the production levels of 14 RseP orthologs prior to selecting RseP from *K. koreensis* as a promising candidate (137). Protein production levels of were further optimized in a small-scale expression screen, indicating 10 hours post-induction at 30 °C as the optimal expression conditions. To evaluate the folding and functionality of the purified proteins, the biological activity of the purified protein is commonly assessed. Indeed, previous studies on RseP orthologs have exploited the native substrate in cleavage-based assays to evaluate proper protein expression and folding (137, 163, 168). However, the substrate of *E. faecium* RseP is unknown, making cleavage-based assays challenging to establish. It should be noted that the proteolytic activity of IMP has also been assessed using non-native substrates. Indeed, the proteolytic activity of *Mj*S2P

was evaluated using the membrane associated protein CED-9 *in vitro* (104, 193). Thus, we attempted to evaluate the proteolytic activity of purified *Efm*RseP using fluorescently tagged casein. Casein is regarded as a general protease substrate, known to be degraded by several proteases (194). However, no proteolytic activity was detected following incubation of casein with purified *Efm*RseP (data not shown). Lipids are known to influence the activity of membrane proteins (195-197). For example, Subramani and colleagues observed a drastic reduction in activity of the magnesium transporter A during the course of purification, with more than 90 % loss in activity from the soluble membrane fraction to the final SEC fractions (195). Addition of lipid extract recovered activity of the enzyme, highlighting the effect of lipids on membrane protein activity. Similarly, the presence of specific lipids has been demonstrated to affect the activity of other IMP (198). So far, detection of proteolytic activity using the purified *Efm*RseP has only been attempted in the absence of lipids. Thus, it would be interesting to explore addition of lipids and/or the use of the soluble membrane fraction in future attempts to establish the proteolytic activity of *Efm*RseP.

To overcome the challenges of establishing an activity-based assay, the functionality and fold of the purified *Efm*RseP was evaluated in two ways. First, a simple spot-on-lawn assay was performed to determine the EntK1 sensitivity of *L. plantarum* expressing various *rseP* orthologs. *L. plantarum* is naturally resistant to EntK1, thus the observed increased sensitivity towards the bacteriocin indicated that the *rseP* ortholog is functionally expressed *in vivo* (Paper IV; Figure S1). A similar approach was also used in paper III to confirm proper expression of *rseP* in EntK1-resistant mutants. Secondly, the structural integrity of purified *Efm*RseP was confirmed using CD-analysis (Paper IV; Figure 5). Taken together, these results indicate that *Efm*RseP is functional when expressed and that the protein is properly folded when purified. Following the protocol outlined in paper IV, *Efm*RseP was purified by immobilized metal ion affinity chromatography followed by size-exclusion chromatography (Paper IV; Figure 3). The purification resulted in a final yield of approximately 1 mg per 3 gram of wet cell pellet of highly pure protein (Paper IV; Figure 4). Crystallization screens with *Efm*RseP purified from *L. plantarum* have been initiated, however, no crystal formation has been observed so far (data not shown). X-ray

crystallography has long been the gold standard for determining the three-dimensional structure of biological macromolecules (199). However, protein crystallization can be a challenging endeavor as (i) it requires substantial amounts of highly pure and concentrated protein and (ii) identification of crystal conditions normally require comprehensive screening (187, 199). Advances in structural biology have accelerated the number of structures determined for membrane proteins. In particular, cryo-EM has greatly impacted structural determination of membrane protein (200, 201). Most notably, cryo-EM does not require the formation of a crystal and generally requires less sample material than traditional crystallography-based methods. Cryo-EM was long considered to only result in low-resolution structures, however recent advances in detection and image processing now allow determination of 3D-structures at near-atomic resolution (200-203). Nevertheless, even with the increasing number of cryo-EM structures, transmembrane proteins remain heavily underrepresented in the Protein Data Bank.

The introduction of AlphaFold2 has revolutionized the field of structural biology (184). As discussed in section 3.2, AlphaFold is a protein prediction tool based on artificial intelligence that predicts protein structure with a greater accuracy than previously established in silico methods (184). Indeed, the predicted AlphaFold2 structure of *Mj*S2P and *Ec*RseP greatly resembles the experimentally determined structure (data not shown). While AlphaFold2 holds tremendous potential, the AI-based prediction tool has some limitations compared to experimentally determination of protein structures. First, several proteins function in complex with other proteins, nucleic acids, or ligands. While an extension of AlphaFold2, AlphaFold-Multimer (discussed section 3.2), allow protein-protein interaction predictions, AlphaFold2 does not currently support the prediction of protein:nucleic acid or protein:ligand interaction (185, 204). Secondly, while proteins are often dynamic, AlphaFold2 predicts only a single conformational state (204). Thus, AlphaFold does not capture the structural plasticity of proteins. Lastly, AlphaFold2 has been shown to be less successful in predicting peptides with flexible and/or unstructured regions (205). EntK1 has previously been shown to be disordered in aqueous environment when analyzed by NMR spectroscopy (37), which may account for the low confidence score observed for EntK1 in the predicted EntK1:*Efm*RseP complex (section 3.2)

4. Concluding remarks

Advances in the field of intramembrane proteases have increased our understanding of the role of S2P-mediated signaling in bacterial pathogenesis, raising the exciting possibility that S2P may serve as novel antimicrobial targets. Today, the members of the LsbB family are the only known antimicrobials specifically targeting S2P. While members of the LsbB family depend on interactions with the S2P RseP for their antimicrobial activity, little is known about how these bacteriocins recognize and interact with RseP, and how this interaction eventually results in cell death. The work presented in this thesis sheds light on the molecular mechanism underlying EntK1:RseP interaction and the construction of novel bacteriocins. Collectively, these results contribute to establish RseP as a antimicrobial target and highlighting the potential of EntK1 and EntK1-dervied bacteriocins as novel antimicrobial agents.

The results presented in paper I demonstrate that the LsbB family is amenable to engineering. The EntK1-derived bacteriocin H1 showed superior activity against *S. haemolyticus* and contributed to the complete eradication of biofilm formation for this human pathogen. These results not only provide evidence that the members of the LsbB family can be engineered to improve potency, but also describe a unique non-antibiotic bacteriocin-based combination for targeting a biofilm forming human pathogen.

The antimicrobial activity of EntK1 was revealed to depend on an interaction with the PDZ-domain and regions of the third transmembrane helix of *E. faecium* RseP. Most notably, Asn359 was found to be essential for the antimicrobial activity of EntK1, as a mutation of this residue abolished EntK1 sensitivity and binding. It is interesting to note that the region needed for the antimicrobial activity of EntK1 is found in the RseP homologs of several bacteria, including the prominent human pathogens discussed in paper I. Taken together with the ability of the members of the LsbB family to be engineered, it is tempting to speculate that these bacteriocins could be modified to target RseP homologs in additional human pathogens. However, such rational design of bacteriocins would depend on further structural characterization of RseP, with the ultimate goal being resolving the structure of a RseP:EntK1 complex. The established platform for the production and purification of RseP

lays the foundation for further structural and biochemical characterization of RseP. Data provided from such investigation, taken together with data presented in this thesis, will provide a powerful basis for rational design of novel bacteriocins and further contribute to develop bacteriocins for clinical applications.

5. References

1. Ventola CL. 2015. The antibiotic resistance crisis: part 1: causes and threats. PT 40:277-83.
2. Antimicrobial-Resistance-Collaborators. 2022. Global burden of bacterial antimicrobial resistance in 2019: a systematic analysis. Lancet 399:629-655.
3. Holmes AH, Moore LS, Sundsfjord A, Steinbakk M, Regmi S, Karkey A, Guerin PJ, Piddock LJ. 2016. Understanding the mechanisms and drivers of antimicrobial resistance. Lancet 387:176-87.
4. O'Neill J. 2016. Tackling drug-resistant infections globally: final report and recommendations. Government of the United Kingdom.
5. Van Boeckel TP, Brower C, Gilbert M, Grenfell BT, Levin SA, Robinson TP, Teillant A, Laxminarayan R. 2015. Global trends in antimicrobial use in food animals. Proc Natl Acad Sci U S A 112:5649-54.
6. Patel SJ, Wellington M, Shah RM, Ferreira MJ. 2020. Antibiotic Stewardship in Food-producing Animals: Challenges, Progress, and Opportunities. Clin Ther 42:1649-1658.
7. Ventola CL. 2015. The antibiotic resistance crisis: part 2: management strategies and new agents. PT 40:344-52.
8. Yim G, Thaker MN, Koteva K, Wright G. 2014. Glycopeptide antibiotic biosynthesis. J Antibiot 67:31-41.
9. Kumariya R, Garsa AK, Rajput YS, Sood SK, Akhtar N, Patel S. 2019. Bacteriocins: Classification, synthesis, mechanism of action and resistance development in food spoilage causing bacteria. Microb Pathog 128:171-177.
10. Cotter PD, Ross RP, Hill C. 2013. Bacteriocins - a viable alternative to antibiotics? Nat Rev Microbiol 11:95-105.
11. Soltani S, Hammami R, Cotter PD, Rebuffat S, Said LB, Gaudreau H, Bédard F, Biron E, Drider D, Fliss I. 2021. Bacteriocins as a new generation of antimicrobials: toxicity aspects and regulations. FEMS Microbiol Rev 45.
12. Rea MC, Sit CS, Clayton E, O'Connor PM, Whittal RM, Zheng J, Vederas JC, Ross RP, Hill C. 2010. Thuricin CD, a posttranslationally modified bacteriocin with a narrow spectrum of activity against *Clostridium difficile*. Proc Natl Acad Sci U S A 107:9352-7.
13. Tymoszewska A, Diep DB, Wirtek P, Aleksandrzak-Piekarczyk T. 2017. The non-lantibiotic bacteriocin garvicin Q targets man-PTS in a broad spectrum of sensitive bacterial genera. Sci Rep 7:8359.
14. Alvarez-Sieiro P, Montalbán-López M, Mu D, Kuipers OP. 2016. Bacteriocins of lactic acid bacteria: extending the family. Appl Microbiol Biotechnol 100:2939-51.
15. Azevedo AC, Bento CB, Ruiz JC, Queiroz MV, Mantovani HC. 2015. Distribution and genetic diversity of bacteriocin gene clusters in rumen microbial genomes. Appl Environ Microbiol 81:7290-304.
16. Arnison PG, Bibb MJ, Bierbaum G, Bowers AA, Bugni TS, Bulaj G, Camarero JA, Campopiano DJ, Challis GL, Clardy J, Cotter PD, Craik DJ, Dawson M, Dittmann E, Donadio S, Dorrestein PC, Entian KD, Fischbach MA, Garavelli JS, Göransson U,

Gruber CW, Haft DH, Hemscheidt TK, Hertweck C, Hill C, Horswill AR, Jaspars M, Kelly WL, Klinman JP, Kuipers OP, Link AJ, Liu W, Marahiel MA, Mitchell DA, Moll GN, Moore BS, Müller R, Nair SK, Nes IF, Norris GE, Olivera BM, Onaka H, Patchett ML, Piel J, Reaney MJ, Rebuffat S, Ross RP, Sahl HG, Schmidt EW, Selsted ME, et al. 2013. Ribosomally synthesized and post-translationally modified peptide natural products: overview and recommendations for a universal nomenclature. Nat Prod Rep 30:108-60.

17. Fimland G, Johnsen L, Dalhus B, Nissen-Meyer J. 2005. Pediocin-like antimicrobial peptides (class IIa bacteriocins) and their immunity proteins: biosynthesis, structure, and mode of action. J Pept Sci 11:688-96.
18. Nissen-Meyer J, Oppegård C, Rogne P, Haugen HS, Kristiansen PE. 2010. Structure and mode-of-action of the two-peptide (Class-IIb) bacteriocins. Probiotics Antimicrob Proteins 2:52-60.
19. Perez RH, Zendo T, Sonomoto K. 2018. Circular and leaderless bacteriocins: biosynthesis, mode of action, applications, and prospects. Front Microbiol 9:2085.
20. Nes IF, Diep DB, Håvarstein LS, Brurberg MB, Eijsink V, Holo H. 1996. Biosynthesis of bacteriocins in lactic acid bacteria. Antonie Van Leeuwenhoek 70:113-28.
21. Håvarstein LS, Diep DB, Nes IF. 1995. A family of bacteriocin ABC transporters carry out proteolytic processing of their substrates concomitant with export. Mol Microbiol 16:229-240.
22. Cintas LM, Casaus P, Håvarstein LS, Hernandez PE, Nes IF. 1997. Biochemical and genetic characterization of enterocin P, a novel sec-dependent bacteriocin from *Enterococcus faecium* P13 with a broad antimicrobial spectrum. Appl Environ Microbiol 63:4321-4330.
23. Plat A, Kluskens LD, Kuipers A, Rink R, Moll GN. 2011. Requirements of the engineered leader peptide of nisin for inducing modification, export, and cleavage. Appl Environ Microbiol 77:604-11.
24. Thibodeaux CJ, Wagoner J, Yu Y, van der Donk WA. 2016. Leader peptide establishes dehydration order, promotes efficiency, and ensures fidelity during lacticin 481 biosynthesis. J Am Chem Soc 138:6436-44.
25. Gajic O, Buist G, Kojic M, Topisirovic L, Kuipers OP, Kok J. 2003. Novel mechanism of bacteriocin secretion and immunity carried out by lactococcal multidrug resistance proteins. J Biol Chem 278:34291-8.
26. Sánchez-Hidalgo M, Maqueda M, Gálvez A, Abriouel H, Valdivia E, Martínez-Bueno M. 2003. The genes coding for enterocin EJ97 production by *Enterococcus faecalis* EJ97 are located on a conjugative plasmid. Appl Environ Microbiol 69:1633-41.
27. Stein T, Heinzmann S, Solovieva I, Entian KD. 2003. Function of *Lactococcus lactis* nisin immunity genes *nisI* and *nisFEG* after coordinated expression in the surrogate host *Bacillus subtilis*. J Biol Chem 278:89-94.
28. Zhu L, Zeng J, Wang J. 2022. Structural basis of the immunity mechanisms of pediocin-like bacteriocins. Appl Environ Microbiol 88:e0048122.
29. Diep DB, Skaugen M, Salehian Z, Holo H, Nes IF. 2007. Common mechanisms of target cell recognition and immunity for class II bacteriocins. Proc Natl Acad Sci U S A 104:2384-9.
30. Mierau I, Kleerebezem M. 2005. 10 years of the nisin-controlled gene expression system (NICE) in *Lactococcus lactis*. Appl Microbiol Biotechnol 68:705-17.

31. Sørvik E, Grõnqvist S, Naterstad K, Mathiesen G, Eijsink VGH, Axelsson L. 2003. Construction of vectors for inducible gene expression in *Lactobacillus sakei* and *L. plantarum*. FEMS Microbiol Lett 229:119-126.
32. Mathiesen G, Axelsson L, Eijsink VGH. 2022. Heterologous Protein Production in *Lactobacillus (plantarum)* Using pSIP Vectors. Methods Mol Biol 2406:205-217.
33. Sørvig E, Mathiesen G, Naterstad K, Eijsink VGH, Axelsson L. 2005. High-level, inducible gene expression in *Lactobacillus sakei* and *Lactobacillus plantarum* using versatile expression vectors. Microbiology (Reading) 151:2439-2449.
34. Kleerebezem M, Beerthuyzen MM, Vaughan EE, de Vos WM, Kuipers OP. 1997. Controlled gene expression systems for lactic acid bacteria: transferable nisin-inducible expression cassettes for *Lactococcus, Leuconostoc,* and *Lactobacillus s*pp. Appl Environ Microbiol 63:4581-4.
35. Ibarra-Sánchez LA, El-Haddad N, Mahmoud D, Miller MJ, Karam L. 2020. Invited review: Advances in nisin use for preservation of dairy products. J Dairy Sci 103:2041-2052.
36. Reinseth I, Tønnesen HH, Carlsen H, Diep DB. 2021. Exploring the Therapeutic Potenital of the Leaderless Enterocins K1 and EJ97 in the Treatment of Vancomycin-Resistant Enterococcal Infection. Front Microbiol 12:248.
37. Ovchinnikov KV, Kristiansen PE, Straume D, Jensen MS, Aleksandrzak-Piekarczyk T, Nes IF, Diep DB. 2017. The Leaderless Bacteriocin Enterocin K1 Is Highly Potent against *Enterococcus faecium*: A Study on Structure, Target Spectrum and Receptor. Front Microbiol 8:774.
38. Ovchinnikov KV, Kranjec C, Thorstensen T, Carlsen H, Diep DB. 2020. Successful development of bacteriocins into therapeutic formulation for treatment of MRSA skin infection in a murine model. Antimicrob Agents Chemother 64:e00829-20.
39. Piper C, Draper LA, Cotter PD, Ross RP, Hill C. 2009. A comparison of the activities of lacticin 3147 and nisin against drug-resistant *Staphylococcus aureus* and *Enterococcus* species. J Antimicrob Chemother 64:546-51.
40. Kranjec C, Ovchinnikov KV, Grønseth T, Ebineshan K, Srikantam A, Diep DB. 2020. A bacteriocin-based antimicrobial formulation to effectively disrupt the cell viability of methicillin-resistant *Staphylococcus aureus* (MRSA) biofilms. npj Biofilms and Microbiomes 6:58.
41. Trzasko A, Leeds JA, Praestgaard J, Lamarche MJ, McKenney D. 2012. Efficacy of LFF571 in a hamster model of *Clostridium difficile* infection. Antimicrob Agents Chemother 56:4459-62.
42. Liu S, Deng S, Liu H, Tang L, Wang M, Xin B, Li F. 2022. Four novel leaderless bacteriocins, bacin A1, A2, A3, and A4 exhibit potent antimicrobial and antibiofilm activities against methicillin-resistant *Staphylococcus aureus*. Microbiol Spectr 10:e0094522.
43. Brumfitt W, Salton MR, Hamilton-Miller JM. 2002. Nisin, alone and combined with peptidoglycan-modulating antibiotics: activity against methicillin-resistant *Staphylococcus aureus* and vancomycin-resistant enterococci. J Antimicrob Chemother 50:731-4.
44. Ovchinnikov KV, Kranjec C, Telke A, Kjos M, Thorstensen T, Scherer S, Carlsen H, Diep DB. 2021. A strong synergy between the thiopeptide bacteriocin micrococcin

P1 and rifampicin qgainst MRSA in a murine skin infection model. Front Immunol 12:676534.
45. Salvucci E, Hebert EM, Sesma F, Saavedra L. 2010. Combined effect of synthetic enterocin CRL35 with cell wall, membrane-acting antibiotics and muranolytic enzymes against *Listeria* cells. Lett Appl Microbiol 51:191-5.
46. Draper LA, Cotter PD, Hill C, Ross RP. 2013. The two peptide lantibiotic lacticin 3147 acts synergistically with polymyxin to inhibit Gram negative bacteria. BMC Microbiol 13:212.
47. Mathur H, Field D, Rea MC, Cotter PD, Hill C, Ross RP. 2017. Bacteriocin-antimicrobial synergy: A medical and food perspective. Front Microbiol 8:1205.
48. Hetz C, Bono MR, Barros LF, Lagos R. 2002. Microcin E492, a channel-forming bacteriocin from *Klebsiella pneumoniae*, induces apoptosis in some human cell lines. Proc Natl Acad Sci U S A 99:2696-701.
49. Rea MC, Dobson A, O'Sullivan O, Crispie F, Fouhy F, Cotter PD, Shanahan F, Kiely B, Hill C, Ross RP. 2011. Effect of broad- and narrow-spectrum antimicrobials on *Clostridium difficile* and microbial diversity in a model of the distal colon. Proc Natl Acad Sci U S A 108 Suppl 1:4639-44.
50. Dabour N, Zihler A, Kheadr E, Lacroix C, Fliss I. 2009. *In vivo* study on the effectiveness of pediocin PA-1 and *Pediococcus acidilactici* UL5 at inhibiting *Listeria monocytogenes*. Int J Food Microbiol 133:225-33.
51. Arnusch CJ, Bonvin AM, Verel AM, Jansen WT, Liskamp RM, de Kruijff B, Pieters RJ, Breukink E. 2008. The vancomycin-nisin(1-12) hybrid restores activity against vancomycin resistant Enterococci. Biochemistry 47:12661-3.
52. Field D, Begley M, O'Connor PM, Daly KM, Hugenholtz F, Cotter PD, Hill C, Ross RP. 2012. Bioengineered nisin A derivatives with enhanced activity against both Gram positive and Gram negative pathogens. PLoS One 7:e46884.
53. Fimland G, Johnsen L, Axelsson L, Brurberg MB, Nes IF, Eijsink VG, Nissen-Meyer J. 2000. A C-terminal disulfide bridge in pediocin-like bacteriocins renders bacteriocin activity less temperature dependent and is a major determinant of the antimicrobial spectrum. J Bacteriol 182:2643-8.
54. O'Shea EF, O'Connor PM, Cotter PD, Ross RP, Hill C. 2010. Synthesis of trypsin-resistant variants of the *Listeria*-active bacteriocin salivaricin P. Appl Environ Microbiol 76:5356-62.
55. Fields FR, Carothers KE, Balsara RD, Ploplis VA, Castellino FJ, Lee SW. 2018. Rational design of syn-safencin, a novel linear antimicrobial peptide derived from the circular bacteriocin safencin AS-48. J Antibiot 71:592-600.
56. Fields FR, Manzo G, Hind CK, Janardhanan J, Foik IP, Carmo Silva PD, Balsara RD, Clifford M, Vu HM, Ross JN, Kalwajtys VR, Gonzalez AJ, Bui TT, Ploplis VA, Castellino FJ, Siryaporn A, Chang M, Sutton JM, Mason AJ, Lee S. 2020. Synthetic Antimicrobial Peptide Tuning Permits Membrane Disruption and Interpeptide Synergy. ACS Pharmacol Transl Sci 3:418-424.
57. Uzelac G, Kojic M, Lozo J, Aleksandrzak-Piekarczyk T, Gabrielsen C, Kristensen T, Nes IF, Diep DB, Topisirovic L. 2013. A Zn-dependent metallopeptidase is responsible for sensitivity to LsbB, a class II leaderless bacteriocin of *Lactococcus lactis* subsp. lactis BGMN1-5. J Bacteriol 195:5614-21.

58. Cotter PD. 2014. An 'Upp'-turn in bacteriocin receptor identification. Mol Microbiol 92:1159-63.
59. Parks WM, Bottrill AR, Pierrat OA, Durrant MC, Maxwell A. 2007. The action of the bacterial toxin, microcin B17, on DNA gyrase. Biochimie 89:500-7.
60. Braffman NR, Piscotta FJ, Hauver J, Campbell EA, Link AJ, Darst SA. 2019. Structural mechanism of transcription inhibition by lasso peptides microcin J25 and capistruin. Proc Natl Acad Sci U S A 116:1273-1278.
61. Breukink E, de Kruijff B. 2006. Lipid II as a target for antibiotics. Nat Rev Drug Discov 5:321-32.
62. Bakhtiary A, Cochrane SA, Mercier P, McKay RT, Miskolzie M, Sit CS, Vederas JC. 2017. Insights into the mechanism of action of the two-peptide lantibiotic lacticin 3147. J Am Chem Soc 139:17803-17810.
63. Wiedemann I, Böttiger T, Bonelli RR, Schneider T, Sahl HG, Martínez B. 2006. Lipid II-based antimicrobial activity of the lantibiotic plantaricin C. Appl Environ Microbiol 72:2809-14.
64. Breukink E, Wiedemann I, van Kraaij C, Kuipers OP, Sahl HG, de Kruijff B. 1999. Use of the cell wall precursor lipid II by a pore-forming peptide antibiotic. Science 286:2361-4.
65. Hsu ST, Breukink E, Tischenko E, Lutters MA, de Kruijff B, Kaptein R, Bonvin AM, van Nuland NA. 2004. The nisin-lipid II complex reveals a pyrophosphate cage that provides a blueprint for novel antibiotics. Nat Struct Mol Biol 11:963-7.
66. Wiedemann I, Breukink E, van Kraaij C, Kuipers OP, Bierbaum G, de Kruijff B, Sahl HG. 2001. Specific binding of nisin to the peptidoglycan precursor lipid II combines pore formation and inhibition of cell wall biosynthesis for potent antibiotic activity. J Biol Chem 276:1772-9.
67. Sheldrick GM, Jones PG, Kennard O, Williams DH, Smith GA. 1978. Structure of vancomycin and its complex with acetyl-D-alanyl-D-alanine. Nature 271:223-5.
68. Nitanai Y, Kikuchi T, Kakoi K, Hanamaki S, Fujisawa I, Aoki K. 2009. Crystal structures of the complexes between vancomycin and cell-wall precursor analogs. J Mol Biol 385:1422-32.
69. Oftedal TF, Ovchinnikov KV, Hestad KA, Goldbeck O, Porcellato D, Narvhus J, Riedel CU, Kjos M, Diep DB. 2021. Ubericin K, a new pore-forming bacteriocin targeting mannose-PTS. Microbiol Spectr 9:e0029921.
70. Tymoszewska A, Walczak P, Aleksandrzak-Piekarczyk T. 2020. BacSJ-another bacteriocin with distinct spectrum of activity that targets man-PTS. Int J Mol Sci 21.
71. Kjos M, Nes IF, Diep DB. 2009. Class II one-peptide bacteriocins target a phylogenetically defined subgroup of mannose phosphotransferase systems on sensitive cells. Microbiology (Reading) 155:2949-2961.
72. Tymoszewska A, Diep DB, Aleksandrzak-Piekarczyk TJSr. 2018. The extracellular loop of Man-PTS subunit IID is responsible for the sensitivity of Lactococcus garvieae to garvicins A, B and C. 8:15790.
73. Jeckelmann JM, Erni B. 2020. The mannose phosphotransferase system (Man-PTS) - Mannose transporter and receptor for bacteriocins and bacteriophages. Biochim Biophys Acta Biomembr 1862:183412.

74. Bieler S, Silva F, Soto C, Belin D. 2006. Bactericidal activity of both secreted and nonsecreted microcin E492 requires the mannose permease. J Bacteriol 188:7049-61.
75. Kjos M, Salehian Z, Nes IF, Diep DB. 2010. An extracellular loop of the mannose phosphotransferase system component IIC is responsible for specific targeting by class IIa bacteriocins. J Bacteriol 192:5906-13.
76. Zhu L, Zeng J, Wang C, Wang J. 2022. Structural basis of pore formation in the mannose phosphotransferase system by pediocin PA-1. Appl Environ Microbiol 88:e0199221.
77. Huang K, Zeng J, Liu X, Jiang T, Wang J. 2021. Structure of the mannose phosphotransferase system (man-PTS) complexed with microcin E492, a pore-forming bacteriocin. Cell Discov 7:20.
78. Swe PM, Cook GM, Tagg JR, Jack RW. 2009. Mode of action of dysgalacticin: a large heat-labile bacteriocin. J Antimicrob Chemother 63:679-686.
79. Campelo AB, Gaspar P, Roces C, Rodríguez A, Kok J, Kuipers OP, Neves AR, Martínez B. 2011. The Lcn972 bacteriocin-encoding plasmid pBL1 impairs cellobiose metabolism in *Lactococcus lactis*. Appl Environ Microbiol 77:7576-85.
80. Biswas S, Wu C, van der Donk WA. 2021. The antimicrobial activity of the glycocin sublancin is dependent on an active phosphoenolpyruvate-sugar phosphotransferase system. ACS Infect Dis 7:2402-2412.
81. Garcia De Gonzalo CV, Denham EL, Mars RA, Stülke J, van der Donk WA, van Dijl JM. 2015. The phosphoenolpyruvate:sugar phosphotransferase system is involved in sensitivity to the glucosylated bacteriocin sublancin. Antimicrob Agents Chemother 59:6844-54.
82. Kjos M, Oppegård C, Diep DB, Nes IF, Veening JW, Nissen-Meyer J, Kristensen T. 2014. Sensitivity to the two-peptide bacteriocin lactococcin G is dependent on UppP, an enzyme involved in cell-wall synthesis. Mol Microbiol 92:1177-87.
83. Miljkovic M, Uzelac G, Mirkovic N, Devescovi G, Diep DB, Venturi V, Kojic M. 2016. LsbB bacteriocin interacts with the third transmembrane domain of the YvjB receptor. Appl Environ Microbiol 82:5364-5374.
84. Gabrielsen C, Brede DA, Hernández PE, Nes IF, Diep DB. 2012. The maltose ABC transporter in *Lactococcus lactis* facilitates high-level sensitivity to the circular bacteriocin garvicin ML. Antimicrob Agents Chemother 56:2908-15.
85. Oppegård C, Kjos M, Veening JW, Nissen-Meyer J, Kristensen T. 2016. A putative amino acid transporter determines sensitivity to the two-peptide bacteriocin plantaricin JK. Microbiologyopen 5:700-8.
86. Ekblad B, Nissen-Meyer J, Kristensen T. 2017. Whole-genome sequencing of mutants with increased resistance against the two-peptide bacteriocin plantaricin JK reveals a putative receptor and potential docking site. PLoS One 12:e0185279.
87. Heeney DD, Yarov-Yarovoy V, Marco ML. 2019. Sensitivity to the two peptide bacteriocin plantaricin EF is dependent on CorC, a membrane-bound, magnesium/cobalt efflux protein. Microbiologyopen 8:e827.
88. Gérard F, Pradel N, Wu LF. 2005. Bactericidal activity of colicin V is mediated by an inner membrane protein, SdaC, of *Escherichia coli*. J Bacteriol 187:1945-50.
89. Kjos M, Nes IF, Diep DB. 2011. Mechanisms of resistance to bacteriocins targeting the mannose phosphotransferase system. Appl Environ Microbiol 77:3335-42.

90. Opsata M, Nes IF, Holo H. 2010. Class IIa bacteriocin resistance in *Enterococcus faecalis* V583: the mannose PTS operon mediates global transcriptional responses. BMC Microbiol 10:224.
91. Ovchinnikov KV, Kristiansen PE, Uzelac G, Topisirovic L, Kojic M, Nissen-Meyer J, Nes IF, Diep DB. 2014. Defining the structure and receptor binding domain of the leaderless bacteriocin LsbB. J Biol Chem 289:23838-45.
92. Gálvez A, Valdivia E, Abriouel H, Camafeita E, Mendez E, Martínez-Bueno M, Maqueda M. 1998. Isolation and characterization of enterocin EJ97, a bacteriocin produced by *Enterococcus faecalis* EJ97. Archives of Microbiology 171:59-65.
93. Cintas LM, Casaus P, Herranz C, Håvarstein LS, Holo H, Hernández PE, Nes IF. 2000. Biochemical and genetic evidence that *Enterococcus faecium* L50 produces enterocins L50A and L50B, thesec-dependent enterocin P, and a novel bacteriocin secreted without an N-terminal extension termed enterocin Q. J Bacteriol 182:6806-6814.
94. Arias CA, Murray B. 2012. The rise of the Enterococcus: beyond vancomycin resistance. Nat Rev Microbiol 10:266.
95. Cattoir V, Leclercq R. 2013. Twenty-five years of shared life with vancomycin-resistant enterococci: is it time to divorce? J Antimicrob Chemother 68:731-42.
96. Varahan S, Iyer VS, Moore WT, Hancock LE. 2013. Eep confers lysozyme resistance to *Enterococcus faecalis* via the activation of the extracytoplasmic function sigma factor SigV. J Biol Chem 195:3125-3134.
97. Benachour A, Muller C, Dabrowski-Coton M, Le Breton Y, Giard JC, Rincé A, Auffray Y, Hartke A. 2005. The *Enterococcus faecalis* sigV protein is an extracytoplasmic function sigma factor contributing to survival following heat, acid, and ethanol treatments. J Bacteriol 187:1022-35.
98. Sun L, Li X, Shi Y. 2016. Structural biology of intramembrane proteases: mechanistic insights from rhomboid and S2P to γ-secretase. Curr Opin Struct Biol 37:97-107.
99. Urban S. 2009. Making the cut: central roles of intramembrane proteolysis in pathogenic microorganisms. Nat Rev Microbiol 7:411-23.
100. Wolfe MS, Kopan R. 2004. Intramembrane proteolysis: theme and variations. Science 305:1119-1123.
101. Beard HA, Barniol-Xicota M, Yang J, Verhelst SHL. 2019. Discovery of cellular roles of intramembrane proteases. ACS chemical biology 14:2372-2388.
102. Wolfe MS. 2009. Intramembrane proteolysis. Chemical reviews 109:1599-1612.
103. Chen G, Zhang X. 2010. New insights into S2P signaling cascades: regulation, variation, and conservation. Protein Science 19:2015-2030.
104. Feng L, Yan H, Wu Z, Yan N, Wang Z, Jeffrey PD, Shi Y. 2007. Structure of a site-2 protease family intramembrane metalloprotease. Science 318:1608-1612.
105. Manolaridis I, Kulkarni K, Dodd RB, Ogasawara S, Zhang Z, Bineva G, Reilly NO, Hanrahan SJ, Thompson AJ, Cronin N, Iwata S, Barford D. 2013. Mechanism of farnesylated CAAX protein processing by the intramembrane protease Rce1. Nature 504:301-5.
106. Wu Z, Yan N, Feng L, Oberstein A, Yan H, Baker RP, Gu L, Jeffrey PD, Urban S, Shi Y. 2006. Structural analysis of a rhomboid family intramembrane protease reveals a gating mechanism for substrate entry. Nat Struct Mol Biol 13:1084-91.

107. Bai X-c, Yan C, Yang G, Lu P, Ma D, Sun L, Zhou R, Scheres SH, Shi Y. 2015. An atomic structure of human γ-secretase. Nature 525:212-217.
108. Li X, Dang S, Yan C, Gong X, Wang J, Shi Y. 2013. Structure of a presenilin family intramembrane aspartate protease. Nature 493:56-61.
109. McCarthy AJ, Coleman-Vaughan C, McCarthy JV. 2017. Regulated intramembrane proteolysis: emergent role in cell signalling pathways. Biochem Soc Trans 45:1185-1202.
110. Rawson RB, Zelenski NG, Nijhawan D, Ye J, Sakai J, Hasan MT, Chang TY, Brown MS, Goldstein JL. 1997. Complementation cloning of S2P, a gene encoding a putative metalloprotease required for intramembrane cleavage of SREBPs. Mol Cell 1:47-57.
111. Sakai J, Duncan EA, Rawson RB, Hua X, Brown MS, Goldstein JL. 1996. Sterol-regulated release of SREBP-2 from cell membranes requires two sequential cleavages, one within a transmembrane segment. Cell 85:1037-46.
112. Brown MS, Ye J, Rawson RB, Goldstein JL. 2000. Regulated intramembrane proteolysis: a control mechanism conserved from bacteria to humans. Cell 100:391-398.
113. Sakai J, Rawson RB, Espenshade PJ, Cheng D, Seegmiller AC, Goldstein JL, Brown MS. 1998. Molecular identification of the sterol-regulated luminal protease that cleaves SREBPs and controls lipid composition of animal cells. Mol Cell 2:505-14.
114. Rawson RB. 2003. The SREBP pathway--insights from Insigs and insects. Nat Rev Mol Cell Biol 4:631-40.
115. Nohturfft A, DeBose-Boyd RA, Scheek S, Goldstein JL, Brown MS. 1999. Sterols regulate cycling of SREBP cleavage-activating protein (SCAP) between endoplasmic reticulum and Golgi. Proc Natl Acad Sci U S A 96:11235-40.
116. Espenshade PJ, Li WP, Yabe D. 2002. Sterols block binding of COPII proteins to SCAP, thereby controlling SCAP sorting in ER. Proc Natl Acad Sci U S A 99:11694-9.
117. Yang T, Espenshade PJ, Wright ME, Yabe D, Gong Y, Aebersold R, Goldstein JL, Brown MS. 2002. Crucial step in cholesterol homeostasis: sterols promote binding of SCAP to INSIG-1, a membrane protein that facilitates retention of SREBPs in ER. Cell 110:489-500.
118. Yabe D, Brown MS, Goldstein JL. 2002. Insig-2, a second endoplasmic reticulum protein that binds SCAP and blocks export of sterol regulatory element-binding proteins. Proc Natl Acad Sci U S A 99:12753-8.
119. Lindert U, Cabral WA, Ausavarat S, Tongkobpetch S, Ludin K, Barnes AM, Yeetong P, Weis M, Krabichler B, Srichomthong C. 2016. *MBTPS2* mutations cause defective regulated intramembrane proteolysis in X-linked osteogenesis imperfecta. Nat Commun 7:1-12.
120. Caengprasath N, Theerapanon T, Porntaveetus T, Shotelersuk V. 2021. MBTPS2, a membrane bound protease, underlying several distinct skin and bone disorders. J Transl Med 19:114.
121. Yu YT, Kroos L. 2000. Evidence that SpoIVFB is a novel type of membrane metalloprotease governing intercompartmental communication during *Bacillus subtilis* sporulation. J Bacteriol 182:3305-3309.
122. Rudner DZ, Fawcett P, Losick R. 1999. A family of membrane-embedded metalloproteases involved in regulated proteolysis of membrane-associated transcription factors. Proc Natl Acad Sci U S A 96:14765-14770.

123. Kanehara K, Akiyama Y, Ito K. 2001. Characterization of the *yaeL* gene product and its S2P-protease motifs in *Escherichia coli*. Gene 281:71-79.
124. Schneider JS, Glickman MS. 2013. Function of site-2 proteases in bacteria and bacterial pathogens. Biochimi Biophys Acta 1828:2808-2814.
125. Draper RC, Martin LW, Beare PA, Lamont IL. 2011. Differential proteolysis of sigma regulators controls cell-surface signalling in *Pseudomonas aeruginosa*. Mol Microbiol 82:1444-1453.
126. Bastiaansen KC, Ibañez A, Ramos JL, Bitter W, Llamas MA. 2014. The Prc and RseP proteases control bacterial cell-surface signalling activity. Environ Microbiol 16:2433-2443.
127. Otero-Asman JR, García-García AI, Civantos C, Quesada JM, Llamas MA. 2019. *Pseudomonas aeruginosa* possesses three distinct systems for sensing and using the host molecule haem. Environ Microbiol 21:4629-4647.
128. Alba BM, Leeds JA, Onufryk C, Lu CZ, Gross CA. 2002. DegS and YaeL participate sequentially in the cleavage of RseA to activate the sigma(E)-dependent extracytoplasmic stress response. Genes Dev 16:2156-68.
129. Chen JC, Hottes AK, McAdams HH, McGrath PT, Viollier PH, Shapiro L. 2006. Cytokinesis signals truncation of the PodJ polarity factor by a cell cycle-regulated protease. EMBO J 25:377-386.
130. Chen JC, Viollier PH, Shapiro L. 2005. A membrane metalloprotease participates in the sequential degradation of a *Caulobacter* polarity determinant. Mol Microbiol 55:1085-103.
131. Campo N, Rudner DZ. 2006. A branched pathway governing the activation of a developmental transcription factor by regulated intramembrane proteolysis. Mol Cell 23:25-35.
132. Makinoshima H, Glickman MS. 2005. Regulation of *Mycobacterium tuberculosis* cell envelope composition and virulence by intramembrane proteolysis. Nature 436:406-409.
133. Teoh WP, Matson JS, DiRita VJ. 2015. Regulated intramembrane proteolysis of the virulence activator TcpP in *Vibrio cholerae* is initiated by the tail-specific protease (Tsp). Mol Microbiol 97:822-31.
134. Matson JS, DiRita VJ. 2005. Degradation of the membrane-localized virulence activator TcpP by the YaeL protease in *Vibrio cholerae*. Proc Natl Acad Sci U S A 102:16403-16408.
135. Makinoshima H, Glickman MS. 2006. Site-2 proteases in prokaryotes: regulated intramembrane proteolysis expands to microbial pathogenesis. Microbes and infection 8:1882-1888.
136. Kinch LN, Ginalski K, Grishin NV. 2006. Site-2 protease regulated intramembrane proteolysis: sequence homologs suggest an ancient signaling cascade. Protein Sci 15:84-93.
137. Imaizumi Y, Takanuki K, Miyake T, Takemoto M, Hirata K, Hirose M, Oi R, Kobayashi T, Miyoshi K, Aruga R. 2022. Mechanistic insights into intramembrane proteolysis by *E. coli* site-2 protease homolog RseP. Sci Adv 34.
138. Lewis AP, Thomas PJ. 1999. A novel clan of zinc metallopeptidases with possible intramembrane cleavage properties. Protein Sci 8:439-42.

139. Koide K, Maegawa S, Ito K, Akiyama Y. 2007. Environment of the active site region of RseP, an *Escherichia coli* regulated intramembrane proteolysis protease, assessed by site-directed cysteine alkylation. J Biol Chem 282:4553-4560.
140. Saito A, Hizukuri Y, Matsuo E-i, Chiba S, Mori H, Nishimura O, Ito K, Akiyama Y. 2011. Post-liberation cleavage of signal peptides is catalyzed by the site-2 protease (S2P) in bacteria. Proc Natl Acad Sci U S A 108:13740-13745.
141. Kanehara K, Ito K, Akiyama Y. 2002. YaeL (EcfE) activates the sigma(E) pathway of stress response through a site-2 cleavage of anti-sigma(E), RseA. Genes Dev 16:2147-55.
142. De Las Peñas A, Connolly L, Gross CA. 1997. The sigmaE-mediated response to extracytoplasmic stress in *Escherichia coli* is transduced by RseA and RseB, two negative regulators of sigmaE. Mol Microbiol 24:373-85.
143. Missiakas D, Mayer MP, Lemaire M, Georgopoulos C, Raina S. 1997. Modulation of the *Escherichia coli* sigmaE (RpoE) heat-shock transcription-factor activity by the RseA, RseB and RseC proteins. Mol Microbiol 24:355-71.
144. Walsh NP, Alba BM, Bose B, Gross CA, Sauer RT. 2003. OMP peptide signals initiate the envelope-stress response by activating DegS protease via relief of inhibition mediated by its PDZ domain. Cell 113:61-71.
145. Ades SE, Connolly LE, Alba BM, Gross CA. 1999. The *Escherichia coli* sigma(E)-dependent extracytoplasmic stress response is controlled by the regulated proteolysis of an anti-sigma factor. Genes Dev 13:2449-61.
146. Akiyama Y, Kanehara K, Ito K. 2004. RseP (YaeL), an *Escherichia coli* RIP protease, cleaves transmembrane sequences. EMBO J 23:4434-42.
147. Flynn JM, Levchenko I, Sauer RT, Baker TA. 2004. Modulating substrate choice: the SspB adaptor delivers a regulator of the extracytoplasmic-stress response to the AAA+ protease ClpXP for degradation. Genes Dev 18:2292-2301.
148. Schöbel S, Zellmeier S, Schumann W, Wiegert T. 2004. The *Bacillus subtilis* simaW anti-sigma factor RsiW is degraded by intramembrane proteolysis through YluC. Mol Microbiol 52:1091-1105.
149. Heinrich J, Wiegert T. 2006. YpdC determines site-1 degradation in regulated intramembrane proteolysis of the RsiW anti-sigma factor of *Bacillus subtilis*. Mol Microbiol 62:566-79.
150. Ellermeier CD, Losick R. 2006. Evidence for a novel protease governing regulated intramembrane proteolysis and resistance to antimicrobial peptides in *Bacillus subtilis*. Genes Dev 20:1911-1922.
151. Damron FH, Hongwei DY. 2011. Pseudomonas aeruginosa MucD regulates the alginate pathway through activation of MucA degradation via MucP proteolytic activity. Journal of bacteriology 193:286-291.
152. Li X, Wang B, Feng L, Kang H, Qi Y, Wang J, Shi Y. 2009. Cleavage of RseA by RseP requires a carboxyl-terminal hydrophobic amino acid following DegS cleavage. Proc Natl Acad Sci U S A 106:14837-14842.
153. Cezairliyan BO, Sauer RT. 2007. Inhibition of regulated proteolysis by RseB. Proc Natl Acad Sci U S A 104:3771-3776.
154. Kim DY, Kwon E, Choi J, Hwang HY, Kim KK. 2010. Structural basis for the negative regulation of bacterial stress response by RseB. Protein Sci 19:1258-63.

155. Chaba R, Alba BM, Guo MS, Sohn J, Ahuja N, Sauer RT, Gross CA. 2011. Signal integration by DegS and RseB governs the σ E-mediated envelope stress response in *Escherichia coli*. Proc Natl Acad Sci U S A 108:2106-2111.
156. Wollmann P, Zeth K. 2007. The structure of RseB: a sensor in periplasmic stress response of *E. coli*. J Mol Biol 372:927-941.
157. Lima S, Guo MS, Chaba R, Gross CA, Sauer RT. 2013. Dual molecular signals mediate the bacterial response to outer-membrane stress. Science 340:837-41.
158. Hizukuri Y, Oda T, Tabata S, Tamura-Kawakami K, Oi R, Sato M, Takagi J, Akiyama Y, Nogi T. 2014. A structure-based model of substrate discrimination by a noncanonical PDZ tandem in the intramembrane-cleaving protease RseP. Structure 22:326-336.
159. Kanehara K, Ito K, Akiyama Y. 2003. YaeL proteolysis of RseA is controlled by the PDZ domain of YaeL and a Gln-rich region of RseA. EMBO J 22:6389-6398.
160. Inaba K, Suzuki M, Maegawa K-i, Akiyama S, Ito K, Akiyama Y. 2008. A pair of circularly permutated PDZ domains control RseP, the S2P family intramembrane protease of *Escherichia coli*. J Biol Chem 283:35042-35052.
161. Bohn C, Collier J, Bouloc P. 2004. Dispensable PDZ domain of *Escherichia coli* YaeL essential protease. Mol Microbiol 52:427-35.
162. Parrell D, Zhang Y, Olenic S, Kroos L. 2017. *Bacillus subtilis* intramembrane protease RasP activity in *Escherichia coli* and *in vitro*. J Bacteriol 199.
163. Koide K, Ito K, Akiyama Y. 2008. Substrate recognition and binding by RseP, an *Escherichia coli* intramembrane protease. J Biol Chem 283:9562-9570.
164. Akiyama K, Mizuno S, Hizukuri Y, Mori H, Nogi T, Akiyama Y. 2015. Roles of the membrane-reentrant β-hairpin-like loop of RseP protease in selective substrate cleavage. Elife 4:e08928.
165. Miyake T, Hizukuri Y, Akiyama Y. 2020. Involvement of a membrane-bound amphiphilic helix in substrate discrimination and binding by an *Escherichia coli* S2P peptidase RseP. Front Microbiol 11.
166. Akiyama K, Hizukuri Y, Akiyama Y. 2017. Involvement of a conserved GFG motif region in substrate binding by RseP, an *Escherichia coli* S2P protease. Mol Microbiol 104:737-751.
167. Zhang Y, Luethy PM, Zhou R, Kroos L. 2013. Residues in conserved loops of intramembrane metalloprotease SpoIVFB interact with residues near the cleavage site in pro-σK. J Bacteriol 195:4936-4946.
168. Olenic S, Buchanan F, VanPortfliet J, Parrell D, Kroos L. 2022. Conserved proline residues of *Bacillus subtilis* intramembrane metalloprotease SpoIVFB are important for substrate interaction and cleavage. J Bacteriol 204:e0038621.
169. Maskos K. 2005. Crystal structures of MMPs in complex with physiological and pharmacological inhibitors. Biochimie 87:249-63.
170. Bieniossek C, Niederhauser B, Baumann UM. 2009. The crystal structure of apo-FtsH reveals domain movements necessary for substrate unfolding and translocation. Proc Natl Acad Sci U S A 106:21579-84.
171. Ovchinnikov KV, Chi H, Mehmeti I, Holo H, Nes IF, Diep DB. 2016. Novel Group of Leaderless Multipeptide Bacteriocins from Gram-Positive Bacteria. Appl Environ Microbiol 82:5216-24.

172. Degiacomi G, Personne Y, Mondésert G, Ge X, Mandava CS, Hartkoorn RC, Boldrin F, Goel P, Peisker K, Benjak A, Barrio MB, Ventura M, Brown AC, Leblanc V, Bauer A, Sanyal S, Cole ST, Lagrange S, Parish T, Manganelli R. 2016. Micrococcin P1 - A bactericidal thiopeptide active against Mycobacterium tuberculosis. Tuberculosis (Edinb) 100:95-101.
173. Harms JM, Wilson DN, Schluenzen F, Connell SR, Stachelhaus T, Zaborowska Z, Spahn CM, Fucini P. 2008. Translational regulation via L11: molecular switches on the ribosome turned on and off by thiostrepton and micrococcin. Mol Cell 30:26-38.
174. Montalbán-López M, Cebrián R, Galera R, Mingorance L, Martín-Platero AM, Valdivia E, Martínez-Bueno M, Maqueda M. 2020. Synergy of the bacteriocin AS-48 and antibiotics against uropathogenic *Enterococci*. Antibiotics (Basel) 9:567.
175. Delgado MA, Rintoul MR, Farías RN, Salomón RA. 2001. *Escherichia coli* RNA polymerase is the target of the cyclopeptide antibiotic microcin J25. J Bacteriol 183:4543-50.
176. Yuzenkova J, Delgado M, Nechaev S, Savalia D, Epshtein V, Artsimovitch I, Mooney RA, Landick R, Farias RN, Salomon R, Severinov K. 2002. Mutations of bacterial RNA polymerase leading to resistance to microcin j25. J Biol Chem 277:50867-75.
177. Jonsson M, Juuti JT, Francois P, AlMajidi R, Pietiäinen M, Girard M, Lindholm C, Saller MJ, Driessen AJ, Kuusela P. 2010. Inactivation of the Ecs ABC transporter of *Staphylococcus aureus* attenuates virulence by altering composition and function of bacterial wall. PLoS One 5.
178. Varahan S, Harms N, Gilmore MS, Tomich JM, Hancock L. 2014. An ABC transporter is required for secretion of peptide sex pheromones in *Enterococcus faecalis*. mBio 5:e01726-14.
179. Yokoyama T, Niinae T, Tsumagari K, Imami K, Ishihama Y, Hizukuri Y, Akiyama Y. 2021. The *Escherichia coli* S2P intramembrane protease RseP regulates ferric citrate uptake by cleaving the sigma factor regulator FecR. J Biol Chem 296.
180. Chandler JR, Dunny GM. 2008. Characterization of the sequence specificity determinants required for processing and control of sex pheromone by the intramembrane protease Eep and the plasmid-encoded protein PrgY. J Bacteriol 190:1172-1183.
181. An FY, Sulavik MC, Clewell DB. 1999. Identification and characterization of a determinant (*eep*) on the *Enterococcus faecalis* chromosome that is involved in production of the peptide sex pheromone cAD1. J Bacteriol 181:5915-21.
182. Manjunath GP, Ramanujam PL, Galande S. 2018. Structure function relations in PDZ-domain-containing proteins: Implications for protein networks in cellular signalling. J Biosci 43:155-171.
183. Cezairliyan BO, Sauer RT. 2009. Control of *Pseudomonas aeruginosa* AlgW protease cleavage of MucA by peptide signals and MucB. Mol Microbiol 72:368-79.
184. Callaway E. 2020. 'It will change everything': DeepMind's AI makes gigantic leap in solving protein structures. Nature 588:203-205.
185. Evans R, O'Neill M, Pritzel A, Antropova N, Senior AW, Green T, Žídek A, Bates R, Blackwell S, Yim J. 2021. Protein complex prediction with AlphaFold-Multimer. Biorxiv.

186. Bill RM, Henderson PJ, Iwata S, Kunji ER, Michel H, Neutze R, Newstead S, Poolman B, Tate CG, Vogel H. 2011. Overcoming barriers to membrane protein structure determination. Nat Biotechnol 29:335-40.
187. Carpenter EP, Beis K, Cameron AD, Iwata S. 2008. Overcoming the challenges of membrane protein crystallography. Curr Opin Struct Biol 18:581-6.
188. Rogl H, Kosemund K, Kühlbrandt W, Collinson I. 1998. Refolding of *Escherichia coli* produced membrane protein inclusion bodies immobilised by nickel chelating chromatography. FEBS Lett 432:21-6.
189. Kaur J, Kumar A, Kaur J. 2018. Strategies for optimization of heterologous protein expression in *E. coli*: Roadblocks and reinforcements. Int J Biol Macromol 106:803-822.
190. Straume D, Axelsson L, Nes IF, Diep DB. 2006. Improved expression and purification of the correctly folded response regulator PlnC from lactobacilli. J Microbiol Methods 67:193-201.
191. Nguyen HA, Nguyen TH, Nguyen TT, Peterbauer CK, Mathiesen G, Haltrich D. 2012. Chitinase from Bacillus licheniformis DSM13: expression in *Lactobacillus plantarum* WCFS1 and biochemical characterisation. Protein Expr Purif 81:166-74.
192. Halbmayr E, Mathiesen G, Nguyen TH, Maischberger T, Peterbauer CK, Eijsink VG, Haltrich D. 2008. High-level expression of recombinant beta-galactosidases in *Lactobacillus plantarum* and *Lactobacillus sakei* using a Sakacin P-based expression system. J Agric Food Chem 56:4710-9.
193. Guan M, Su L, Yuan Y-C, Li H, Chow WA. 2015. Nelfinavir and nelfinavir analogs block site-2 protease cleavage to inhibit castration-resistant prostate cancer. Sci Rep 5:1-8.
194. Jones LJ, Upson RH, Haugland RP, Panchuk-Voloshina N, Zhou M, Haugland RP. 1997. Quenched BODIPY dye-labeled casein substrates for the assay of protease activity by direct fluorescence measurement. Anal Biochem 251:144-52.
195. Subramani S, Perdreau-Dahl H, Morth JP. 2016. The magnesium transporter A is activated by cardiolipin and is highly sensitive to free magnesium *in vitro*. Elife 5:e11407.
196. Arias-Cartin R, Grimaldi S, Pommier J, Lanciano P, Schaefer C, Arnoux P, Giordano G, Guigliarelli B, Magalon A. 2011. Cardiolipin-based respiratory complex activation in bacteria. Proc Natl Acad Sci U S A 108:7781-6.
197. Osenkowski P, Ye W, Wang R, Wolfe MS, Selkoe DJ. 2008. Direct and potent regulation of gamma-secretase by its lipid microenvironment. J Biol Chem 283:22529-40.
198. Paschkowsky S, Oestereich F, Munter LM. 2018. Embedded in the membrane: how lipids confer activity and specificity to intramembrane proteases. J Membr Biol 251:369-378.
199. Holcomb J, Spellmon N, Zhang Y, Doughan M, Li C, Yang Z. 2017. Protein crystallization: Eluding the bottleneck of X-ray crystallography. AIMS Biophys 4:557-575.
200. Choy BC, Cater RJ, Mancia F, Pryor EE, Jr. 2021. A 10-year meta-analysis of membrane protein structural biology: Detergents, membrane mimetics, and structure determination techniques. Biochim Biophys Acta Biomembr 1863:183533.

201. Bai XC, McMullan G, Scheres SH. 2015. How cryo-EM is revolutionizing structural biology. Trends Biochem Sci 40:49-57.
202. Renaud JP, Chari A, Ciferri C, Liu WT, Rémigy HW, Stark H, Wiesmann C. 2018. Cryo-EM in drug discovery: achievements, limitations and prospects. Nat Rev Drug Discov 17:471-492.
203. Yip KM, Fischer N, Paknia E, Chari A, Stark H. 2020. Atomic-resolution protein structure determination by cryo-EM. Nature 587:157-161.
204. Perrakis A, Sixma TK. 2021. AI revolutions in biology: The joys and perils of AlphaFold. EMBO Rep 22:e54046.
205. McDonald EF, Jones T, Plate L, Meiler J, Gulsevin A. 2023. Benchmarking AlphaFold2 on peptide structure prediction. Structure 31:111-119.e2.

6. Publications

Paper I

The Role of Site-2-Proteases in Bacteria: A Review on Physiology, Virulence, and Therapeutic Potential

Sofie S. Kristensen[1,*], Dzung B. Diep[1,†], Morten Kjos[1,§] and Geir Mathiesen[1,§,*]

1. Faculty of Chemistry, Biotechnology, and Food Science, Norwegian University of Life Sciences (NMBU), Ås, Norway.

† This author is deceased (7th of December 2022)

§ These authors share last authorship

* Address correspondence to: Sofie S. Kristensen (sofie.kristensen@nmbu.no) or Geir Mathiesen (geir.mathiesen@nmbu.no).

Abstract

Site-2-proteases (S2P) are a class of intramembrane proteases involved in regulated intramembrane proteolysis. Regulated intramembrane proteolysis is a highly conserved signaling mechanism, which commonly involves sequentially degradation of an anti-sigma factor by a site-1- and site-2-protease in response to external stimuli, resulting in an adaptive transcriptional response. Variation of this signaling cascade continues to emerge as the role of S2P in bacteria continues to be explored. S2P are highly conserved among bacteria and play a key role in multiple processes including iron uptake, stress response and pheromone production. Additionally, an increasing number of S2P have been found to play a pivotal role in the virulence properties of multiple human pathogens, such as alginate production in *Pseudomonas aeruginosa*, toxin production in *Vibrio cholerae*, resistance to lysozyme in enterococci and antimicrobials in several *Bacillus* spp, and cell-envelope lipid composition of *Mycobacterium tuberculosis*. The prominent role of S2P in bacterial pathogenicity highlights the potential of S2P as novel targets for therapeutic intervention. In this review, we summarize the role of S2P in bacterial physiology and virulence, as well as evaluate the therapeutic potential of S2P.

Introduction

Bacteria depend on transmembrane signaling to sense and quickly respond to a changing environment. A fast response is particularly crucial for pathogenic bacteria, which encounter a rapidly changing environment within the host throughout the infection process. Regulated intramembrane proteolysis (RIP) is a signaling mechanism known to mediate transmembrane signaling in Gram-positive and Gram-negative bacteria (1-3). In the most general terms, RIP cleaves a substrate within the membrane, causing releasing a regulator able to modify gene expression. RIP is mediated by a unique class of intramembrane proteases (IMP). IMP are divided into four subgroups based on their catalytic mechanisms: The rhomboid serine proteases, the site-2-metalloproteases (S2P), the glutamyl protease and the aspartyl proteases. In the present review, the role of S2P-mediated RIP signaling in

bacteria will be discussed. The remaining IMP families have been extensively reviewed in other articles (2, 4-7)

In bacteria, gene expression is commonly controlled at the transcriptional level. S2P-mediated RIP signaling allow regulated gene expression in bacteria by activating an alternative sigma factor of the extracytoplasmic function (ECF) family in response to environmental cues. As reviewed in detail here and by others, S2P-mediated RIP signaling contribute to a vast array of cellular processes, including cell polarity, iron acquisition and sporulation (8-11). Most notably, RIP-mediated activation of sigma factors has been linked to virulence in several human pathogens (1, 2, 12). While regulating a vast array of cellular processes, S2P-mediated RIP signaling generally adheres to the same general principle (Figure 1) (13). A membrane bound anti-sigma factor, commonly a single-spanning membrane protein, binds to the ECF sigma factor, thereby negatively regulating ECF sigma factor activity. Following the detection of an environmental signal, a primary site-1-protease (S1P) cleaves the anti-sigma factor (site-1-cleavage). This primary cleavage triggers an intramembrane protease (IMP) to cleave the anti-sigma factor within the lipid bilayer (site-2-cleave), thereby releasing the activated σ-factor from the membrane. The RIP cascade is a widely distributed signaling pathway in the bacterial world, and variations of this blueprint are emerging as the role of S2P in different bacteria are explored.

In this review, the roles and mechanisms of RIP and S2P in bacteria will be explored, starting with the implications of S2P in bacterial adaptation to a rapidly changing environment. Next, RIP-mediated virulence will be reviewed, focusing on the role of S2P in important human pathogens. Finally, we will discuss the therapeutic potential of S2P and highlight the challenges and opportunities of targeting this unique class of proteins.

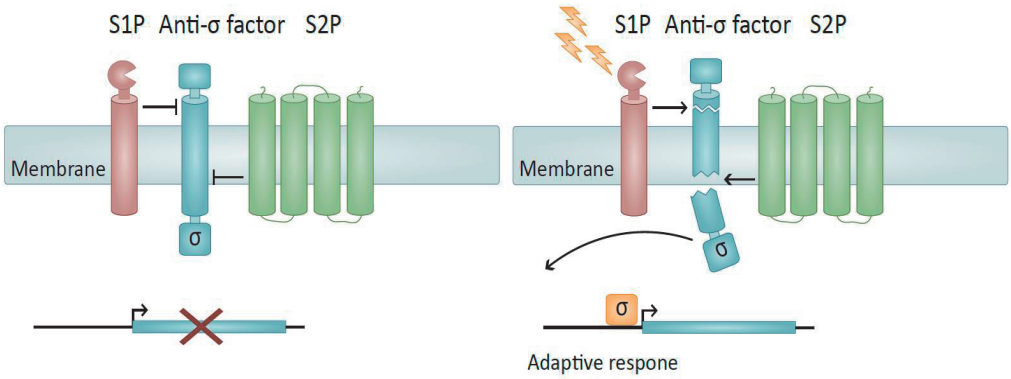

Figure 1 | The general S2P-mediated RIP paradigm. In the absence of environmental cues (left panel), the degradation of the anti-sigma factor is inhibited, leaving the σ-factor in an inactive state. When extracytoplasmic stimuli is detected (right panel), a site-1-protease (S1P) cleaves a membrane-bound anti-sigma factor. The primary cleavages trigger a secondary cleavage by a site-2-protease (S2P), resulting in release of the σ-factor from the membrane, and activation of genes involved in adaptive response.

The role of S2P in response to changes in the extracytoplasmic environment

Bacteria depend on signal transduction across the membrane to respond appropriately to environmental cues. Proteolysis is a rapid process, thus, multiple signaling pathways depend on proteases to generate an immediate response (3). Following the discovery of the S2P RseP in *Escherichia* coli and the S2P SpoIVFB in *Bacillus subtilis* at the beginning of this millennium, several S2P have been implied in adaptive response (14-16) (Figure 2, Table 1). The following section will discuss the role of S2P in response to changes in the extracytoplasmic environment.

The role of RseP in regulation of the σ^E-dependent stress response in *Escherichia coli*

E. coli RseP (Regulator of sigma E, protease; *Ec*RseP), previously known as YaeL, is one of the most extensively studied members of the S2P family and was first identified as a key regulator of the σ^E-dependent stress response (Figure 2A) (14, 17, 18). In *E. coli*, the extracytoplasmic stress response is initiated following the sequential degradation of the anti-sigma factor RseA by the S1P DegS and the S2P *Ec*RseP (17-19). *Ec*RseP-mediated degradation of RseA is one of the best understood transmembrane signaling pathways involving a S2P and is viewed as the blueprint for the bacterial RIP-cascades.

In the absence of stress, σ^E is sequestered in the membrane by the anti-sigma factor RseA (20, 21) (Figure 2A). During stress conditions, such as heat, unfolded or misfolded outer membrane proteins (OMPs) will accumulate in the periplasm. Unfolding of outer membrane proteins results in exposure of hydrophobic amino acids that is directly recognized by the periplasmic PDZ domain of the S1P DegS (22). Recognition of unfolded OMPs triggers DegS-mediated cleavage of the periplasmic region of RseA, which subsequently initiates a secondary cleavage by the S2P *Ec*RseP (17-19, 22, 23). *Ec*RseP cleaves RseA within the transmembrane segment, thereby releasing the cytoplasmic region of RseA in complex with σ^E (23, 24). The protease ClpXP performs the final degradation of RseA to release the σ^E into the cytosol, which activates the transcription of target genes involved in the stress response (25).

The RIP-mediated activation of σ^E is tightly regulated at multiple levels to ensure that σ^E activation is strictly stress-dependent (Figure 2A). Most importantly, *Ec*RseP can only efficiently process RseA following site-1-cleavage (24). Many proteins involved in RIP, including both DegS and *Ec*RseP, harbors extracellular PDZ domains which are thought to be important for structuring of signal complexes. It has been suggested that the *Ec*RseP PDZ domain acts as a size-exclusion filter, preventing interaction with larger substrates such as full-length RseA (26). Two lines of evidence support this notion. Firstly, mutational analysis has demonstrated that disruption of the *Ec*RseP PDZ domain results in *Ec*RseP-mediated degradation of RseA in the absence of site-1-cleavage (27-29) Secondly, structural analysis

indicates that the PDZ tandem forms a pocket-like structure facing the catalytic center (26, 30), thereby blocking the access of bulky substrates to the active site. Notably, the newly exposed C-terminal of DegS-cleavage RseA is suggested to interact directly with the PDZ domain (24), further highlighting the importance of this domain in substrate discrimination. In addition, the periplasmic stress sensor protein RseB function as a negative regulator of σ^E activity. RseB interacts with the periplasmic region of RseA, presumably inhibiting DegS cleavage by masking the site-1-cleavage site (20, 21, 31, 32). During stress, misfolded OMPs and lipoprotein intermediates are suggested to promote RseB release from RseA (33-35). These regulation mechanisms collectively ensure that *Ec*RseP-mediated activation of σ^E is strictly stress-dependent.

SpoIVFB and endosporulation in *Bacillus subtilis*

SpoIVFB (Stage IV sporulation protein FV), the S2P of B. subtilis controlling the transcription factor σ^K, is another well-characterized member of the S2P family (Figure 2B) (15, 16, 36). Under harsh environmental conditions, actively growing B. subtilis differentiates into a dormant state, known as endospores, one of the most advanced and long-lasting forms of stress response found among bacteria (37). The regulatory mechanisms of endospore formation are complex, involving a set of sigma factors which are active at certain time points during sporulation. The transcription factor σ^K controls the final stage of the endospore formation. σ^K is synthesized as an inactive precursor, Pro-σ^K, which is sequestered in the outer forespore membrane (38). SpoIVFB cleaves the N-terminal pro-region of Pro-σ^K, resulting in mature σ^K being released into the mother cell (15, 36). Once released, σ^K activates genes needed in the final stage of endospore maturation (Figure 2B).

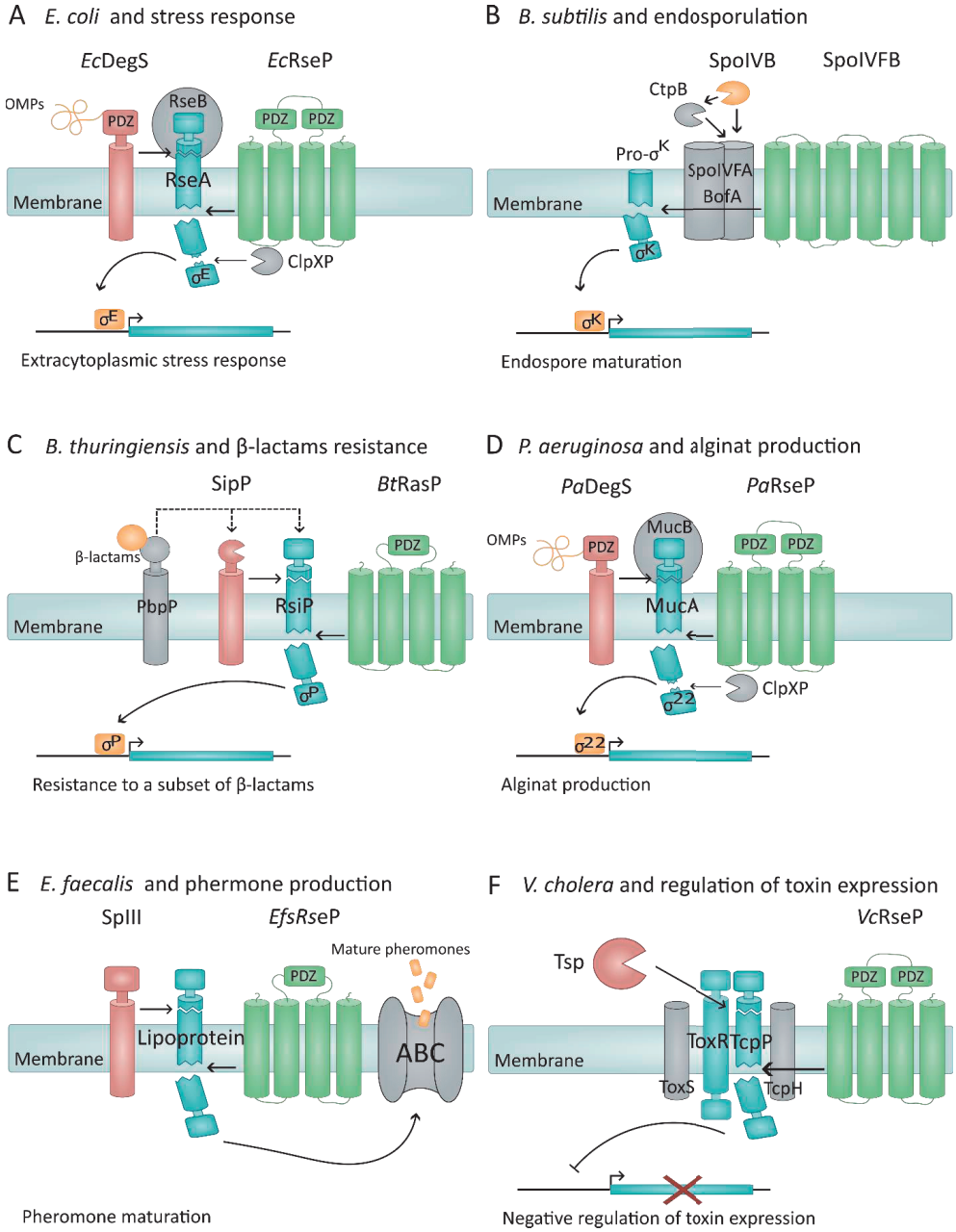
A E. coli and stress response
EcDegS
EcRseP
OMPs
PDZ
RseB
PDZ
PDZ
RseA
Membrane
ClpXP
σE
σE
Extracytoplasmic stress response
B B. subtilis and endosporulation
SpoIVB
SpoIVFB
CtpB
Pro-σK
SpoIVFA
BofA
Membrane
σK
σK
Endospore maturation
C B. thuringiensis and β-lactams resistance
SipP
BtRasP
β-lactams
PDZ
PbpP
RsiP
Membrane
σP
σP
Resistance to a subset of β-lactams
D P. aeruginosa and alginat production
PaDegS
PaRseP
OMPs
PDZ
MucB
PDZ
PDZ
MucA
Membrane
ClpXP
σ22
σ22
Alginat production
E E. faecalis and phermone production
SpIII
EfsRseP
Mature pheromones
PDZ
Lipoprotein
ABC
Membrane
Pheromone maturation
F V. cholera and regulation of toxin expression
VcRseP
Tsp
PDZ
PDZ
ToxRTcpP
Membrane
ToxS
TcpH
Negative regulation of toxin expression

Figure 2 |The role of S2P in RIP signaling mechanism in selected bacteria. A) The *E. coli* RseP activation of the extracytoplasmic stress response serves as a blueprint for S2P-mediated signaling. Accumulation of unfolded outer membrane proteins (OMPs) is a known stress cue sensed by the PDZ domain of the S1P DegS. Accumulation of OMPs results in sequential degradation of the anti-sigma factor RseA by DegS (site-1-cleavage) and RseP (site-2-cleavage). ClpXP further degrades RseA in the cytosol, finally releasing the σ^E which subsequently activates genes involved in the adaptive stress response. RseB, a periplasmic protein, negatively regulates σ^E activity by blocking DegS/RseP cleavage under non-stress conditions. B-F) Variants of RIP involving S2P are shown for various species. In all panels: Suggested stimuli signal is shown in yellow, the substrate in blue, presumed S1P in red, S2P in green, substrates in active form in yellow, and additional components in grey. See the text for more details.

Analogous to *Ec*RseP cleavage of RseA (Figure 2A), the SpoIVFB cleavage of Pro-σ^K is tightly regulated (Figure 2B), to make sure that σ^K is activated only at the correct developmental stage of sporulation. As discussed above, regulation of *Ec*RseP activity largely relies on substrate priming by a S1P and the size-excluding role of the *Ec*RseP PDZ domain. In contrast, the processing of Pro-σ^K by SpoIVFB, which does not contain a PDZ domain, occurs independently of a S1P. BofA and SpoIVFA, two regulatory membrane proteins, form a complex with SpoIVFB in the outer forespore membrane (39, 40). The formation of the complex is suggested to allow BofA to directly interact with the SpoIVFB active site, thereby inhibiting Pro-σ^K processing (39, 41). The serine proteases SpoIVB and CtbP are suggested to sequentially degrade the BofA:SpoIVFA complex, thereby liberating the active SpoIVFB to cleave Pro-σ^K (42-44). Importantly, transcription of serine protease is only activated in the forespore after it has been completely engulfed (37, 42), thereby making sure that σ^K can be released into the mother cell to activate genes at the onset of the final sporulation stage. In this sense, SpoIVFB acts as the primary mediator of signaling from the forespore to σ^K activation in the mother cell.

The SpoIVFB-mediated cleavage of Pro-σ^K differs from the RIP-cascade paradigm in *E.coli* in multiple aspects. Most notably, SpoIVFB directly cleaves the transcription factor, not an anti-sigma factor, to produce the active form of σ^K. Moreover, SpoIVFB mediated processing of Pro-σ^K appears to be independent of canonical S1P cleavage, although proteolytic degradation of the BofA:SpoIVFA complex is needed for SpoIVFB activation (Figure 2B).

S2P-mediated lysozyme resistance in Gram-positive bacteria

Lysozyme is a key component of the innate immune response. Lysozyme acts as a hydrolase, degrading the glycosidic bonds between N-acetylmuramic acid (NAM) and N-acetylglucosamide (NAG) in peptidoglycan in the bacterial cell wall, resulting in increased cell wall permeability and ultimately cell death (45). Several bacteria have developed sophisticated mechanisms to counteract the effect of lysozyme (45-50).

In *B. subtilis,* lysozyme resistance is mediated through S2P-dependent activation of the ECF sigma factor σ^V (47, 51). In the absence of lysozyme, σ^V activity is hindered by the anti-sigma factor RisV (51, 52). In the presence of lysozyme, an extracellular domain of RisV directly binds lysozyme resulting in conformational changes within the anti-sigma factor, thereby initiating the RIP-cascade (53, 54). The signal peptidases SipS and SipT are suggested to cleave the extracellular region of RisV (53, 55). Following this primary cleavage, the S2P RasP (regulator of sigma protease, *Bs*RasP) cleaves RisV, thereby releasing the cytoplasmic region of RisV containing σ^V (51). It is presumed that cytosolic proteases further processes RisV, however, such proteases have not yet been identified. Once released into the cytosol, σ^V activates genes involved in lysozyme resistance, including *oatA* and *dltA*. OatA and DltA modifies cell wall properties and charge through O-acetylation of the peptidoglycan and D-alanylation of teichoic acids, respectively (47, 56).

A similar cascade is observed in the opportunistic pathogens *Clostridioides difficile* and *Enterococcus faecalis*. Deletion of RasP (*Cd*RasP) and RseP (*Efs*RseP, also known as Eep) the S2Ps of *C. difficile* and *E. faecalis,* respectively, results in decreased σ^V activity and lysozyme resistance (48, 49, 57). In *C. difficile*, *Cd*RasP mediates σ^V activation by degrading RsiV in response to lysozyme in a dose-dependent manner (49). *C. difficile* σ^V regulates the expression of several genes in response to lysozyme, including the peptidoglycan deacetylase PdaV, which removes acetyl groups from peptidoglycan in the cell wall (58-61). In this bacterium, deacetylation of the peptidoglycan results in reduced affinity for lysozyme, thereby increasing lysozyme resistance. Interestingly, deletion of *pda*V results in only a modest increase in lysozyme susceptibility. However, the combined loss of *pdaV* and another deacetylase, *pgdA*, resulted in a 1 000-fold reduction in lysozyme resistance, suggesting that

these two deacetylases are redundant (60). In a similar manner, σ^V of *E. faecalis* regulates expression of peptidoglycan deacetylase PgdA (48, 61-63), but also here, deletion of *pgdA* alone does not affect lysozyme resistance (48, 61, 63, 64). It is possible that a similar redundancy as observed in *C. difficile*, is found in *E. faecalis*, or that other σ^V-dependent genes also contribute to the decrease in lysozyme resistance observed for the *E. faecalis* strains depleted of RseP and σ^V.

Thus, the S2P-mediated activation of σ^V dependent lysozyme resistance appears highly conserved in *B. subtilis*, *C. difficile* and *E. faecalis*. To date, no S1P has been identified for RsiV in *E. faecalis* or *C. difficile*. However, a signal peptidase cleavage site has been identified in RsiV for both species, suggesting that the S1P is a so far unknown signal peptidase (49, 53). In *E. faecalis*, σ^V is also suggested to contribute to a general stress response, as Δ*rseP* and Δ*sigV* significantly attenuated survival in response to multiple stressors, including heat, acid, and ethanol (48, 65). Similar observations have been made in *Enterococcus faecium*, where mutations within *rseP* results in a 6-8 fold increase in lysozyme susceptibly as well as a reduction in desiccation tolerance (66). A more general role in stress response has so far not been observed for RasP and σ^V in *B. subtilis or C. difficile.*

RseP and iron acquisition in Gram-negative bacteria

Iron acquisition is a key factor for colonization and infection of several pathogens (67, 68). For pathogenic bacteria, iron resources in the environment are limited, as most of the host iron is present in high affinity iron binding complexes, such as hemoglobin and transferrin. To circumvent these limitations, bacteria have developed several sophisticated iron acquisition systems, including the production of siderophores and heme utilization (67, 68). To ensure rapid adaption to changing environment, iron acquisition is regulated by ECF sigma factors in several Gram-negative bacteria.

In *Pseudomonas aeruginosa*, an opportunistic human pathogen causing a range of different infections, particularly in immunocompromised and cystic fibrosis patients, the involvement of ECF sigma factors in iron acquisition has been extensively reviewed (67, 69, 70).

Interestingly, the S2P RseP, also known as MucP, is required for complete proteolysis of the anti-sigma factor and thus ECF sigma factor activity, in at least five pathways related to iron acquisition in *P. aeruginosa*: The pyoverdine, ferrichome and ferrioxamine siderophore pathways, and the Has and Hxu heme pathways (71-74). S2P mediated iron acquisition appears to be conserved in *Pseudomonas* species, as the deletion of *rseP* additionally eradicates the activity of multiple iron acquisition pathways in *Pseudomonas putida* (73). Interestingly, several of the RseP-regulated iron acquisition pathways have also been implied in pathogenicity of *P. aeruginosa* (75-77). Most notably, the deletion of the sigma factor PvdS, which regulates pyoverdine production in a RseP-dependent manner, resulted in attenuated virulence in mouse lung infection (71, 78, 79). In addition to pyoverdine production, σ^{PvdS} regulated the expression of the major virulence factors exotoxin A and PrpL, thereby showing a dual role in *P. aeruginosa* virulence (77, 78, 80, 81). The role of S2P and the RIP-cascade in *P. aeruginosa* will be further discussed below.

S2P-mediated iron acquisition has also been implied in other Gram-negative species. In *Bordetella bronchispetica*, a pathogen colonizing the respiratory tract of animals and humans, the S2P HurP (heme utilization receptor protease) is essential for heme utilization through the expression of the outer membrane receptor BhuR (10). The complete regulation mechanism has not been fully elucidated; however, it is suggested that HurP cleaves the anti-sigma factor HurR in a heme-dependent manner. The modification of HurR is proposed to release the sigma factor HurI, which subsequently regulates the cellular response to the iron depleted environment and heme uptake. The S1P of this proposed RIP cascade has not yet been identified (10). Curiously, *hurP* complements mutations in the S2P *rseP* in *Vibrio cholerae* while *rseP* from *E. coli* complements *hurP* deletions in *B. bronchispetica* (10), indicating that substrate recognition and processing must be highly conserved in these species. To date, RseP has not been implied in iron acquisition in *V. cholerae*, however, *Ec*RseP was recently found to activate the ECF sigma factor FecI in response to ferric-citrate (9).

RasP and resistance to antimicrobials in *Bacillus* spp.

Several bacteria utilize alternative sigma factors to regulate genes in response to stressors such as antibiotics and antimicrobial peptides (82). In *Bacillus thuringiensis*, a Gram-positive bacterium commonly found in the soil, resistances to selected β-lactams are controlled by the ECF sigma factor σ^P (Figure 2C). Upon activation, σ^P regulates expression of multiple β-lactamases and penicillin binding proteins (PBP) (83), providing *B. thuringiensis* with an arsenal of protection strategies. The activity of σ^P is hindered by the anti-sigma factor RsiP, which, in response to selected β-lactams, is successively degraded by the S1P SipP and the S2P RasP (84, 85). It is suggested that penicillin binding protein P (PbpP) acts as a sensor for β-lactams, somehow activating the S1P cleavage of the RIP cascade (86). Δ*pbpP*, Δ*sipP* and Δ*rasP* increase susceptibility to ampicillin and cefoxitin (84-86), underpinning the RIP cascade's role in σ^P mediated β-lactam resistance. A similar cascade is observed in *B. subtilis*, where σ^W participates in response to a variety of cell wall inhibiting antibiotics and antimicrobial peptides (87-89). Activation of σ^W depends on the RIP-mediated degradation of the anti-sigma factor RsiW by the S1P PrsW and the S2P RasP (90-92). Although primarily considered as an antibiosis regulon, the *B. subtilis* σ^W responds to various stressors compromising cell wall integrity (88-90, 92, 93). In contrast, *B. thuringiensis* σ^P is activated only by a specific subset of β-lactams, not other cell wall-targeting antibiotics, suggesting that σ^P is not activated in response to general cell wall stress (84). It should be noted that σ^P also has been linked to resistance against β-lactams in *Bacillus cereus* and *Bacillus anthracis.* RasP is conserved in these closely related human pathogens, suggesting a role of RIP-mediated antibiotic resistance in these species. However, the role of RIP-mediated resistance to antibiotics in *B. cereus* and *B. anthracis* has not been extensively studied (85, 94)

Table 1 | Suggested components of the RIP signaling pathway in selected bacteria

Organism	S1P	Substrate	S2P	Transcriptional regulation	Function	Ref.
B. bronchiseptica	Unknown	HurR	HurP	σ^{HurI}	Iron acquisition	(10)
B. subtilis	Not required	Pro-σ^{K}	SpoIVFB	σ^{K}	Sporulation	(15, 16, 42)
	SipS and SipT	RsiV	RasP	σ^{V}	Lysozyme resistance	(51, 55)
	PrsW	RsiW	RasP	σ^{W}	Cell envlope stress response	(87, 90-92)
B. thuringiensis	SipP	RsiP	RasP	σ^{P}	Resistance to a subset of β-lactams	(84, 85)
C. crescentus	PerP	$PodJ_S$	MmpA	None	Cell polarity	(8, 95)
C. difficile	Unknown	RsiV	RasP	σ^{V}	Lysozyme resistance	(49)
E. coli	DegS	RseA	RseP	σ^{E}	Cell envelope stress response	(18)
	Unknown	FecR	RseP	σ^{FecI}	Iron acquisition	(9)
E. faecalis	Unknown	RsiV	RseP	σ^{v}	Lysozyme resistance	(48)
	SPII	Signal peptides	RseP	None	Pheromone production	(96-99)
L. monocytogenes	Unknown	Signal peptides	Eep	None	Pheromone production	(100)
M. tuberculosis	Unknown	RslA,	Rip1	σ^{L}	Regulation of membrane composition, virulence, stress	(101)
	Unknown	RsmA,	Rip1	σ^{M}		(101)
	Uknown	RskA	Rip1	σ^{K}		(101)
	Unknown	RsdA	Rip1	σ^{D}		(102)
P. aeruginosa	Unknown	FpvR	RseP	σ^{FpvI} and σ^{PvdS}	Iron acquisition	(71)
	Unknown	FoxR	RseP	σ^{FoxI}		(71)
	Unknown	FiuR	RseP	σ^{FiuI}		(71, 73)
	Unknown	HasS	RseP	σ^{HasI}		(72)
	Unknown	HxuR	RseP	σ^{HxuI}		(72)
	DegS	MucA	RseP	σ^{22}	Alginate production	(103)

P. putida	Prc	LutY	RseP	σ^{lutY}	Iron acquisition	(73)
S. aureus	Unknown	Signal peptides	Eep	None	Peptide maturation, Virulence	(104, 105)
Streptococcus	Unknown	Signal peptides	Eep	None	Signal peptide production	(106-108)
V. cholera	TsP	TcpP	RseP	TcpP	Downregulates toxin production	(109, 110)
	Unknown	ToxR	RseP	ToxR	Downregulates toxin production	(109)

The role of S2P in bacterial pathogenesis

As discussed above, S2P-mediated activation of ECF sigma factors plays a key role in the quick adaptation to extracytoplasmic stimuli in many bacteria. Rapid adaptation to changing environments is crucial for establishing infections, however S2P-mediated RIP have also been implied in the direct activation of virulence related genes (Figure 2, Table 1). In the following section the role of S2P in prominent human pathogens will be discussed.

MucP and mucoid production in *Pseudomonas aeruginosa*

P. aeruginosa is an opportunistic pathogen causing a wide range of nosocomial infections. Most notably, *P. aeruginosa* is a major cause of morbidity among patients with cystic fibrosis. Clinical *P. aeruginosa* isolated from patients with cystic fibrosis generally exhibit mucoid phenotype resulting from an overproduction of alginate (111, 112) It is suggested that alginate production contributes to protecting the bacteria against various stressors, including antibiotics and oxidative stress, thereby promoting persistence in the lungs and thereby virulence. In *P. aeruginosa*, genes involved in alginate production is controlled by the ECF sigma factor σ^{22}, also known as σ^{AlgT} or σ^{AlgU} (113, 114). Activation of σ^{22} is regulated in a RIP-depended manner in response to envelope stress, highly resembling the RseP-mediated activation of the extracytoplasmic stress response in *E. coli* (Figure 2D) (103, 113, 114). It has indeed been suggested that alginate production plays a part in a general stress response, as σ^{22} also regulates genes involved in protection against extracytoplasmic stress (113, 114).

Under non-stress conditions, the anti-sigma factor MucA sequesters σ^{22} in the membrane, thereby inactivating the sigma factor (115) (Figure 2D). The PDZ domain of *P aeruginosa* DegS (*Pa*DegS), also known as AlgW, is suggested to recognize C-terminal residues of the envelope protein MucE and possibly other outer membrane protein, which are accumulated under cell wall stress (116, 117). This interaction initiates *Pa*DegS mediated cleavage of MucA, which is proposed to subsequently trigger a secondary cleavage by *Pa*RseP, also known as MucP (103, 113, 116-118). MucA is suggested to be further processed by proteases such as ClpXP in the cytosol, finally resulting in a activate σ^{22} (119). Under non-stress conditions, MucB, the equivalent to RseB in *E. coli*, binds to MucA, thereby inhibiting RIP-mediated degradation of the anti-sigma factor (Figure 2A & D) (113, 115, 117).

It is interesting to note that clinical *Pseudomonas* isolates from cystic fibrosis patients often contain mutation within MucA, commonly resulting in a C-terminal truncation of the anti-sigma factor and subsequent increased σ^{22} activity (120, 121). In *E. coli*, truncation of RseA results in *Ec*RseP degradation of RseA independent of site-1 cleavage (24, 26). A similar mechanism is proposed for degradation of truncated MucA in *P. aeruginosa*, explaining the constitutive mucoid phenotype commonly observed for MucA mutants (103). As discussed above, RseP of *P. aeruginosa* has also been implicated in iron-uptake and regulation of virulence determinators exotoxin A and PrpL. The combined role of RseP-mediated regulation of iron uptake, alginate production and expression of virulence enhancing genes, makes it tempting to speculate that a *rseP* deletion would have a striking effect of *P. aeruginosa* pathogenicity. However, the role of pseudomonal RseP has not yet been investigated in infection models *in vivo.*

Rip1 and virulence in *Mycobacterium tuberculosis*

Mycobacterium tuberculosis is an obligate human pathogen, which despite the Bacille-Calmete-Guerine (BCG) vaccine, remains a leading cause of infection worldwide (122). The complex composition of the *M. tuberculosis* cell envelope makes these infections difficult to treat and is known to play a key role in the persistence and virulence of this pathogen (123, 124). Transcriptional analysis in the presence or absence of detergents revealed that the *M.*

tuberculosis S2P Rip1 regulates genes involved in lipid metabolism in response to a changing environment (125). In line with this evidence, Δ*rip1* displays altered cell morphology and loss of ability to cord (125), which is an established virulence trait relying on a glycolipid known as the cord-factor in the mycobacterial cell-envelope. When challenged in an aerosol murine model, Δ*rip1* showed impaired growth during both the acute and chronic phase of infection (102, 125, 126). Specifically, by 22 weeks, bacterial titers from the lungs were 10 000-fold lower for Δ*rip1* compared to wild-type, while Δ*rip1* was completely abolished from the liver (125), and by 43 weeks, Δ*rip1* was completely cleared from the lungs, showing no detectable CFU in the majority of the mice (102). The deletion phenotype was rescued when complemented with the wild-type Rip1, showing that attenuated virulence is Rip1 dependent (125).

Although the severe attenuation of *M. tuberculosis* virulence caused by the single gene deletion of *rip1* is striking, the mechanism of Rip1 in *M. tuberculosis* virulence remains somewhat elusive. In fact, Rip1 degrades four independent anti-sigma factors controlling the activity of σ^K, σ^L, σ^M and σ^D (101, 102). Interestingly, Δ*sigKLM* does not attenuate bacterial growth in aerosol murine model, suggesting that the Rip1-dependent virulence observed for Δ*rip1* is independent of these pathways (102). This points to a key role of σ^D in the virulence mechanism, which notably controls expression of multiple virulence factors, including *fbpA* and the resuscitation promoting factor RpfC (127, 128). Thus, it was surprising to note that single deletion Δ*sigD* only caused modest decrease in virulence compared to the ΔRip1 (127, 128). So far, the effect of the quadruple mutant (Δ*sigKLMD*) not been investigate *in vivo.*

Adding to the complexity of Rip1s role in virulence, a recent study revealed that Rip1 contributes to defense against host-imposed stressors (126). When challenging Δ*rip1* with various stressors, Rip1 was found to be essential for protection against metal and nitrosative stress. Most importantly, the observed attenuated growth of Δ*rip1* in acute infection in mice was reversed in the absence of nitric oxide production, suggesting that Rip1 directly contributes to pathways defending *M. tuberculosis* against host-produced nitic oxide (126). Interestingly, no Rip1-dependent defects were observed when challenging the *Δrip1* mutant

with starvation, lysozyme, iron deficiency or an acidic environment (126), as previously observed for other S2P mutants (as discussed above).

RseP and pheromone production in *Enterococcus faecalis*

S2P was generally believed only to regulate transcription factor activity. However non-anti-sigma factor substrates have been identified for S2P in multiple species, with *E. faecalis* being the earliest example (8, 109, 129-131). Although considered commensal enterococci have emerged as important healthcare-associated pathogens in the last decades, causing a wide range of infections, including urinary tract infections, endocarditis, and bacteremia (132, 133). The S2P of *E. faecalis*, *EFm*RseP, also known as Eep (enhanced expression of pheromone), increases the production of multiple sex pheromones, including cCF10, cAD1 and cPD1 (96, 97, 99, 134), which are critical for conjugation of plasmids between bacterial cells. A model has been proposed in which lipoprotein signal peptides is sequentially degraded by a type II signaling peptidase and *Efs*RseP, before a ABC transporters actively transport the resulting, mature pheromones outside the cell (135) (Figure 2E). S2P involvement in pheromone maturation has also been suggested in several species of *Streptococcus* as well as *Listeria monocytogenes* and *Staphylococcus aureus*, indicating that S2P-mediated pheromone processing may be a conserved mechanism among some Gram-positive bacteria (100, 104-108).

In addition to its role in pheromone processing, *Efs*RseP has been suggested as a key factor in *E. faecalis* virulence (136, 137). When challenged in a rabbit endocarditis model, Δ*rseP* was severely attenuated, showing a 4-$\log_{10}$ decrease in colony forming units (CFU) recovered from the heart valves compared to the wild-type. The attenuation defects observed for Δ*rseP* could be rescued by *in trans* expression of *rseP* (136). Moreover, Δ*rseP* resulted in a reduced bacterial load recovered from the kidneys in a murine catheter-associated urinary tract infection model (137). It should be noted that the defects in virulence observed for the Δ*rseP* is likely not attributed to loss of plasmid conjugation, as both *in vivo* studies were performed using *E. faecalis* OG1RF – a well characterized laboratory strain which almost completely lacks mobile genetic elements (138). *Efs*RseP dependent virulence is therefor most likely not related to lack of sex pheromones maturation. On the other hand, σ^V may be involved. As

discussed above, *Efs*RseP induces lysozyme resistance through RIP-mediated activation of the ECF σ^V (48). Indeed, Δ*sigV* attenuated *E. faecalis* virulence in a murine UTI and systemic infection (62). This indicates that, at least to some extent, reduction in σ^V activation may contribute to the reduced virulence observed for strains deficient in *Efs*RseP. Nevertheless, the exact mechanisms underlying *Efs*RseP-mediated virulence remains to be confirmed.

Eep and virulence in *Staphylococcus aureus*

S. aureus is a major human pathogen causing a wide range of both nosocomial and community acquired infections. Small linear peptides are suggesting a key role in multiple cellular processes in Gram-positive bacteria, including signaling, competence development and virulence (100, 108, 139, 140). Similar to what was discussed above for *E. faecalis*, the *S. aureus* S2P (*Sa*Eep) is involved in maturation of multiple small linear peptides, including the sex pheromone cAM373 (104, 105). A proteomic analysis showed that Δ*eep* in *S. aureus* affected the release of more than 55 proteins, including a significant decrease of several proteins involved in bacterial adhesion (i.e. SpA, SasG and FnbA) (104). Indeed, Δ*eep* showed reduced adhesion to human epithelial cells two hours post-infection. Overexpression of Spa, SasG and FnbA increased adhesion in the Δ*eep* strain, suggesting that the reduced ability to adhere is directly linked to reduced production of important adhesion proteins in the mutant (104). Furthermore, when challenging a murine blood infection model, Δ*eep* showed significantly decreased virulence and survival (104). In this study, CFU counts retrieved from the liver, but not the kidneys, could be restored to wild-type levels when SpA was overexpressed in the Δ*eep* mutant, suggesting that *Sa*Eep may affect other aspects of infection besides adhesion (104).

ECF factors σ^S and σ^B have been suggested to play a role in *S. aureus* virulence (141-144). Interestingly, *fnbA*, which is downregulated in *Sa*Eep deficient strain, is controlled by the σ^B regulon, while a *S. aureus* homolog of the S1P of *B. subtilis* is suggested to be involved in σ^S activation (145-147). These observations, taken together with the fact that *Sa*Eep controls the expression of a vast range of proteins make it tempting to speculate that *Sa*Eep and RIP-

mediated activation of ECF factors play important roles in *S. aureus* virulence. However, the potential role of Eep in *S. aureus* ECF factor activity remains to be elucidated.

RseP and virulence regulation in *Vibrio cholera*

As reviewed above, RIP is a common mechanism for activating transcriptional factors by releasing them from the membrane. In contrast, TcpP, a transcription factor needed for activation of the master virulence regulator ToxT in *V. cholera*, is active when bound to the membrane but inactive following proteolysis (Figure 2E). ToxT directly activates multiple virulence associated genes in *V. cholerae*, including genes encoding cholera toxin and the toxin-co-regulated pilus (148). Under non-virulence inducing conditions, TcpP is degraded in a RIP-dependent manner, thereby repressing the expression of *toxT* and downstream virulence associated genes (109, 110). The periplasmic protein Tsp (tail-specific protease) performs the primary cleavage of TcpP, while the S2P cleavage is performed by *V. cholerae* RseP (*Vc*RseP, also known as Yael) (109, 110). During virulence promoting conditions, another protein known as TcpH is suggested to interact with TcpP, thereby protecting it from RIP mediated degradation, thereby allowing *toxT* expression (109, 149).

Another level of regulatory complexity in this system is added by another membrane-bound transcription factor known as ToxR and its effector protein ToxS (Figure 2E). ToxR is thought to additionally enhanced the TcpP mediated activation of *toxT* (Figure 2E) (150, 151). Notably, *Vc*RseP has been implied in ToxR degradation under nutrient limitation at alkaline pH (152). ToxR degradation has been associated with entry of *V. cholerae* to a dormant state, suggesting that RIP-mediated inactivation of virulence regulators TcpP/ToxR and entry into an nonculturable state are linked (152).

Targeting S2P in the context of antimicrobial therapy

Despite the evident role of S2P in bacterial physiology and virulence, only a limited number of inhibitors have been shown to target S2P. Several challenges hamper the development of specific S2P inhibitors. Most notably, S2P are conserved among all kingdoms of life (153), making adverse interaction between an inhibitor and the host S2P a potential concern. Increased biochemical and structural understanding of S2P may contribute to the development of specific inhibitors with minimal off-target effects. Novel protease inhibitors are generally rationally designed based on the known structure of the protease itself, or by mimicking the interaction with known protease substrates and/or inhibitors. To date, only three S2P has been fully structurally characterized: *Ec*RseP, RseP of *Kangiella koreensis* and the S2P of *Methanocaldococcus jannaschii* (30, 154).

Despite these challenges, S2P remains attractive drug targets and a limited number of inhibitors targeting S2P has been identified. Most notably, a subgroup of bacteriocins known as the LsbB family, target the S2P of selected Gram-positive bacteria (155-158). Bacteriocins are small, ribosomally synthesized peptides produced by bacteria that inhibit the growth of other bacteria in competition for nutrient and ecological niches. These antimicrobial peptides have predominantly been exploited as food preservatives; however, bacteriocins are receiving increased scientific interest as promising alternatives and/or complements to antibiotics due to their potent activity against multiple human pathogens (159, 160). Among the members of the LsbB family, Enterocin EJ97 (EntEJ97) and Enterocin K1 (EntK1) show the greatest therapeutic potential. EntEJ97 and EntK1 show potent activity against vancomycin-resistant enterococci at nanomolar concentrations *in vitro* (66, 158). Notably, EntEJ97 and EntK1 are autoclavable and retain antimicrobial activity in blood, highlighting their therapeutic potential against systemic infections (66). The potent activity of EntK1 and EntEJ97 have been attributed to specific interaction with the enterococcal S2P (158, 161). As discussed above, enterococcal RseP is suggested to be important for stress tolerance and virulence in enterococci (48, 65, 66, 136, 137). Indeed, while spontaneous EntK1- and EntEJ97 resistant mutants can emerge due to mutations in *rseP*, these mutants show a 6-8-fold increase in lysozyme susceptibility, reduced tolerance to heat and a significant reduction

in desiccation tolerance (66, 158). Thus, resistance development seems to come at a high cost for the bacteria cell.

EntK1 and EntEJ97 are particularly attractive bacteriocins, not only because they act on VRE, but also because they are synthesized without a N-terminal leader sequence and contain no post-translational modifications (158, 161). This makes EntK1 and EntEJ97 an ideal starting point for bioengineering of novel S2P targeting antimicrobials. Indeed, the construction of a EntK1/EntEJ97 hybrid bacteriocin, designated Hybrid 1 (H1), exhibited a novel inhibition spectrum and improved activity compared to the parental bacteriocins (157). It was recently shown that the antimicrobial activity of EntK1 is dependent on its interactions with the PDZ-domain and Asn359 in the extended LDG motif of RseP in *E. faecium* (161). Interestingly, these regions have been implicated in substrate interaction for other bacterial S2P (e.g *Ec*RseP, Bacillus SpoIVFB) (162-166), and are conserved among several of the human pathogens discussed in this review.

Besides antimicrobial peptides, two commercially available protease inhibitors have been shown to have a surprising effect on S2P activity. Nelfinavir (Viacept), an FDA-approved protease inhibitor used in HIV therapy, is suggested to inhibit human S2P. The drug results in increased accumulation of the human S2P substrates AFT6 and SREBP1 (167, 168). In humans, S1P and S2P are involved in lipid metabolism and unfolded protein response (endoplasmatic reticulum stress) (169). Interestingly, nelfinavir shows promising anti-cancer properties, and the therapeutic potential of nelfinavir is currently being investigated for several types of cancers (168, 170-172). Nelfinavir and nelfinavir-analogs inhibit the proteolytic activity of *Mj*S2P, the S2P in *M. Jannaschii, in vitro,* indicating that this drug may be a potent inhibitor of bacterial S2P (168). However, the antimicrobial potential of nelfinavir is largely unexplored.

Additionally, Konovalova and colleagues recently identified batimastat, a broad-spectrum protease inhibitor known to target eukaryotic metalloproteases, as a potent inhibitor of *Ec*RseP (173). Structural analysis of the *Ec*RseP in complex with batimastat revealed that the binding mode of batimastat to *Ec*RseP depends on residues and regions known to be crucial for interaction with the native substrate RseA (Fig. 1A) (30). Notably, as also seen for

RseP:EntK1 interaction, this includes the extended LDG domain (30, 161). However, batimastat was identified as *Ec*RseP inhibitor in a screen using an efflux-deficient (Δ*tolC*) strain, with batimastat having no inhibitory effect on the wild-type efflux-intact strains (173). This likely hampers the therapeutic potential of batimastat in antimicrobial infections.

Future perspective and concluding remarks

S2P-mediated RIP is a well conserved signaling mechanism common to all forms of life. Notably, S2P and RIP play a key role in physiology and virulence in multiple human pathogens, including enterococci, staphylococci, and *M. tuberculosis*. The recent advances in the field have increased our understanding of the variety molecular mechanisms underlying S2P-mediated signaling and has raised the exiting possibility the S2P may serve as novel antimicrobial targets. So far, the small antimicrobial EntK1 and EntEJ97 are the only known antimicrobials specifically targeting S2P; however, as our structural and biochemical insights into S2P increase, more inhibitors are likely to be developed. Tools like Alphafold and artificial intelligence (AI) are revolutionizing the field of drug discovery by providing new ways to predict protein structures and identify potential inhibitors. The use of these technologies is expected to grow in the future as they will help researchers to understand the structure of S2P better and screen large libraries of potential inhibitors for those that effectively bind and inhibit S2P.

Acknowledgments

This study was financed by the Research Council of Norway through project number 275190. The founder had no role in conceptualization, data collection or interpretation, or the decision to submit the work for publication.

References

1. Schneider JS, Glickman MS. 2013. Function of site-2 proteases in bacteria and bacterial pathogens. Biochimi Biophys Acta 1828:2808-2814.
2. Urban S. 2009. Making the cut: central roles of intramembrane proteolysis in pathogenic microorganisms. Nat Rev Microbiol 7:411-23.
3. Wettstadt S, Llamas MA. 2020. Role of regulated proteolysis in the communication of bacteria with the environment. Front Mol Biosci 7:586497.
4. Sun L, Li X, Shi Y. 2016. Structural biology of intramembrane proteases: mechanistic insights from rhomboid and S2P to γ-secretase. Curr Opin Struct Biol 37:97-107.
5. Wolfe MS, Kopan R. 2004. Intramembrane proteolysis: theme and variations. Science 305:1119-1123.
6. Verhelst SHL. 2017. Intramembrane proteases as drug targets. FEBS J 284:1489-1502.
7. Beard HA, Barniol-Xicota M, Yang J, Verhelst SHL. 2019. Discovery of cellular roles of intramembrane proteases. ACS chemical biology 14:2372-2388.
8. Chen JC, Viollier PH, Shapiro L. 2005. A membrane metalloprotease participates in the sequential degradation of a *Caulobacter* polarity determinant. Mol Microbiol 55:1085-103.
9. Yokoyama T, Niinae T, Tsumagari K, Imami K, Ishihama Y, Hizukuri Y, Akiyama Y. 2021. The *Escherichia coli* S2P intramembrane protease RseP regulates ferric citrate uptake by cleaving the sigma factor regulator FecR. J Biol Chem 296.
10. King-Lyons ND, Smith KF, Connell TD. 2007. Expression of hurP, a gene encoding a prospective site 2 protease, is essential for heme-dependent induction of bhuR in *Bordetella bronchiseptica*. J Bacteriol 189:6266-6275.
11. Schöbel S, Zellmeier S, Schumann W, Wiegert T. 2004. The *Bacillus subtilis* sigmaW anti-sigma factor RsiW is degraded by intramembrane proteolysis through YluC. Mol Microbiol 52:1091-1105.
12. Makinoshima H, Glickman MS. 2006. Site-2 proteases in prokaryotes: regulated intramembrane proteolysis expands to microbial pathogenesis. Microbes and infection 8:1882-1888.
13. Chen G, Zhang X. 2010. New insights into S2P signaling cascades: regulation, variation, and conservation. Protein Science 19:2015-2030.
14. Kanehara K, Akiyama Y, Ito K. 2001. Characterization of the *yaeL* gene product and its S2P-protease motifs in *Escherichia coli*. Gene 281:71-79.
15. Rudner DZ, Fawcett P, Losick R. 1999. A family of membrane-embedded metalloproteases involved in regulated proteolysis of membrane-associated transcription factors. Proc Natl Acad Sci U S A 96:14765-14770.
16. Yu YT, Kroos L. 2000. Evidence that SpoIVFB is a novel type of membrane metalloprotease governing intercompartmental communication during *Bacillus subtilis* sporulation. J Bacteriol 182:3305-3309.
17. Kanehara K, Ito K, Akiyama Y. 2002. YaeL (EcfE) activates the sigma(E) pathway of stress response through a site-2 cleavage of anti-sigma(E), RseA. Genes Dev 16:2147-55.

18. Alba BM, Leeds JA, Onufryk C, Lu CZ, Gross CA. 2002. DegS and YaeL participate sequentially in the cleavage of RseA to activate the sigma(E)-dependent extracytoplasmic stress response. Genes Dev 16:2156-68.
19. Ades SE, Connolly LE, Alba BM, Gross CA. 1999. The *Escherichia coli* sigma(E)-dependent extracytoplasmic stress response is controlled by the regulated proteolysis of an anti-sigma factor. Genes Dev 13:2449-61.
20. De Las Peñas A, Connolly L, Gross CA. 1997. The sigmaE-mediated response to extracytoplasmic stress in *Escherichia coli* is transduced by RseA and RseB, two negative regulators of sigmaE. Mol Microbiol 24:373-85.
21. Missiakas D, Mayer MP, Lemaire M, Georgopoulos C, Raina S. 1997. Modulation of the *Escherichia coli* sigmaE (RpoE) heat-shock transcription-factor activity by the RseA, RseB and RseC proteins. Mol Microbiol 24:355-71.
22. Walsh NP, Alba BM, Bose B, Gross CA, Sauer RT. 2003. OMP peptide signals initiate the envelope-stress response by activating DegS protease via relief of inhibition mediated by its PDZ domain. Cell 113:61-71.
23. Akiyama Y, Kanehara K, Ito K. 2004. RseP (YaeL), an *Escherichia coli* RIP protease, cleaves transmembrane sequences. EMBO J 23:4434-42.
24. Li X, Wang B, Feng L, Kang H, Qi Y, Wang J, Shi Y. 2009. Cleavage of RseA by RseP requires a carboxyl-terminal hydrophobic amino acid following DegS cleavage. Proc Natl Acad Sci U S A 106:14837-14842.
25. Flynn JM, Levchenko I, Sauer RT, Baker TA. 2004. Modulating substrate choice: the SspB adaptor delivers a regulator of the extracytoplasmic-stress response to the AAA+ protease ClpXP for degradation. Genes Dev 18:2292-2301.
26. Hizukuri Y, Oda T, Tabata S, Tamura-Kawakami K, Oi R, Sato M, Takagi J, Akiyama Y, Nogi T. 2014. A structure-based model of substrate discrimination by a noncanonical PDZ tandem in the intramembrane-cleaving protease RseP. Structure 22:326-336.
27. Kanehara K, Ito K, Akiyama Y. 2003. YaeL proteolysis of RseA is controlled by the PDZ domain of YaeL and a Gln-rich region of RseA. EMBO J 22:6389-6398.
28. Inaba K, Suzuki M, Maegawa K-i, Akiyama S, Ito K, Akiyama Y. 2008. A pair of circularly permutated PDZ domains control RseP, the S2P family intramembrane protease of *Escherichia coli*. J Biol Chem 283:35042-35052.
29. Bohn C, Collier J, Bouloc P. 2004. Dispensable PDZ domain of *Escherichia coli* YaeL essential protease. Mol Microbiol 52:427-35.
30. Imaizumi Y, Takanuki K, Miyake T, Takemoto M, Hirata K, Hirose M, Oi R, Kobayashi T, Miyoshi K, Aruga R. 2022. Mechanistic insights into intramembrane proteolysis by *E. coli* site-2 protease homolog RseP. Sci Adv 34.
31. Cezairliyan BO, Sauer RT. 2007. Inhibition of regulated proteolysis by RseB. Proc Natl Acad Sci U S A 104:3771-3776.
32. Kim DY, Kwon E, Choi J, Hwang HY, Kim KK. 2010. Structural basis for the negative regulation of bacterial stress response by RseB. Protein Sci 19:1258-63.
33. Chaba R, Alba BM, Guo MS, Sohn J, Ahuja N, Sauer RT, Gross CA. 2011. Signal integration by DegS and RseB governs the σ E-mediated envelope stress response in *Escherichia coli*. Proc Natl Acad Sci U S A 108:2106-2111.
34. Wollmann P, Zeth K. 2007. The structure of RseB: a sensor in periplasmic stress response of *E. coli*. J Mol Biol 372:927-941.

35. Lima S, Guo MS, Chaba R, Gross CA, Sauer RT. 2013. Dual molecular signals mediate the bacterial response to outer-membrane stress. Science 340:837-41.
36. Zhou R, Cusumano C, Sui D, Garavito RM, Kroos L. 2009. Intramembrane proteolytic cleavage of a membrane-tethered transcription factor by a metalloprotease depends on ATP. Proc Natl Acad Sci U S A 106:16174-9.
37. Tan IS, Ramamurthi KS. 2014. Spore formation in *Bacillus subtilis*. Environ Microbiol Rep 6:212-25.
38. Zhang B, Hofmeister A, Kroos L. 1998. The prosequence of pro-sigmaK promotes membrane association and inhibits RNA polymerase core binding. J Bacteriol 180:2434-41.
39. Zhou R, Kroos L. 2004. BofA protein inhibits intramembrane proteolysis of pro-σK in an intercompartmental signaling pathway during *Bacillus subtilis* sporulation. Proc Natl Acad Sci U S A 101:6385-6390.
40. Rudner DZ, Losick R. 2002. A sporulation membrane protein tethers the pro-sigmaK processing enzyme to its inhibitor and dictates its subcellular localization. Genes Dev 16:1007-18.
41. Olenic S, Heo L, Feig M, Kroos L. 2022. Inhibitory proteins block substrate access by occupying the active site cleft of *Bacillus subtilis* intramembrane protease SpoIVFB. Elife 11.
42. Campo N, Rudner DZ. 2006. A branched pathway governing the activation of a developmental transcription factor by regulated intramembrane proteolysis. Mol Cell 23:25-35.
43. Zhou R, Kroos L. 2005. Serine proteases from two cell types target different components of a complex that governs regulated intramembrane proteolysis of pro-sigmaK during *Bacillus subtilis* development. Mol Microbiol 58:835-46.
44. Dong TC, Cutting SM. 2003. SpoIVB-mediated cleavage of SpoIVFA could provide the intercellular signal to activate processing of Pro-sigmaK in *Bacillus subtilis*. Mol Microbiol 49:1425-34.
45. Ragland SA, Criss AK. 2017. From bacterial killing to immune modulation: Recent insights into the functions of lysozyme. PLoS Pathog 13:e1006512.
46. Ho TD, Ellermeier CD. 2019. Activation of the extracytoplasmic function σ factor σV by lysozyme. Mol Microbiol 112:410-419.
47. Ho TD, Hastie JL, Intile PJ, Ellermeier CD. 2011. The *Bacillus subtilis* extracytoplasmic function σ factor σ(V) is induced by lysozyme and provides resistance to lysozyme. J Bacteriol 193:6215-22.
48. Varahan S, Iyer VS, Moore WT, Hancock LE. 2013. Eep confers lysozyme resistance to *Enterococcus faecalis* via the activation of the extracytoplasmic function sigma factor SigV. J Biol Chem 195:3125-3134.
49. Pannullo AG, Ellermeier CD. 2022. Activation of the extracytoplasmic function σ factor σV in *Clostridioides difficile* requires regulated intramembrane proteolysis of the anti-σ factor RsiV. mSphere 7:e00092-22.
50. Bera A, Herbert S, Jakob A, Vollmer W, Götz F. 2005. Why are pathogenic staphylococci so lysozyme resistant? The peptidoglycan O-acetyltransferase OatA is the major determinant for lysozyme resistance of *Staphylococcus aureus*. Mol Microbiol 55:778-87.

51. Hastie JL, Williams KB, Ellermeier CD. 2013. The activity of σV, an extracytoplasmic function σ factor of *Bacillus subtilis*, is controlled by regulated proteolysis of the anti-σ factor RsiV. J Bacteriol 195:3135-44.
52. Yoshimura M, Asai K, Sadaie Y, Yoshikawa H. 2004. Interaction of *Bacillus subtilis* extracytoplasmic function (ECF) sigma factors with the N-terminal regions of their potential anti-sigma factors. Microbiology (Reading) 150:591-599.
53. Hastie JL, Williams KB, Sepúlveda C, Houtman JC, Forest KT, Ellermeier CD. 2014. Evidence of a bacterial receptor for lysozyme: binding of lysozyme to the anti-σ factor RsiV controls activation of the ecf σ factor σV. PLoS Genet 10:e1004643.
54. Hastie JL, Williams KB, Bohr LL, Houtman JC, Gakhar L, Ellermeier CD. 2016. The anti-sigma factor RsiV Is a bacterial receptor for lysozyme: co-crystal structure determination and demonstration that binding of lysozyme to RsiV Is required for σV activation. PLoS Genet 12:e1006287.
55. Castro AN, Lewerke LT, Hastie JL, Ellermeier CD. 2018. Signal peptidase is necessary and sufficient for site 1 cleavage of RsiV in *Bacillus subtilis* in response to lysozyme. J Bacteriol 200.
56. Guariglia-Oropeza V, Helmann JD. 2011. *Bacillus subtilis* σ(V) confers lysozyme resistance by activation of two cell wall modification pathways, peptidoglycan O-acetylation and D-alanylation of teichoic acids. J Bacteriol 193:6223-32.
57. Rouchon CN, Harris J, Zubair-Nizami Z, Weinstein AJ, Roky M, Frank KL. 2022. The cationic antimicrobial peptide activity of lysozyme reduces viable *Enterococcus faecalis* cells in biofilms. Antimicrob Agents Chemother

66:e02339-21.
58. Ho TD, Williams KB, Chen Y, Helm RF, Popham DL, Ellermeier CD. 2014. *Clostridium difficile* extracytoplasmic function σ factor σV regulates lysozyme resistance and is necessary for pathogenesis in the hamster model of infection. Infect Immun 82:2345-55.
59. Woods EC, Nawrocki KL, Suárez JM, McBride SM. 2016. The *Clostridium difficile* Dlt pathway is controlled by the extracytoplasmic function sigma factor σV in response to lysozyme. Infect Immun 84:1902-1916.
60. Kaus GM, Snyder LF, Müh U, Flores MJ, Popham DL, Ellermeier CD. 2020. Lysozyme resistance in *Clostridioides difficile* is dependent on two peptidoglycan deacetylases. J Bacteriol 202:e00421-20.
61. Parthasarathy S, Wang X, Carr KR, Varahan S, Hancock EB, Hancock LE. 2021. SigV mediates lysozyme resistance in *Enterococcus faecalis* via RsiV and PgdA. J Bacteriol 203:e0025821.
62. Le Jeune A, Torelli R, Sanguinetti M, Giard JC, Hartke A, Auffray Y, Benachour A. 2010. The extracytoplasmic function sigma factor SigV plays a key role in the original model of lysozyme resistance and virulence of *Enterococcus faecalis*. PLoS One 5:e9658.
63. Benachour A, Ladjouzi R, Le Jeune A, Hébert L, Thorpe S, Courtin P, Chapot-Chartier MP, Prajsnar TK, Foster SJ, Mesnage S. 2012. The lysozyme-induced peptidoglycan N-acetylglucosamine deacetylase PgdA (EF1843) is required for *Enterococcus faecalis* virulence. J Bacteriol 194:6066-73.

64. Hébert L, Courtin P, Torelli R, Sanguinetti M, Chapot-Chartier MP, Auffray Y, Benachour A. 2007. *Enterococcus faecalis* constitutes an unusual bacterial model in lysozyme resistance. Infect Immun 75:5390-8.
65. Benachour A, Muller C, Dabrowski-Coton M, Le Breton Y, Giard JC, Rincé A, Auffray Y, Hartke A. 2005. The *Enterococcus faecalis* sigV protein is an extracytoplasmic function sigma factor contributing to survival following heat, acid, and ethanol treatments. J Bacteriol 187:1022-35.
66. Reinseth I, Tønnesen HH, Carlsen H, Diep DB. 2021. Exploring the Therapeutic Potenital of the Leaderless Enterocins K1 and EJ97 in the Treatment of Vancomycin-Resistant Enterococcal Infection. Front Microbiol 12:248.
67. Llamas MA, Sánchez-Jiménez A. 2022. Iron Homeostasis in *Pseudomonas aeruginosa*: Targeting Iron Acquisition and Storage as an Antimicrobial Strategy. Adv Exp Med Biol 1386:29-68.
68. Sheldon JR, Laakso HA, Heinrichs DE. 2016. Iron Acquisition Strategies of Bacterial Pathogens. Microbiol Spectr 4.
69. Chevalier S, Bouffartigues E, Bazire A, Tahrioui A, Duchesne R, Tortuel D, Maillot O, Clamens T, Orange N, Feuilloley MG. 2019. Extracytoplasmic function sigma factors in *Pseudomonas aeruginosa*. Biochim Biophys Acta Gene Regul Mech 1862:706-721.
70. Llamas MA, Imperi F, Visca P, Lamont IL. 2014. Cell-surface signaling in Pseudomonas: stress responses, iron transport, and pathogenicity. FEMS microbiology reviews 38:569-597.
71. Draper RC, Martin LW, Beare PA, Lamont IL. 2011. Differential proteolysis of sigma regulators controls cell-surface signalling in *Pseudomonas aeruginosa*. Molecular microbiology 82:1444-1453.
72. Otero-Asman JR, García-García AI, Civantos C, Quesada JM, Llamas MA. 2019. *Pseudomonas aeruginosa* possesses three distinct systems for sensing and using the host molecule haem. Environ Microbiol 21:4629-4647.
73. Bastiaansen KC, Ibañez A, Ramos JL, Bitter W, Llamas MA. 2014. The Prc and RseP proteases control bacterial cell-surface signalling activity. Environ Microbiol 16:2433-2443.
74. Bastiaansen KC, Otero-Asman JR, Luirink J, Bitter W, Llamas MA. 2015. Processing of cell-surface signalling anti-sigma factors prior to signal recognition is a conserved autoproteolytic mechanism that produces two functional domains. Environ Microbiol 17:3263-77.
75. Cai Z, Yang F, Shao X, Yue Z, Li Z, Song Y, Pan X, Jin Y, Cheng Z, Ha UH, Feng J, Yang L, Deng X, Wu W, Bai F. 2022. ECF sigma factor HxuI is critical for in vivo fitness of *Pseudomonas aeruginosa* during Infection. Microbiol Spectr 10:e0162021.
76. Damron FH, Oglesby-Sherrouse AG, Wilks A, Barbier M. 2016. Dual-seq transcriptomics reveals the battle for iron during *Pseudomonas aeruginosa* acute murine pneumonia. Sci Rep 6:39172.
77. Minandri F, Imperi F, Frangipani E, Bonchi C, Visaggio D, Facchini M, Pasquali P, Bragonzi A, Visca P. 2016. Role of iron uptake systems in *Pseudomonas aeruginosa* virulence and airway infection. Infect Immun 84:2324-2335.
78. Wilderman PJ, Vasil AI, Johnson Z, Wilson MJ, Cunliffe HE, Lamont IL, Vasil ML. 2001. Characterization of an endoprotease (PrpL) encoded by a PvdS-regulated gene in *Pseudomonas aeruginosa*. Infect Immun 69:5385-94.

79. Imperi F, Massai F, Facchini M, Frangipani E, Visaggio D, Leoni L, Bragonzi A, Visca P. 2013. Repurposing the antimycotic drug flucytosine for suppression of *Pseudomonas aeruginosa* pathogenicity. Proc Natl Acad Sci U S A 110:7458-63.
80. Hunt TA, Peng WT, Loubens I, Storey DG. 2002. The *Pseudomonas aeruginosa* alternative sigma factor PvdS controls exotoxin A expression and is expressed in lung infections associated with cystic fibrosis. Microbiology (Reading) 148:3183-3193.
81. Ochsner UA, Wilderman PJ, Vasil AI, Vasil ML. 2002. GeneChip expression analysis of the iron starvation response in *Pseudomonas aeruginosa*: identification of novel pyoverdine biosynthesis genes. Mol Microbiol 45:1277-87.
82. Woods EC, McBride SM. 2017. Regulation of antimicrobial resistance by extracytoplasmic function (ECF) sigma factors. Microbes Infect 19:238-248.
83. Ho TD, Nauta KM, Luhmann EK, Radoshevich L, Ellermeier CD. 2022. Identification of the extracytoplasmic function σ Factor σ(P) regulon in *Bacillus thuringiensis*. mSphere 7:e0096721.
84. Ho TD, Nauta KM, Müh U, Ellermeier CD. 2019. Activation of the extracytoplasmic function σ factor σP by β-lactams in *Bacillus thuringiensis* requires the site-2 protease RasP. Msphere 4:e00511-19.
85. Nauta KM, Ho TD, Ellermeier CD. 2022. Signal peptidase-mediated cleavage of the anti-σ factor RsiP at site 1 controls σP activation and β-lactam resistance in *Bacillus thuringiensis*. Mbio 13:e03707-21.
86. Nauta KM, Ho TD, Ellermeier CD. 2021. The penicillin-binding protein PbpP is a sensor of β-Lactams and is required for activation of the extracytoplasmic function σ factor σP in *Bacillus thuringiensis*. Mbio 12:e00179-21.
87. Cao M, Wang T, Ye R, Helmann JD. 2002. Antibiotics that inhibit cell wall biosynthesis induce expression of the *Bacillus subtilis* σW and σM regulons. Mol Microbiol 45:1267-1276.
88. Pietiäinen M, Gardemeister M, Mecklin M, Leskelä S, Sarvas M, Kontinen VP. 2005. Cationic antimicrobial peptides elicit a complex stress response in *Bacillus subtilis* that involves ECF-type sigma factors and two-component signal transduction systems. Microbiology (Reading) 151:1577-1592.
89. Butcher BG, Helmann JD. 2006. Identification of *Bacillus subtilis* σW-dependent genes that provide intrinsic resistance to antimicrobial compounds produced by Bacilli. Mol Microbiol 60:765-782.
90. Schöbel S, Zellmeier S, Schumann W, Wiegert T. 2004. The *Bacillus subtilis* simaW anti-sigma factor RsiW is degraded by intramembrane proteolysis through YluC. Mol Microbiol 52:1091-1105.
91. Heinrich J, Wiegert T. 2006. YpdC determines site-1 degradation in regulated intramembrane proteolysis of the RsiW anti-sigma factor of *Bacillus subtilis*. Mol Microbiol 62:566-79.
92. Ellermeier CD, Losick R. 2006. Evidence for a novel protease governing regulated intramembrane proteolysis and resistance to antimicrobial peptides in *Bacillus subtilis*. Genes Dev 20:1911-1922.
93. Petersohn A, Brigulla M, Haas S, Hoheisel JrD, Völker U, Hecker M. 2001. Global analysis of the general stress response of *Bacillus subtilis*. J Bacteriol 183:5617-5631.

94. Ross CL, Thomason KS, Koehler TM. 2009. An extracytoplasmic function sigma factor controls β-Lactamase gene expression in *Bacillus anthracis* and other *Bacillus cereus* group Species. J Bacteriol 191:6683-6693.
95. Chen JC, Hottes AK, McAdams HH, McGrath PT, Viollier PH, Shapiro L. 2006. Cytokinesis signals truncation of the PodJ polarity factor by a cell cycle-regulated protease. EMBO J 25:377-386.
96. An FY, Sulavik MC, Clewell DB. 1999. Identification and characterization of a determinant (*eep*) on the *Enterococcus faecalis* chromosome that is involved in production of the peptide sex pheromone cAD1. J Bacteriol 181:5915-21.
97. An FY, Clewell DB. 2002. Identification of the cAD1 sex pheromone precursor in *Enterococcus faecalis*. J Bacteriol 184:1880-7.
98. Antiporta MH, Dunny GM. 2002. *ccfA*, the genetic determinant for the cCF10 peptide pheromone in *Enterococcus faecalis* OG1RF. J Bacteriol 184:1155-62.
99. Chandler JR, Flynn AR, Bryan EM, Dunny GM. 2005. Specific control of endogenous cCF10 pheromone by a conserved domain of the pCF10-encoded regulatory protein PrgY in *Enterococcus faecalis*. J Bacteriol 187:4830-4843.
100. Xayarath B, Alonzo III F, Freitag NE. 2015. Identification of a peptide-pheromone that enhances *Listeria monocytogenes* escape from host cell vacuoles. PLoS Pathog 11:e1004707.
101. Sklar JG, Makinoshima H, Schneider JS, Glickman MS. 2010. *M. tuberculosis* intramembrane protease Rip1 controls transcription through three anti-sigma factor substrates. Mol Microbiol 77:605-617.
102. Schneider JS, Sklar JG, Glickman MS. 2014. The Rip1 protease of *Mycobacterium tuberculosis* controls the SigD regulon. J Bacteriol 196:2638-2645.
103. Damron FH, Goldberg JB. 2012. Proteolytic regulation of alginate overproduction in *Pseudomonas aeruginosa*. Mol Microbiol 84:595-607.
104. Cheng D, Lv H, Yao Y, Cheng S, Huang Q, Wang H, Liu X, Bae T, Li M, Liu Q. 2020. The roles of the site-2 protease Eep in *Staphylococcus aureus*. J Bacteriol doi:10.1128/JB.00046-20.
105. Schilcher K, Caesar LK, Cech NB, Horswill AR. 2020. Processing, export, and identification of novel linear peptides from *Staphylococcus aureus*. Mbio 11:e00112-20.
106. Denham E, Ward P, Leigh J. 2008. Lipoprotein signal peptides are processed by Lsp and Eep of *Streptococcus uberis*. J Bacteriol 190:4641-4647.
107. Pérez-Pascual D, Gaudu P, Fleuchot B, Besset C, Rosinski-Chupin I, Guillot A, Monnet V, Gardan R. 2015. RovS and its associated signaling peptide form a cell-to-cell communication system required for *Streptococcus agalactiae* pathogenesis. mBio 6:e02306-14.
108. Chang JC, LaSarre B, Jimenez JC, Aggarwal C, Federle MJ. 2011. Two group A streptococcal peptide pheromones act through opposing Rgg regulators to control biofilm development. PLoS Pathog 7:e1002190.
109. Matson JS, DiRita VJ. 2005. Degradation of the membrane-localized virulence activator TcpP by the YaeL protease in *Vibrio cholerae*. Proc Natl Acad Sci U S A 102:16403-16408.

110. Teoh WP, Matson JS, DiRita VJ. 2015. Regulated intramembrane proteolysis of the virulence activator TcpP in *Vibrio cholerae* is initiated by the tail-specific protease (Tsp). Mol Microbiol 97:822-31.
111. Hogardt M, Heesemann J. 2010. Adaptation of *Pseudomonas aeruginosa* during persistence in the cystic fibrosis lung. Int J Med Microbiol 300:557-62.
112. Pritt B, O'Brien L, Winn W. 2007. Mucoid Pseudomonas in cystic fibrosis. Am J Clin Pathol 128:32-4.
113. Wood LF, Ohman DE. 2009. Use of cell wall stress to characterize sigma 22 (AlgT/U) activation by regulated proteolysis and its regulon in *Pseudomonas aeruginosa*. Mol Microbiol 72:183-201.
114. Wood LF, Leech AJ, Ohman DE. 2006. Cell wall-inhibitory antibiotics activate the alginate biosynthesis operon in Pseudomonas aeruginosa: Roles of sigma (AlgT) and the AlgW and Prc proteases. Mol Microbiol 62:412-26.
115. Li S, Lou X, Xu Y, Teng X, Liu R, Zhang Q, Wu W, Wang Y, Bartlam M. 2019. Structural basis for the recognition of MucA by MucB and AlgU in *Pseudomonas aeruginosa*. FEBS J 286:4982-4994.
116. Qiu D, Eisinger VM, Rowen DW, Yu HD. 2007. Regulated proteolysis controls mucoid conversion in *Pseudomonas aeruginosa*. Proc Natl Acad Sci U S A 104:8107-8112.
117. Cezairliyan BO, Sauer RT. 2009. Control of *Pseudomonas aeruginosa* AlgW protease cleavage of MucA by peptide signals and MucB. Mol Microbiol 72:368-79.
118. Damron FH, Hongwei DY. 2011. Pseudomonas aeruginosa MucD regulates the alginate pathway through activation of MucA degradation via MucP proteolytic activity. Journal of bacteriology 193:286-291.
119. Qiu D, Eisinger VM, Head NE, Pier GB, Yu HD. 2008. ClpXP proteases positively regulate alginate overexpression and mucoid conversion in *Pseudomonas aeruginosa*. Microbiology (Reading) 154:2119-2130.
120. Bragonzi A, Wiehlmann L, Klockgether J, Cramer N, Worlitzsch D, Döring G, Tümmler B. 2006. Sequence diversity of the *mucABD* locus in *Pseudomonas aeruginosa* isolates from patients with cystic fibrosis. Microbiology (Reading) 152:3261-3269.
121. Pulcrano G, Iula DV, Raia V, Rossano F, Catania MR. 2012. Different mutations in *mucA* gene of *Pseudomonas aeruginosa* mucoid strains in cystic fibrosis patients and their effect on *algU* gene expression. New Microbiol 35:295-305.
122. Antimicrobial-Resistance-Collaborators. 2022. Global burden of bacterial antimicrobial resistance in 2019: a systematic analysis. Lancet 399:629-655.
123. Maitra A, Munshi T, Healy J, Martin LT, Vollmer W, Keep NH, Bhakta S. 2019. Cell wall peptidoglycan in *Mycobacterium tuberculosis*: An Achilles' heel for the TB-causing pathogen. FEMS Microbiol Rev 43:548-575.
124. Garcia-Vilanova A, Chan J, Torrelles JB. 2019. Underestimated manipulative roles of *Mycobacterium tuberculosis* cell envelope glycolipids during infection. Front Immunol 10:2909.
125. Makinoshima H, Glickman MS. 2005. Regulation of *Mycobacterium tuberculosis* cell envelope composition and virulence by intramembrane proteolysis. Nature 436:406-409.
126. Buglino JA, Sankhe GD, Lazar N, Bean JM, Glickman MS. 2021. Integrated sensing of host stresses by inhibition of a cytoplasmic two-component system controls *M. tuberculosis* acute lung infection. Elife 10:e65351.

127. Calamita H, Ko C, Tyagi S, Yoshimatsu T, Morrison NE, Bishai WR. 2005. The *Mycobacterium tuberculosis* SigD sigma factor controls the expression of ribosome-associated gene products in stationary phase and is required for full virulence. Cell Microbiol 7:233-44.
128. Raman S, Hazra R, Dascher CC, Husson RN. 2004. Transcription regulation by the *Mycobacterium tuberculosis* alternative sigma factor SigD and its role in virulence. J Bacteriol 186:6605-6616.
129. Mukherjee P, Sureka K, Datta P, Hossain T, Barik S, Das KP, Kundu M, Basu J. 2009. Novel role of Wag31 in protection of mycobacteria under oxidative stress. Mol Microbiol 73:103-119.
130. Schilcher K, Caesar LK, Cech NB, Horswill AR. 2020. Processing, Export, and Identification of Novel Linear Peptides from Staphylococcus aureus. mBio 11.
131. Saito A, Hizukuri Y, Matsuo E-i, Chiba S, Mori H, Nishimura O, Ito K, Akiyama Y. 2011. Post-liberation cleavage of signal peptides is catalyzed by the site-2 protease (S2P) in bacteria. Proc Natl Acad Sci U S A 108:13740-13745.
132. Reinseth IS, Ovchinnikov KV, Tønnesen HH, Carlsen H, Diep DB. 2019. The Increasing Issue of vancomycin-resistant Enterococci and the bacteriocin solution. Probiotics Antimicrob Proteins 12:1203-1217.
133. Cattoir V, Leclercq R. 2013. Twenty-five years of shared life with vancomycin-resistant enterococci: is it time to divorce? J Antimicrob Chemother 68:731-42.
134. Chandler JR, Dunny GM. 2008. Characterization of the sequence specificity determinants required for processing and control of sex pheromone by the intramembrane protease Eep and the plasmid-encoded protein PrgY. J Bacteriol 190:1172-1183.
135. Varahan S, Harms N, Gilmore MS, Tomich JM, Hancock L. 2014. An ABC transporter is required for secretion of peptide sex pheromones in *Enterococcus faecalis*. mBio 5:e01726-14.
136. Frank KL, Barnes AM, Grindle SM, Manias DA, Schlievert PM, Dunny GM. 2012. Use of recombinase-based in vivo expression technology to characterize *Enterococcus faecalis* gene expression during infection identifies in vivo-expressed antisense RNAs and implicates the protease Eep in pathogenesis. Infect Immun 80:539-549.
137. Frank KL, Guiton PS, Barnes AM, Manias DA, Chuang-Smith ON, Kohler PL, Spaulding AR, Hultgren SJ, Schlievert PM, Dunny GM. 2013. AhrC and Eep are biofilm infection-associated virulence factors in *Enterococcus faecalis*. Infect Immun 81:1696-1708.
138. Bourgogne A, Garsin DA, Qin X, Singh KV, Sillanpaa J, Yerrapragada S, Ding Y, Dugan-Rocha S, Buhay C, Shen H, Chen G, Williams G, Muzny D, Maadani A, Fox KA, Gioia J, Chen L, Shang Y, Arias CA, Nallapareddy SR, Zhao M, Prakash VP, Chowdhury S, Jiang H, Gibbs RA, Murray BE, Highlander SK, Weinstock GM. 2008. Large scale variation in *Enterococcus faecalis* illustrated by the genome analysis of strain OG1RF. Genome Biol 9:R110.
139. Håvarstein LS, Coomaraswamy G, Morrison DA. 1995. An unmodified heptadecapeptide pheromone induces competence for genetic transformation in *Streptococcus pneumoniae*. Proc Natl Acad Sci U S A 92:11140-11144.
140. Thoendel M, Horswill AR. 2010. Biosynthesis of peptide signals in gram-positive bacteria. Adv Appl Microbiol 71:91-112.

141. Shaw LN, Lindholm C, Prajsnar TK, Miller HK, Brown MC, Golonka E, Stewart GC, Tarkowski A, Potempa J. 2008. Identification and characterization of sigma S, a novel component of the *Staphylococcus aureus* stress and virulence responses. PLoS One 3:e3844.
142. Miller HK, Carroll RK, Burda WN, Krute CN, Davenport JE, Shaw LN. 2012. The extracytoplasmic function sigma factor σ S protects against both intracellular and extracytoplasmic stresses in *Staphylococcus aureus*. J Bacteriol 194:4342-54.
143. Mitchell G, Fugère A, Pépin Gaudreau K, Brouillette E, Frost EH, Cantin AM, Malouin F. 2013. SigB is a dominant regulator of virulence in Staphylococcus aureus small-colony variants. PLoS One 8:e65018.
144. Jonsson IM, Arvidson S, Foster S, Tarkowski A. 2004. Sigma factor B and RsbU are required for virulence in *Staphylococcus aureus*-induced arthritis and sepsis. Infect Immun 72:6106-11.
145. Krute CN, Bell-Temin H, Miller HK, Rivera FE, Weiss A, Stevens SM, Shaw LN. 2015. The membrane protein PrsS mimics σ S in protecting *Staphylococcus aureus* against cell wall-targeting antibiotics and DNA-damaging agents. Microbiology (Reading) 161:1136-1148.
146. Entenza JM, Moreillon P, Senn MM, Kormanec J, Dunman PM, Berger-Bächi B, Projan S, Bischoff M. 2005. Role of sigma B in the expression of *Staphylococcus aureus* cell wall adhesins ClfA and FnbA and contribution to infectivity in a rat model of experimental endocarditis. Infect Immun 73:990-8.
147. Goerke C, Fluckiger U, Steinhuber A, Bisanzio V, Ulrich M, Bischoff M, Patti JM, Wolz C. 2005. Role of Staphylococcus aureus global regulators *sae* and sigma B in virulence gene expression during device-related infection. Infect Immun 73:3415-21.
148. Matson JS, Withey JH, DiRita VJ. 2007. Regulatory networks controlling *Vibrio cholerae* virulence gene expression. Infect Immun 75:5542-9.
149. Beck NA, Krukonis ES, DiRita VJ. 2004. TcpH influences virulence gene expression in *Vibrio cholerae* by inhibiting degradation of the transcription activator TcpP. J Bacteriol 186:8309-16.
150. Krukonis ES, Yu RR, Dirita VJ. 2000. The *Vibrio cholerae* ToxR/TcpP/ToxT virulence cascade: distinct roles for two membrane-localized transcriptional activators on a single promoter. Mol Microbiol 38:67-84.
151. Almagro-Moreno S, Root MZ, Taylor RK. 2015. Role of ToxS in the proteolytic cascade of virulence regulator ToxR in *Vibrio cholerae*. Mol Microbiol 98:963-76.
152. Almagro-Moreno S, Kim TK, Skorupski K, Taylor RK. 2015. Proteolysis of virulence regulator ToxR is associated with entry of *Vibrio cholerae* into a dormant state. PLoS Genet 11:e1005145.
153. Kinch LN, Ginalski K, Grishin NV. 2006. Site-2 protease regulated intramembrane proteolysis: sequence homologs suggest an ancient signaling cascade. Protein Sci 15:84-93.
154. Feng L, Yan H, Wu Z, Yan N, Wang Z, Jeffrey PD, Shi Y. 2007. Structure of a site-2 protease family intramembrane metalloprotease. Science 318:1608-1612.
155. Ovchinnikov KV, Kristiansen PE, Uzelac G, Topisirovic L, Kojic M, Nissen-Meyer J, Nes IF, Diep DB. 2014. Defining the structure and receptor binding domain of the leaderless bacteriocin LsbB. J Biol Chem 289:23838-45.

156. Uzelac G, Kojic M, Lozo J, Aleksandrzak-Piekarczyk T, Gabrielsen C, Kristensen T, Nes IF, Diep DB, Topisirovic L. 2013. A Zn-dependent metallopeptidase is responsible for sensitivity to LsbB, a class II leaderless bacteriocin of *Lactococcus lactis* subsp. lactis BGMN1-5. J Bacteriol 195:5614-21.
157. Kranjec C, Kristensen SS, Bartkiewicz KT, Brønner M, Cavanagh JP, Srikantam A, Mathiesen G, Diep DB. 2021. A bacteriocin-based treatment option for *Staphylococcus haemolyticus* biofilms. Sci Rep 11:13909.
158. Ovchinnikov KV, Kristiansen PE, Straume D, Jensen MS, Aleksandrzak-Piekarczyk T, Nes IF, Diep DB. 2017. The Leaderless Bacteriocin Enterocin K1 Is Highly Potent against *Enterococcus faecium*: A Study on Structure, Target Spectrum and Receptor. Front Microbiol 8:774.
159. Cotter PD, Ross RP, Hill C. 2013. Bacteriocins - a viable alternative to antibiotics? Nat Rev Microbiol 11:95-105.
160. Soltani S, Hammami R, Cotter PD, Rebuffat S, Said LB, Gaudreau H, Bédard F, Biron E, Drider D, Fliss I. 2021. Bacteriocins as a new generation of antimicrobials: toxicity aspects and regulations. FEMS Microbiol Rev 45.
161. Kristensen SS, Oftedal TF, Røhr Å K, Eijsink VGH, Mathiesen G, Diep DB. 2022. The extracellular domain of site-2-metalloprotease RseP is important for sensitivity to bacteriocin EntK1. J Biol Chem 298:102593.
162. Koide K, Ito K, Akiyama Y. 2008. Substrate recognition and binding by RseP, an *Escherichia coli* intramembrane protease. J Biol Chem 283:9562-9570.
163. Akiyama K, Hizukuri Y, Akiyama Y. 2017. Involvement of a conserved GFG motif region in substrate binding by RseP, an *Escherichia coli* S2P protease. Mol Microbiol 104:737-751.
164. Akiyama K, Mizuno S, Hizukuri Y, Mori H, Nogi T, Akiyama Y. 2015. Roles of the membrane-reentrant β-hairpin-like loop of RseP protease in selective substrate cleavage. Elife 4:e08928.
165. Zhang Y, Luethy PM, Zhou R, Kroos L. 2013. Residues in conserved loops of intramembrane metalloprotease SpoIVFB interact with residues near the cleavage site in pro-σK. J Bacteriol 195:4936-4946.
166. Olenic S, Buchanan F, VanPortfliet J, Parrell D, Kroos L. 2022. Conserved proline residues of *Bacillus subtilis* intramembrane metalloprotease SpoIVFB are important for substrate interaction and cleavage. J Bacteriol 204:e0038621.
167. Guan M, Fousek K, Jiang C, Guo S, Synold T, Xi B, Shih CC, Chow WA. 2011. Nelfinavir induces liposarcoma apoptosis through inhibition of regulated intramembrane proteolysis of SREBP-1 and ATF6. Clin Cancer Res 17:1796-806.
168. Guan M, Su L, Yuan Y-C, Li H, Chow WA. 2015. Nelfinavir and nelfinavir analogs block site-2 protease cleavage to inhibit castration-resistant prostate cancer. Sci Rep 5:1-8.
169. Danyukova T, Schöneck K, Pohl S. 2021. Site-1 and site-2 proteases: A team of two in regulated proteolysis. Biochim Biophys Acta Mol Cell Res 1869:119138.
170. Kawabata S, Connis N, Gills JJ, Hann CL, Dennis PA. 2021. Nelfinavir Inhibits the Growth of Small-cell Lung Cancer Cells and Patient-derived Xenograft Tumors. Anticancer Res 41:91-99.
171. Gantt S, Casper C, Ambinder RF. 2013. Insights into the broad cellular effects of nelfinavir and the HIV protease inhibitors supporting their role in cancer treatment and prevention. Curr Opin Oncol 25:495-502.

172. Gills JJ, Lopiccolo J, Tsurutani J, Shoemaker RH, Best CJ, Abu-Asab MS, Borojerdi J, Warfel NA, Gardner ER, Danish M, Hollander MC, Kawabata S, Tsokos M, Figg WD, Steeg PS, Dennis PA. 2007. Nelfinavir, A lead HIV protease inhibitor, is a broad-spectrum, anticancer agent that induces endoplasmic reticulum stress, autophagy, and apoptosis *in vitro* and *in vivo*. Clin Cancer Res 13:5183-94.
173. Konovalova A, Grabowicz M, Balibar CJ, Malinverni JC, Painter RE, Riley D, Mann PA, Wang H, Garlisi CG, Sherborne B. 2018. Inhibitor of intramembrane protease RseP blocks the σ E response causing lethal accumulation of unfolded outer membrane proteins. Proc Natl Acad Sci U S A 115:E6614-E6621.

Paper II

scientific reports

Check for updates

OPEN

A bacteriocin-based treatment option for *Staphylococcus haemolyticus* biofilms

Christian Kranjec[1,5], Sofie S. Kristensen[1,5], Karolina T. Bartkiewicz[1], Mikkel Brønner[1], Jorunn P. Cavanagh[2,3], Aparna Srikantam[4], Geir Mathiesen[1] & Dzung B. Diep[1]✉

Bacteriocins are ribosomally-synthesized antimicrobial peptides, showing great potential as novel treatment options for multidrug-resistant pathogens. In this study, we designed a novel hybrid bacteriocin, Hybrid 1 (H1), by combing the N-terminal part and the C-terminal part of the related bacteriocins enterocin K1 (K1) and enterocin EJ97 (EJ97), respectively. Like the parental bacteriocins, H1 used the membrane-bound protease RseP as receptor, however, it differed from the others in the inhibition spectrum. Most notably, H1 showed a superior antimicrobial effect towards *Staphylococcus haemolyticus*—an important nosocomial pathogen. To avoid strain-dependency, we further evaluated H1 against 27 clinical and commensal *S. haemolyticus* strains, with H1 indeed showing high activity towards all strains. To curtail the rise of resistant mutants and further explore the potential of H1 as a therapeutic agent, we designed a bacteriocin-based formulation where H1 was used in combination with the broad-spectrum bacteriocins micrococcin P1 and garvicin KS. Unlike the individual bacteriocins, the three-component combination was highly effective against planktonic cells and completely eradicated biofilm-associated *S. haemolyticus* cells in vitro. Most importantly, the formulation efficiently prevented development of resistant mutants as well. These findings indicate the potential of a bacteriocins-based formulation as a treatment option for *S. haemolyticus*.

Staphylococci are a diverse genus of Gram-positive bacteria, commonly found in the microbiota of skin and mucosal membranes of humans. Generally, staphylococci are divided into two groups: coagulase-negative (CoNS) and coagulase-positive staphylococci (CoPS), depending on the production of the clotting enzyme coagulase. For decades, the CoPS *Staphylococcus aureus* has been recognized as an important human pathogen, while CoNS have been considered commensal and regarded as mere contaminants when found in samples from infections[1,2]. Today, CoNS are recognized as major opportunistic nosocomial pathogens, particularly causing infections in immunocompromised patients and patients with indwelling medical devices[3,4]. Among CoNS, *S. haemolyticus* is receiving increased attention as a nonconical pathogen, being the second most frequently isolated CoNS in clinical settings[1,5].

Compared to the more virulent *S. aureus*, few virulence characteristics have been determined as crucial for *S. haemolyticus* infections. One of these is its multidrug-resistant (MDR) phenotype[6–8]. Clinical isolates of *S. haemolyticus* are ranked as the most antibiotic-resistant CoNS, and they have frequently been reported as resistant to last-line antibiotics such as glycopeptides, making treatment options limited[1,9,10]. A variety of mechanisms contribute to the acquisition of antibiotic resistance. Notably, the *S. haemolyticus* genomes contain multiple insertions and single nucleotide polymorphisms (SNPs), allowing frequent genetic rearrangements[3,8]. The extreme genome plasticity likely allows *S. haemolyticus* to acquire antibiotic-resistant genes from its environment, often resulting in MDR hospital-adapted clones[8]. Equally significant is the horizontal gene transfer of antibiotic-resistance genes from *S. haemolyticus* to *S. aureus* strains observed in hospital outbreaks of methicillin-resistant *S. aureus* (MRSA), indicating that *S. haemolyticus* may act as a reservoir for resistance genes in hospitals[11–13].

The ability to form biofilms and adhere to medical devices is another crutial virulence factor in *S. haemolyticus* infections[14]. Biofilm formation allows microbial adhesion to biotic and abiotic surfaces, as well as shielding the bacteria from the host immune response and antibiotics[15]. Biofilm formation on indwelling medical devices is a major concern, as the increased antibiotic resistance makes infections more difficult to treat, often leaving

[1]Faculty of Chemistry, Biotechnology and Food Science, Norwegian University of Life Sciences, Ås, Norway. [2]Pediatric Infections Group, Department of Pediatrics, University Hospital of North Norway, Tromsö, Norway. [3]Pediatric Infections Group, Department of Clinical Medicine, UiT the Arctic University of Norway, Tromsö, Norway. [4]Blue Peter Public Health and Research Centre, LEPRA Society, Hyderabad, India. [5]These authors contributed equally: Christian Kranjec and Sofie S. Kristensen. ✉email: dzung.diep@nmbu.no

K1 MKFKFNPTGTIVKKLTQYEIAWFKNKHGYYPWEIPR

EJ97 MLAKIKAMIKKFPNPYTLAAKLTTYEINWYKQQYGRYPWERPVA

H1 MKFKFNPTGTIVKKLTQYEINWYKQQYGRYPWERPVA

Figure 1. Predicted Structure and amino acid sequence of the hybrid bacteriocin and its parental bacteriocins. The predicted structure of the hybrid bacteriocin 1 (H1), formed by the N-terminal part of K1 (green) and the C-terminal part of EJ97 (orange). The central tripeptide sequence (YEI—underlined) in K1 and EJ97 serves as the joining segment in the fusion protein. The structure of H1 was modeled based on the NMR structural data of K1[23] using the structure prediction tool Swiss model[35].

surgical removal of the device as the only option[14,15]. There is limited knowledge about the molecular mechanisms underlying the formation of *S. haemolyticus* biofilm. However, their primary importance in infections is evident. Compared to the polysaccharide biofilms formed by *S. epidermidis, S. haemolyticus* forms biofilms mainly composed of proteins and DNA[6]. The ability to form biofilms combined with their high degree of MDR makes infections caused by *S. haemolyticus* increasingly challenging to combat. Due to their ability to form biofilms, persist and thrive in the hospital environment[16], *S. haemolyticus* strains are emerging as a severe nosocomial threat.

To better control the increasing number of MDR pathogens, novel treatment options are needed. In this context, bacteriocins are receiving increased scientific and medical interest. Bacteriocins are small ribosomally synthesized antimicrobial peptides which are produced by bacteria to compete with other bacterial species for nutrients and ecological niches. Bacteriocins are generally believed to be produced by most bacteria, with the *Staphylococcus* genus being no exception. Several bacteriocins produced by staphylococci show prominent anti-staphylococcal and bacteriolytic activities[17].

Compared with traditional antibiotics, bacteriocins have several advantages, including low toxicity (particularly those expressed by lactc acid bacteria (LAB)), the ability to be bioengineered and high efficacy[18]. The high potency of bacteriocins has been demonstrated both in vitro and in vivo. Notably, bacteriocins exhibit high activity towards several clinically important species, including *Streptococcus pneumonia*[19], MRSA[17,20], *Clostridium difficile*[21,22] and vancomycin resistant enterococci (VRE)[23,24], thereby underlining the potential of bacteriocins as antimicrobial therapeutics. More importantly, bacteriocins have different modes of action than traditional antibiotics, making them active against MDR pathogens[18].

Leaderless bacteriocins are synthesized without an N-terminal leader sequence and contain no post-translational modifications. This, along with their relatively small size (30–50 amino acids), makes them ideal for synthetic production. Enterocins K1 and EJ97 are two leaderless bacteriocins with potent and specific activity towards enterococcal species through an interaction with the membrane-bound site-2-protease RseP (Regulator of Sigma-E Protease)[23]. RseP is a virulence factor[25,26] involved in the stress response and processing of signaling peptides in several bacteria[27–30], thus serving as a potential antimicrobial target. It is proposed that EJ97 and K1 interact specifically with RseP to create pores in the cell membrane, thereby leading to disrupted membrane integrity and cell death[23]. In the present study, we designed a novel hybrid bacteriocin designated Hybrid 1 (H1), which is composed of the N-terminal half of Enterocin K1 and the C-terminal half of Enterocin EJ97[23,31]. Here we show that RseP serves as the receptor for H1 and that the hybrid bacteriocin has superior antimicrobial properties towards clinical *S. haemolyticus* isolates when compared with the parental bacteriocins. Moreover, we demonstrate that H1 acts synergistically with the broad-spectrum bacteriocins garvicin KS and micrococcin P1, not only to kill planktonic and biofilm-associated *S. haemolyticus* cells but also to prevent resistance development.

Results

The inhibition spectrum of the novel hybrid bacteriocin H1. Previous studies have indicated that the generation of hybrid bacteriocins can be an effective way to create novel antimicrobials with new and/or improved properties[32–34]. Inspired by these works we created a hybrid bacteriocin, called H1, formed by two sequence related enterocins: K1 and EJ97, the former being most active against *E. faecium* while the latter being most active against *E. faecalis*. H1 contains the N-terminal half of K1 and the C-terminal half of EJ97, sequence and predicted structure[23,35], guided by the NMR data of K1, is shown in Fig. 1. When testing the antimicrobial activity against a panel of 50 bacteria from different genera and species (Table S1), the hybrid bacteriocin displayed good activity against selected species within the genera *Staphylococcus* and *Streptococcus*. Within the

	Bacteriocins (*)		
S. haemolyticus strains	K1	EJ97	H1
4068**	–	++*	+++*
4069**	–	++*	+++*
4070**	–	++*	+++*
4071**	–	++*	+++*
4072**	–	++*	+++*
4073**	–	++*	+++*
7067_4_56	–	++*	+++*
7068_7_63	–	++*	+++*
7067_4_66	–	++*	+++*
7067_4_49	–	++*	+++*
7067_4_84	–	++*	+++*
7067_4_67	–	++*	+++*
7067_4_71	–	+++*	+++*
7067_4_28	–	+++*	+++*
7067_4_48	–	+	+++*
7067_4_21**	–	++*	+++*
7067_4_60**	++	+++*	+++*
SH46	–	++*	+++*
SH01	–	+++*	+++*
SH09	–	+	+++*
SH04	–	+++*	+++*
SH10	+	+++*	+++*
SH47	+	+++*	+++*
SH14**	–	++*	+++*
SH20**	+	++*	+++*
7067_4_39**	–	+	+++*

Table 1. Inhibition spectrum of K1, EJ97 and H1 as assessed by the spot-on-lawn assay against 27 *Staphylococcus haemolyticus* strains. *Mutants observed after 24 h. 5 µl of each bacteriocin at 1 mg/ml was used in the spot-on-lown assay. Average Inhibition score (n = 3) indicates: "–" = No inhibition; "+" = Unclear zone; "++" = zone < 1 cm, and "+++" = zone ≥ 1 cm. **Strains where H1 resistant mutants where isolated from 1 mg/ml spot-on-lawn inhibition zone.

former genus, it is interesting to note that H1 displayed increased activity against *S. epidermidis* and *S. haemolyticus,* compared with the parental bacteriocins. In addition, all three bacteriocins showed weak or no effect on *S. aureus*, *S. arlettae* and *S. simulans*; whereas EJ97 and H1 displayed a comparable antimicrobial effect against *S. hominis*. Similarly, among streptococci, H1 showed increased activity against *S. thermophilus* and *S. uberis,* but no activity against *S. dysgalactiae*. None of the bacteriocins had activity against Gram-negative bacteria (Table S1). Because of the superior effect of H1 against the important human pathogen *S. haemolyticus*, we focused further on the activity of H1 on this species.

To examine whether the activity of H1 was strain-depedent, a collection of 27 clinical and commensal *S. haemolyticus* strains derived from blood, urine and wound-associated infections were tested (Table S2). Using the spot-on-lawn assay, H1 was found to have better activity (i.e., larger inhibition zones) for 74% of the tested *S. haemolyticus* strains compared to K1 or EJ97 (Table 1). However, development of resistant colonies was observed within the inhibition zones for all 27 strains after a 24 h incubation (Table 1). Using the microtiter plate assay to follow the antimicrobial dynamics, H1 had minimum inhibition concentrations (MIC_{50}) in the range 0.1–0.78 mg/ml against the different *S. haemolyticus* strains after 5 h of incubation (Table S2) but resistance to H1 was progressively observed after 24 and 48 h incubation (data not shown).

RseP is required for H1 antimicrobial activity. Previous studies have shown that the enterocins K1 and EJ97 require the membrane-bound protease RseP to recognize and kill enterococcal cells[23]. It is logical to assume that H1, a hybrid of K1 and EJ97, targets the same receptor. To test this, we heterologously expressed the *S. haemolyticus* RseP in *Lactobacillus plantarum* WCFS1[36], which is resistant to the enterocin H1. As expected, *L. plantarum* expressing the *S. haemolyticus rseP*, showed sensitivity comparable to the parental *S. haemolyticus* strain, while *L. plantarum* harbouring the empty vector (pEV) was resistant to H1 (Fig. S1; Table 2).

The *rseP* gene is not the hot spot for mutations in the H1-resistant mutants. Although the role of RseP in the sensitivity of *S. haemolyticus* towards H1 was evident, we sought to confirm whether mutations were within *rseP* among the H1-resistant mutants. The *rseP* gene was therefore sequenced in a pool of

Strain	Relevant characteristics	H1 (μg/ml)
L. plantarum WCFS1	WT of host strain	> 50
L. plantarum WCFS1/pEV	Expressig empty vector	> 50
L. plantarum WCFS1/pSIP401_SHRseP	Expressing RseP from *S. haemolyticus* 7067_4_21	0.39

Table 2. Minimal inhibitory concentration (MIC) values (μg/ml) of H1 towards different *L. plantarum strains*.

H1 resistant *S. haemolyticus* isolate	Mutations*	
	rseP	*escAB*
7076_4_21 M1	–	*escB*: c.855delT p.Phe285fs
7076_4_21 M2	–	*escB*: c.855delT p.Phe285fs
4069 M3	–	*ecsA*: c.113G>A p.Gly38Asp
4071 M3	c.1136_1139dupGTGG p.R381fs	–
4072 M3	–	*escB*: c.51_52insT p.Lys18fs

Table 3. Whole genome sequencing of selected H1 resistant mutants. *: Intact gene, c: Coding DNA, p: Protein, del: deletion, fs: frameshift, >: Substitution, ins: Insertion, dup: duplication.

14 randomly selected H1-resistant mutants of *S. haemolyticus*. Surprisingly, only two mutants (4070 10_2 and 4071 1_4) had mutations within *rseP*, both with amino acid substitutions. In contrast, no mutation within *rseP* was found for the remaining H1-resistant mutants.To solve this puzzle, we performed whole-genome sequencing (WGS) on five additional H1-resistant mutants and the respective wildtype (WT) counterparts (Table 3). Surprisingly, four sequenced mutants contained mutations within the genes *ecsAB,* encoding subunits of the ATP-binding cassette (ABC) transporter Ecs[37,38]. The Ecs ABC transporter is known to be tightly connected with RseP in a secretory pathway in aerobic and facultative anaerobic Firmicutes, including staphylococci[39,40]. The last mutant contained a frame-shift mutation within *rseP* resulting in a truncated product (Table 3).

Micrococcin P1 and garvicin KS potentiate the activity of H1. The frequent resistance to H1 observed above, prompted us to investigate its synergistic effects in combination with other bacteriocins. To this end, the bacteriocins micrococcin P1 (MP1) and garvicin KS (GarKS) were chosen as they have been used in synergy studies before[20,41]. MP1 is a thiopeptide inhibiting protein synthesis[42–45], while GarKS is a three-peptide bacteriocin with a yet unknown mode of action[46]. We initially evaluated the antimicrobial activity of the two bacteriocins against the six *S. haemolyticus* strains isolated from leprosy-associated plantar skin ulcers (4068–4073). For comparison, we also included the parental bacteriocins EJ97 and K1. We used the spot-on-lawn assay where these strains were challenged with three different concentrations of each antimicrobial (0.04, 0.2 and 1.0 mg/ml). As shown in Fig. 2, MP1 gave clear inhibition zones at all three concentrations while H1 gave inhibition only at the two highest concentrations. For GarKS and EJ97, some inhibition was seen only at the highest concentration. K1 did not result in any inhibition.

To investigate whether there was synergy between the three bacteriocins (H1, GarKS and MP1), a checkboard antimicrobial assay was performed. The selected strains were treated for 5, 24 and 48 h with a range of concentrations of H1, GarKS and MP1 alone or in different combinations. The results are summarized in Fig. 3 and further details on individual MIC_{50} values for the tested strains can be found in Table S3. After a 5 h incubation, MP1 showed the strongest antimicrobial activity, with MIC_{50} values ranging between 0.02 and 0.15 μg/ml, whereas H1 had a MIC_{50} of 0.78 μg/ml against all strains. Consistent with the antimicrobial test in Fig. 2, GarKS was the least active bacteriocin, with MIC_{50} values ranging between 3 and 24 μg/ml (Fig. 3; Table S3).

The prolonged exposure for 24 and 48 h resulted in a progressive increase in the MIC_{50} values for all treatments, a sign of resistance development. In agreement with the results above, H1 alone readily led to the generation of resistance among all tested strains (Fig. 3; Table S3). On the other hand, while the double combinatorial treatments (GarKS/MP1; H1/GarKS; H1/MP1) did not significantly increase the antimicrobial activity of the bacteriocins, combining all three bacteriocins (called the tricomponent combination) efficiently inhibited the microbial growth at all time-points. Interestingly, treatment with the tricomponent combination led to contained MIC_{50} values, with reduced inter-strain variability and displayed no sign of resistance development (Fig. 3). This was particularly evident at the 24 and 48 h time-points compared to the other treatments (Table S3).

Taken together these data indicate that the tricomponent combination had not only a superior antimicrobial activity but was also able to prevent resistance development.

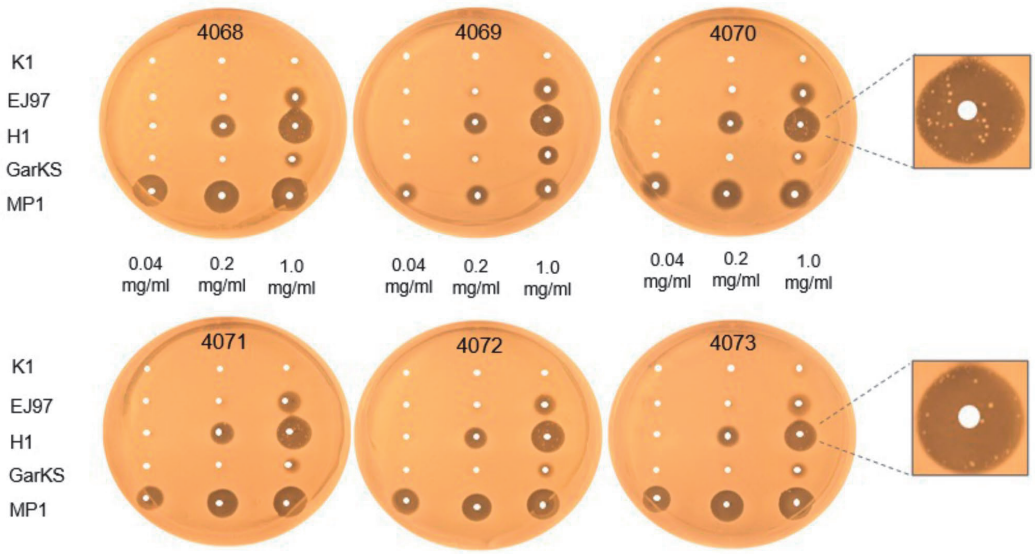

Figure 2. Comparison of the antimicrobial activities of the bacteriocins against *S. haemolyticus*. The antimicrobial activity of the indicated bacteriocins was assessed by "spot-on-lawn" assay against six *S. haemolyticus* strains, 4068–4073. The bacteriocins were applied at three different concentrations (0.04, 0.2, and 1.0 mg/ml), and 5 µl of each was spotted on the lawns of the *S. haemolyticus* strains. All strains developed resistance to H1 after 24 h incubation, as illustrated for strains 4070 and 4073.

The tricomponent combination is effective against *S. haemolyticus* biofilms. The ability to form biofilms is a widespread virulence factor among CoNS; it is significantly associated with the colonization of prosthetic implants, increased antimicrobial resistance and therapeutic failure[47]. Among *S. haemolyticus* the genetic elements conferring adhesive properties and ultimately the ability to form biofilms are widely distributed[48,49]. In order to assess whether our clinical *S. haemolyticus* strains were indeed able to form biofilms in vitro, we performed a crystal violet assay on biofilm-associated cells[50]. Twelve *S. haemolyticus* isolates were included in the study, six of which were isolated from leprosy-associated skin ulcers in India (4068–4073), four were isolated from bacteremia patients and two were commensial isolates. We also included the methicillin-resistant *S. aureus* strain USA300 and a leprosy-associated *S. arlettae* strain as controls for a strong and a poor biofilm-former, respectively (Fig. S2)[41,51]. Using the crystal violet assay, the strong biofilm-former *S. aureus* USA300 produced an average OD value of over 3 (cut-off value for biofilm formers = 1), while the poor biofilm-former *S. arlettae* gave an average OD value of 0.5. All *S. haemolyticus* strains formed biofilms comparable to that of *S. aureus* USA300, except 7067_4_60 which produced an average OD value of 2 (Fig. S2). These results indicate that most pathogenic *S. haemolyticus* strains are strong biofilm-formers.

Given the strong antimicrobial effect of the tricomponent combination identified above, we wanted to examine its efficacy against biofilm-associated *S. haemolyticus* cells. We used a modified version of the biofilm-oriented antimicrobial test (BOAT)[52,53] which allows the quantification of the metabolic activity (via the metabolic indicator triphenyl-tetrazolium chloride) within residual live cells within the biofilms after antimicrobial treatment. To do this, the *S. haemolyticus* biofilms were first allowed to form for 24 h, then the biofilms were treated with the antimicrobials for 5, 24 or 48 h, before the BOAT assay was performed (Fig. 4A; Fig. S3). We exposed biofilm-associated cells to a serial dilution of the tricomponent combination, starting with the highest concentrations (D0) being 625 µg/ml for H1 and garvicin KS and 62.5 µg/ml for micrococcin P1. These high values were 100 times higher the MIC_{50} values for planktonic cells, accounting for the higher resilience to antimicrobial treatment of biofilm-associated cells[15,41,54]. After 5 h the metabolic activity of all tested strains was very low or undetectable at all dilutions, except for 4069, which showed a residual metabolic activity at the highest dilution factors (D6 and D7) (Fig S3A). After a prolonged incubation for 24 and 48 h, most strains showed resilience but only at the lowest concentrations D5 and D7. For strains 4071–4073, 7068_4_63 and SH14, little or no metabolic activity was seen at all dilutions (Fig. 4A; Fig. S3B).

Bacterial cells can remain dormant (with very low or no metabolic activity) within the biofilms[55,56]. If this was the case in our biofilm settings, these cells would be overlooked by the BOAT assay. To examine this issue, biofilm-associated *S. haemolyticus* cells were treated with the tricomponent combination at concentration D0 (e.g. 625 µg/ml for H1 and garvicin KS and 62.5 µg/ml for micrococcin P1) for 24 h. This was followed by CFU counting to identify potential survinving cells in the treated biofilms. As shown in Fig. 4B, this treatment led

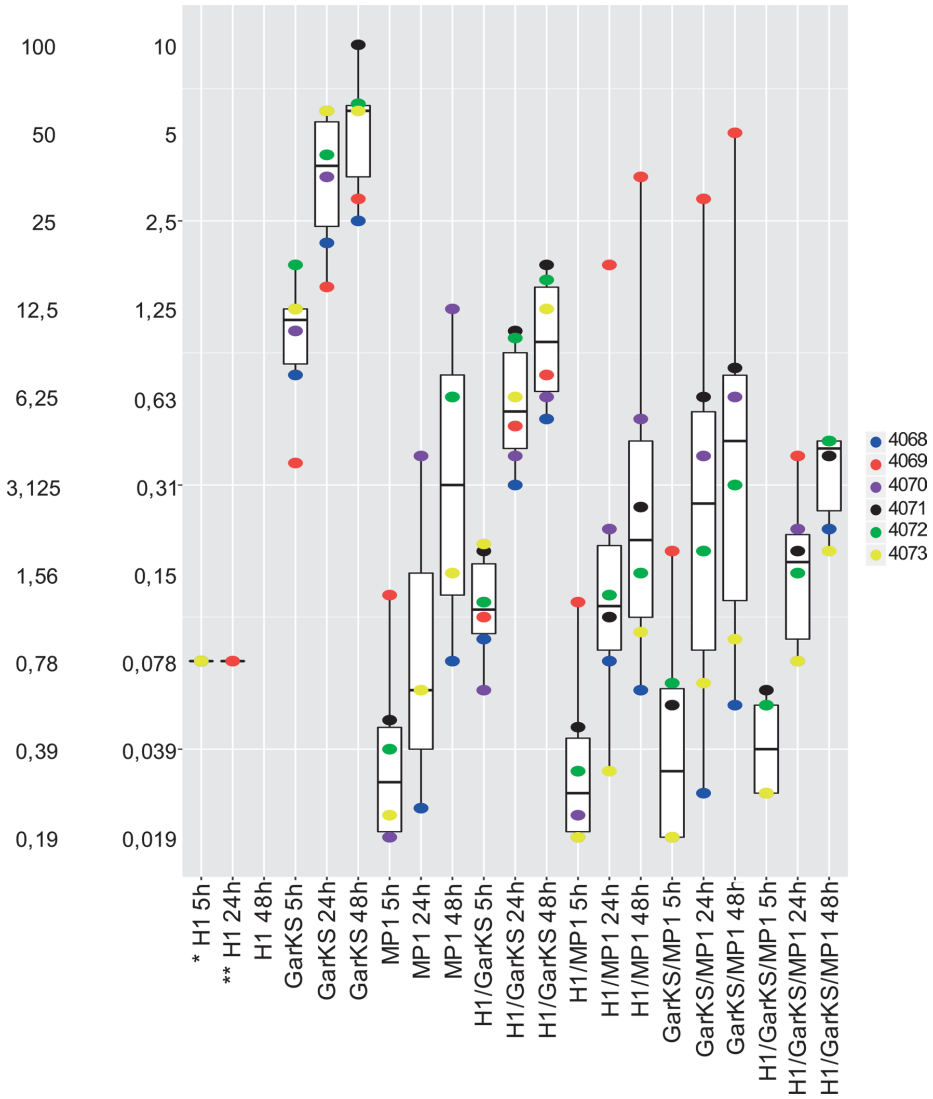

Figure 3. Boxplot of minimal inhibition concentrations (μg/ml) for the treatment with H1, garvicin KS, micrococcin P1 and their combinations against planktonic *S. haemolyticus*. The median distribution is indicated as thick line within boxes and the degree of variability (amplitude of the box or inter quartile region (IQR)) of the MIC_{50} values for the indicated strains obtained at three different time points: 5 h, 24 h and 48 h. Whiskers extending out the boxes mark the minimum and maximum observed values and the variability outside the middle 50% of values (whisker length). Outliers are represented as values that extend out of the whisker limit (1.5×IQR). Note that the treatment with the tricomponent combination (H1/GarKS/MP1) led to contained MIC values and inter-strain variability compared to the other treatments at all time-points. (*)Please note that for the treatment with H1 all strains were sensitive after a 5 h incubation (MIC_{50} = 0.78 μg/ml); (**) all strains were resistant after a 24 h incubation, except 4069 (MIC_{50} = 0.78 μg/ml); all strains were resistant after a 48 h incubation.

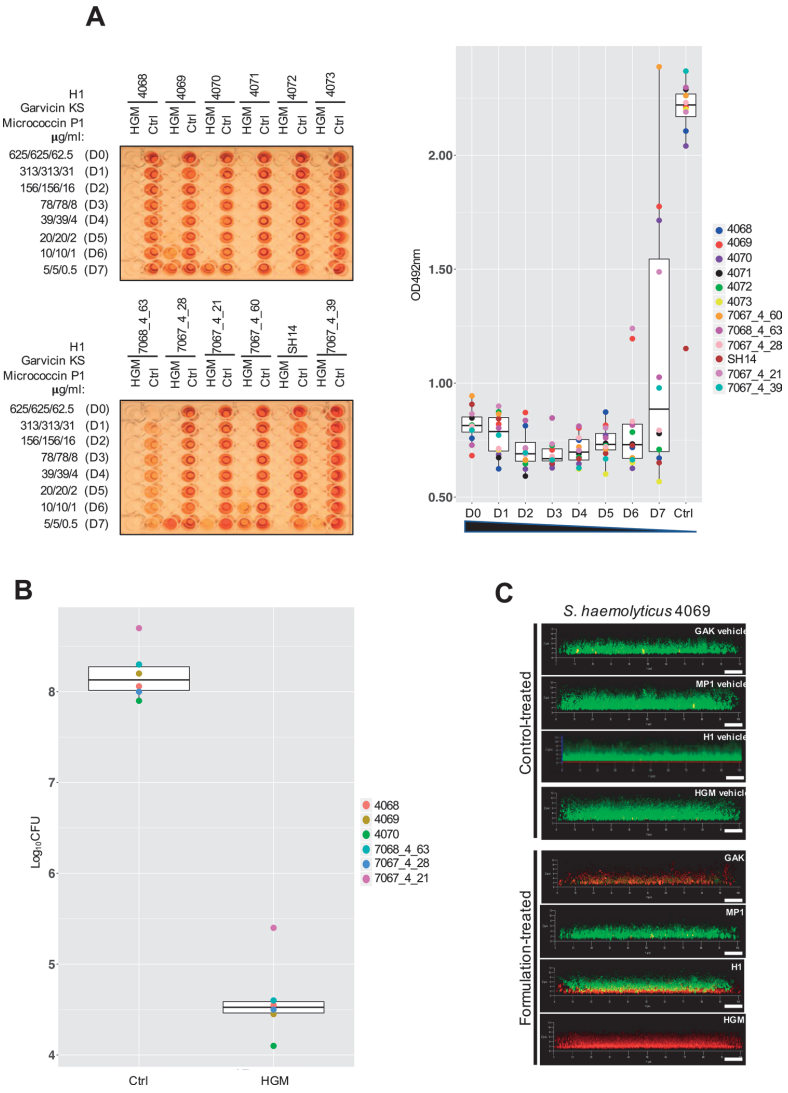

Figure 4. The tricomponent antimicrobial combination effectively inhibits the metabolic activity and viability of *S. haemolyticus* biofilm-associated cells in vitro. (**A**) The left panels show representative images of BOAT assays performed upon 24 h treatment with the tricomponent combination (HGM: H1, GarKS, MP1) for the indicated strains. The concentration (µg/ml) of the individual antimicrobials in the dilutions (dilution factors: D0 to D7) is indicated on the far left of the images. As controls, the assay was performed using the vehicles at their final concentrations (Ctrl). The development of red color indicates the retention of metabolic activity, and its quantification was performed by spectrophotometry at OD_{492}. Metabolic activity values were plotted as a function of the dilution factor for the antimicrobial combination (right panel). Shown is the median distribution (thick line within boxes) and the degree of variability (amplitude of the box or inter quartile region (IQR)) of the metabolic activities for the indicated strains measured at increasing dilution factors (D0–D7). The boxplot components (whiskers and outliers) are displayed as specified in Fig. 3. Note that the treatment maintained the metabolic activitiy under detectable levels up to D6 for most strains. (**B**) The logarithmic colony formation unit ($Log_{10}CFU$) was calculated after the BOAT assays were performed for the indicated strains. BOAT assays were performed as in (**A**), and the boxplot shows the median distribution of the $Log_{10}CFU$ values. The antimicrobial concentrations in the tricomponent combination were 625 µg/ml for H1 and garvicin KS and 62.5 µg/ml for micrococcin P1. The control was performed by using the antimicrobials vehicles at their final concentration. (**C**) The *S. haemolyticus* strain 4069 was allowed to form biofilms on glass-bottomed chambers for 24 h, prior to treatment with the indicated antimicrobials (lower set of panels) or the respective control-vehicles (upper set of panels) as detailed in (**B**). The biofilms were subsequently stained using the LIVE/DEAD biofilm staining kit and confocal microscope images were taken using a 63 × oil immersion objective. Scale bars correspond to 10 µm.

to a dramatic and statistically significant ($p < 0.0001$) reduction of the biofilm-associated cell viability, with a drop in Log_{10}CFU values ranging between 3.3 and 3.8 compared with the non-treated control for all six *S. haemolyticus* strains. These results were further confirmed by LIVE/DEAD biofilm staining followed by confocal microscopy analysis (Fig. 4C) which indeed showed only dead (red) cells within the biofilms when treated with the tricomponent combination. On the other hand, mixtures of live (green) and dead cells were observed when treated with the single antimcrobials. It is interesting to note that the treatment with H1 led to the killing of the bacterial cells in the deepest layers of the biofilm while preserving the cell viability in upper layers. This effect could not be observed for GarKS and MP1, possibly reflecting a mode of action and/or pattern of penetration within the biofilm specific for H1.

Discussion

In this study we described the generation of a hybrid bacteriocin (H1) obtained by the fusion of the N- and C-terminal parts of the enterocins K1 and EJ97, respectively. The resulting H1 shows much better activity against the important human pathogen *S. haemolyticus* compared with EJ97 and especially K1 (Table 1). Both parental enterocins are class-II leaderless antimicrobial peptides. They share high sequence homology with each other and both use the membrane-bound RseP as a receptor on target cells[23]. We have previously shown that within the LsbB-group which contains LsbB, EJ97 and K1, the C-terminal part of these bacteriocins dictates their target specificity while the N-terminal part contains an amphiphilic alpha-helix which likely has the pore-forming function[23,57–60]. Since H1 was composed of the C-terminal half of EJ97 and the N-terminal half of K1, it is reasonable to think that the hybrid bacteriocin would have an inhibition spectrum similar to EJ97. This notion was generally in line with the result presented in Table S1 which showed an overlapping inhibition spectrum between H1 and EJ97. Nevertheless, there were some few important differences: H1 displayed an activity against certain strains of *B. cereus*, *C. pisciola*, *L. garvieae* and *S. arlettae* that overlapped with K1. On the other hand, compared to both parental enterocins, H1 showed a higher activity against members of the genera *Staphylococcus* (*S. aureus, S. epidermidis* and *S. haemolyticus*) and *Streptococcus* (*S. termophilus* and *S. uberis*) (Table S1). This indicates that the K1's N-terminal half in H1, to some extent, also modulates the specificity of H1. Importantly, our analysis on 27 clinical *S. haemolyticus* strains indicated that the antimicrobial activity of K1 and EJ97 was highly strain-dependent, whereas H1 retained a high level of antimicrobial activity against all *S. haemolyticus* strains (Table 1).

It is worth mentioning that another hybrid peptide (H2) with an inverse order to H1 was also made, i.e., with an N-terminal half from EJ97 and a C-terminal half from K1. However, unlike H1, the inverted peptide showed in general very low activity (data not shown), and therefore no further analysis was carried on this version. At present, we do not know why H2 had low antimicrobial activity, but this is beyond the scope of the present study.

Despite the increased activity against *S. haemolyticus*, the antimicrobial potential of H1 was unfortunately hampered by the rapid development of resistance. Previous studies highlighted that multicomponent antimicrobial combinations offer a superior efficacy in terms of antimicrobial activity and prevention of resistance development[20,41,61,62]. In this study, we assessed the efficacy of H1 in combination with garvicin KS and micrococcin P1. The former is a multi-peptide bacteriocin composed of three non-modified peptides and belongs to the leaderless family of bacteriocins (class IId)[46]. Its mode of killing has not been elucidated in detail. However, it is supposed to disrupt the cell membrane integrity leading to the leakage of intracellular fluids, followed by cell lysis and death (unpublished data). On the other hand, micrococcin P1 belongs to a class of microbial ribosomally-synthesized and post-translationally modified peptides (RiPPs) known as thiopeptides[63]; a group of protein synthesis inhibitors[42–45]. The combination of H1 with garvicin KS and micrococcin P1 elicited a significant reduction of the antimicrobial concentrations required to effectively inhibit the growth of both planktonic and biofilm-associated *S. haemolyticus* cells.

Consistent with our recent study on *S. aureus* biofilms[41], a discrepancy between the inhibition of biofilm-associated metabolic activity and cell viability could be observed. Indeed, treatments that led to a complete abolishment of metabolic activity did not translate directly into a corresponding annihilation of the cell viability quantified by CFU counting. A likely explanation for such an effect is biofilm-associated cell dormancy. Bacterial dormancy is a well-documented phenomenon, which significantly contributes to the long-term persistence of bacterial cells[55,56]. The dormant phenotype is characterized by low levels of metabolic activity, which confers the reduced susceptibility to antimicrobials as most antibiotics only attack active metabolic pathways such DNA, RNA, protein, cell wall synthesis[56,64]. Therefore, it is conceivable that if persister cells do exist within the biofilms in our model, their metabolic activity might not be tracked in the BOAT assays; however, metabolic reactivation will occur once cells are transferred to an appropriate growth-promoting environment[65,66].

Bacteriocin-based antimicrobial combinations have been widely explored against a variety of pathogenic bacteria, including biofilm-forming strains[67,68]. However, these studies primarily focused on investigating the interaction between bacteriocins and different classes of antibiotics or other bioactive molecules[68–72]. Recently, also garvicin KS and micrococcin P1 have been tested in combination with penicillin G against MRSA, showing a potent antimicrobial activity[20,41]. To our knowledge, the antimicrobial combination described in the present work is the first bacteriocin-based and antibiotic-free example. In our view, this has a significant advantage as it complies with the health authorities' general recommendations: namely to reduce or, where possible, avoid the use of antibiotics to treat bacterial infections. Similar recommendations were set by the European Commission (2015/C 299/04) also in veterinary medicine, particularly in the food production chain. In treating certain medical conditions, such as mastitis in dairy cows, antibiotic therapy will result in drug accumulation into the milk, leading to short-term withdrawal of milk from antibiotic-treated cows and as a consequence, significant economic loss for farmers. Thus, our bacteriocin-based and antibiotic-free approach can be a valuable solution in this context.

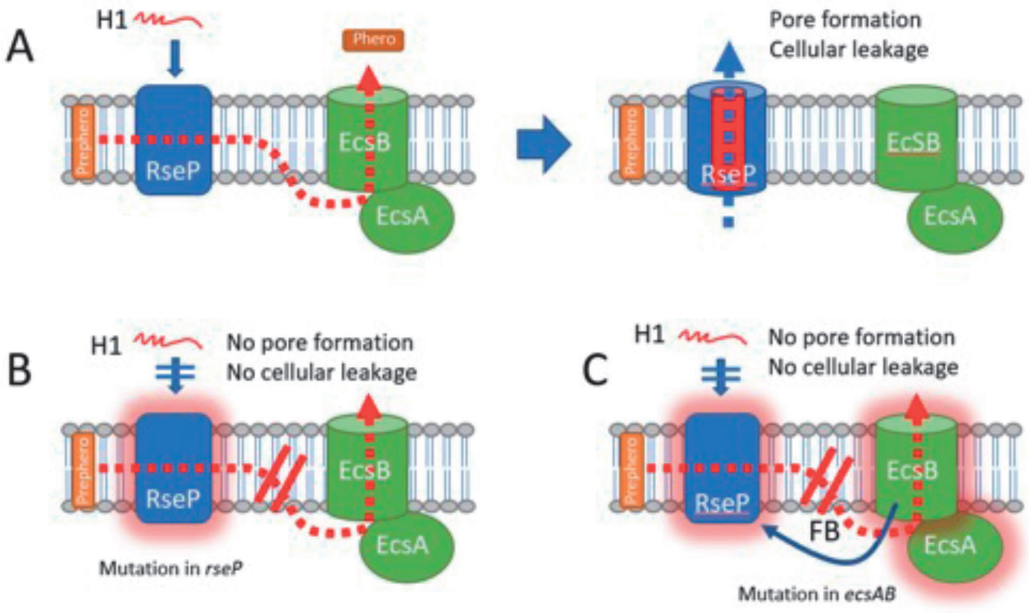

Figure 5. Proposed model for the EcsAB mediated H1-resistance in *S.haemolyticus*. (**A**) RseP is a inner-membrane protease working together the ABC-transporter EcsAB to cleave the hormone prepeptide (Prephero) and export the mature hormone peptide (Phero) to the external milieu. RseP is acting also as the receptor for the bacteriocin H1 which forms pores and causes lethal cellular leakage across the membrane. (**B**) When *rseP* is mutated resulting in a non-functional receptor (RseP with glow), cells become resistant to H1. (**C**) When the *ecs* system is mutated, the malfunctional ABC transporter can no longer export the hormone peptide. This jammed situation of hormone prepeptide/peptide within the membrane results in a feedback (FB) loop somehow causing RseP inactivity. An inactive RseP (RseP with glow) loses its function as a bacteriocin receptor, and cells therefore become resistant to H1.

Our complementation studies using *L. plantarum* confirmed that RseP was indeed the target for H1 on the *S. haemolyticus* cells and was essential for its antimicrobial activity. Therefore it was very surprising to reveal that most *S. haemolyticus* H1-resistant mutants did not possess a disruptive mutation within the *rseP* gene. By WGS, we found that 4 out of 5 mutants contained mutations in the *ecsAB* gene pair, which encodes components of the ATP-binding cassette (ABC) transporter Ecs. The fact that mutations accumulated within the ABC transporter abolished the sensitivity to H1 might indicate a molecular link between Ecs and RseP. Interestingly, similar observations have also been found in other studies. In *Bacillus subtilis* the perturbation of the *ecsAB* gene locus leads to the disruption of RasP function (RasP is a RseP homolog). In addition, inactivation of *rasP* led to an overlapping phenotype with *B. subtilis* strains carrying mutations in *ecsA*[39]. In *Enterococcus faecalis*, EcsAB and Eep (the enterococcal homolog of RseP) are functionally connected in a quorum sensing pathway involved in conjugation[73]. Eep is responsible for the processing of several pheromone precursors, including cCF10, cAD1 and cAD1[30,74], and the secretion of the mature sex pheromones is then mediated by EcsAB[73], resulting in the conjugative transfer of mobile genetic elements; including antibiotic resistance determinants [30,75]. Similarly, the inactivation of an Eep-like metalloprotease in *Streptococcus gordonii* abolishes the secretion of the cAM373 pheromone[76]. Based on these similarities, it is tempting to speculate that a similar mechanism is involved in the H1-resistant *S. haemolyticus ecs* mutants. In such a model as depicted in Fig. 5A, EcsAB is working downstream of RseP, to export an unknown product provided by RseP. Mutations in *rseP* will destroy its receptor function thereby allow cells becoming resistant to H1 (Fig. 5B). Mutations in *ecsAB* will entail the accumulation of RseP-processed peptides in the cell membrane that may affect, in a feedback maner, the functionality of RseP, ultimately rendering RseP no longer suitable as the bacteriocin receptor (Fig. 5C). This model can also probably be applied to enterococci, since *E. faecalis* mutants which are resistant to EJ97 contain mutations either within *ecsAB* or *rseP*; however, a much higher frequency was observed in the latter[77]. Therefore, it was unexpected to find high frequency of mutations in *ecs* relative to *rseP* in *S. haemolyticus*. The molecular nature behind the different mutation rates in *rseP* and *ecsAB* between these two pathogens is unknown, yet it might reflect the different roles of RseP in these two pathogens. Undoubtfully, the role of RseP and its connection with the Ecs system deserves further investigation in future studies.

The high degree of genome plasticity of *S. haemolyticus*[3] allows this bacterium to readily acquire resistance mehcanisms toward many different antibiotics. Here we demonstrated that using multiple bacteriocins with different modes of action can overcome the resistance problem in *S. haemolyticus*. The tricomponent combination with the bacteriocins H1, MP1 and GarKS proves effective both against planktonic and biofilm-associated cells, the latter being much troublesome in therapeutic treatment due to the protective biofilm layers. Our data indicate that the antimicrobials in the mixture were able to peneterate the protective biofilm layer and kill the bacterial cells hiding underneath. Antimicrobial peptides are ubiquitous in nature, and they are very diverse in terms of amino acid sequence, structure, modification, and mode of action. By genetic means, or by de novo synthesis, new hybrid antimicrobial peptides can be easily made to improve potency and/or alter target specificity, as demonstrated in the present study with H1. This approach can be a precious path to create novel antimicrobials and combat bacterial infections and antibiotic resistance.

Materials and methods

Bacterial strains and cultivation conditions. Bacterial strains used in this study are listed in Tables S1, S3 and S4. The following strains were cultivated in Brain heart infusion (BHI) broth (Oxoid): all indicator strains (30 °C, with shaking), all clinical *S. haemolyticus* isolates (Table S2) and *Escherichia coli* (DH5α, TG1) (37 °C, with shaking). *Lactobacillus plantarum* (WCFS1) was cultivated in MRS broth (Oxoid) at 37 °C without shaking. Agar plates were prepared by supplementing the appropriate broth with 1.5% (w/v) agar (VWR chemicals). When appropriate, erythromycin was added to a final concentration of 200 µg/ml for *E.coli* and 10 µg/ml for *L. plantarum*.

Bacteriocins and antimicrobial assays. Bacteriocins used in this study are listed in Table S5. K1[23], EJ97[31], H1 and garvicin KS peptides (Gak-A, -B and -C)[46] were synthesized by Pepmic Co., Ltd, China, with > 95% purity. These bacteriocins were all solubilized in 0.1% (vol/vol) trifluoracetic acid (TFA; Sigma-Aldrich). Micrococcin P1[78] was purchased from Cayman Chemical, Michigan, USA with[3] 95% purity and solubilized in a 50% (v/v) mixture of isopropanol (Merck) with 0.1% (v/v) TFA (Sigma-Aldrich) at a stock concentration of 1 mg/ml.

A semi-quantitative spot-on-lawn inhibitory assay was performed on 51 bacterial indicator strains (Table S1) to determine the bacteriocins inhibition spectra. Overnight cultures were diluted 1:100 in BHI soft agar and distributed on BHI agar plates. Once solidified, bacteriocins with various concentrations were applied on designated spots. The plates were incubated at appropriate temperature O/N and inhibition zones were measured the following day. To determine minimal inhibitory concentration (MIC_{50}) of H1 against clinical *S. haemolyticus* isolates (Table S2), as well as strains heterologously expressing RseP (Table S4), the microtiterplate antimicrobial assay was performed as previously described[41,79]. MIC_{50} was defined as the minimal bacteriocin concentration needs to inhibit the growth of a bacterial strain by at least 50%.

Synergistic interactions between antimicrobials were determined using the fractional inhibition concentration (FIC) as previously described[80]. The FIC values were determined using a mirotiterplate checkerboard assay. Briefly, antimirobial A was applied in wells A1–H1 then diluted two-fold in wells 2–12. In a second microtiter plate, antimicrobial B was applied in wells A1–A12, then diluted two folds in wells B–H. Fifty µl of the serial diluted antimirobial A was transferred to the wells of a third microtiter plate, except for wells H1–H12. Similarly, 50 µl of the serial diluted antimicrobial B was transferred to the same microtiter plate, except for wells A1–A12. Wells H1-12 and wells A1-12 contained only one of the antimicrobials and was used to estimate the MIC value of the pure substance. After combining the antimicrobials, 100 µl of a 1:25 diluted O/N of *S. haemolyticus* was transferred to each well of the third microplate, while 50 µl of medium was added to wells H1-12 and A1-12. The plates where incubated at 37 °C for 5, 24 or 48 h before the MIC values were scored. FIC values were calculated as follows: FIC = FICa + FICb + FICc, where the FICa means MIC of A in combination/MIC of A alone, FICb means MIC of B in combination/MIC of B, and FICc means MIC of C in combination/MIC of C alone. Effects were considered as synergistic if FIC was ≤ 0.5 for two components mixture[81] and ≤ 0.75 for three components mixture[82].

Isolation of H1-resistant mutants. During the spot-on-lawn inhibitory assay on plates, H1-resistant *S. haemolyticus* isolates were observed within the inhibition zones. Resistant colonies within the inhibition zones with various H1-concentrations (1 mg/ml or 10 mg/ml) were re-streaked to obtain pure colonies. Glycerol stocks (15% glycerol v/v) of the pure cultures were made and stored at − 80 °C until use.

DNA sequencing. For *rseP* sequencing, *rseP* was PCR amplified using pure colonies or gDNA isolated from H1-resistant *S. haemolyticus* strains as a template. gDNA was isolated from the resistant mutants using NucleoSpin Genomic DNA kit from Microorganisms (Macherey–Nagel). *rseP* was amplified using Q5 Hot Start High-Fidelity DNA polymerase (New England Biolabs). PCR amplicons were purified using NucleoSpin Gel and PCR clean-up kit (Macherery-Nagel), sequenced at Eurofins GATC, Germany, and analysed using CLC Main Workbench (Qiagen) (https://digitalinsights.qiagen.com). Primers used for sequencing and PCR amplification are listed in Table S6. For whole genome sequencing, genomic DNA was sequenced using Illumina Next Generation Sequencing. Contigs were assembled using Unipro UGENE[83], while SnapGene software (GSL Biotech), Blast (NCBI) and UniProt was applied in further downstream analysis.

Heterologous expression of *rseP*. *rseP* (Uniprot: Q4L5W4) derived from *S. haemolyticus* 7067_4_21 was heterologously expressed in the naturally H1-resistant *L. plantarum* WCFS1[36] using the vector pSIP expression system[84,85]. First, pLp1261_InvS, a pSIP401 derivative[84,86], was linearized using FastDigest Restriction Enzymes NdeI and Acc65I (ThermoFisher Scientific) to isolate the vector part. Second, *rseP* was amplified by PCR using specially designed In-Fusion Primes (Table S6), giving amplicons with complementary ends to the

linearized vector. The In-Fusion HD cloning Kit (Takara Bio) was used to fuse *rseP* into the linearized vector, yielding pSIP401_SHRseP. The plasmid was subsequently transformed to *E.coli* TOP10 (ThermoFischer Scientific). Plasmid DNA from *E. coli* was isolated using NucleoSpin Plasmid Kit (Macherey–Nagel). The DNA sequence of all PCR amplified fragments was verified by sequencing at Eurofins GATC, Germany, and before being electroporated into *L. plantarum* WCSF1 following the procedure described by Aukrust and Blom[87].

Biofilm formation assay. A microtiter dish biofilm formation assay was performed to determine the biofilm forming ability of *S. haemolyticus* strains. Briefly, the optical density measured at 600 nm (OD_{600}) of O/N cultures was adjusted to 0.5 by diluting the cultures in 3% Tryptic Soy Broth (TSB; Sigma-Aldrich). This was followed by further diluting 10 ml of the relevant bacterial supentions in 90 ml of 3% TSB supplemented with 1% glucose in the appropriate wells of a 96-well plate (Sarstedt) and incubated at 37 °C for 24 h. Following incubation, the O/N culture medium was removed and the presence of biofilms within the inoculated wells was first assessed visually. For quantification, the biofilms were washed twice with 100 µl of 0.9% NaCl, incubated at 55 °C for 1 h to fix the biofilm forming cells to the plastic surface and then stained with a 0.5% crystal violet solution for 10 min at room temperature. Excess crystal violet solution was removed, and the biofilms were further washed with 100 µl of 0.9% NaCl three times. The residual biofilm-bound crystal violet was then extracted by incubating the wells with 100 ml of absolute ethanol (Sigma-Aldrich) for 10 min. The extraction procedure was repeated twice, and the amount of crystal violet extracted was quantified at OD_{600}. The quantification of the crystal violet released from the biofilm is a surrogate measure of the biofilm formation ability of a strain.

Biofilm-oriented antimicrobial test (BOAT). To assess the antimicrobial effects of bacteriocins on biofilm-associated *S. haemolyticus* cells, the metabolic activity of biofilm-associated cells was determined by using the biofilm-oriented antimicrobial test (BOAT), as previously described[41,52]. H1, garvicin KS and micrococin P1 were assessed individually or in combinations, using a serial two-fold dilution scheme of their concentration. Unless otherwise stated, the starting dilutions were 625 µg/ml for H1 and garvicin KS, 62.5 µg/ml for micrococcin P1. Biofilms were allowed to form for 24 h as described above and subsequently challenged with the bacteriocins, individually or in combinations, for 5, 24 or 48 h at 37 °C. As negative control, the assay was performed using the vehicles to their working concentration (i.e., without bacteriocins).

Determination of persister cells within biofilms after BOAT. The procedure for the BOAT assay was repeated as above, with one exception. Instead of monitoring the residual metabolic activity of biofilm-associated cells after the bacteriocin challenge, bacteriocin-treated cells were resuspended in TSB and further serially diluted. The serial diluted bacterial cells were plated on BHI agar plates and incubated at 37 °C for 24 h. Colony forming units (CFU/ml) were used to quantify the remaining surviving cells after antimicrobial challenge.

Confocal microscopy of biofilms. Biofilms were allowed to grow for 24 h as described above except that they were formed in the wells of chambered cover-glass plates (Thermo Fisher Scientific) before being challenged for 24 h with the single bacteriocins or combinations diluted in TSB. The biofilms were subsequently analyzed using the LIVE/DEAD Biofilm Viability Kit (Molecular Probes, Thermo Fisher Scientific) according to the manufacturer´s instruction. Z-stacks of the stained biofilms were then taken on a confocal laser scanning microscope (Zeiss), using a 488 nm argon laser line for exciting the SYTO-9 (green—live cells) dye and a 561 nm laser line for the propidium iodide (red—dead cells). The bacteriocin concentrations used were the same as described for the BOAT assay. The control vehicles for the single bacteriocins and their combination were used at the following concentrations: 0,0063% (v/v) TFA for H1; garvicin KS, 0,003% (v/v) TFA; 3,1% (v/v) 2-propanol for micrococcin P1.

Received: 22 April 2021; Accepted: 15 June 2021
Published online: 06 July 2021

References

1. Becker, K., Heilmann, C. & Peters, G. Coagulase-negative staphylococci. *Clin. Microbiol. Rev.* **27**, 870–926. https://doi.org/10.1128/CMR.00109-13 (2014).
2. Czekaj, T., Ciszewski, M. & Szewczyk, E. M. *Staphylococcus haemolyticus*—An emerging threat in the twilight of the antibiotics age. *Microbiology (Reading)* **161**, 2061–2068. https://doi.org/10.1099/mic.0.000178 (2015).
3. Takeuchi, F. *et al.* Whole-genome sequencing of *staphylococcus haemolyticus* uncovers the extreme plasticity of its genome and the evolution of human-colonizing staphylococcal species. *J. Bacteriol.* **187**, 7292–7308. https://doi.org/10.1128/JB.187.21.7292-7308.2005 (2005).
4. Silva, P. V. *et al.* The antimicrobial susceptibility, biofilm formation and genotypic profiles of *Staphylococcus haemolyticus* from bloodstream infections. *Mem. Inst. Oswaldo Cruz* **108**, 812–813. https://doi.org/10.1590/0074-02761080620130 22 (2013).
5. Klingenberg, C. *et al.* Persistent strains of coagulase-negative staphylococci in a neonatal intensive care unit: virulence factors and invasiveness. *Clin. Microbiol. Infect.* **13**, 1100–1111 (2007).
6. Fredheim, E. G. *et al.* Biofilm formation by *Staphylococcus haemolyticus*. *J. Clin. Microbiol.* **47**, 1172–1180. https://doi.org/10.1128/JCM.01891-08 (2009).
7. Barros, E. M., Ceotto, H., Bastos, M. C., Dos Santos, K. R. & Giambiagi-deMarval, M. *Staphylococcus haemolyticus* as an important hospital pathogen and carrier of methicillin resistance genes. *J. Clin. Microbiol.* **50**(1), 166–8 (2012).
8. Cavanagh, J. P. *et al.* Whole-genome sequencing reveals clonal expansion of multiresistant *Staphylococcus haemolyticus* in European hospitals. *J. Antimicrob. Chemother.* **69**, 2920–2927. https://doi.org/10.1093/jac/dku271 (2014).

9. Froggatt, J. W., Johnston, J. L., Galetto, D. W. & Archer, G. L. Antimicrobial resistance in nosocomial isolates of *Staphylococcus haemolyticus*. *Antimicrob. Agents Chemother.* **33**, 460–466. https://doi.org/10.1128/aac.33.4.460 (1989).
10. Veach, L., Pfaller, M., Barrett, M., Koontz, F. & Wenzel, R. Vancomycin resistance in *Staphylococcus haemolyticus* causing colonization and bloodstream infection. *J. Clin. Microbiol.* **28**, 2064–2068 (1990).
11. Hanssen, A. M., Kjeldsen, G. & Sollid, J. U. Local variants of Staphylococcal cassette chromosome mec in sporadic methicillin-resistant *Staphylococcus aureus* and methicillin-resistant coagulase-negative *Staphylococci*: evidence of horizontal gene transfer?. *Antimicrob. Agents Chemother.* **48**, 285–296. https://doi.org/10.1128/aac.48.1.285-296.2004 (2004).
12. Berglund, C. & Soderquist, B. The origin of a methicillin-resistant *Staphylococcus aureus* isolate at a neonatal ward in Sweden-possible horizontal transfer of a staphylococcal cassette chromosome mec between methicillin-resistant *Staphylococcus haemolyticus* and *Staphylococcus aureus*. *Clin. Microbiol. Infect.* **14**, 1048–1056. https://doi.org/10.1111/j.1469-0691.2008.02090.x (2008).
13. Fluit, A. C., Carpaij, N., Majoor, E. A., Bonten, M. J. & Willems, R. J. Shared reservoir of *ccrB* gene sequences between coagulase-negative staphylococci and methicillin-resistant *Staphylococcus aureus*. *J. Antimicrob. Chemother.* **68**, 1707–1713. https://doi.org/10.1093/jac/dkt121 (2013).
14. Mack, D. *et al.* Biofilm formation in medical device-related infection. *Int. J. Artif. Organs* **29**, 343–359 (2006).
15. Mah, T. F. & O'Toole, G. A. Mechanisms of biofilm resistance to antimicrobial agents. *Trends Microbiol.* **9**, 34–39. https://doi.org/10.1016/s0966-842x(00)01913-2 (2001).
16. Neely, A. N. & Maley, M. P. Survival of enterococci and staphylococci on hospital fabrics and plastic. *J. Clin. Microbiol.* **38**, 724–726. https://doi.org/10.1128/JCM.38.2.724-726.2000 (2000).
17. Nascimento, J. *et al.* Bacteriocins as alternative agents for control of multiresistant staphylococcal strains. *Lett. Appl. Microbiol.* **42**, 215–221 (2006).
18. Cotter, P. D., Ross, R. P. & Hill, C. Bacteriocins—a viable alternative to antibiotics?. *Nat. Rev. Microbiol.* **11**, 95–105. https://doi.org/10.1038/nrmicro2937 (2013).
19. Goldstein, B. P., Wei, J., Greenberg, K. & Novick, R. Activity of nisin against *Streptococcus pneumoniae*, *in vitro*, and in a mouse infection model. *J. Antimicrob. Chemother.* **42**, 277–278 (1998).
20. Ovchinnikov, K. V., Kranjec, C., Thorstensen, T., Carlsen, H. & Diep, D. B. Successful development of bacteriocins into therapeutic formulation for treatment of MRSA skin infection in a murine model. *Antimicrob. Agents Chemother.* https://doi.org/10.1128/AAC.00829-20 (2020).
21. Bartoloni, A. *et al. In-vitro* activity of nisin against clinical isolates of *Clostridium difficile*. *J. Chemother.* **16**, 119–121 (2004).
22. Hanchi, H. *et al.* Inhibition of MRSA and of *Clostridium difficile* by durancin 61A: Synergy with bacteriocins and antibiotics. *Future Microbiol.* **12**, 205–212. https://doi.org/10.2217/fmb-2016-0113 (2017).
23. Ovchinnikov, K. V. *et al.* The leaderless bacteriocin enterocin K1 is highly potent against *Enterococcus faecium*: A study on structure, target spectrum and receptor. *Front. Microbiol.* **8**, 774. https://doi.org/10.3389/fmicb.2017.00774 (2017).
24. Reinseth, I. S., Ovchinnikov, K. V., Tonnesen, H. H., Carlsen, H. & Diep, D. B. The increasing issue of vancomycin-resistant enterococci and the bacteriocin solution. *Probiot. Antimicrob. Proteins* **12**, 1203–1217. https://doi.org/10.1007/s12602-019-09618-6 (2020).
25. Frank, K. L. *et al.* Use of recombinase-based in vivo expression technology to characterize *Enterococcus faecalis* gene expression during infection identifies *in vivo*-expressed antisense RNAs and implicates the protease Eep in pathogenesis. *Infect. Immun.* **80**, 539–549. https://doi.org/10.1128/IAI.05964-11 (2012).
26. Frank, K. L. *et al.* AhrC and Eep are biofilm infection-associated virulence factors in *Enterococcus faecalis*. *Infect. Immun.* **81**, 1696–1708. https://doi.org/10.1128/IAI.01210-12 (2013).
27. Kanehara, K., Ito, K. & Akiyama, Y. YaeL (EcfE) activates the sigma(E) pathway of stress response through a site-2 cleavage of anti-sigma(E), RseA. *Genes Dev.* **16**, 2147–2155. https://doi.org/10.1101/gad.1002302 (2002).
28. Ellermeier, C. D. & Losick, R. Evidence for a novel protease governing regulated intramembrane proteolysis and resistance to antimicrobial peptides in *Bacillus subtilis*. *Genes Dev.* **20**, 1911–1922. https://doi.org/10.1101/gad.1440606 (2006).
29. Kroos, L. & Akiyama, Y. Biochemical and structural insights into intramembrane metalloprotease mechanisms. *Biochim. Biophys. Acta* **2873–2885**, 2013. https://doi.org/10.1016/j.bbamem.2013.03.032 (1828).
30. An, F. Y., Sulavik, M. C. & Clewell, D. B. Identification and characterization of a determinant (*eep*) on the *Enterococcus faecalis* chromosome that is involved in production of the peptide sex pheromone cAD1. *J. Bacteriol.* **181**, 5915–5921. https://doi.org/10.1128/JB.181.19.5915-5921.1999 (1999).
31. Galvez, A. *et al.* Isolation and characterization of enterocin EJ97, a bacteriocin produced by *Enterococcus faecalis* EJ97. *Arch. Microbiol.* **171**, 59–65. https://doi.org/10.1007/s002030050678 (1998).
32. Tiwari, S. K., Sutyak Noll, K., Cavera, V. L. & Chikindas, M. L. Improved antimicrobial activities of synthetic-hybrid bacteriocins designed from enterocin E50–52 and pediocin PA-1. *Appl. Environ. Microbiol.* **81**, 1661–1667. https://doi.org/10.1128/AEM.03477-14 (2015).
33. Acuna, L., Picariello, G., Sesma, F., Morero, R. D. & Bellomio, A. A new hybrid bacteriocin, Ent35-MccV, displays antimicrobial activity against pathogenic Gram-positive and Gram-negative bacteria. *FEBS Open Bio* **2**, 12–19. https://doi.org/10.1016/j.fob.2012.01.002 (2012).
34. Fimland, G. *et al.* New biologically active hybrid bacteriocins constructed by combining regions from various pediocin-like bacteriocins: The C-terminal region is important for determining specificity. *Appl. Environ. Microbiol.* **62**, 3313–3318. https://doi.org/10.1128/AEM.62.9.3313-3318.1996 (1996).
35. Waterhouse, A. *et al.* SWISS-MODEL: Homology modelling of protein structures and complexes. *Nucleic Acids Res.* **46**, W296–W303 (2018).
36. Kleerebezem, M. *et al.* Complete genome sequence of *Lactobacillus plantarum* WCFS1. *Proc. Natl. Acad. Sci. USA* **100**, 1990–1995. https://doi.org/10.1073/pnas.0337704100 (2003).
37. Kontinen, V. P. & Sarvas, M. Mutants of *Bacillus subtilis* defective in protein export. *J. Gen. Microbiol.* **134**, 2333–2344. https://doi.org/10.1099/00221287-134-8-2333 (1988).
38. Leskela, S., Kontinen, V. P. & Sarvas, M. Molecular analysis of an operon in *Bacillus subtilis* encoding a novel ABC transporter with a role in exoprotein production, sporulation and competence. *Microbiology (Reading)* **142**(Pt 1), 71–77. https://doi.org/10.1099/13500872-142-1-71 (1996).
39. Heinrich, J., Lunden, T., Kontinen, V. P. & Wiegert, T. The *Bacillus subtilis* ABC transporter EcsAB influences intramembrane proteolysis through RasP. *Microbiology (Reading)* **154**, 1989–1997. https://doi.org/10.1099/mic.0.2008/018648-0 (2008).
40. Jonsson, I. M. *et al.* Inactivation of the Ecs ABC transporter of *Staphylococcus aureus* attenuates virulence by altering composition and function of bacterial wall. *PLoS ONE* **5**, e14209. https://doi.org/10.1371/journal.pone.0014209 (2010).
41. Kranjec, C. *et al.* A bacteriocin-based antimicrobial formulation to effectively disrupt the cell viability of methicillin-resistant *Staphylococcus aureus* (MRSA) biofilms. *NPJ Biofilms Microbiomes* **6**, 58. https://doi.org/10.1038/s41522-020-00166-4 (2020).
42. Otaka, T. & Kaji, A. Micrococcin: Acceptor-site-specific inhibitor of protein synthesis. *Eur. J. Biochem.* **50**, 101–106. https://doi.org/10.1111/j.1432-1033.1974.tb03876.x (1974).
43. Ciufolini, M. A. & Lefranc, D. Micrococcin P1: Structure, biology and synthesis. *Nat. Prod. Rep.* **27**, 330–342. https://doi.org/10.1039/b919071f (2010).
44. Mikolajka, A. *et al.* Differential effects of thiopeptide and orthosomycin antibiotics on translational GTPases. *Chem. Biol.* **18**, 589–600. https://doi.org/10.1016/j.chembiol.2011.03.010 (2011).

45. Zheng, Q. *et al.* Thiopeptide antibiotics exhibit a dual mode of action against intracellular pathogens by affecting both host and microbe. *Chem. Biol.* **22**, 1002–1007. https://doi.org/10.1016/j.chembiol.2015.06.019 (2015).
46. Ovchinnikov, K. V. *et al.* Novel group of leaderless multipeptide bacteriocins from gram-positive bacteria. *Appl. Environ. Microbiol.* **82**, 5216–5224. https://doi.org/10.1128/AEM.01094-16 (2016).
47. Rogers, K. L., Fey, P. D. & Rupp, M. E. Coagulase-negative staphylococcal infections. *Infect. Dis. Clin. North Am.* **23**, 73–98. https://doi.org/10.1016/j.idc.2008.10.001 (2009).
48. Soumya, K. R., Philip, S., Sugathan, S., Mathew, J. & Radhakrishnan, E. K. Virulence factors associated with Coagulase Negative Staphylococci isolated from human infections. *3 Biotech* **7**, 140. https://doi.org/10.1007/s13205-017-0753-2 (2017).
49. Tremblay, Y. D. *et al.* Characterization of the ability of coagulase-negative staphylococci isolated from the milk of Canadian farms to form biofilms. *J. Dairy Sci.* **96**, 234–246. https://doi.org/10.3168/jds.2012-5795 (2013).
50. Stepanovic, S. *et al.* Quantification of biofilm in microtiter plates: Overview of testing conditions and practical recommendations for assessment of biofilm production by staphylococci. *APMIS* **115**, 891–899. https://doi.org/10.1111/j.1600-0463.2007.apm_630.x (2007).
51. Vanhommerig, E. *et al.* Comparison of biofilm formation between major clonal lineages of methicillin resistant *Staphylococcus aureus*. *PLoS ONE* **9**, e104561. https://doi.org/10.1371/journal.pone.0104561 (2014).
52. Gronseth, T. *et al.* Lugol's solution eradicates *Staphylococcus aureus* biofilm in vitro. *Int. J. Pediatr. Otorhinolaryngol.* **103**, 58–64. https://doi.org/10.1016/j.ijporl.2017.09.025 (2017).
53. Moussa, S. H. & Farouk, A. Tetrazolium/formazan test as anefficient method to determine fungal chitosan antimicrobial activity. *J. Mycol.* https://doi.org/10.1155/2013/753692 (2013).
54. Ito, A., Taniuchi, A., May, T., Kawata, K. & Okabe, S. Increased antibiotic resistance of *Escherichia coli* in mature biofilms. *Appl. Environ. Microbiol.* **75**, 4093–4100. https://doi.org/10.1128/AEM.02949-08 (2009).
55. Pu, Y., Ke, Y. & Bai, F. Active efflux in dormant bacterial cells—New insights into antibiotic persistence. *Drug Resist. Updat.* **30**, 7–14. https://doi.org/10.1016/j.drup.2016.11.002 (2017).
56. Wood, T. K., Knabel, S. J. & Kwan, B. W. Bacterial persister cell formation and dormancy. *Appl. Environ. Microbiol.* **79**, 7116–7121. https://doi.org/10.1128/AEM.02636-13 (2013).
57. Johnsen, L., Fimland, G. & Nissen-Meyer, J. The C-terminal domain of pediocin-like antimicrobial peptides (class IIa bacteriocins) is involved in specific recognition of the C-terminal part of cognate immunity proteins and in determining the antimicrobial spectrum. *J. Biol. Chem.* **280**, 9243–9250. https://doi.org/10.1074/jbc.M412712200 (2005).
58. Fimland, G., Johnsen, L., Dalhus, B. & Nissen-Meyer, J. Pediocin-like antimicrobial peptides (class IIa bacteriocins) and their immunity proteins: Biosynthesis, structure, and mode of action. *J. Pept. Sci.* **11**, 688–696. https://doi.org/10.1002/psc.699 (2005).
59. Saavedra, L., Minahk, C., de Ruiz Holgado, A. P. & Sesma, F. Enhancement of the enterocin CRL35 activity by a synthetic peptide derived from the NH2-terminal sequence. *Antimicrob. Agents Chemother.* **48**, 2778–2781. https://doi.org/10.1128/AAC.48.7.2778-2781.2004 (2004).
60. Salvucci, E., Saavedra, L. & Sesma, F. Short peptides derived from the NH2-terminus of subclass IIa bacteriocin enterocin CRL35 show antimicrobial activity. *J. Antimicrob. Chemother.* **59**, 1102–1108. https://doi.org/10.1093/jac/dkm096 (2007).
61. Xu, X. *et al.* Synergistic combination of two antimicrobial agents closing each other's mutant selection windows to prevent antimicrobial resistance. *Sci. Rep.* **8**, 7237. https://doi.org/10.1038/s41598-018-25714-z (2018).
62. Doern, C. D. When does 2 plus 2 equal 5? A review of antimicrobial synergy testing. *J. Clin. Microbiol.* **52**, 4124–4128. https://doi.org/10.1128/JCM.01121-14 (2014).
63. Zhang, Y., Chen, M., Bruner, S. D. & Ding, Y. Heterologous production of microbial ribosomally synthesized and post-translationally modified peptides. *Front. Microbiol.* **9**, 1801. https://doi.org/10.3389/fmicb.2018.01801 (2018).
64. Dawson, C. C., Intapa, C. & Jabra-Rizk, M. A. Persisters": Survival at the cellular level. *PLoS Pathog* **7**, e1002121. https://doi.org/10.1371/journal.ppat.1002121 (2011).
65. Marimon, O. *et al.* An oxygen-sensitive toxin–antitoxin system. *Nat. Commun.* **7**, 13634. https://doi.org/10.1038/ncomms13634 (2016).
66. Dworkin, J. & Shah, I. M. Exit from dormancy in microbial organisms. *Nat. Rev. Microbiol.* **8**, 890–896. https://doi.org/10.1038/nrmicro2453 (2010).
67. Newstead, L. L., Varjonen, K., Nuttall, T. & Paterson, G. K. Staphylococcal-produced bacteriocins and antimicrobial peptides: Their potential as alternative treatments for *Staphylococcus aureus* infections. *Antibiotics (Basel)* https://doi.org/10.3390/antibiotics9020040 (2020).
68. Mathur, H. *et al.* Fighting biofilms with lantibiotics and other groups of bacteriocins. *NPJ Biofilms Microbiomes* **4**, 9. https://doi.org/10.1038/s41522-018-0053-6 (2018).
69. Zgheib, H., Drider, D. & Belguesmia, Y. Broadening and enhancing bacteriocins activities by association with bioactive substances. *Int. J. Environ. Res. Public Health.* https://doi.org/10.3390/ijerph17217835 (2020).
70. Fahim, H. A., Khairalla, A. S. & El-Gendy, A. O. Nanotechnology: A valuable strategy to improve bacteriocin formulations. *Front. Microbiol.* **7**, 1385. https://doi.org/10.3389/fmicb.2016.01385 (2016).
71. Mataraci, E. & Dosler, S. In vitro activities of antibiotics and antimicrobial cationic peptides alone and in combination against methicillin-resistant *Staphylococcus aureus* biofilms. *Antimicrob. Agents Chemother.* **56**, 6366–6371. https://doi.org/10.1128/AAC.01180-12 (2012).
72. Dosler, S. & Mataraci, E. *In vitro* pharmacokinetics of antimicrobial cationic peptides alone and in combination with antibiotics against methicillin resistant *Staphylococcus aureus* biofilms. *Peptides* **49**, 53–58. https://doi.org/10.1016/j.peptides.2013.08.008 (2013).
73. Varahan, S., Harms, N., Gilmore, M. S., Tomich, J. M. & Hancock, L. E. An ABC transporter is required for secretion of peptide sex pheromones in *Enterococcus faecalis*. *mBio* **5**, e01726–e01714. https://doi.org/10.1128/mBio.01726-14 (2014).
74. Chandler, J. R. & Dunny, G. M. Characterization of the sequence specificity determinants required for processing and control of sex pheromone by the intramembrane protease Eep and the plasmid-encoded protein PrgY. *J. Bacteriol.* **190**, 1172–1183. https://doi.org/10.1128/JB.01327-07 (2008).
75. Dunny, G., Funk, C. & Adsit, J. Direct stimulation of the transfer of antibiotic resistance by sex pheromones in *Streptococcus faecalis*. *Plasmid* **6**, 270–278. https://doi.org/10.1016/0147-619x(81)90035-4 (1981).
76. Vickerman, M. M. *et al.* A genetic determinant in *Streptococcus gordonii* Challis encodes a peptide with activity similar to that of enterococcal sex pheromone cAM373, which facilitates intergeneric DNA transfer. *J. Bacteriol.* **192**, 2535–2545. https://doi.org/10.1128/JB.01689-09 (2010).
77. Reinseth, I., Tonnesen, H. H., Carlsen, H. & Diep, D. B. Exploring the therapeutic potenital of the leaderless enterocins K1 and EJ97 in the treatment of vancomycin-resistant enterococcal infection. *Front. Microbiol.* **12**, 649339. https://doi.org/10.3389/fmicb.2021.649339 (2021).
78. Su, T. L. Micrococcin, an antibacterial substance formed by a strain of *Micrococcus*. *Br. J. Exp. Pathol.* **29**, 473–481 (1948).
79. Chi, H. & Holo, H. Synergistic antimicrobial activity between the broad spectrum bacteriocin garvicin KS and nisin, farnesol and polymyxin B against gram-positive and gram-negative bacteria. *Curr. Microbiol.* **75**, 272–277. https://doi.org/10.1007/s00284-017-1375-y (2018).
80. Orhan, G., Bayram, A., Zer, Y. & Balci, I. Synergy tests by E test and checkerboard methods of antimicrobial combinations against *Brucella melitensis*. *J. Clin. Microbiol.* **43**, 140–143. https://doi.org/10.1128/JCM.43.1.140-143.2005 (2005).

81. Neu, H. C. & Fu, K. P. Synergy of azlocillin and mezlocillin combined with aminoglycoside antibiotics and cephalosporins. *Antimicrob. Agents Chemother.* **13**, 813–819. https://doi.org/10.1128/aac.13.5.813 (1978).
82. Bhusal, Y., Shiohira, C. M. & Yamane, N. Determination of *in vitro* synergy when three antimicrobial agents are combined against *Mycobacterium tuberculosis*. *Int. J. Antimicrob. Agents* **26**, 292–297. https://doi.org/10.1016/j.ijantimicag.2005.05.005 (2005).
83. Okonechnikov, K., Golosova, O. & Fursov, M.; UGENE Team. Unipro UGENE: A unified bioinformatics toolkit. *Bioinformatics* **28**, 1166–1167. https://doi.org/10.1093/bioinformatics/bts091 (2012).
84. Sorvig, E. *et al.* Construction of vectors for inducible gene expression in *Lactobacillus sakei* and *L. plantarum*. *FEMS Microbiol. Lett.* **229**, 119–126. https://doi.org/10.1016/S0378-1097(03)00798-5 (2003).
85. Sorvig, E., Mathiesen, G., Naterstad, K., Eijsink, V. G. H. & Axelsson, L. High-level, inducible gene expression in *Lactobacillus sakei* and *Lactobacillus plantarum* using versatile expression vectors. *Microbiology (Reading)* **151**, 2439–2449. https://doi.org/10.1099/mic.0.28084-0 (2005).
86. Fredriksen, L. *et al.* Surface display of N-terminally anchored invasin by *Lactobacillus plantarum* activates NF-kappaB in monocytes. *Appl. Environ. Microbiol.* **78**, 5864–5871. https://doi.org/10.1128/AEM.01227-12 (2012).
87. Holck, A., Axelsson, L., Birkeland, S. E., Aukrust, T. & Blom, H. Purification and amino acid sequence of sakacin A, a bacteriocin from *Lactobacillus sakei* Lb706. *J. Gen. Microbiol.* **138**, 2715–2720. https://doi.org/10.1099/00221287-138-12-2715 (1992).

Acknowledgements

This study was financed by the Research Council of Norway (Project Nos. 275190 and 273646) and by Grant support from Indian Council for Medical Research, GoI (Grant No.: AMR/IN/113/2013/2017-ECD/II). The funders had no role in study design, data collection and interpretation, or the decision to submit the work for publication.

Author contributions

C.K. and S.K. designed the experiments, analysed the data and wrote the paper. K.T.B and M.B. performed the experiments and contributed to the data analysis. J.P.C. and A.S. provided the *S. haemolyticus* clinical strains used in the study. G.M. and D.B.D. obtained funding, designed the experiments and revised the paper.

Competing interests

The authors declare no competing interests.

Additional information

Supplementary Information The online version contains supplementary material available at https://doi.org/10.1038/s41598-021-93158-z.

Correspondence and requests for materials should be addressed to D.B.D.

Reprints and permissions information is available at www.nature.com/reprints.

Publisher's note Springer Nature remains neutral with regard to jurisdictional claims in published maps and institutional affiliations.

Supplementary

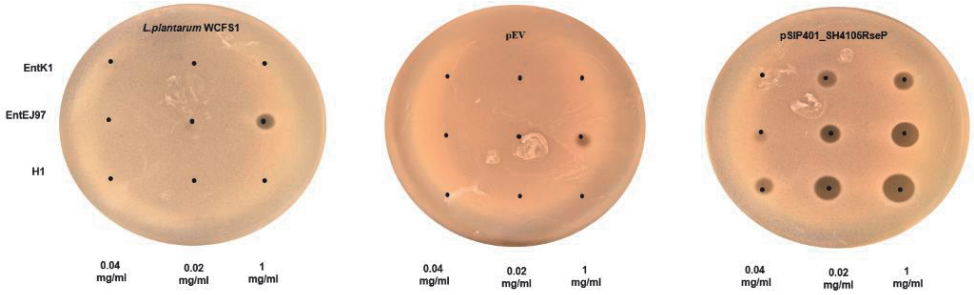

Figure S1| Heterologous expression of *S. haemolyticus* RseP in *L. plantarum* WCFS1. Spot-on-lawn assay on the wild-type *L. plantarum* WCFS1 (A), WCSF1 expressing the empty expression vector pEV (B) or pSIP401-SH4106RseP (a derivative of pEV) containing the *S. haemolyticus rseP* (C). *rsep* was derived from *S. haemolyticus* LMGT 4106. The antimicrobials were EJ97, K1 and H1, each at three concentrations (0.04, 0.2 and 1.0 mg/ml). Five ul of each concentration was applied to each spot. Inhibition is seen as dark zones around the white dots.

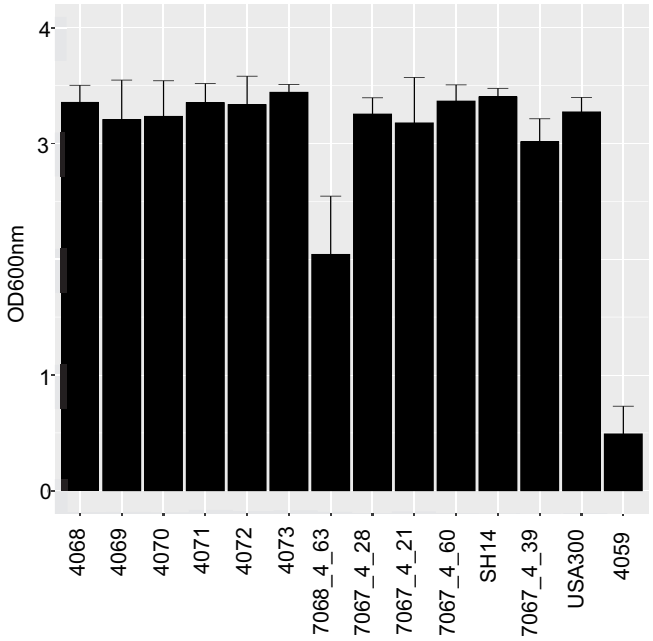

Figure S2| Evaluation of *S. haemolyticus* biofilm formation abilitiy. The indicated *S. haemolyticus* strains were allowed to form for 24 hours prior to staining with a crystal violet solution. The amount of dye bound to the cells is an indirect measure of the biofilm-forming ability and was quantified by optical density readings at 600 nm (OD_{600}) for each strain. The bar chart shows the average values (± s.d.) obtained from three independent experiments. *S. aureus* USA300 and *S.arlettae* (4059) served as a positive and negative control for biofilm formation, respectively. Cut-off OD values for biofilm formation were set to 1.

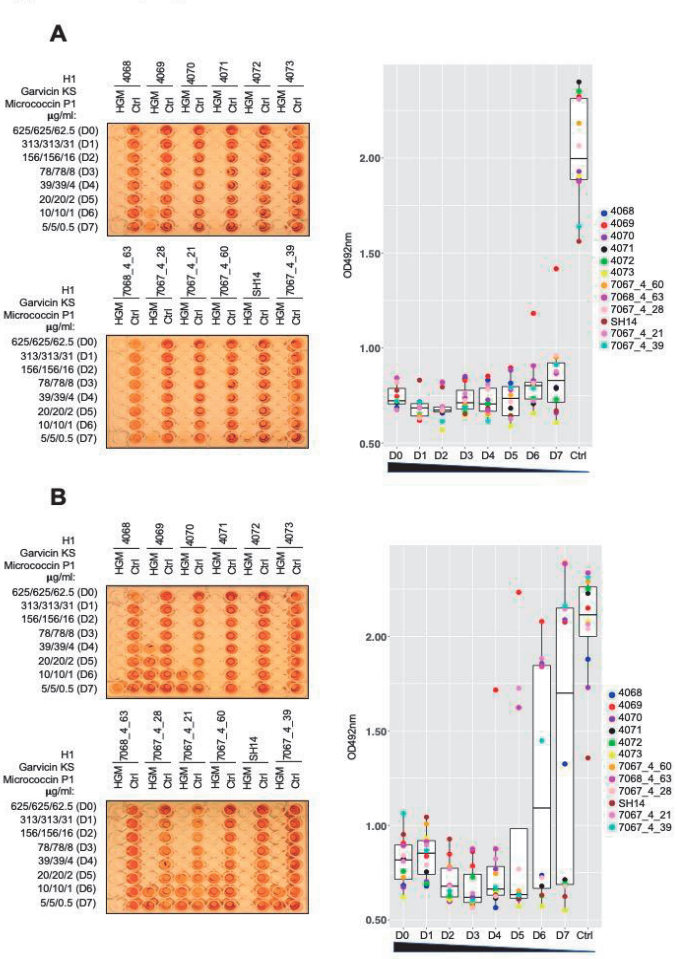

Figure S3| Evaluation of the three-component combination antibiofilm activity. Representative images of BOAT assays (left panels) obtained after a 5 hour treatment (A) or after a 48 hours treatment (B) with the tricomponent antimicrobial combination (HGM - short for H1, GarKS and MP1) or with the control (Ctrl) vehicle. The assays were performed as described in Figure 4A. The boxplot in the right panel describes the recovery of metabolic activity after the antimicrobial treatment (refer to figure 4A for details). Note that the metabolic activity after a 5 hours treatemtn with the antimicrobials remained below detectable levels up to D6 for most stains. Increased levels of metabolic activity were seen when the treatment was extended to 48 hours, especially at high dilution factors (D5-D7).

Table S1| Inhibition spectrum of K1, EJ97 and H1 as assessed by the spot-on-lawn assay against a collection of indicator species (n=50).

Indicator species	Source or reference (*)	Bacteriocins (**)		
		K1	EJ97	H1
Bacillus cereus LMG 2805	LMG	+	-	+
B. cereus LMG 2711	LMG	+	-	+
B. cereus LMG 2731	LMG	+	-	-
Carnobacterium divergens NCDO 2306	NCDO	-	-	-
C. piscicola LMG 2332	LMG	+	-	+
Enterococcus avium LMG 3465	LMG	+	+++	+++
E. faecalis V583	[1]	+	+	++
E. faecalis LMG 2333	LMG	+	+++	+++
E. faecalis LMG 3331	LMG	+	+++	+++
E. faecalis LMG 3330	LMG	+	+++	+++
E. faecalis LMG 3332	LMG	+	+++	++
E. faecium L50	[2]	++	+++	++
E. faecium P13	[3]	+++	+++	+++
E. faecium P21	[4]	++	+++	+++
E. faecium AL41	[5]	++	+++	+++
Esherichia coli DH5α	ThermoFischer Scientific	-	-	-
E. coli TG1	LMG	-	-	-
Lactobacillus curvatus LTH 1174	[6]	+++	+++	++
L. curvatus LMG 2353	LMG	+++	+++	++
L. plantarum LMG 2352	LMG	+	++	-
L. sakei LMG 2380	LMG	++	-	-
L. sakei 148	[7]	+++	-	-
L. salivarius UCC118	[8]	-	-	-
Lactococcus garvieae DCC43	[9]	+++	+	+++
L. lactis LMG 2081	LMG	-	-	-
L. lactis IL1403	[10]	+++	+++	+++
L. gelidum LMG 2386	LMG	-	-	-
L. innocua LMG 2785	LMG	+++	-	+++
L. innocua LMG 2710	LMG	++	+++	+++
L. ivanovii Li4	Nofima	+	+	+
L. monocytogenes 400	VET	-	-	-
L. monocytogenes 223	VET	-	-	+
L. monocytogenes 279	VET	-	-	+
L. monocytogenes EDGe	[11]	+	+++	+++
L. monocytogenes 403	VET	-	-	+
Staphylococcus arlettae LMG 4134	LMG	-	+	-
S. epidermidis LMG 3522	LMG	-	+	++
S. haemolyticus LMG 4133	LMG	+	++	+++

S. homonis LMG 3129	LMG	++	+++	+++
S. simulans LMG 3233	LMG	-	-	-
S. aureus LMG 3326	LMG	-	+	++
S. aureus LMG 3328	LMG	-	-	+
S. aureus LMG 3263	LMG	-	+	+
S. aureus LMG 3325	LMG	-	-	-
S. aureus LMG 3329	LMG	-	-	+
S. aureus ATCC14458	Nofima	-	-	-
Streptococcus dysgalactiae 7649-3	MLM	-	-	-
S. thermophilus Sfi13	[12]	-	-	+++
S. uberis 8008-1	MLM	-	-	++
S. uberis 7904-3	MLM	+	-	++

*LMG: Laboratory of Microbial Gene Technology, Norwegian University of Life Sciences
NCDO: National Collection of Dairy Organisms, United Kingdom
Nofima: Norwegian Food Research Institute, Norway
VET: Faculty of Veterinary Medicine, Norwegian University of Life Science
MLM: Mastitis laboratorium in Molde, Norway

** 5 µl of each bacteriocin at 1 mg/ml. Average inhibition score (n=3) indicates: "-" = No inhibition; "+" = Unclear zone; "++" = zone < 1 cm; "+++"= zone > 1 cm.

Table S2| Minimal inhibitory concentration (MIC) values (µg/ml) of H1 towards clinical and commensial *S. haemolyticus* isolates.

***S.haemolyticus* strain**	**Isolation source (*)**	**MIC_{50} H1 (µg/ml)**	**ENA Acc. No.**	**Reference**
7067_4_39	Blood culture, OUH	0.78	ERS066281	[13]
SH20	Commensal, skin, UNN	0.78	GCA_903969795	[13]
SH14	Commensal, skin, UNN	0.78	GCA_903969855	[13]
SH47	Commensal, skin, UNN	0.10	GCA_903969995	[13]
SH10	Commensal, skin, UNN	0.10	GCA_903969755	[13]
SH04	Commensal, skin, UNN	0.78	GCA_903969785	[13]
SH09	Commensal, skin, UNN	0.78	GCA_903969725	[13]
SH01	Commensal, skin, UNN	0.78	GCA_903969685	[13]
SH46	Commensal, skin, UNN	0.78	GCA_903969985.1	[13]
7067_4_60	Blood, Switzerland	0.10	ERS066392	[14]
7067_4_21	Commensal, Japan	0.39	ERS066353	[14]
7067_4_48	Blood, OUH	0.78	ERS066290	[14]
7067_4_28	Blood, OUH	0.78	ERS066270	[14]
7067_4_71	Urine, OUH	0.78	ERS066313	[14]
7076_4_67	Blood, UNN	0.78	ERS066309	[14]
7067_4_84	Blood, United Kingdom	0.78	N/A	[14]
7067_4_49	Blood, OUH	0.78	ERS066291	[14]
7067_4_66	Blood, UNN	0.78	ERS066308	[14]
7067_4_63	Blood, Switzerland	0.78	ERS066395	[14]
7067_4_56	Blood, OUH	0.78	ERS066298	[14]
7068_7_48	Blood, Switzerland	0.78	ERS066380	[14]
4068	Leprosy-associated plantar skin ulcers, BPHRC	0.39	N/A	This study
4069	Leprosy-associated plantar skin ulcers, BPHRC	0.78	N/A	This study
4070	Leprosy-associated plantar skin ulcers, BPHRC	0.78	N/A	This study
4071	Leprosy-associated plantar skin ulcers, BPHRC	0.78	N/A	This study

4072	Leprosy-associated plantar skin ulcers, BPHRC	0.78	N/A	This study
4073	Leprosy-associated plantar skin ulcers, BPHRC	0.78	N/A	This study

* OUH: Oslo University Hospital, Rikshospitalet, Norway; UNN: University hospital of North Norway; BPHRC: Blue Peter Public Health and Research Centre, India

Table S3| MIC values (µg/ml) determined for planktonic cells after 5, 24 or 48 hour exposure to H1, GarKS, MP1 or the indicated combinations.

Antimicrobial		Strains					
		4068	4069	4070	4071	4072	4073
Individual component							
H1	5h	0.78	0.78	0.78	0.78	0.78	0.78
	24h	>100	0.78	>100	>100	>100	>100
	48h	>100	>100	>100	>100	>100	>100
GarKS	5h	6.5	3.3	12	12.5	23.6	12.5
	24h	24	13	48	51	49	51
	48h	25	26	51	100	52	51
MP1	5h	0.02	0.15	0.02	0.043	0.039	0.022
	24h	0.023	>10	0.33	>10	>10	0.072
	48h	0.078	>10	0.13	>10	0.63	0.14
Combination							
H1	5h	0.83	1.4	0.72	1.6	1.5	1.7
	24h	3.1	6	3.3	12	12	6.3
	48h	6	6.5	6.3	24	13	12
GarKS	5h	0.83	1.4	0.72	1.6	1.5	1.7
	24h	3.1	6	3.3	12	12	6.3
	48h	6	6.5	6.3	24	13	12
FIC*	5h	1.2	2.2	1.0	2.2	2.0	2.3

	24h	0.16	8.16	0.1	0.36	0.36	0.19
	48h	0.3	0.3	0.2	4.8	1.6	1.4
Combination							
H1	5h	0.2	1.5	0.2	0.42	0.36	0.2
	24h	0.78	23	2.8	1.4	1.5	0.36
	48h	0.72	48	6	3	1.6	0.85
MP1	5h	0.02	0.15	0.02	0.042	0.036	0.02
	24h	0.078	2.3	0.28	0.14	0.15	0.036
	48h	0.072	4.8	0.6	0.3	0.16	0.01
FIC*	5h	0.36	2.0	0.36	0.64	0.55	0.36
	24h	0.35	29.7	0.11	0.028	0.03	0.05
	48h	0.1	5.3	0.1	0.06	0.04	0.01
Combination							
GarKS	5h	0.2	1.6	0.2	0.68	0.73	0.2
	24h	0.32	25	3.3	6.3	1.6	0.73
	48h	0.68	50	6.3	6.5	3.1	0.83
MP1	5h	0.02	0.16	0.02	0.068	0.073	0.02
	24h	0.032	2.5	0.33	0.63	0.16	0.073
	48h	0.068	5	0.63	0.65	0.31	0.083
FIC*	5h	0.13	0.6	0.12	0.06	0.2	0.1
	24h	0.15	2.2	0.17	0.19	0.05	0.12
	48h	0.12	1.3	0.2	0.13	0.1	0.7
Combination							
H1	5h	0.32	0.68	0.32	0.72	0.68	0.33
	24h	0.78	3.3	2.8	1.6	1.6	0.78

	48h	2.8	5.8	5.8	3.3	5.8	1.6
GarKS	5h	0.32	0.68	0.32	0.72	0.68	0.33
	24h	0.78	3.3	2.8	1.6	1.6	0.78
	48h	2.8	5.8	5.8	3.3	5.8	1.6
MP1	5h	0.032	0.068	0.032	0.072	0.068	0.033
	24h	0.078	0.33	0.28	0.16	0.16	0.078
	48h	0.28	0.58	0.58	0.33	0.58	0.16
FIC**	5h	0.62	1.12	0.6	1.2	1.1	0.6
	24h	0.38	4.5	0.17	0.06	0.06	0.14
	48h	0.5	0.4	0.2	0.1	0.26	0.15

* Synergy with fractional inhibition concentration (FIC) ≤ 0.5.
** Synergy with fractional inhibition concentration (FIC) ≤ 0.75.

Table S4| Bacterial strains and plasmids used for heterologous expression of RseP.

Strain or plasmid	Relevant characteristics (*)	Reference
Strain		
S.haemolyticus 7076_4_21	Template for *rseP*	[14]
E. coli TOP10	Cloning host	ThermoFischer Scientific
L. plantarum WCFS1	Host strain	[15]
Plasmid		
pEV	Em^r; empty expression vector, a derivative of pSIP401	[16]
pLp1261_InvS	Em^r; a derivative of the *spp*-based expression vector pSIP401.	[16,17]
pSIP401_SHRseP	Em^r; a derivative of pLp1261_InvS, containing a *S. haemolyticus rseP*	This study

*Em^r: Erythromycin resistant

Table S5| Bacteriocins used in this study

Bacteriocins (*)	Amino acid sequence	Reference
K1	MKFKFNPTGTIVKKLTQYEIAWFKNKHGYYPWEIPRC	[18]
Ej97	MLAKIKAMIKKFPNPYTLAAKLTTYEINWYKQQYGRYPWERPVA	[19]
H1	MKFKFNPTGTIVKKLTQYEINWYKQQYGRYPWERPVA	This study
GakA*	MGAIIKAGAKIVGKGVLGGGASWLGWNVGEKIWK	[20]
GakB*	MGAIIKAGAKIIGKGLLGGAAGGATYGGLKKIFG	[20]
GakC*	MGAIIKAGAKIVGKGALTGGGVWLAEKLFGGK	[20]
Micrococcin P1**	SCTTCVCTCSCCTT	[21]

* Components of garvicin KS; ** Micrococcin P1 has exstensive post-translational modifications

Table S6| Primers used in this study

Primer and category	Sequence (5'-3')
RseP amplification	
SH_7076_4_21 _RseP_F	GGA GTA TGA TTC ATA TGA GCT ATT TAA TCA CTA TTG TCT CAT TT
SH_7076_4_21 _RseP_R	TCG AAC CCG GGG TAC CTT ACA AGA AAT AAC GTT GTA TAT CGT TC
Sequencing	
SH_7076_4_21_RseP_Seq_F1	TTG AGT GCA CAT TTG ACT AGA C
SH_7076_4_21_RseP_Seq_F2	ATC GCT CCA CGA CAT CGA C
SH_7076_4_21_RseP_Seq_F3	GAA CGA AAC TTT GTA TAC CAT CCG
SH_7076_4_21_RseP_Seq_R1	ACT CAA TGC TTC TGC TTC AGC
SH_7076_4_21_RseP_Seq_R2	GCT GCA GAC TGA ATG TCA TC
SH_7076_4_21_RseP_Seq_R3	ATG TAC TGG CAC TAA CAA ACT G
SH_7076_4_21_RseP_Seq_R4	AAA TTC GAC CAC CAT CAA GTG C

Supplementary references

1 McShan, W. M. & Shankar, N. in *The Enterococci* 409-415 (2002).

2 Cintas, L. M. *et al.* Enterocins L50A and L50B, two novel bacteriocins from *Enterococcus faecium* L50, are related to staphylococcal hemolysins. *J Bacteriol* **180**, 1988-1994, doi:10.1128/JB.180.8.1988-1994.1998 (1998).

3 Cintas, L. M., Casaus, P., Havarstein, L. S., Hernandez, P. E. & Nes, I. F. Biochemical and genetic characterization of enterocin P, a novel sec-dependent bacteriocin from *Enterococcus faecium* P13 with a broad antimicrobial spectrum. *Appl Environ Microbiol* **63**, 4321-4330, doi:10.1128/AEM.63.11.4321-4330.1997 (1997).

4 Herranza C, P. C. P., Mukhopadhyaya S, Martínez JM, Rodríguez JM, Nes IF, Hernández PE, Cintas LM. *Enterococcus faecium* P21: a strain occurring naturally in dry-fermented sausages producing the class II bacteriocins enterocin A and enterocin B. *Food Microbiology* **18**, 115-131, doi:https://doi.org/10.1006/fmic.2000.0382 (2001).

5 Marekova, M., Laukova, A., Skaugen, M. & Nes, I. Isolation and characterization of a new bacteriocin, termed enterocin M, produced by environmental isolate *Enterococcus faecium* AL41. *J Ind Microbiol Biotechnol* **34**, 533-537, doi:10.1007/s10295-007-0226-4 (2007).

6 Petra S.Tichaczek, J.-M., Ingolf F.Nes, Rudi F.Vogel, Walter P.Hammes. Characterization of the Bacteriocins Curvacin A from Lactobacillus curvatus LTH1174 and Sakacin P from *L. sake* LTH673. *Systematic and Applied Microbiology* **15**, 460-468, doi:https://doi.org/10.1016/S0723-2020(11)80223-7 (1992).

7 Sobrino, O. J. *et al.* Sakacin M, a bacteriocin-like substance from *Lactobacillus sake* 148. *Int J Food Microbiol* **16**, 215-225, doi:10.1016/0168-1605(92)90082-e (1992).

8 Claesson, M. J. *et al.* Multireplicon genome architecture of *Lactobacillus salivarius*. *Proc Natl Acad Sci U S A* **103**, 6718-6723, doi:10.1073/pnas.0511060103 (2006).

9 Sanchez, J. *et al.* Antimicrobial and safety aspects, and biotechnological potential of bacteriocinogenic enterococci isolated from mallard ducks (Anas platyrhynchos). *Int J Food Microbiol* **117**, 295-305, doi:10.1016/j.ijfoodmicro.2007.04.012 (2007).

10 Bolotin, A. *et al.* The complete genome sequence of the lactic acid bacterium *Lactococcus lactis* ssp. lactis IL1403. *Genome Res* **11**, 731-753, doi:10.1101/gr.gr-1697r (2001).

11 Hechard, Y., Pelletier, C., Cenatiempo, Y. & Frere, J. Analysis of sigma(54)-dependent genes in *Enterococcus faecalis*: a mannose PTS permease (EII(Man)) is involved in sensitivity to a bacteriocin, mesentericin Y105. *Microbiology (Reading)* **147**, 1575-1580, doi:10.1099/00221287-147-6-1575 (2001).

12 Marciset, O., Jeronimus-Stratingh, M. C., Mollet, B. & Poolman, B. Thermophilin 13, a nontypical antilisterial poration complex bacteriocin, that functions without a receptor. *J Biol Chem* **272**, 14277-14284, doi:10.1074/jbc.272.22.14277 (1997).

13 Pain, M., Hjerde, E., Klingenberg, C. & Cavanagh, J. P. Comparative Genomic Analysis of *Staphylococcus haemolyticus* Reveals Key to Hospital Adaptation and Pathogenicity. *Front Microbiol* **10**, 2096, doi:10.3389/fmicb.2019.02096 (2019).

14 Cavanagh, J. P. *et al.* Whole-genome sequencing reveals clonal expansion of multiresistant *Staphylococcus haemolyticus* in European hospitals. *J Antimicrob Chemother* **69**, 2920-2927, doi:10.1093/jac/dku271 (2014).

15 Kleerebezem, M. *et al.* Complete genome sequence of *Lactobacillus plantarum* WCFS1. *Proc Natl Acad Sci U S A* **100**, 1990-1995, doi:10.1073/pnas.0337704100 (2003).

16 Sorvig, E. *et al.* Construction of vectors for inducible gene expression in *Lactobacillus sakei* and *L. plantarum*. *FEMS Microbiol Lett* **229**, 119-126, doi:10.1016/S0378-1097(03)00798-5 (2003).

17 Sorvig, E., Mathiesen, G., Naterstad, K., Eijsink, V. G. H. & Axelsson, L. High-level, inducible gene expression in *Lactobacillus sakei* and *Lactobacillus plantarum* using versatile expression vectors. *Microbiology (Reading)* **151**, 2439-2449, doi:10.1099/mic.0.28084-0 (2005).

18 Ovchinnikov, K. V. *et al.* The Leaderless Bacteriocin Enterocin K1 Is Highly Potent against *Enterococcus faecium*: A Study on Structure, Target Spectrum and Receptor. *Front Microbiol* **8**, 774, doi:10.3389/fmicb.2017.00774 (2017).

19 Frank, K. L. *et al.* Use of recombinase-based in vivo expression technology to characterize *Enterococcus faecalis* gene expression during infection identifies *in vivo*-expressed antisense RNAs and implicates the protease Eep in pathogenesis. *Infect Immun* **80**, 539-549, doi:10.1128/IAI.05964-11 (2012).

20 Ovchinnikov, K. V. *et al.* Novel Group of Leaderless Multipeptide Bacteriocins from Gram-Positive Bacteria. *Appl Environ Microbiol* **82**, 5216-5224, doi:10.1128/AEM.01094-16 (2016).

21 Ciufolini, M. A. & Lefranc, D. Micrococcin P1: structure, biology and synthesis. *Nat Prod Rep* **27**, 330-342, doi:10.1039/b919071f (2010).

Paper III

JBC RESEARCH ARTICLE

The extracellular domain of site-2-metalloprotease RseP is important for sensitivity to bacteriocin EntK1

Received for publication, July 8, 2022, and in revised form, October 1, 2022 Published, Papers in Press, October 14, 2022,
https://doi.org/10.1016/j.jbc.2022.102593

Sofie S. Kristensen[‡], Thomas F. Oftedal[‡], Åsmund K. Røhr, Vincent G. H. Eijsink, Geir Mathiesen[§], and Dzung B. Diep[*,§]

From the Faculty of Chemistry, Biotechnology, and Food Science, Norwegian University of Life Sciences (NMBU), Ås, Norway

Edited by Chris Whitfield

Enterocin K1 (EntK1), a bacteriocin that is highly potent against vancomycin-resistant enterococci, depends on binding to an intramembrane protease of the site-2 protease family, RseP, for its antimicrobial activity. RseP is highly conserved in both EntK1-sensitive and EntK1-insensitive bacteria, and the molecular mechanisms underlying the interaction between RseP and EntK1 and bacteriocin sensitivity are unknown. Here, we describe a mutational study of RseP from EntK1-sensitive *Enterococcus faecium* to identify regions of RseP involved in bacteriocin binding and activity. Mutational effects were assessed by studying EntK1 sensitivity and binding with strains of naturally EntK1-insensitive *Lactiplantibacillus plantarum*–expressing various RseP variants. We determined that site-directed mutations in conserved sequence motifs related to catalysis and substrate binding, and even deletion of two such motifs known to be involved in substrate binding, did not abolish bacteriocin sensitivity, with one exception. A mutation of a highly conserved asparagine, Asn359, in the extended so-called LDG motif abolished both binding of and killing by EntK1. By constructing various hybrids of the RseP proteins from sensitive *E. faecium* and insensitive *L. plantarum*, we showed that the extracellular PDZ domain is the key determinant of EntK1 sensitivity. Taken together, these data may provide valuable insight for guided construction of novel bacteriocins and may contribute to establishing RseP as an antibacterial target.

Site-2-metalloproteases (S2Ps) are a family of intramembrane-cleaving proteases involved in regulated intramembrane proteolysis (RIP) (1, 2). In the RIP cascade, an S2P cleaves its substrate, for example, a membrane-bound anti-sigma factor, within the cell membrane, thereby mediating transmembrane signaling to trigger an adaptive response. S2Ps are conserved in all kingdoms of life and are crucial in several biological processes, including stress response, sporulation, cell polarity, virulence, and nutrient uptake (3–9). Due to its vital role in both animal and human pathogens, RseP is regarded as an attractive antimicrobial target. In fact, nature itself targets RseP, which is a known target for antimicrobial peptides belonging to the LsbB family of bacteriocins in selected Gram-positive bacteria (10, 11). Little is known about how these bacteriocins recognize and bind RseP and how this interaction eventually leads to killing of target cells. More insight into these issues is crucial for understanding bacteriocin function and for understanding how RseP may be targeted in antimicrobial therapy.

The hallmarks of the S2P family are the conserved catalytic motifs (HExxH and LDG) located on transmembrane segments (TMSs) of the protease (12). The S2P family of proteases is divided into four subgroups based on membrane topology and domain structure (13). Among the four groups, only a few members have been characterized; these include *Escherichia coli* RseP (*Ec*RseP) from group I and the group III members MjS2P and SpolVFB from *Methanocaldococcus jannaschii* and *Bacillus subtilis*, respectively (12, 14, 15). *Ec*RseP is the most extensively studied S2P and was first identified as a key modulator of stress response (16, 17). When *E. coli* cells are exposed to stress, a site-1-protease cleaves the membrane-bound anti-σ^E factor RseA. This primary cleavage triggers a secondary cleavage by the S2P *Ec*RseP, which leads to release of RseA into the cytosol (16–18). RseA is further processed in the cytosol to form the mature σ^E, which activates genes involved in the stress response (19). It is believed that most S2P signaling pathways follow this same general cascade.

Next to the catalytic motifs, several conserved regions are thought to be involved in substrate interaction and catalysis by *Ec*RseP. These include the membrane-reentrant β-hairpin–like loop (MRE β-loop), the GxG motif, and the PDZ domain (Fig. 1) (20–22). The PDZ domain has been suggested to work as a size-exclusion filter, preventing interaction with the substrate prior to site-1-protease cleavage (21, 23).

In addition, conserved residues near the LDG catalytic motif located in the third transmembrane segment (TMS3) have been implicated in substrate binding and recognition, in particular two asparagines and prolines in the sequence motif NxxxxNxxPxPxLDG (24), here referred to as the extended LDG motif. Despite the identification of these potentially important features, the mechanism of substrate recognition and binding by *Ec*RseP remains somewhat enigmatic.

[‡] These authors contributed equally to this work. Author order was determined by mutual agreement.
[§] These authors share last authorship.
* For correspondence: Dzung B. Diep, dzung.diep@nmbu.no.

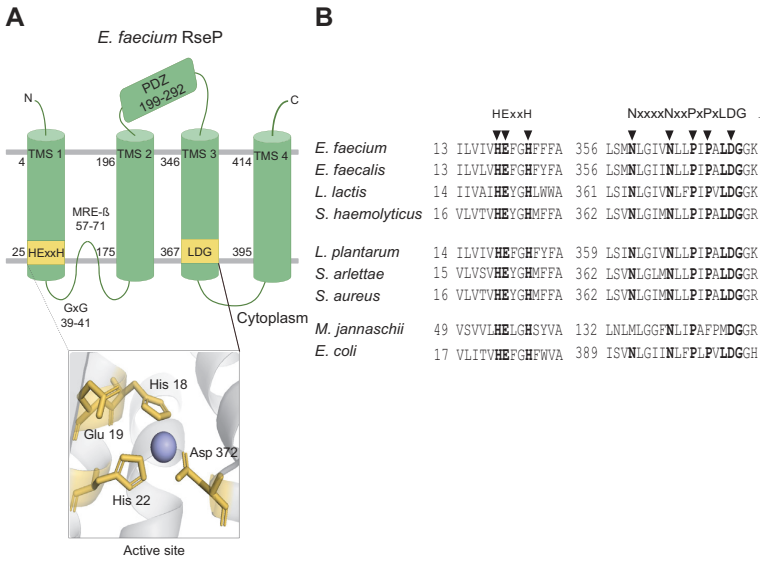

Figure 1. Schematic representation of the topology of *Efm*RseP and alignment of conserved S2P regions. *A*, schematic representation of the predicted topology of *Enterococcus faecium* RseP with conserved S2P motifs indicated. TMS1-4 indicates the four predicted transmembrane segments. The GxG motif, MRE β-loop, and the predicted PDZ domain are indicated. The *box* below shows the predicted active site, consisting of the conserved HEXXH and LDG motifs. *B*, alignment of the amino acid sequences of active site and the extended LDG motif in RseP from four EntK1-sensitive species (*E. faecium*, *Enterococus faecalis*, *Lactococcus lactis*, and *Staphylococcus haemolyticus*) and three EntK1-insensitive species (*Lactiplantibacillus plantarum*, *Staphylococcus arlettae*, and *Staphylococcus aureus*), as well as Gram-negative *Escherichia coli* and *Methanocaldococcus jannaschii*. *Arrow heads* indicate residues subjected to alanine substitutions. EntK1, Enterocin K1; MRE β-loop, membrane-reentrant β-hairpin–like loop; S2P, site-2-metalloprotease; TMS, transmembrane segment.

Bacteriocins are antimicrobial peptides produced by bacteria to inhibit other bacteria in competition for nutrition and ecological niches. They are considered promising alternatives and/or complements to antibiotics, mainly due to their potent activity against multidrug resistant pathogens. We have previously demonstrated that enterocin K1 (EntK1), a leaderless bacteriocin belonging to the LsbB family, is especially potent against *Enterococcus faecium*, including vancomycin-resistant strains (11, 25). Leaderless bacteriocins are synthesized without an N-terminal leader sequence and do not have post-translational modifications, making this group of bacteriocins ideal for synthetic production. Members of the LsbB family are small (30–44 amino acids), cationic, and amphiphilic, with an N-terminal helical structure and a disordered C-terminal end (11, 26). Interestingly, members of the LsbB family of bacteriocins differ in their inhibition spectrum, with LsbB being active only against *Lactococcus lactis*, while the inhibitory spectrum of EntK1 and enterocin EJ97 (EntEJ97) is broader, including high activity toward *E. faecium* and *Enterococcus faecalis*, respectively (11). It has previously been shown that the antimicrobial activity of bacteriocins of the LsbB family depends on RseP being present in target cells (10, 11).

RseP of *E. faecium* (*Efm*RseP) and *Ec*RseP, both from subgroup 1, shares a 28% sequence identity and has the same predicted membrane topology and conserved domains (Fig. 1). Little is known about the function of RseP in *E. faecium*; however, recent phenotypic analysis of *rseP* mutants suggests a role in stress response (25). For *E. faecalis*, it has been shown that RseP (*Efs*RseP) is a key regulator of the stress response through RIP-mediated activation of the sigma factor SigV. Deletion of either *EfsrseP* or *sigV* increases the susceptibility of *E. faecalis* to multiple stressors, such as lysozyme, heat, ethanol, and acid (27). In addition, *Efs*RseP is involved in sex pheromone maturation and is therefore also referred to as Eep (enhanced expression of pheromone) in this organism (28). Lastly, deletion of *EfsrseP* has been shown to result in severely attenuated virulence in a rabbit endocarditis model and a catheter-associated urinary tract infection model, suggesting an important role for *Efs*RseP in pathogenesis (7, 29).

Despite the evident role of RseP in enterococcal virulence, critical features of enterococcal RseP, such as the substrate recognition mechanism, remain unknown. The known substrates of RseP-like S2P share no apparent sequence homology; however, amphiphilic helices in the substrates have been indicated as necessary for recognition (20, 30). Considering the helical structure of EntK1, it is conceivable that EntK1 interacts with enterococcal RseP in a similar manner as the native substrates. Therefore, to gain more insight into bacteriocin action and possibly the interaction between RseP and its natural substrates, we have studied the EntK1–RseP interaction, focusing on the role of conserved regions of RseP. The impact of mutations in these regions was assessed by bacteriocin-binding assays and by analyzing bacteriocin sensitivity of strains carrying mutated RseP. The results shed

light on the interaction between EntK1 and RseP, providing insights into bacteriocin specificity and giving valuable information for the design of novel bacteriocins.

Results

Heterologous expression of RseP renders insensitive Lactiplantibacillus plantarum *sensitive to EntK1*

L. plantarum WCFS1 is a Gram-positive bacterium for which pSIP-based vectors have been developed for heterologous protein expression (31, 32). In addition, the bacterium is insensitive to EntK1 despite having an *rseP* ortholog on the chromosome. Together, these properties make *L. plantarum* a suitable host for expressing *E. faecium* RseP for binding and sensitivity studies. As shown in Table 1, expression of RseP from *E. faecium* renders *L. plantarum* sensitive to EntK1, with a minimum inhibitory concentration (MIC_{50}) of 0.01 μM, while *L. plantarum* carrying the empty vector (pEV) exhibited a MIC_{50} greater than 22 μM, which is considered fully resistant. We also overexpressed *L. plantarum* RseP (*Lp*RseP) in *L. plantarum*, to confirm the inability of *Lp*RseP to be a receptor for EntK1. As expected, the *Lp*RseP-overexpressing strain ($LpRseP^{-His}$; see Table 2 for a description of strain names) remained insensitive (i.e., MIC_{50} greater than 22 μM) (Table 1). These results suggest that the *L. plantarum* strain is a suitable host for heterologous expression of *Efm*RseP. Moreover, a pairwise sequence alignment of *Efm*RseP and *Lp*RseP indicates that subtle sequence differences between *Efm*RseP and *Lp*RseP define the sensitivity toward EntK1 (Fig. S1).

Of note, while the pSIP vectors used for expression (Table 2) have an inducible promoter, regulated by the inducer peptide SppIP (31), all sensitivity and binding experiments were performed using noninducing conditions. Under inducing conditions (3–30 ng/ml SppIP), the transformants showed aberrant growth on agar plates (data not shown), indicating a cytotoxic effect likely due to the high amounts of the membrane-protein RseP. Noninduced cells appeared to grow normally. The inducible promotor *sppA* in the pSIP vector has a low basal activity in *L. plantarum*, which permits low expression of *rseP* genes under noninducing conditions (as demonstrated by the results presented in Table 1).

Antimicrobial activity and binding of EntK1 to sensitive cells depend on RseP

To examine whether the antimicrobial activity observed above is directly linked to the ability of EntK1 to bind target cells, we developed a binding assay for EntK1 to *L. plantarum*. For this assay, EntK1 was chemically synthesized with an N-terminal FITC fluorescent tag. The N-terminal fusion was chosen as the C-terminal half of the LsbB family of bacteriocins and is thought to be necessary for receptor interaction (26). The labeling of EntK1 with FITC reduced the antimicrobial potency, which, however, remained high for *L. plantarum*–expressing *Efm*RseP (Table 1). Fluorescence microscopy of EntK1-sensitive *L. plantarum*–expressing plasmid-encoded *Efm*RseP showed strong fluorescent signals following exposure to FITC-EntK1, consistent with EntK1 binding. In contrast, nonsensitive *L. plantarum* carrying the empty vector (pEV) did not show any visible fluorescent signals under the same conditions, thus confirming lack of EntK1 binding (Fig. 2).

In accordance with the fluorescence microscopy, flow cytometry analysis revealed that FITC-EntK1–exposed *L. plantarum*–expressing RseP derived from *E. faecium* exhibited strong fluorescent signals, while cells containing the empty vector or overexpressing the *Lp*RseP protein showed no signal (Fig. 3). We have previously observed that EntK1 has some antimicrobial activity toward strains of *L. lactis*, *E. faecalis*, and *Staphylococcus haemolyticus* but not strains of *Staphylococcus aureus* and *Staphylococcus arlettae* (33). To confirm that the sensitivity is linked to RseP binding, *rseP* genes derived from these sensitive and insensitive species were heterologously expressed in *L. plantarum*. Table 1 shows that, indeed, *L. plantarum* strains expressing *rseP* genes derived from the sensitive strains of *L. lactis* ($LlRseP^{-His}$), *E. faecalis* ($EfsRseP^{-His}$), and *S. haemolyticus* ($ShRseP^{-His}$) were indeed inhibited by EntK1. In addition, Figure 3 shows that these strains had distinctly higher FITC signals than *L. plantarum* strains expressing RseP from the insensitive strains *S. aureus* ($SasRseP^{-His}$) and *S. arlettae* ($SaeRseP^{-His}$). Taken together, these results provide strong evidence that there is a specific interaction between EntK1 and RseP from bacteria that are naturally sensitive to EntK1 but not between EntK1 and RseP from bacteria that are insensitive to EntK1.

Defining the role of conserved S2P motifs in the EntK1:RseP interaction

To define the regions of RseP involved in EntK1 sensitivity, we initially focused on conserved regions that, based on previous studies of other members of the S2P family, seem to be involved in substrate binding and catalysis. In addition to the

Table 1
MIC for EntK1 and FITC-EntK1 towards *Lactiplantibacillus plantarum* strains expressing heterologous RseP

Strains	Characteristics	MIC_{50} (μM)	
		EntK1	FITC-EntK1
$EfmRseP^{-His}$	Expressing RseP from *Enterococcus faecium*	0.01	0.15
$LpRseP^{-His}$	Expressing RseP from *Lactiplantibacillus plantarum*	>22	>20
$EfsRseP^{-His}$	Expressing RseP from *Enterococcus faecalis*	0.04	0.6
$LlRseP^{-His}$	Expressing RseP from *Lactococcus lactis*	0.09	>20
$ShRseP^{-His}$	Expressing RseP from *Staphylococcus haemolyticus*	0.17	>20
$SaeRseP^{-His}$[a]	Expressing RseP from *Staphylococcus arlettae*	>22	>20
$SasRseP^{-His}$[a]	Expressing RseP from *Staphylococcus aureus*	>22	>20
pEV	Empty vector	>22	>20

[a] Control experiments (Fig. S2) indicated low expression, which may contribute to low sensitivity.

Table 2
Plasmids and bacterial strains used in this study

Strain or plasmid	Relevant characteristic(s)	Reference
Plasmid		
pLp1261_InvS	Spp-based expression vector, pSIP401 backbone, Ery^R	(31, 41)
Strain		
L. plantarum WCFS1 (*Lp*)	Template for *rseP* (*Lp*RseP) and expression host	(53)
E. faecium P21 (*Efm*)	Template for *rseP* (*Efm*RseP)	(54)
E. faecalis V583 (*Efs*)	Template for *rseP* (*Efs*RseP)	NCBI:txid226185
L. lactis IL1403 (*Ll*)	Template for *rseP* (*Ll*RseP)	NCBI:txid272623
S. aureus ATCC 14458 (*Sas*)	Template for *rseP* (*Sas*RseP)	Nofima
S. arlettae LMGT 4134 (*Sae*)	Template for *rseP* (*Sae*RseP)	LMGT
S. haemolyticus LMGT 4106 (*Sh*)	Template for *rseP* (*Sh*RseP)	LMGT
E. coli TOP10	Cloning host	Thermo Fisher Scientific
L. plantarum WCFS1	Harboring pSIP401 encoding various RseP derivates, Ery^R	
pEV	Empty vector	(41)
$EfmRseP^{-His}$	*rseP* from *E. faecium* P21	This study
EfmRseP[a]	*rseP* from *E. faecium* P21, C-terminal 6× His-tag	This study
$EfsRseP^{-His}$	*rseP* from *E. faecalis* V583	This study
$LlRseP^{-His}$	*rseP* from *L. lactis* IL1403	This study
$LpRseP^{-His}$	*rseP* from *L. plantarum* WCFS1	This study
LpRseP[a]	*rseP* from *L. plantarum* WCFS1, C-terminal 6× His-tag	This study
$ShRseP^{-His}$	*rseP from S. haemolyticus* 7067	(33)
$SasRseP^{-His}$	*rseP* from *S. aureus* ATCC 14458	This study
$SaeRseP^{-His}$	*rseP* from *S. arlettae* LMGT 4134	This study
EfmH18A[a]	*Efm*RseP with substitution H18A	This study
EfmE19A[a]	*Efm*RseP with substitution H19A	This study
EfmH22A[a]	*Efm*RseP with substitution H22A	This study
EfmAAxxA[a]	*Efm*RseP with substitutions H18A, H19A, H22A	This study
EfmN359A[a]	*Efm*RseP with substitution N359A	This study
EfmN364A[a]	*Efm*RseP with substitution N364A	This study
EfmP367A[a]	*Efm*RseP with substitution P367A	This study
EfmP369A[a]	*Efm*RseP with substitution P369A	This study
EfmD372A[a]	*Efm*RseP with substitution D372A	This study
Hyb1[a]	Fusion of *Lp*RseP (1–221) and *Efm*RseP (222–422)	This study
Hyb2[a]	Fusion of *Lp*RseP (1–328) and *Efm*RseP (329–422)	This study
Hyb3[a]	Fusion of *Efm*RseP (1–221) and *Lp*RseP (222–425)	This study
Hyb4[a]	Fusion of *Efm*RseP (1–325) and *Lp*RseP (326–425)	This study
Hyb5[a]	Fusion of *Efm*RseP (1–200) and *Lp*RseP (201–425)	This study
Hyb6[a]	Fusion of *Efm*RseP (1–170) and *Lp*RseP (171–425)	This study
Hyb7[a]	Fusion of *Efm*RseP (1–32) and *Lp*RseP (33–425)	This study
Hyb8[a]	Fusion of *Lp*RseP (1–171, 222–425) and *Efm*RseP (172–221)	This study
Hyb9[a]	Fusion of *Lp*RseP (1–201, 222–425) and *Efm*RseP (202–221)	This study
Hyb10[a]	Fusion of *Lp*RseP (1–171, 326–425) and *Efm*RseP (172–325)	This study
Hyb11[a]	Fusion of *Lp*RseP (1–201, 328–425) and *Efm*RseP (202–327)	This study
Trunc[a]	Truncation of *Efm*RseP (1–39, 139–422) Δ40–138	This study

RseP homologs from the respective species are abbreviated with the species initials italicized (*e.g.*, *Sh*RseP is the RseP homolog in *S. haemolyticus*), while the strain names for each *L. plantarum* strain expressing a variant of RseP is not italicized (*e.g.*, ShRseP is *L. plantarum* WCFS1 harboring pSIP401 encoding *Sh*RseP). For cases where the species initials are ambiguous, both the first and last letter of the specific name is used (*e.g.*, *E. faecium* and *E. faecalis*).
Abbreviations: Em^R, erythromycin resistance; LMGT, laboratory of microbial gene technology; Nofima, norwegian institute of food, fisheries and aquaculture research.
[a] Harboring a C-terminal 6× His-tag.

conserved residues of the active site found in all members of the S2P family, *E. faecium* RseP contain multiple other conserved motifs, including the MRE β-loop and the extended LDG motif. These domains are conserved among members of subgroup I and III in the S2P family, as well as the GxG motif and PDZ domain which are only present in subgroup I (Fig. 1). To examine how these conserved motifs of *E. faecium* RseP affect the binding of and sensitivity toward EntK1, mutational analysis of each motif was performed, by site-directed mutagenesis, by creating hybrids of *Efm*RseP and *Lp*RseP, and by a truncation in *Efm*RseP.

The active site

The conserved motifs HExxH and LDG make up the active site of the S2P family (Fig. 1) (14). It has previously been shown that mutations of residues corresponding to *Efm*RseP His18, Glu19, His22, and Asp372 substantially affect the protease activity of RseP homologs from multiple species (12, 14, 34). To examine whether proteolytic activity of RseP is needed for EntK1 sensitivity, alanine substitutions were introduced in all conserved residues in the active site. Single alanine substitutions in the active site (EfmH18A, EfmE19A, EfmH22A, and EfmD372A) resulted in a slight increase of the MIC_{50} from ≤0.002 μM for 6His-tagged WT *Efm*RseP to 0.01 to 0.7 μM for the 6His-tagged mutants (Table 3). In line with these observations, measurements of the populations with the single alanine substitutions in the binding assay described above showed only a slight reduction in binding with 59 to 80% of the median fluorescence intensity of the *L. plantarum* population expressing the native *Efm*RseP. The triple alanine substitution (EfmAAxxA) resulted in a considerable increase in the MIC_{50}, to 2.7 μM (Table 3). However, the triple mutant was still more than 8-fold more sensitive to EntK1 than pEV. The impact of the mutations on the MIC_{50} values could be partly due to variation in RseP expression, which was not assessed in detail. For example, it is conceivable that the triple mutant is rather unstable and was produced in lower amounts, leading to a higher MIC_{50} value and low EntK1 binding. Nevertheless, the fact that all variants remained sensitive and bound the

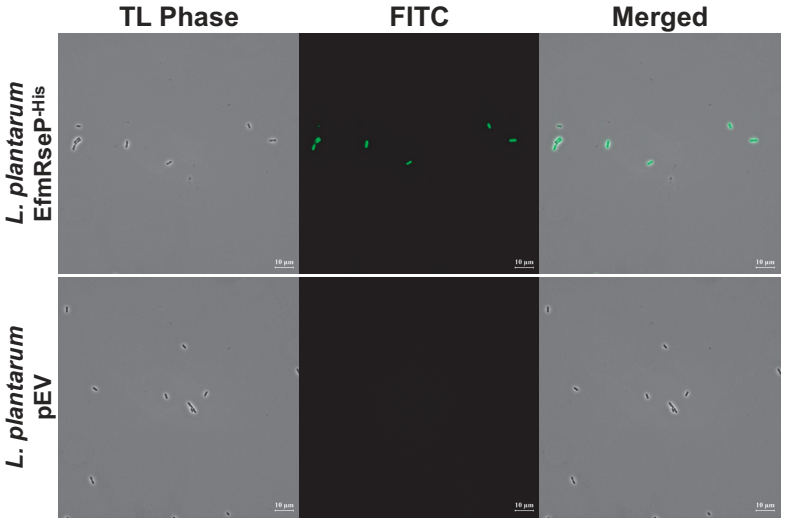

Figure 2. Transmitted light phase contrast and fluorescence microscopy of *Lactiplantibacillus plantarum* expressing *Efm*RseP (EfmRseP^{-His}) or containing the empty vector (pEV) after exposure to FITC-EntK1. EfmRseP cells (*upper panel*) show strong fluorescent signals upon exposure to FITC-EntK1 compared to the negative control containing pEV (*lower panel*). An overlay of the fluorescence and phase-contrast images is shown to the right (Merged). *Efm*RseP, *Enterococcus faecium* RseP; EntK1, Enterocin K1.

bacteriocin clearly shows that the mutant proteins were produced and that the catalytic activity of RseP does not play an essential role in RseP binding and strain sensitivity.

The MRE β-loop and the GxG motif region

Previous studies on *Ec*RseP indicate that the MRE β-loop and the GxG motif region (Fig. 1) interact directly with the substrate (20, 22). To examine the significance of this region for the RseP:EntK1 interaction, residues 39 to 138 encompassing the MRE β-loop and the GxG motif were deleted (Trunc, Fig. S1). The truncation significantly reduced EntK1 sensitivity, as judged by the increase in MIC_{50} of Trunc to 2.7 μM (Table 3). Using the binding assay, we observed that FITC signals were also significantly reduced to 7.4% compared to the full-length protein (Table 3). Nonetheless, the FITC signal reflecting binding (7.4% *versus* 0.4%) and the sensitivity towards EntK1 (MIC_{50} of 2.7 μM *versus* 22 μM) were higher than that of the empty vector control strain (Table 3). It would thus seem that the MRE β-loop and the GxG motif region are not involved in the RseP:EntK1 interaction.

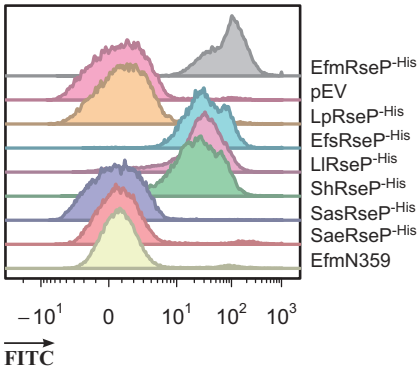

Figure 3. FITC-EntK1 binding assay of *Lactiplantibacillus plantarum* clones expressing RseP from naturally EntK1-sensitive and EntK1-insensitive bacteria. The figure shows representative histograms for *L. plantarum* cells expressing RseP from EntK1-sensitive species *Enterococcus faecium* (EfmRseP^{-His}), *Enterococcus faecalis* (EfsRseP^{-His}), *Lactococcus lactis* (LlRseP^{-His}), and *Staphylococcus haemolyticus* (ShRseP^{-His}), and from EntK1-insensitive species *L. plantarum* (LpRseP^{-His}), *Staphylococcus arlettae* (SaeRseP^{-His}), and *Staphylococcus aureus* (SasRseP^{-His}), in addition to *L. plantarum* carrying the empty vector and the N359A mutant of *Efm*RseP. An increase in fluorescence indicates binding of the bacteriocin to the cells. EntK1, Enterocin K1.

The extended LDG motif

A conserved motif in TMS3 (NxxPxPxLDG), which includes the LDG catalytic site motif (Fig. 1*B*), has been suggested as a prime candidate for S2P substrate binding (13). Moreover, previous substrate-binding studies with *Ec*RseP (24) suggest a longer version of the LDG motif, referred as the extended LDG motif (N359xxxxN364xxP367xP369xLD372G in *Efm*RseP), may be important for substrate binding. The two asparagines and two prolines in the extended motif were individually mutated to alanine. Three of the four mutants remained sensitive to EntK1 and showed strong EntK1 binding (Table 3). However, the alanine substitution of Asn359 in *Efm*RseP (named EfmN359A) resulted in complete resistance to EntK1, and the binding of the bacteriocin was abolished (Fig. 3 and Table 3).

The absence of EntK1 sensitivity and EntK1 binding could be caused by failure to express the *rseP* variant. Therefore,

Table 3
EntK1 sensitivity and EntK1 binding of *Lactiplantibacillus plantarum* expressing variants of RseP

Strain[a]	EntK1 MIC_{50} (μM)	FITC-EntK1 rMFI % (RSD)
EfmRseP	≤0.002	100 (8.3)
pEV	>22	0.4 (4.2)
LpRseP	>22	0.41 (9.7)
Active site		
EfmH18A	0.02	61.6 (3.8)
EfmE19A	0.01	65.4 (3.3)
EfmH22A	0.01	59 (8.1)
EfmAAxxA	2.7	0.5 (5.2)
EfmD372A	0.7	80.6 (3.5)
GxG motif and the MRE β-loop		
Trunc	2.7	7.4 (12.2)
Extended LDG		
EfmN359A	>22	0.41 (22.6)
EfmN364A	0.004	83.4 (3.4)
EfmP367A	0.004	89.1 (4.6)
EfmP369A	≤0.02	84.4 (6.9)
RseP hybrids		
Hyb1	>22	0.42 (25.2)
Hyb2	>22	0.47 (18.3)
Hyb3	0.7	37.6 (24.4)
Hyb4	≤0.002	97.6 (8.5)
Hyb5	>22	0.82 (36.6)
Hyb6	>22	0.51 (6.8)
Hyb7[b]	>22	0.29 (10.4)
Hyb8	>22	0.82 (26.6)
Hyb9	>22	0.53 (18.2)
Hyb10	≤0.002	78 (7.6)
Hyb11	0.09	54.8 (2.4)

The middle column shows MIC for EntK1 towards *L. plantarum* strains expressing various RseP variants (see text, Figs. 1 and S1 for details). The strains are named by the protein variant they express. The right column shows the binding of FITC-labeled EntK1 to indicated strains. The FITC signals, indicating binding of the bacteriocin, are presented as the relative median fluorescence intensity (rMFI) compared to the MFI obtained for EfmRseP6His (100%) with percent relative standard deviations (RSD).
[a] All RseP variants contain a C-terminal 6× His-tag.
[b] Control experiments (Fig. S2) indicated low expression, which may contribute to low sensitivity.

EfmN359A (and all other variants displaying a complete loss of sensitivity, discussed below) were exposed to EntEJ97, another bacteriocin from the LsbB family. EntEJ97 targets RseP but has a different antimicrobial spectrum compared to EntK1 (11), which implies that its interaction with RseP differs from EntK1. Fig. S2 shows that the control pEV clone displayed limited sensitivity towards EntEJ97, while EfmN359A was highly sensitive to the bacteriocin, showing that the alanine substitution did not drastically alter the protein structure nor the expression level and that the removal of the asparagine side chain alone is likely responsible for the alteration in EntK1 sensitivity and binding. Interestingly, Asn359 and the extended LDG motif are highly conserved among both EntK1-sensitive and EntK1-insensitive species (Fig. 1*B*). Thus, the impact of this residue on EntK1 sensitivity must relate to its interaction with other less conserved regions of the protein.

Mapping the regions involved in EntK1 specificity.

To further identify regions determining EntK1 sensitivity, we constructed several hybrid proteins in which parts of the RseP from insensitive *L. plantarum* were replaced with the corresponding parts of RseP from sensitive *E. faecium* (Hyb1-11, Fig. S3). Previous studies had suggested that residues 328 to 428 in the C-terminal region of RseP from *L. lactis* (YvjB) determine the sensitivity of *L. lactis* to LsbB (35). As LsbB and EntK1 target the same receptor, belong to the same bacteriocin family, and have a similar structure (10, 11, 26), we hypothesized that the C-terminal region of RseP from *E. faecium* would confer EntK1 sensitivity. To test the hypothesis, varying parts of the C-terminal region of *Lp*RseP were replaced with the corresponding region of *E. faecium* RseP (Fig. S3). Surprisingly, the resulting hybrid proteins, Hyb1 and Hyb2, did not confer sensitivity to EntK1 (MIC_{50} > 22 μM) nor did they show bacteriocin binding (Table 3). Control experiments with EntEJ97 (Fig. S2) showed that Hyb1 and Hyb2 were produced.

Next, Hyb3 and Hyb4 (inverts of Hyb1 and Hyb2), containing the N-terminal region of *Efm*RseP and the C-terminal region of *Lp*RseP were constructed (Fig. S3). Unlike Hyb1 and Hyb2, Hyb3 and Hyb4 conferred sensitivity to EntK1 with MIC_{50} values of 0.7 μM and ≤0.002 μM, respectively. Hyb3 and Hyb4 also showed binding of the bacteriocin (Table 3). The results obtained with Hyb1-4 show that the N-terminal region of *E. faecium* RseP (residues 1–324) is involved in EntK1 binding. Although quantitative comparison of MIC_{50} values is risky due to possible differences in expression, it is worth noting that Hyb4, containing the complete *Efm*RseP PDZ domain, was the most sensitive of the four hybrids.

To further narrow down the RseP region needed for EntK1 sensitivity, three additional hybrid proteins containing a decreasing portion of *Efm*RseP were constructed (Hyb5-7, Fig. S3). None of these hybrids, all lacking the PDZ domain from *E. faecium*, could confer sensitivity to or binding of EntK1 (Table 3), indicating that the PDZ domain is required for activity. The control experiments of Fig. S2 showed that Hyb5 and Hyb6 were produced, whereas Hyb7 likely has reduced expression. To confirm the importance of the PDZ region, we constructed four additional hybrid proteins in which different parts of the PDZ domain of *Lp*RseP were replaced with the corresponding sequences of *Efm*RseP (Fig. 3, Hyb8-11). Interestingly, only Hyb10 and Hyb11, which contained the entire PDZ domain from *Efm*RseP were EntK1-sensitive, with MIC_{50} values of 0.002 μM and 0.09 μM, respectively (Table 3). Hyb8 and Hyb9, only containing parts of the *Efm*RseP PDZ domain, were not sensitive to EntK1 with MIC_{50} >22 μM (Table 3). A control experiment showed that both Hyb8 and Hyb9 were highly sensitive to EntEJ97, indicating that these hybrids are produced (Fig. S2).

Importantly, as noted above, all hybrids that did not confer sensitivity or binding to EntK1, except for Hyb7, were sensitive (*i.e.*, inhibition zone >10 mm for EntEJ97; Fig. S2). This indicates that Hyb1-6 and Hyb8-11 were properly expressed and folded. Moreover, all clones of *L. plantarum*–expressing recombinant RseP showed growth comparable to EfmRseP, suggesting that expression of the hybrids had no obvious toxic effect on the host (data not shown).

Discussion

The S2P RseP is highly conserved in multiple species, yet the potency of EntK1 varies considerably between species (11, 33). To further develop EntK1 as a novel treatment option for bacterial infections, a detailed understanding of the determinants of

bacteriocin sensitivity and binding to RseP is essential. Therefore, in this study, we explored the contribution of conserved S2P motifs to the EntK1:RseP interaction and EntK1 sensitivity. To do so, we first needed to establish a sensitivity and binding assay. Although the antimicrobial activity of EntK1 depends on RseP (11), it remains elusive whether the difference in EntK1 sensitivity between species is solely due to variations in the RseP protein or if other factors, such as cell surface composition and gene expression levels, contribute. To avoid potential problems related to these uncertainties, we expressed *rseP* from insensitive and sensitive species in the same expression vector (pSIP) and EntK1-insensitive host (*L. plantarum*). We demonstrated that only *rseP* from sensitive bacterial species confers EntK1 sensitivity to *L. plantarum*. Binding of the bacteriocin to the RseP-producing *L. plantarum* strains was assessed using FITC-labeled EntK1. The levels of FITC-EntK1 signals correlated well with the MIC_{50} values (Table 3; higher binding correlates with lower MIC_{50} values). These observations show that subtle differences in the receptor alone likely determine variation in EntK1 sensitivity.

*Efm*RseP belongs to group I of the S2P family, for which the involvement of several conserved motifs in substrate binding and substrate specificity has been explored to some extent (20, 22, 24, 34). We considered that these motifs could be involved in EntK1 sensitivity and, therefore, we targeted these motifs in the mutagenesis studies to identify their role(s) in RseP as a bacteriocin receptor. We initially focused on the active site of *E. faecium* RseP, as there were indications in the literature that alterations in the active site of RseP in *E. faecalis* affects the sensitivity to a member of the LsbB bacteriocin family (11). However, none of the mutations in the catalytic center, including mutations known to abolish protease activity in *Ec*RseP (16, 36), led to EntK1 resistance, demonstrating that the proteolytic activity of RseP is not essential for interaction and the antimicrobial action of EntK1.

Two motifs of *Ec*RseP known to interact with the substrate are the MRE β-loop and a conserved GxG motif located on a membrane-associated region between TMS1 and TMS2 (Fig. 1) (20, 22). If RseP-targeting bacteriocins mimic the interaction of natural substrates with the receptor, these two regions would likely interact with EntK1. Although deletion of the MRE β-loop and the GxG motif led to a significant reduction in EntK1 sensitivity, the removal of these nearly 100 amino acids did not result in total resistance toward EntK1 (Table 3), indicating that neither the MRE β-loop nor the GxG motif is essential for the EntK1:RseP interaction. The reduced sensitivity and binding upon truncation are likely due to global structural changes in the receptor resulting from the large deletion. Of note, the MRE β-loop and GxG motif of *Efm*RseP are both predicted to be located on the cytoplasmic side of the cell membrane (Fig. 1*A*); such a location would likely not allow direct interaction with the bacteriocin which attacks target cells from the outside. It should be noted that the predicted topology of *Efm*RseP and the RseP hybrids was not confirmed experimentally in this study. However, a similar topology for the group 1 S2P *Ec*RseP and *Sas*RseP has been confirmed by the fusion of alkaline phosphatase to specific regions of RseP (6, 15), suggesting that the predicted topology may be conserved among group 1 S2Ps.

Next, we explored the role of the extended LDG motif in EntK1:RseP interaction. Substituting Asn364, Pro367, and Pro369 with alanine in *Efm*RseP resulted in only minor changes in EntK1 sensitivity and binding (Table 3). This was surprising, as these conserved asparagine and proline residues are known to be important for substrate binding and correct processing in both *Ec*RseP and S2P from *B. subtilis*, known as SpoIVFB (12, 24, 37, 38). On the other hand, Asn359 was shown to be essential for EntK1 sensitivity and binding (Table 3). Under noninduced conditions, we were not able to detect RseP expression from N359A, or any other clone, using a standard Western blot (Fig. S4). However, when induced, expression levels of N359A and *Efm*RseP were comparable, suggesting that the insensitivity of the clone was due to the N359A substitution but not due to a failure in expression. Moreover, EfmN359A remained highly sensitive to EntEJ97, another bacteriocin of the LsbB family targeting RseP, which strongly indicates that the observed changes in sensitivity and binding were not caused by failure to express mutated *rseP* (Fig. S2). Previous studies have exploited the known substrates of RseP homologs to perform cleavage-based activity assays to confirm proper protein folding and expression following the introduction of mutations (24). However, RseP has no known substrates in *E. faecium*, which explains why cleavage-based activity assays could not be used. Interestingly, Asn389 in *Ec*RseP, which corresponds to Asn359 in *Efm*RseP, plays an important role in substrate recognition. When this asparagine was replaced by cysteine, *Ec*RseP showed reduced substrate binding as well as reduced proteolytic activity (24). Despite the evident role of Asn359 in EntK1:RseP binding, it is interesting to note that Asn359 and the surrounding extended LDG domain are highly conserved in the RseP proteins of both EntK1-sensitive and EntK1-insensitive species (Fig. 1*B*). This suggests that other regions of RseP play a role in bacteriocin binding and sensitivity.

Of the 11 constructed *Efm*RseP-*Lp*RseP hybrid proteins, only four (Hyb3, Hyb4, Hyb10, Hyb11) were EntK1 sensitive (Table 3). Importantly, all EntK1-sensitive hybrids contain parts of the *Efm*PDZ domain, with Hyb4, Hyb10, and Hyb11 containing the entire domain. Of the four sensitive hybrids, hybrids containing the entire *Efm*PDZ domain exhibited the lowest MIC_{50} (*i.e.*, most sensitive), underpinning the important contribution of this domain to the EntK1:RseP interaction. Previous studies have shown that the PDZ domain is involved in substrate recognition by RseP-like S2P (21, 23). It has been suggested that the PDZ domain of *Ec*RseP acts as a size-exclusion filter, preventing substrates with large periplasmic domains access to the active site (21). A similar role has been suggested for the PDZ domain of the *B. subtilis* S2P homolog, RasP (23). Several S2Ps process multiple substrates *in vitro* and *in vivo*, yet the substrate specificity of these proteins is poorly understood. We conclude that the PDZ domain of *Efm*RseP is the defining region for EntK1 binding and thus the major determinant of variation in EntK1 sensitivity.

To better understand the positions of *Efm*RseP motifs investigated in this study, we predicted the structure of *Efm*RseP using AlphaFold. AlphaFold is a protein structure prediction

program based on artificial intelligence that predict protein structures with greater accuracy than any other in silico method (39). As illustrated in Figure 4, AlphaFold predicted that the PDZ domain of *Efm*RseP forms a pocket which may prevent direct access to core residues. Among the regions investigated in this study, Asn359 in the extended LDG domain is located the closest to the PDZ domain, while the GxG motif and the MRE-β loop appears to be more distant (Fig. 4). Taken together with our experimental data, it is conceivable that the initial docking of EntK1 to the PDZ domain leads to subsequent interactions with core residues such as Asn359.

During the finalization of this article, AlphaFold-Multimer was published (R. Evans *et al.*, Preprint at bioRxiv). AlphaFold-Multimer is an extension of AlphaFold2 using an artificial intelligence model explicitly trained for multimeric input. This allowed us to predict the EntK1:RseP complex, which strikingly predicted the interaction between EntK1 and RseP to primarily involve the PDZ domain and the region near Asn359 (data not shown). However, while most of the residues of RseP in the complex exhibited a high confidence score (pLDDT > 90), most of the residues of EntK1 were ranked poorly (pLDDT < 50). Confidence scores below 50 is a strong predictor of disorder, suggesting that the peptide chain is unstructured at physiological conditions or only structured as part of a complex. Indeed, EntK1 has been shown to be disordered in an aqueous environment by NMR spectroscopy (11). Due to the low confidence scores produced for EntK1 in the complex, these structure predictions are highly speculative and should be used cautiously.

While it remains unknown how the EntK1:RseP complex eventually leads to cell death, the present study reveals molecular details of the interaction of EntK1 with its receptor. Previous studies have shown that bacteriocins of the LsbB family can be engineered to improve both potency and alter the activity spectrum (33). The interpretation of these previous results, as well as future efforts to develop improved RseP-binding bacteriocins, will benefit from the deeper insight into the bacteriocin–receptor interaction that we provide here. Importantly, LsbB family of bacteriocins are attractive not only because they act on vancomycin-resistant strains but also because the bacteriocins are short, synthesized without an N-terminal leader sequence, and contain no posttranslational modification, which enables low-cost synthetic production. The fact that RseP homologs have important roles in virulence in several animal and human pathogens highlights RseP as an attractive antimicrobial target in multiple species (9, 40). The mutational analysis performed in this study combined with the predicted *Efm*RseP structure may provide a powerful basis for guided construction of novel bacteriocins and may contribute to further development of RseP as a drug target.

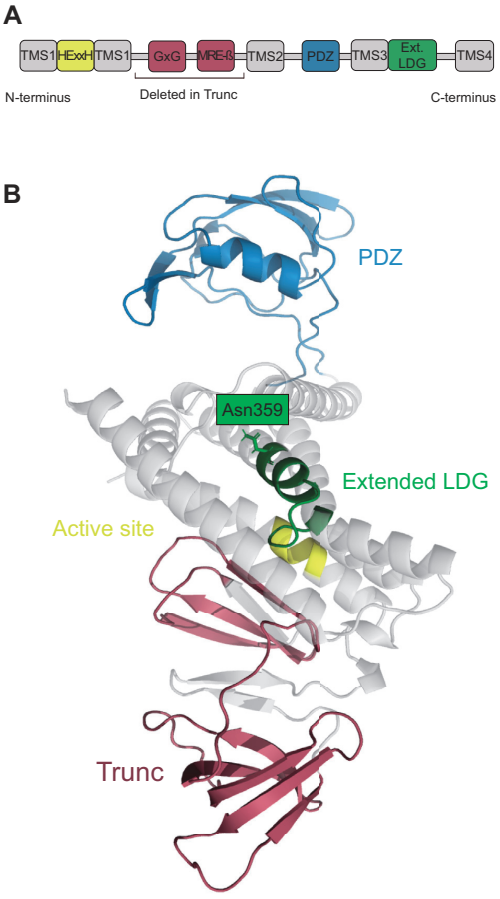

Figure 4. RseP from *Enterococcus faecium* as predicted by AlphaFold. *A*, schematic overview of the conserved RseP-like S2P motifs found in RseP from *E. faecium*. *B*, structure of RseP from *E. faecium* as predicted by AlphaFold with RseP-like S2P motifs highlighted. The HExxH motif of the active site is indicated in *yellow*, the predicted PDZ domain is indicated in *blue*, and the extended LDG domain is indicated in *green*. The region deletion from Trunc, which encompasses the GxG and the MRE β-loop motifs, is indicated in *purple*. MRE β-loop, membrane-reentrant β-hairpin–like loop; S2P, site-2-metalloprotease.

Experimental procedures

Bacterial strains and cultivation conditions

Bacterial strains used in this study are listed in Table 2. The following strains were cultivated in Brain heart infusion broth (Thermo Scientific Oxoid): enterococcal strains (37 °C, without agitation), staphylococcal strains (37 °C, 220 rpm), and *E. coli* (37 °C, 220 rpm). *L. plantarum* and *L. lactis* were cultivated without shaking in DeMan, Rogosa and Sharp (MRS) broth (Thermo Scientific Oxoid) at 37 °C and M17 broth (Thermo Scientific Oxoid) supplemented with 0.5% glucose at 30 °C, respectively. Agar plates were prepared by supplementing the appropriate broth with 1.5% (w/v) agar (VWR chemicals). Erythromycin was added to a final concentration of 200 μg/ml for *E. coli* and 10 μg/ml for *L. plantarum* when appropriate.

Construction of rseP *orthologs,* rseP *hybrids, and site-directed mutagenesis*

Seven orthologs of *rseP* from EntK1-sensitive and EntK1-insensitive species were expressed in *L. plantarum* using the pSIP expression system (31, 32) (Table 2). Briefly,

pLp1261_InvS, a pSIP derivative, was digested with NdeI and Acc65I or XmaI (Thermo Fisher Scientific) (41). Genomic DNA from the seven native *rseP*-containing strains was used as a template for the amplification of *rseP*. PCR amplification of all *rseP* variants was performed using Q5 Hot Start High-fidelity DNA polymerase (New England BioLabs) with In-Fusion primers to yield amplicons with ends complementary to the linearized pSIP vector (Table S1). The amplified PCR fragments were fused with the linearized vector using In-Fusion HD cloning Kit (Takara Bio) and transformed into competent *E. coli* TOP10 (ThermoFisher Scientific).

Site-directed mutants, truncations of RseP and RseP hybrids were constructed using splicing by overlap extension PCR. Briefly, two fragments of the *rseP* sequences were amplified in separate PCR reactions using two primer pairs, each consisting of an inner and outer primer (Table S1). The inner primers generated overlapping complementary ends and acted as mutagenic primers when introducing point-mutations. The overlapping fragments were fused by a second PCR reaction using the outer primers. Fused amplicons containing a mutated *rseP* gene were purified, fused to the linearized vector, and transformed to *E. coli* as described above.

All constructed plasmids were verified by DNA sequencing at Eurofins GATC Biotech (Germany) and subsequently transferred into electrocompetent *L. plantarum* as previously described (42). Fig. S3 shows a schematic representation of all hybrids and the truncated versions of RseP. Protein topology and the PDZ domain were predicted using CCTOP and Pfam, respectively (43, 44).

Antimicrobial assays

The bacteriocins used in this study, EntK1, EntEJ97, and FITC-EntK1, were produced by Pepmic Co, LtD with >95% purity. Bacteriocins were solubilized in 0.1% (vol/vol) TFA (Sigma-Aldrich), except for FITC-EntK1 which was solubilized in dH_2O. For semiquantitative assessment of antimicrobial activity, a spot-on-lawn assay was performed. Briefly, an overnight culture was diluted 1:100 in soft-agar and distributed on agar plates containing appropriate antibiotics. Bacteriocins with various concentrations were applied on designated spots on the solidified soft-agar. The agar plates were incubated at appropriate temperatures overnight and inhibition zones were measured the following day. For more accurate quantification, EntK1 sensitivity was determined using a microtiter plate assay to define MIC_{50} (45). The MIC_{50} was defined as the lowest bacteriocin concentration needed to inhibit bacterial growth by ≥50%. MIC assays were performed with three biological replicates.

Binding assays

Overnight cultures of *L. plantarum* strains were diluted 50-fold and grown until mid-log phase (4 h), after which cells were harvested by centrifugation at 16,000*g* for 3 min and resuspended in sterile 0.9 % (w/v) NaCl to an A_{600} of 1 (assessed using a SPECTROstar Nano reader; BMG Labtech). Cell suspensions were diluted 20-fold in binding buffer [1 μM FITC-labeled EntK1 in 100 μM triammonium citrate pH 6.5 (Sigma-Aldrich)]. The cells were incubated in the binding buffer on a rotator (Multi Bio RS-24, Biosan, Latvia) at 6 rpm for 20 min at room temperature. After incubation, cells were harvested by centrifugation (16,000*g*, 3 min) and the binding buffer was discarded. The cell pellets were resuspended in sterile PBS to an appropriate cell density and analyzed using a MACSQuant Analyzer flow cytometer with excitation at 488 nm and emission at 475 to 575 nm (500 V PMT). The instrument was set to trigger on side-scattered light (SSC-A, 370 V PMT) with the threshold set to 8 to reduce false events.

Data and figures were prepared using the CytoExploreR package (v 1.1.0) for the R programming language (v 4.0.5) (https://github.com/DillonHammill/CytoExploreR [accessed June 25, 2022], https://www.R-project.org/ [accessed June 28, 2022]). All binding assays were performed in triplicate. The median fluorescence intensity (MFI) was calculated as the average of three runs for each strain and expressed as a percent relative to *L. plantarum* expressing RseP from *E. faecium* (rMFI). Percent relative standard deviations were calculated as the ratio of the sample SD to the MFI mean multiplied by 100%.

Phase contrast and fluorescence microscopy

The cells were stained with the FITC-labeled EntK1 as described for the binding assay. After discarding the remaining binding buffer, cells were resuspended in 25 μl of PBS, spotted on a microscopy slide, and overlayed with 2% low melting agarose in PBS to immobilize the cells. Phase-contrast images and FITC fluorescence images were obtained using a Zeiss Axio Observer with ZEN Blue software and an ORCA-Flash 4.0 V2 Digital CMOS camera (Hamamatsu Photonics) using a 100 × phase-contrast objective. The excitation light source was an HXP 120 Illuminator (Zeiss).

AlphaFold and structure analysis

The structure of RseP and complexes between RseP and EntK1 were predicted using the published open source code for AlphaFold according to the instructions by the AlphaFold team (46). All required databases were downloaded on February 10th 2022 and all templates prior to 2022 were included (–max_template_date = 2022-01-01). Interactions present in the predicted complexes were determined by the fully automated protein-ligand interactions profiler (47) and the interactions function implemented in the web-based molecular viewer iCn3D (48, 49). Figures were generated using PyMOL (http://www.pymol.org/pymol). Amino acid sequences used for *Efm*RseP and EntK1 are presented in Table S2.

Data availability

The AlphaFold computations were performed on resources provided by Sigma2 (allocations NN1003K and NS1003K) - the National Infrastructure for High Performance Computing and Data Storage in Norway. For DNA sequence of the

mutants and flow cytometry, the data will be shared upon request.

Supporting information—This article contains supporting information (50–52).

Acknowledgments—This study was financed by the Research Council of Norway through project 275190. The funder had no role in study design, data collection and interpretation, or the decision to submit the work for publication.

Author contributions—S. S. K., T. F. O., G. M., and D. B. D. conceptualization; S. S. K. and T. F. O. methodology; T. F. O. and A. K. R. software; S. S. K., T. F. O., G. M., and D. B. D. validation; S. S. K., T. F. O., G. M., and D. B. D. formal analysis; S. S. K., T. F. O., G. M., and D. B. D. investigation; S. S. K. and T. F. O. data curation; S. S. K. and T. F. O. writing–original draft; S. S. K., T. F. O., V. G. H. E., G. M., and D. B. D. writing–review and editing; A. K. R., G. M., and D. B. D. supervision; D. B. D. project administration; V. G. H. E., G. M., and D. B. D. funding acquisition.

Conflict of interest—The authors declare that they have no conflicts of interest with the contents of this article.

Abbreviations—The abbreviations used are: *Ec*RseP, *Escherichia coli* RseP; *Efm*RseP, *Enterococcus faecium* RseP; *Efs*RseP, *Enterococcus faecalis* RseP; EntK1, Enterocin K1; *Lp*RseP, *Lactiplantibacillus plantarum* RseP; MFI, median fluorescence intensity; MIC50, minimal inhibitory concentration; MRE β-loop, membrane-reentrant β-hairpin–like loop; RIP, regulated intramembrane proteolysis; S2P, site-2-metalloprotease; TMS, transmembrane segment.

References

1. Brown, M. S., Ye, J., Rawson, R. B., and Goldstein, J. L. (2000) Regulated intramembrane proteolysis: a control mechanism conserved from bacteria to humans. *Cell* **100**, 391–398
2. Kroos, L., and Akiyama, Y. (2013) Biochemical and structural insights into intramembrane metalloprotease mechanisms. *Biochim. Biophys. Acta* **1828**, 2873–2885
3. Chen, J. C., Viollier, P. H., and Shapiro, L. (2005) A membrane metalloprotease participates in the sequential degradation of a Caulobacter polarity determinant. *Mol. Microbiol.* **55**, 1085–1103
4. Yokoyama, T., Niinae, T., Tsumagari, K., Imami, K., Ishihama, Y., Hizukuri, Y., *et al.* (2021) The *Escherichia coli* S2P intramembrane protease RseP regulates ferric citrate uptake by cleaving the sigma factor regulator FecR. *J. Biol. Chem.* **296**, 100673
5. King-Lyons, N. D., Smith, K. F., and Connell, T. D. (2007) Expression of hurP, a gene encoding a prospective site 2 protease, is essential for heme-dependent induction of bhuR in *Bordetella bronchiseptica*. *J. Bacteriol.* **189**, 6266–6275
6. Cheng, D., Lv, H., Yao, Y., Cheng, S., Huang, Q., Wang, H., *et al.* (2020) The roles of the site-2 protease Eep in *Staphylococcus aureus*. *J. Bacteriol.* **202**, e00046-20
7. Frank, K. L., Barnes, A. M., Grindle, S. M., Manias, D. A., Schlievert, P. M., and Dunny, G. M. (2012) Use of recombinase-based *in vivo* expression technology to characterize *Enterococcus faecalis* gene expression during infection identifies in vivo-expressed antisense RNAs and implicates the protease Eep in pathogenesis. *Infect. Immun.* **80**, 539–549
8. Schöbel, S., Zellmeier, S., Schumann, W., and Wiegert, T. (2004) The *Bacillus subtilis* sigmaW anti-sigma factor RsiW is degraded by intramembrane proteolysis through YluC. *Mol. Microbiol.* **52**, 1091–1105
9. Schneider, J. S., and Glickman, M. S. (2013) Function of site-2 proteases in bacteria and bacterial pathogens. *Biochim. Biophys. Acta Biomembr.* **1828**, 2808–2814
10. Uzelac, G., Kojic, M., Lozo, J., Aleksandrzak-Piekarczyk, T., Gabrielsen, C., Kristensen, T., *et al.* (2013) A Zn-dependent metallopeptidase is responsible for sensitivity to LsbB, a class II leaderless bacteriocin of *Lactococcus lactis* subsp. lactis BGMN1-5. *J. Bacteriol.* **195**, 5614–5621
11. Ovchinnikov, K. V., Kristiansen, P. E., Straume, D., Jensen, M. S., Aleksandrzak-Piekarczyk, T., Nes, I. F., *et al.* (2017) The leaderless bacteriocin enterocin K1 is highly potent against *Enterococcus faecium*: a study on structure, target spectrum and receptor. *Front Microbiol.* **8**, 774
12. Rudner, D. Z., Fawcett, P., and Losick, R. (1999) A family of membrane-embedded metalloproteases involved in regulated proteolysis of membrane-associated transcription factors. *Proc. Natl. Acad. Sci. U. S. A.* **96**, 14765–14770
13. Kinch, L. N., Ginalski, K., and Grishin, N. V. (2006) Site-2 protease regulated intramembrane proteolysis: sequence homologs suggest an ancient signaling cascade. *Protein Sci.* **15**, 84–93
14. Feng, L., Yan, H., Wu, Z., Yan, N., Wang, Z., Jeffrey, P. D., *et al.* (2007) Structure of a site-2 protease family intramembrane metalloprotease. *Science* **318**, 1608–1612
15. Kanehara, K., Akiyama, Y., and Ito, K. (2001) Characterization of the yaeL gene product and its S2P-protease motifs in *Escherichia coli*. *Gene* **281**, 71–79
16. Alba, B. M., Leeds, J. A., Onufryk, C., Lu, C. Z., and Gross, C. A. (2002) DegS and YaeL participate sequentially in the cleavage of RseA to activate the σE-dependent extracytoplasmic stress response. *Genes Dev.* **16**, 2156–2168
17. Kanehara, K., Ito, K., and Akiyama, Y. (2002) YaeL (EcfE) activates the sigma(E) pathway of stress response through a site-2 cleavage of anti-sigma(E), RseA. *Genes Dev.* **16**, 2147–2155
18. Alba, B. M., and Gross, C. A. (2004) Regulation of the *Escherichia coli* sigma-dependent envelope stress response. *Mol. Microbiol.* **52**, 613–619
19. Flynn, J. M., Levchenko, I., Sauer, R. T., and Baker, T. A. (2004) Modulating substrate choice: the SspB adaptor delivers a regulator of the extracytoplasmic-stress response to the AAA+ protease ClpXP for degradation. *Genes Dev.* **18**, 2292–2301
20. Akiyama, K., Mizuno, S., Hizukuri, Y., Mori, H., Nogi, T., and Akiyama, Y. (2015) Roles of the membrane-reentrant β-hairpin-like loop of RseP protease in selective substrate cleavage. *Elife* **4**, e08928
21. Hizukuri, Y., Oda, T., Tabata, S., Tamura-Kawakami, K., Oi, R., Sato, M., *et al.* (2014) A structure-based model of substrate discrimination by a noncanonical PDZ tandem in the intramembrane-cleaving protease RseP. *Structure* **22**, 326–336
22. Akiyama, K., Hizukuri, Y., and Akiyama, Y. (2017) Involvement of a conserved GFG motif region in substrate binding by RseP, an *Escherichia coli* S2P protease. *Mol. Microbiol.* **104**, 737–751
23. Parrell, D., Zhang, Y., Olenic, S., and Kroos, L. (2017) *Bacillus subtilis* intramembrane protease RasP activity in *Escherichia coli* and *in vitro*. *J. Bacteriol.* **199**, e00381-17
24. Koide, K., Ito, K., and Akiyama, Y. (2008) Substrate recognition and binding by RseP, an *Escherichia coli* intramembrane protease. *J. Biol. Chem.* **283**, 9562–9570
25. Reinseth, I., Tønnesen, H. H., Carlsen, H., and Diep, D. B. (2021) Exploring the therapeutic potenital of the leaderless enterocins K1 and EJ97 in the treatment of vancomycin-resistant enterococcal infection. *Front. Microbiol.* **12**, 248
26. Ovchinnikov, K. V., Kristiansen, P. E., Uzelac, G., Topisirovic, L., Kojic, M., Nissen-Meyer, J., *et al.* (2014) Defining the structure and receptor binding domain of the leaderless bacteriocin LsbB. *J. Biol. Chem.* **289**, 23838–23845
27. Varahan, S., Iyer, V. S., Moore, W. T., and Hancock, L. E. (2013) Eep confers lysozyme resistance to Enterococcus faecalis via the activation of the extracytoplasmic function sigma factor SigV. *J. Biol. Chem.* **195**, 3125–3134
28. An, F. Y., Sulavik, M. C., and Clewell, D. B. (1999) Identification and characterization of a determinant (eep) on the *Enterococcus faecalis* chromosome that is involved in production of the peptide sex pheromone cAD1. *J. Bacteriol.* **181**, 5915–5921
29. Frank, K. L., Guiton, P. S., Barnes, A. M., Manias, D. A., Chuang-Smith, O. N., Kohler, P. L., *et al.* (2013) AhrC and Eep are biofilm infection-

associated virulence factors in *Enterococcus faecalis*. *Infect. Immun.* **81**, 1696–1708
30. Akiyama, Y., Kanehara, K., and Ito, K. (2004) RseP (YaeL), an *Escherichia coli* RIP protease, cleaves transmembrane sequences. *EMBO J.* **23**, 4434–4442
31. Sørvig, E., Grönqvist, S., Naterstad, K., Mathiesen, G., Eijsink, V. G. H., and Axelsson, L. (2003) Construction of vectors for inducible gene expression in *Lactobacillus sakei* and *L. plantarum*. *FEMS Microbiol. Lett.* **229**, 119–126
32. Sørvig, E., Mathiesen, G., Naterstad, K., Eijsink, V. G. H., and Axelsson, L. (2005) High-level, inducible gene expression in *Lactobacillus sakei* and *Lactobacillus plantarum* using versatile expression vectors. *Microbiology (Reading)* **151**, 2439–2449
33. Kranjec, C., Kristensen, S. S., Bartkiewicz, K. T., Brønner, M., Cavanagh, J. P., Srikantam, A., *et al.* (2021) A bacteriocin-based treatment option for *Staphylococcus haemolyticus* biofilms. *Sci. Rep.* **11**, 13909
34. Koide, K., Maegawa, S., Ito, K., and Akiyama, Y. (2007) Environment of the active site region of RseP, an *Escherichia coli* regulated intramembrane proteolysis protease, assessed by site-directed cysteine alkylation. *J. Biol. Chem.* **282**, 4553–4560
35. Miljkovic, M., Uzelac, G., Mirkovic, N., Devescovi, G., Diep, D. B., Venturi, V., *et al.* (2016) LsbB bacteriocin interacts with the third transmembrane domain of the YvjB receptor. *Appl. Environ. Microbiol.* **82**, 5364–5374
36. Dartigalongue, C., Loferer, H., and Raina, S. (2001) EcfE, a new essential inner membrane protease: its role in the regulation of heat shock response in *Escherichia coli*. *EMBO J.* **20**, 5908–5918
37. Zhang, Y., Luethy, P. M., Zhou, R., and Kroos, L. (2013) Residues in conserved loops of intramembrane metalloprotease SpoIVFB interact with residues near the cleavage site in pro-σK. *J. Bacteriol.* **195**, 4936–4946
38. Olenic, S., Buchanan, F., VanPortfliet, J., Parrell, D., and Kroos, L. (2022) Conserved proline residues of *Bacillus subtilis* intramembrane metalloprotease SpoIVFB are important for substrate interaction and cleavage. *J. Bacteriol.* **204**, e0038621
39. Callaway, E. (2020) 'It will change everything': DeepMind's AI makes gigantic leap in solving protein structures. *Nature* **588**, 203–205
40. Urban, S. (2009) Making the cut: central roles of intramembrane proteolysis in pathogenic microorganisms. *Nat. Rev. Microbiol.* **7**, 411–423
41. Fredriksen, L., Kleiveland, C. R., Hult, L. T. O., Lea, T., Nygaard, C. S., Eijsink, V. G. H., *et al.* (2012) Surface display of N-terminally anchored invasin by *Lactobacillus plantarum* activates NF-κB in monocytes. *Appl. Environ. Microbiol.* **78**, 5864–5871
42. Aukrust, T., and Blom, H. (1992) Transformation of Lactobacillus strains used in meat and vegetable fermentations. *Food Res. Int.* **25**, 253–261
43. Dobson, L., Reményi, I., and Tusnády, G. E. (2015) Cctop: a consensus constrained TOPology prediction web server. *Nucleic Acids Res.* **43**, W408–W412
44. Mistry, J., Chuguransky, S., Williams, L., Qureshi, M., Salazar, G. A., Sonnhammer, E. L., *et al.* (2021) Pfam: the protein families database in 2021. *Nucleic Acids Res.* **49**, D412–D419
45. Holo, H., Nilssen, Ø., and Nes, I. (1991) Lactococcin A, a new bacteriocin from *Lactococcus lactis* subsp. cremoris: isolation and characterization of the protein and its gene. *J. Bacteriol.* **173**, 3879–3887
46. Jumper, J., Evans, R., Pritzel, A., Green, T., Figurnov, M., Ronneberger, O., *et al.* (2021) Highly accurate protein structure prediction with AlphaFold. *Nature* **596**, 583–589
47. Salentin, S., Schreiber, S., Haupt, V. J., Adasme, M. F., and Schroeder, M. (2015) Plip: fully automated protein–ligand interaction profiler. *Nucleic Acids Res.* **43**, W443–W447
48. Wang, J., Youkharibache, P., Zhang, D., Lanczycki, C. J., Geer, R. C., Madej, T., *et al.* (2020) iCn3D, a web-based 3D viewer for sharing 1D/2D/3D representations of biomolecular structures. *Bioinformatics* **36**, 131–135
49. Wang, J., Youkharibache, P., Marchler-Bauer, A., Lanczycki, C., Zhang, D., Lu, S., *et al.* (2022) iCn3D: from web-based 3D viewer to structural analysis tool in batch mode. *Front Mol. Biosci.* **9**, 831740
50. Wiull, K., Boysen, P., Kuczkowska, K., Moen, L. F., Carlsen, H., Eijsink, V. G. H., *et al.* (2022) Comparison of the immunogenic properties of Lactiplantibacillus plantarum carrying the mycobacterial Ag85B-ESAT-6 antigen at various cellular localizations. *Front. Microbiol.* **13**, 900922
51. Rice, P., Longden, I., and Bleasby, A. (2000) Emboss: the European molecular biology open software suite. *Trends Genet.* **16**, 276–277
52. Robert, X., and Gouet, P. (2014) Deciphering key features in protein structures with the new ENDscript server. *Nucleic Acids Res.* **42**, W320–W324
53. Kleerebezem, M., Boekhorst, J., van Kranenburg, R., Molenaar, D., Kuipers, O. P., Leer, R., *et al.* (2003) Complete genome sequence of *Lactobacillus plantarum* WCFS1. *Proc. Natl. Acad. Sci. U. S. A.* **100**, 1990–1995
54. Herranz, C., Casaus, P., Mukhopadhyay, S., Martınez, J., Rodrıguez, J., Nes, I., *et al.* (2001) *Enterococcus faecium* P21: a strain occurring naturally in dry-fermented sausages producing the class II bacteriocins enterocin A and enterocin B. *Food Microbiol.* **18**, 115–131

Supplementary

Table S1| Primers used in this study. Amino acid substitutions are highlighted in bold and underlined.

Name	Sequence (5'-3')
In-Fusion primers for amplification of *rseP*	
EfmRseP_F	GAGTATGATTCATATGAAAACGATTCTGACATTTATC
EfmRseP_R	TCGAACCCGGGGTACCCTAGAAAAAGAATCGTTGAATATCGTTCC
EfmRseP6His_R	CGAACCCGGGGTACCCTAATGATGATGATGATGATGGAAAAAGAATCGTTG
LlsRseP_RseP_F	GGAGTATGATTCATATGATAGAAACACTGATTACTTTTATT
LlsRseP_RseP_R	TCGAACCCGGGGTACCTTAATTTACAAAGGCTCGGAGAATATC
EfsRseP_F	GGAGTATGATTCATATGAAAACAATTATCACATTCATTATT
EfsRseP_R	TCGAACCCGGGGTACCTTAAAAGAAAAAGCGTTGAATATCGTTC
LpRseP_F	GGAGTATGATTCATATGATCGTTACAATTATTACGTTCATTA
LpRseP_R	CTGTAATTTGAAGCTTTTAGAAGAAATATCGCTGAATATCATTC
LpRseP6His_R	CTGTAATTTGAAGCTTTTAATGATGATGATGATGATGGAAGAAATATCGCTGAATATCATTC
SasRseP_F	GGAGTATGATTCATATGGTGAGCTATTTAGTTACAATAATTGCAT
SasRseP_R	TCGAACCCGGGGTACCTTATAAGAAATATCGTCGAATATCATTC
SaeRseP_F	GGAGTATGATTCATATGATAAAAATACGAGGTGTAGTTAATTTGA
SaeRseP_R	TCGAACCCGGGGTACCTTATAAGAAATAACGTTGTATATCATTCCTTCC
Primers for site-directed mutagenesis	
EfmH18A_F	TCTGACATTTATCATCGTTTTTGGTATATTAGTGATTGTT**GCG**GAGTTTGGTCATTTCTTCTTT
EfmH18A_R	AAAGAAGAAATGACCAAACTC**CGC**AACAATCACTAATATACCAAAAACGATGATAAATGTCAGA
EfmE19A_F	GGTATATTAGTGATTGTTCAT**GCG**TTTGGTCATTTCTTCTTTGCG
EfmE19A_R	CGCAAAGAAGAAATGACCAAA**CGC**ATGAACAATCACTAATATACC
EfmH22A_F	ATATTAGTGATTGTTCATGAGTTTGGT**GCG**TTCTTCTTTGCGAAACGATCAGGAATC
EfmH22A_R	GATTCCTGATCGTTTCGCAAAGAAGAA**CGC**ACCAAACTCATGAACAATCACTAATAT
EfmAAxxA_F	CGATTCTGACATTTATCATCGTTTTTGGTATATTAGTGATTGTT**GCGGCG**TTTGGT**GCG**TTCTTCTTTGCGAAACGATCAGG
EfmAAxxA_R	CCTGATCGTTTCGCAAAGAAGAA**CGC**ACCAAA**CGCCGC**AACAATCACTAATATACCAAAAACGATGATAAATGTCAGAATCG
EfmN359A_F	GATGGCGCTTCTTTCAATG**GCT**CTCGGAATCGTCAATCTG

EfmN359A_R	CAGATTGACGATTCCGAG**AGC**CATTGAAAGAAGCGCCATC
EfmN364A_F	AATGAATCTCGGAATCGTC**GCT**CTGCTTCCGATTCCTGCC
EfmN364A_R	GGCAGGAATCGGAAGCAG**AGC**GACGATTCCGAGATTCATT
EfmP367A_F	CGGAATCGTCAATCTGCTT**GCG**ATTCCTGCCTT
EfmP367A_R	AAGGCAGGAAT**CGC**AAGCAGATTGACGATTCCG
EfmP369A_F	CGTCAATCTGCTTCCGATT**GCT**GCCTTAGATGG
EfmP369A_R	CCATCTAAGGC**AGC**AATCGGAAGCAGATTGACG
Efm_D372A_F	TGCTTCCGATTCCTGCCTTA**GCT**GGCGGGAAATTA
Efm_D372A_R	TAATTTCCCGCC**AGC**TAAGGCAGGAATCGGAAGCA

Primers used for construction of *rseP* hybrids

Hyb1_F	GCCCGTACGGCCGGTTTAAAAGAAAATGATGAGGTAGTCAGTGT
Hyb1_R	ATCATTTTCTTTTAAACCGGCCGTACGGG
Hyb2_F	CACGGGTTCAGTTTGGATAAATTAGGCGGACCTGTCA
Hyb2_R	TCCGCCTAATTTATCCAAACTGAACCCGTGAGTGA
Hyb3_F	TGCGGCAGAAGCAGGCATTCAAAAGGGCGATCAAATC
Hyb3_R	TCGCCCTTTTGAATGCCTGCTTCTGCCGCA
LpRseP_XmaI_R	TTGGCGCCTTCGAACCCGGGTTAATGATGATGATGATGATGGAAGAAATATCGCT
Hyb4_F	ACAGGTTTCAGTTTAAACGATTTAGGTGGGCC
Hyb4_R	CCCACCTAAATCGTTTAAACTGAAACCTGTAAATAGTGATC
Hyb5_F	ATGCAAGGTGGTGTTACGAGTACAACGACCCA
Hyb5_R	GGTCGTTGTACTCGTAACACCACCTTGCATAAATGCCA
Hyb6_F	TCGGCTAAATTGTGGCAACGAATGTTGACGAATTTTGC
Hyb6_R	CGTCAACATTCGTTGCCACAATTTAGCCGATTGGA
Hyb7_F	CGATCAGGAATCCTCGTGCGTGAATTTTCTGTCGGGA
Hyb7_F2	CGATCAGGAATCCTCGTGCGTGAATTTTCTGTCGGGA
Hyb8_R	GTTGGTCAGCATACGTTGCCATAACTTGGCCGATT
Hyb8_F	GCCAAGTTATGGCAACGTATGCTGACCAACTTTGC
Hyb9a_R	AGTGTTCGTCACTTGAACACCACCCTGCATAAA
Hyb9b_F	ATGCAGGGTGGTGTTCAAGTGACGAACACTAATCGC

Primers used for construction of truncated *rseP*

Trunc_F	GCGAATTTGCTATCAAAGACGTACAGTTCCAATCGGCT
Trunc_R	GGAACTGTACGTCTTTGATAGCAAATTCGCGGACGA

Table S2| Amino acids sequences employed in AlphaFold-Multimer and structure analysis

Name	Sequence
EntK1	MKFKFNPTGTIVKKLTQYEIAWFKNKHGYYPWEIPRC
RseP from *E. faecium*	MKTILTFIIVFGILVIVHEFGHFFFAKRSGILVREFAIGMGPKIYGHQAKDGTTYTLRLLPIGGY VRMAGNGDDETEMAPGMPLSLLLNSDGIVEKINLSKKIQLTNAIPMELSRYDLEDELTITGY VNGDETEVVTYPVDHDATIIENDGTEIRIAPKDVQFQSAKLWQRMLTNFAGPMNNFILAI VLFIILAFMQGGVQVTNTNRVGEIMPNGAAAEAGLKENDEVVSVDGKEIHSWNDLTTVIT KNPGKTLDFKIEREGQVQSVDVTPKSVESNGEKVGQLGIKAPMNTGFMDKIIGGTRQAFS GSLEIFKALGSLFTGFSLDKLGGPVMMYQLSSEAANQGITTVISLMALLSMNLGIVNLLPIPA LDGGKLVLNIFEGIRGKPLSQEKEGILTLAGFGFLMLLMVLVTWNDIQRFFF

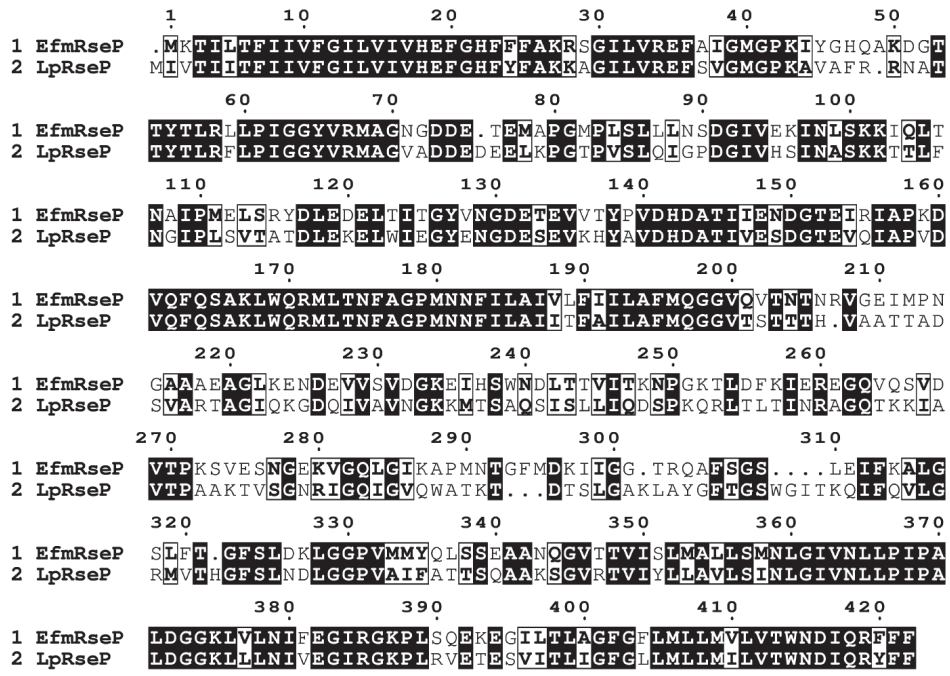

Figure S1| Pairwise sequence alignment of *Efm*RseP and *Lp*RseP. Identical amino acids are shaded in black while amino acids of similar chemical properties are boxed. Alignment was generated using EMBOSS Needle and the figure was exported using ESPript 3 web-serve (51,52).

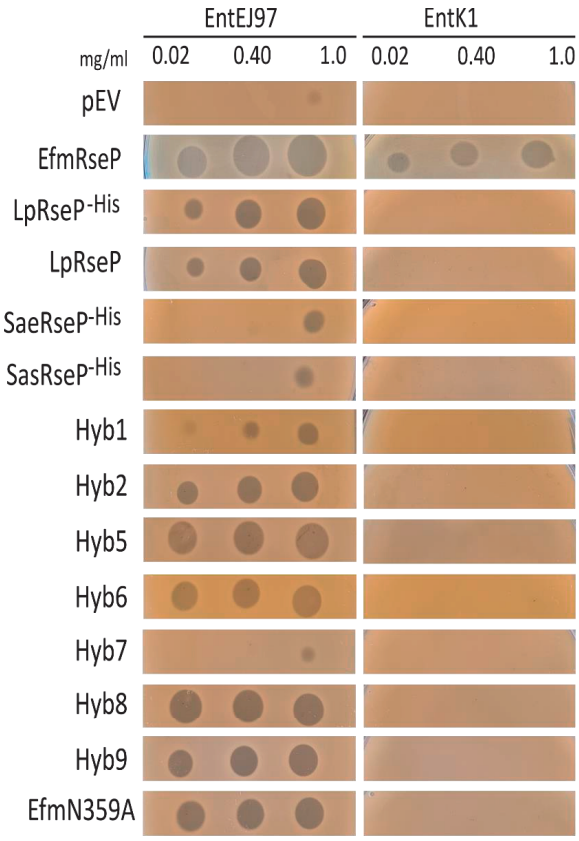

Figure S2| EJ97 inhibition zones in spot-on-lawn assays. 3 µl of EntEJ97 and EntK1 (4–220 µM) was spotted on lawns of *L. plantarum* clones expressing different modified versions of RseP. Since RseP is the receptor for EntEJ97, increased sensitivity towards EntEJ97 compared to the empty vector pEV may indicate proper production and folding of the target protein expression. An inhibition zone of >10 mm was observed for all hybrids and point mutants tested, except for Hyb7, SaeRseP, SasRseP and pEV. A zone comparable to pEV was observed for Hyb7, SaeRseP and SasRseP (<6 mm).

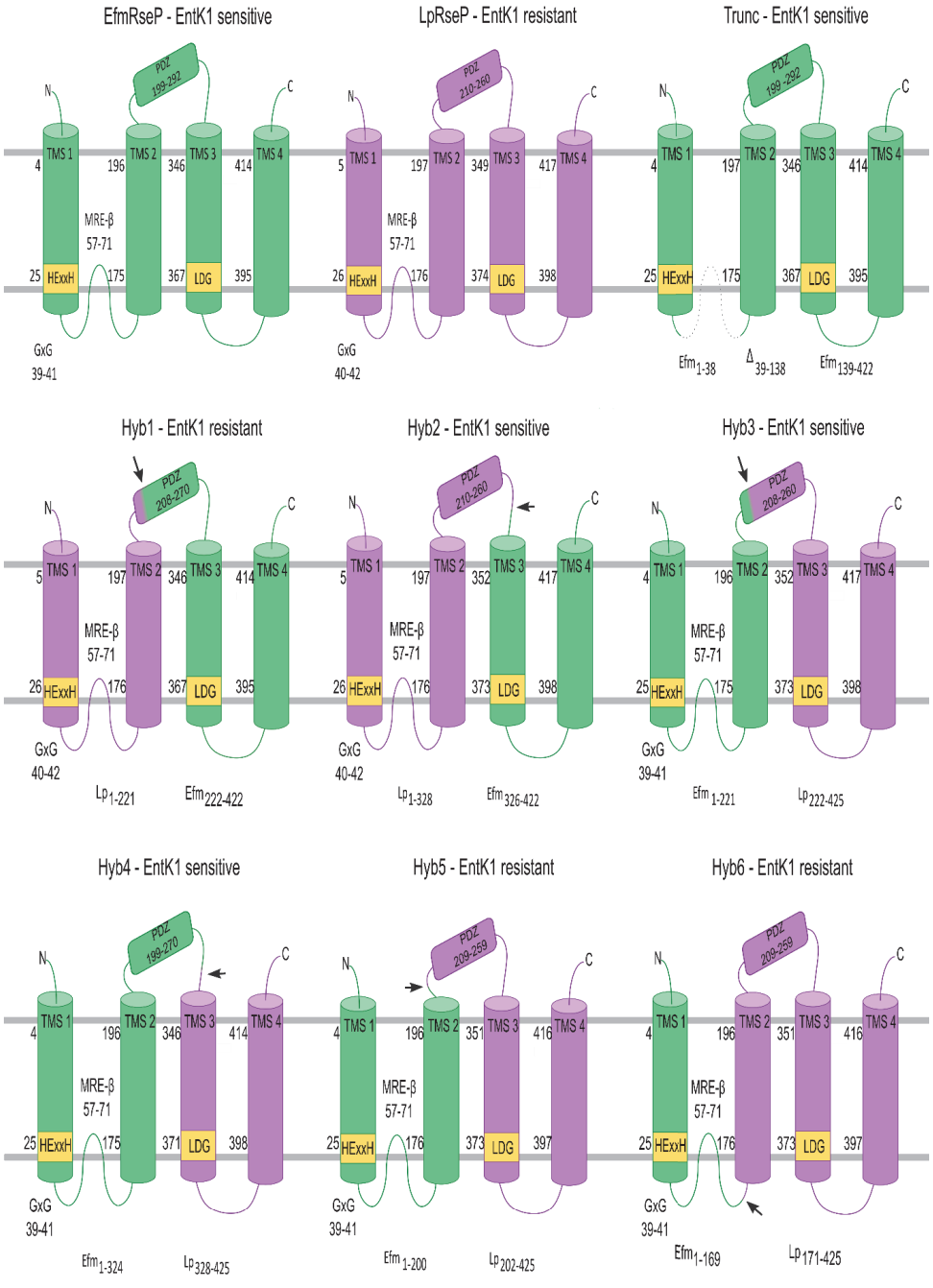
EfmRseP - EntK1 sensitive
LpRseP - EntK1 resistant
Trunc - EntK1 sensitive
Hyb1 - EntK1 resistant
Hyb2 - EntK1 sensitive
Hyb3 - EntK1 sensitive
Hyb4 - EntK1 sensitive
Hyb5 - EntK1 resistant
Hyb6 - EntK1 resistant
N
C
PDZ
TMS 1
TMS 2
TMS 3
TMS 4
HExxH
LDG
MRE-β
57-71
GxG
39-41
40-42
Efm1-38
Δ39-138
Efm139-422
Lp1-221
Efm222-422
Lp1-328
Efm326-422
Efm 1-221
Lp222-425
Efm1-324
Lp328-425
Efm 1-200
Lp202-425
Efm1-169
Lp171-425

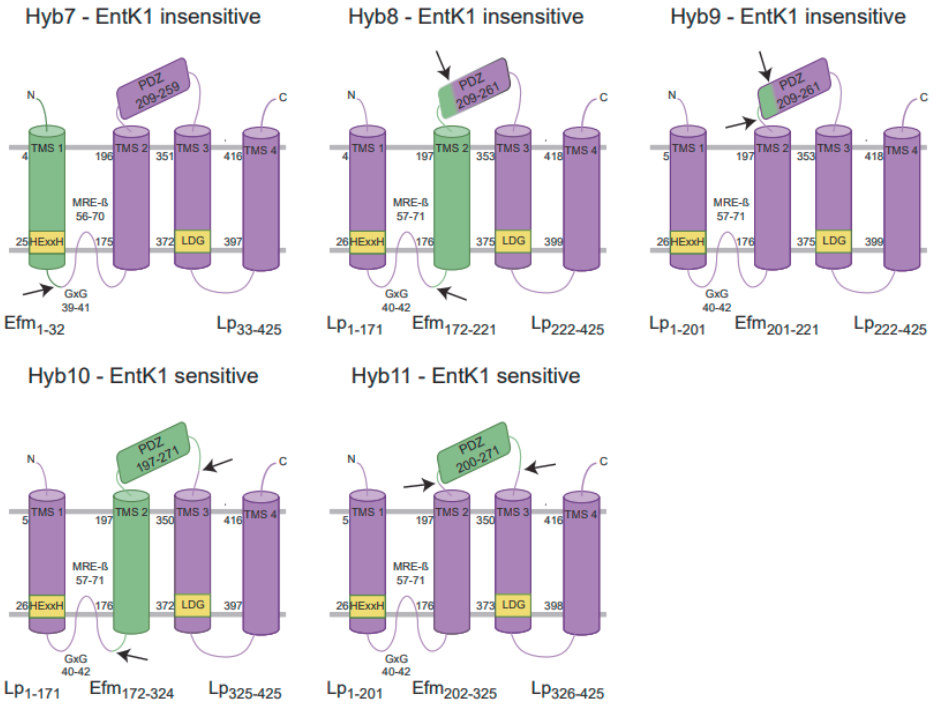

Figure S3 A&B| Schematic representation of all RseP hybrids and truncated RseP. Hybrid proteins in which parts of *Lp*RseP (from the EntK1-insensitive *L. plantarum*, indicated in *purple*) were replaced with the corresponding sequence from *Efm*RseP (from the EntK1-sensitive *E. faecium*, indicated in *green*), were constructed. Conserved S2P motifs are indicated (HExxH, GxG, MRE-ß, PDZ, LDG). TMS1-4 indicate the four predicted transmembrane segments (TMS), while the black arrows indicate the point(s) of fusion between *Lp*RseP and *Efm*RseP regions. The gray dashed line indicates part of the full-length *Efm*RseP deleted in Trunc. Protein variants giving a MIC_{50} ≥22 µM EntK1 are marked as fully EntK1-resistant, while protein variants giving MIC_{50} values below 2.7 µM are marked as EntK1-sensitive. Note that sensitivity data for Hyb7 are uncertain due to possible expression issues visible in the control experiment of Fig. S2. For MIC_{50} values, see Table 3.

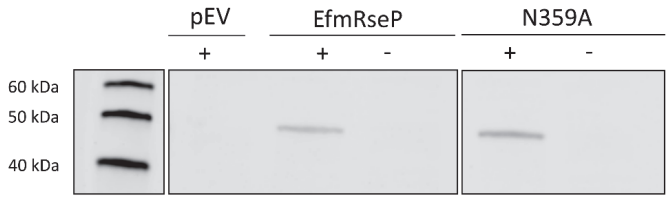

Figure S4| Western blot. pEV, EfmRseP and the N359A mutant under inducing (+) and non-inducing (-) conditions. Cells were harvested, lysed and subjected to SDS-PAGE as previously described (50), with minor modifications. The harvested cells were resuspended in 250 µl NP-40 lysis buffer containing 1 mM PMSF (phenylmethylsulfonyl fluoride). Samples where not boiled prior to SDS-PAGE. Following electrophoresis, proteins were electroblotted onto nitrocellulose mini membranes using iBlot™ Transfer Stack (Invitrogen) and the iBLot Gel transfer device (Invitrogen). The membrane was washed with Tris-Buffered Saline (TBS; 2 × 10 min), then subsequently incubated with blocking buffer (5% Bovine Serum Albumin (BSA) dissolved in TBS) for 1 h and washed again (2 × 10 min Tween-TBS (TTBS; 0.05% Tween-20), 1 × 10 min TBS). The membrane was incubated with Penta-His (Qiagen) (1:1000 in Blocking buffer) for 30 min, following an overnight incubation at 4 °C. The subsequent day the membrane was incubated for 30 min at room temperature, washed (2 × 10 min, TTBS), and incubated with the polyclonal HRP-conjugated anti-mouse IgG (Sigma-Aldrich) secondary antibody (1:5000) in blocking buffer for 1 h. To remove unbound secondary antibodies the membrane was washed 4 × 10 min with TTBS. The blots were subsequently visualized using the SuperSignal West Pico PLUS Chemiluminescent substrate (Thermo Fisher Scientific) and image using the Azure c400 system (Azure Biosystem, Dublin, CA).

Paper IV

A novel platform for production and purification of integral membrane proteins using *Lactiplantibacillus plantarum* as expression host

Sofie S. Kristensen[1*], Suzana Siebenhaar[2], Dzung Diep[1†], J. Preben Morth[2] and Geir Mathiesen[1*].

[1] Faculty of Chemistry, Biotechnology and Food Science, Norwegian University of Life Sciences (NMBU), Ås, Norway

[2] Department of Biotechnology and Biomedicine, Technical University of Denmark (DTU), Kongens Lyngby, Denmark

* Address correspondence to: Sofie S. Kristensen (sofie.kristensen@nmbu.no) or Geir Mathiesen (geir.mathiesen@nmbu.no).

† This author is deceased (7th of December 2022).

Abstract

In the present study, we describe a detailed procedure for expressing and purifying the integral membrane protein RseP using the pSIP system and *Lactiplantibacillus plantarum* as an expression host. RseP is a membrane-bound site-2-protease and a known antibacterial target in multiple human pathogens. Several antimicrobial peptides, known as bacteriocins, depend on RseP for their antimicrobial activity; however, there is limited knowledge on the bacteriocin-RseP interaction and the structure of RseP. Heterologous overexpression and purification of functional membrane proteins is a major bottleneck in the characterization of membrane proteins, thus the development of an efficient protocol for the overproduction and purification of RseP is of interest. In the present study, we screened five RseP orthologs from Gram-positive bacteria and found RseP from *Enterococcus faecium* (EfmRseP) to yield the highest protein levels. The production conditions were optimized and EfmRseP was purified by immobilized metal ion affinity chromatography followed by size-exclusion chromatography. The purification resulted in the overall yield of approximately 1 mg of highly pure protein per 3 gram of wet cell pellet. The structural integrity of the purified protein was confirmed using circular dichroism. We further assessed the expression and purification of RseP from *E. faecium* in the Gram-negative *Escherichia coli*. Detection of soluble protein failed in two of three *E. coli* strains tested. Purification of EfmRseP expressed in *E. coli* C43(DE3) resulted in protein with lower purity compared to EfmRseP expressed in *L. plantarum*. To our knowledge, this is the first time *L. plantarum* and the pSIP expression system have been applied for production of membrane proteins.

Introduction

Integral membrane proteins (IMPs) reside within the lipid membrane surrounding cells and organelles and play a pivotal role in multiple cellular processes, including nutrient transport, molecular recognition, and maintenance of cell integrity. It is estimated that membrane proteins account for 20-30 % of the proteome in most organisms and 60 % of all drug targets, highlighting the importance of membrane proteins in the cell (1-4).

Escherichia coli is the most widely used expression host for recombinant expression of IMPs (Figure 1); however, many membrane proteins fail to fold and get trafficked to the membrane correctly in *E. coli,* resulting in the formation of inclusion bodies (5, 6). Several factors may contribute to insolubility and protein misfolding in *E. coli*, including lack of specific chaperones, mismatch in codon usage and differences in membrane lipid composition. Several alternative expression systems have been developed to circumvent these limitations, with the central principle being that protein expression may be more successful in a host organism more closely related to the organism from which the protein of interest is derived (Figure 1) (7, 8).

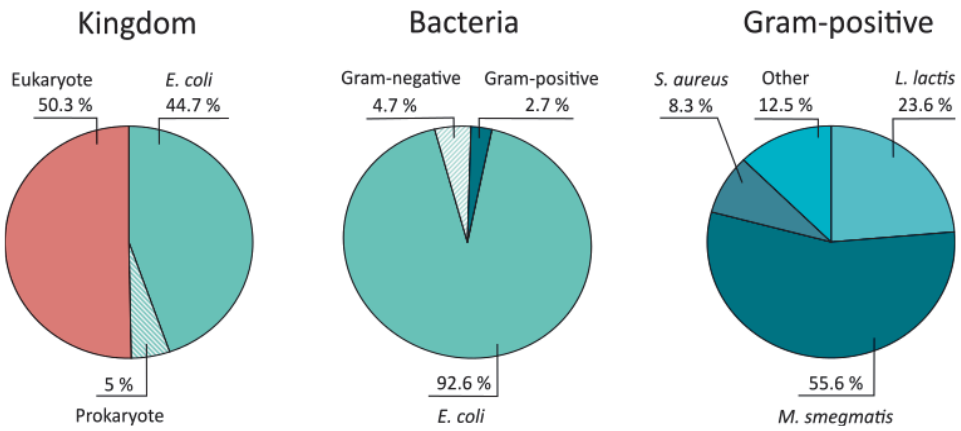

Figure 1 | Comparison of the expression hosts used for production of transmembrane proteins used in structural studies. The number of entries in the Protein Data Bank annotated as transmembrane proteins distributed according to expression host.

Atomic structures of IMPs are generally underrepresented in the Protein Data Bank (https://www.rcsb.org/), only accounting for approximately 3.75 % of the total entries (per. November 2022). Various technical challenges impede the structural characterization of IMPs, with obtaining sufficient amounts of pure and homogeneous protein generally being the first major bottleneck. Among Gram-positive expression hosts used for protein

production to generate IMP structures in the Protein Data Bank, *Mycobacterium smegmatis* and *Lactococcus lactis* are the most commonly used (Figure 1). *M. smegmatis* has been developed as an alternative expression host for mycobacterial proteins, as the expression of proteins from mycobacterial species, such as *Mycobacterium tuberculosis*, are particularly challenging to express in *E. coli* (9, 10). *M. smegmatis* has so far not been extensively used for the expression of proteins from non-mycobacterial species. In contrast, *L. lactis* has been applied in the production of both eukaryotic and prokaryotic proteins, highlighting the versatility of this expression system (11-14).

The use of *L. lactis* for membrane protein production has several advantages, including i) a small genome with limited proteolytic activity; ii) the monoderm cell envelope; iii) a well-developed genetic tool-box; and iv) the ability to reach high cell densities without aeration, thereby allowing expression at industrial scale using bioreactors (14-18). Several inducible and constitutive expression system has been developed for use in *L. lactis*, with the nisin-controlled expression system (NICE) being the most extensively used (19). Various membrane proteins have successfully been structurally characterized using the NICE system in *L. lactis* (20-24) (Figure 1).

Other lactic acid bacteria, such as *Lactiplantibacillus plantarum*, also show significant potential for the overproduction of heterologous proteins (25, 26). Several inducible and constitutive expression systems are compatible with lactobacillal *s*pecies, including the pheromone inducible pSIP vectors, which have been extensively used for the expression, secretion, and surface anchoring of a range of heterologous proteins (25, 27-31). The pSIP system is based on the promotors and regulatory genes involved in the production of the class-II bacteriocin sakacin P in *Latilactobacillus sakei.* The pSIP expression system offers tight regulation of gene expression. The promotor upstream of the target gene is strictly controlled by the two-component system *sppKR*, which depends on the external addition of the peptide pheromone SppIP for induction (27, 28).

While intracellular production of heterologous proteins is well established in *L. plantarum*, expression of IMPs has not yet been evaluated. In the present study, we explore the potential of the pSIP-expression system in *L. plantarum* as a novel platform for production and purification of the site-2-protease RseP. RseP is a membrane-embedded

metalloprotease involved in regulated intramembrane proteolysis, which is a widely distributed signaling mechanism used by bacteria to regulate a diverse array of cellular processes, including stress response, nutrient uptake, and virulence (32-36). Due to its prominent role in bacterial physiology and virulence, RseP is considered an attractive antimicrobial target (37). RseP of selected Gram-positive bacteria acts as a receptor for a specific group of bacteriocins known as the LsbB-family, further highlighting the potential RseP as an antimicrobial target (38-42). Notably, the bacteriocin enterocin K1 (EntK1), which is highly potent against vancomycin resistant bacteria, depends on interaction with enterococcal RseP for its antimicrobial activity (39, 43). The pSIP system has recently been exploited to perform mutational analysis of RseP, revealing molecular details on the interaction between EntK1 and RseP from *Enterococcus faecium* (42). This knowledge, in combination with further structural characterization of RseP, may provide a powerful basis for the rational design of novel bacteriocins. Thus, in this study, we express and purify RseP derived from the Gram-positive *E. faecium* using the pSIP system and *L. plantarum* as the expression host. To our knowledge, this is the first time *L. plantarum* and the pSIP expression system have been applied for the production of membrane proteins.

Materials and methods

Bacterial strains and cultivation conditions

The bacterial strains used in this study are listed in Table 1. Enterococcal strains and *Staphylococcus haemolyticus* were cultivated in brain heart infusion (BHI) broth (Thermo Scientific™, Oxoid™) at 37 °C. All *E. coli* strains were cultivated in Tryptic Soy Broth (TBS) or BHI broth (Thermo Scientific™, Oxoid™) at temperatures ranging from 12-37 °C, depending on the experiment. *Lactococcus lactis* was cultivated in M17 broth (Thermo Scientific™ Oxoid ™) supplemented with 0.5 % glucose at 30 °C while *L. plantarum* was cultivated in De Man, Rogosa and Sharpe (MRS) broth (Thermo Scientific™, Oxoid™) at temperatures ranging from 23-37 °C, depending on the experiment. The enterococcal strains, *L. lactis* and *L. plantarum* were cultivated without shaking, while *E. coli* strains and *S. haemolyticus* were cultivated with agitation at 190 rpm.

Agar plates were prepared by supplementing the appropriate broth with 1.5 % (w/v) agar (VWR chemicals). When appropriate, gentamycin, ampicillin or erythromycin were added to a final concentration of 20 μg/ml, 200 μg/ml, and 200 μg/ml, respectively, for *E. coli*, while erythromycin was added to a final concentration of 10 μg/mL for *L. plantarum.*

Plasmid construction

Five orthologs of the *rseP* gene were expressed in *L. plantarum* using the pSIP expression system (27, 28) (Table 1). The construction of pEfmRseP and pLpRseP containing *rseP* derived from *Enterococcus faecium* P21 and *L. plantarum* WCFS1, respectively, has previously been described(42). *rseP* gene from *L. lactis* IL1430 (*LlRseP*), *S. haemolyticus* 7076_4_21 (*ShRseP*), and *Enterococcus faecalis* V583 (*EfsRseP*), was amplified using genomic DNA as template for PCR amplification with target specific In-Fusion primers (Table S1) that yield amplicons with complementary ends to a linearized vector. A 6xHis-tag was included in all reverse primers, thereby incorporating a C-terminal 6xHis-tag in the final protein product. The resulting PCR fragments were inserted into *Nde*I and *Acc*65I (both ThermoFisher Scientific™) digested pLp_1261_InvS (44), a pSIP401 derivative, following the In-Fusion protocol (Takara Bio Inc, Goteborg, Sweden). The In-Fusion mix was transformed to competent *E. coli* TOP10 (ThermoFisher Scientific™) as described by the manufacturers. The resulting three plasmids (pLIRseP, pShRseP and pEfsRseP) were isolated from *E. coli* using the NucleoSpin Plasmid Kit (Macherey-Nagle) and verified by sequencing at Eurofins GATC Biotech (Germany) and subsequently transformed to electrocompetent *L. plantarum* WCSF1 as previously described(45). An overview of the constructed plasmids is given in Table 1.

Table 1 | Plasmids and bacterial strains used in this study

Strain or plasmid	Relevant characteristic(s)	Reference
Plasmids		
pLp1261_InvS	pSIP-based expression vector, pSIP401 backbone, Ery^R	(27, 44)
pET22b_EFmRseP6His	pET-based expression vector, TEV cleavable C-terminal 6xHis-tag, Amp^R	This study/Genscript
pEV	Empty vector	(44)
pEfmRseP	pSIP401 derivative containing *rseP* derived from *E. faecium* P21. C-terminal 6xHis-tag	(42)
pLpRseP	pSIP401 derivative containing native *L. plantarum* WCSF1 *rseP*. C-terminal 6xHis-tag	(42)
pEfsRseP	pSIP401 derivative containing *rseP* derived from *E. faecalis* V583. C-terminal 6xHis-tag	This study
pLlRseP	pSIP401 derivative containing *rseP* derived from *L. lactis* IL1430. C-terminal 6xHis-tag	This study
pShRseP	pSIP401 derivative containing *rseP* derived from *S. haemolyticus* 7076_4_21. C-terminal 6xHis-tag	This study
Strains		
E. faecalis V583 (*Efs*)	Template for *rseP* (*EfsrseP*)	NCBI:txid226185
L. lactis IL1403 (*Ll*)	Template for *rseP* (*LlrseP*)	NCBI:txid272623
S. haemolyticus 7076_4_21 (*Sh*)	Template for *rseP* (*ShrseP*)	ERS066353
L. plantarum WCFS1	Expression host.	(46)
E. coli TOP10	Cloning host	ThermoFisher Scientific
E. coli Artic Express	Expression host, suitable for low growth temperatures.	Agilent Technologies
E. coli BL21 Star™ (DE3)	Expression host	ThermoFisher Scientific
E. coli C43 (DE3)	Expression host, suitable for expression of toxic proteins	Sigma-Aldrich

Expression screen to determine optimal protein expression conditions

A small-scale expression screen was conducted to determine optimal protein expression conditions using *L. plantarum*. Briefly, an overnight culture was diluted in falcon tubes containing 50 ml pre-warmed MRS to an OD_{600} of 0.10-0.15 followed by incubation at 37 °C without agitation. When reaching an OD_{600} of 0.27-0.35, the cultures were induced with concentrations of SppIP ranging from 12.5 to 50 ng/ml and incubated for 3h, 6h, 10h or 24h before harvesting. The small-scale expression screen was performed at three temperatures: 23 °C, 30 °C and 37 °C. The cultures were harvested by centrifugation for 10 min at 5 000 x g (4 °C). Harvested cell pellets were stored at -20 °C prior to Western Blot analysis. A schematic overview of plasmid construction and expression optimization is given in Figure 2A.

Plasmid construction and expression in *E. coli*

A codon-optimized *EfmRseP* was synthesized and inserted into the pET22b vector by GenScript, resulting in the plasmid pEt22b-EfmRseP6His. The plasmid was transformed into various *E. coli* strains (Table 1) according to the manufacturer's instruction. All clones were verified with colony PCR using the Red Taq DNA polymerase Master Mix (VWR).

For the overproduction of RseP in *E. coli,* two different growth media (BHI and TBS) were tested, and the bacteria were harvested at two different time points (3h and 24h after induction). The expression protocol was based on the protocol provided by the manufacturer, as well as protocols from previous expression studies of RseP derived from Gram-negative bacteria in *E. coli* (47). Briefly, an overnight culture was diluted to an OD_{600} of ~ 0.1. *E. coli* BL21 Star and *E. coli* C43(DE3) were incubated at 37°C, while *E. coli* ArcticExpress was incubated at 30°C. All strains were incubated with agitation until reaching an OD_{600} of 1.0-1.5. *E. coli* ArcticExpress was incubated with agitation at 10°C for 10 minutes before induction with IPTG to a final concentration of 1 mM, while *E. coli* BL21 Star and *E. coli* C43(DE3) were induced directly with IPTG to a final concentration of 200 µM. *E. coli* ArcticExpress was incubated at 10°C post-induction, while *E. coli* BL21 Star and

E. coli C43(DE3) were incubated at 23°C post-induction. The cells were harvested by centrifugation (5000 x g, 10 min, 4 °C), at 3- and 24 hours post-induction and stored at -20 °C before Western Blot analysis.

Western blot analysis

Western blot analysis was performed to investigate protein production levels at the various expression conditions. *E. coli* and *L. plantarum* harboring expression plasmids were lysed and applied to SDS-PAGE as previously described (31), with minor adjustments. Briefly, harvested cells were resuspended in 250 µl NP-40 buffer (150 mM NaCl; 1.0 % Triton X-100; 50mM Tris, pH 8.0) containing 1 mM phenylmethylsulfonyl fluoride (PMFS) and lysed using a FastPrep FP120 Cell Disrupter (MP Biomedicals, Santa Ana, CA). *L. plantarum* cells were lysed using three cycles of shaking at 6.5 m/s for 30 s, while *E. coli* cells were lysed using a single cycle of shaking at 6.0 m/s for 30 s. The volume of the protein extract applied to the SDS-PAGE was normalized based on OD_{600} at the harvesting time point, if not otherwise stated. Following electrophoresis, the proteins were blotted to a nitrocellulose mini membrane using iBlot™ Transfer Stack (Invitrogen) and the iBLot™ Gel transfer device (Invitrogen). The membrane was washed with Tris-buffered Saline (TBS) (2 x 10 min), prior to blocking (1h, 5 % Bovine Serum Albumin (BSA)). Following blocking, the membrane was washed (2 x 10 min Tween-TBS (TTBS; 0,05 % Tween-20), 1 x 10 min TBS), prior to incubation with the primary antibody (Penta-His™ (Qiagen), 1:1000 in 5 % BSA) for 30 min at room temperature. The membrane was subsequently incubated with the primary antibody at 4 °C overnight, followed by a 30 min incubation at room temperature the following day. The membrane was washed (2 x 10 min, TTBS), and incubated with the polyclonal HRP-conjugated anti-mouse IgG (Sigma-Aldrich) secondary antibody, diluted 1:5000 in the blocking buffer, for 1 hour. Unbound secondary antibodies were removed by washing 4 x 10 min with TTBS. All incubations and washing steps were performed with agitation. The blots were visualized using the SuperSignal West Pico PLUS Chemiluminescent substrate (Thermo Fisher Scientific) and the Azure c400 system (Azure Biosystem, Dublin, CA). Band intensity was estimated using ImageJ and protein

concentration was estimated based on the known concentration of the positive control (48).

Antimicrobial assays

To verify RseP production in *L. plantarum*, the antimicrobial activity of bacteriocins targeting RseP was assessed using a spot-on-lawn assay. Briefly, an overnight culture was diluted in soft-agar (1:1000) and distributed on agar plates containing erythromycin. Once solidified, bacteriocins were applied to designated spots. All bacteriocins used in this study were produced by Pepmic Co., Ltd (Suzhou, China) with >95% purity, and solubilized in 0.1 % (vol/vol) trifluoroacetic acid (TFA; Sigma Aldrich). Agar plates were incubated at appropriate temperatures overnight and inhibition zones were measured the following day.

Purification of recombinant EfmRseP

The conditions used during large-scale production of EfmRseP were based on the results from the small-scale optimization. Due to the facultative anaerobic nature of *L. plantarum*, the bacteria were cultivated in 1 L Schott Duran bottles (30 °C, 10h). *E. coli* was cultivated in Erlenmeyer flasks to ensure proper aeration (23 °C, overnight). The cell was harvested by centrifugation (1 227 x g, 4 °C, 20 min), and stored at -20 °C.

The protein was purified as previously described (49), with minor modifications. Briefly, cell pellets were resuspended in a 1:10 ratio in lysis buffer (50 mM HEPES, pH 7.0; 200 mM KCl, 10% Glycerol, 1 mM PMFS, 1 unit/10 ml buffer with DNase I (ThermoFisher Scientific)). *L. plantarum* cells were lysed using an LM20 Microfluidizer® Processer (Microfluidics®) using two passages at 30 000 PSI, while *E. coli* cells were lysed using a single passage at 15 000 PSI. Intact cells were pelleted by centrifugation (8 000 x g, 4 °C for 20 min). The supernatant was subsequently centrifuged at 150 000 x g for 1 hour at 4°C using the Sorvall™ WX ultracentrifuge (Thermo Scientific™). The resulting pelleted membrane was resuspended in a 1:20 ratio in membrane resuspension buffer (50 mM HEPES, pH 7.0; 200 mM KCl, 10 % Glycerol, 1 mM PMFS) using a Potter-Elvehjem PTFE

pestle (Sigma-Aldrich). The solubilized membrane was aliquoted and flash-frozen in liquid nitrogen or directly solubilized in 1 % β-DDM (ap. 1h, 200 rpm, 4 °C). A 5ml HisTrap™ HP column (Cytiva) was equilibrated with 4 x column volume (CV) of buffer A (50 mM Hepes, pH 7.0; 200 mM KCl; Imidazole 20 mM; Glycerol 10 %, 3 x CMC β-DDM, 1 PMFS) before the solubilized membrane suspension was loaded onto the column at 0.5 ml/ml flow rate using the Äkta Start protein purification system.

The column was washed with buffer A until the UV was reduced to 50 mAu at a 1 ml/min flow rate. The protein was eluted with 4 CV of 50 % buffer B (50 mM HEPES, pH 7.0; 200 mM KCl; Imidazole 500 mM; Glycerol 10 %, 3 x CMC β-DDM, 1 PMFS) with a flow rate at 2 ml/min. The eluted fractions containing the target protein were pooled and concentrated to ≤ 1 ml using the Amicon® Ultra Centrifugal filters (Sigma-Aldrich), before being subjected to size-exclusion chromatography using a HiLoad® 16/600 Superdex® 200 pg (Sigma-Aldrich) with buffer C (25 mM HEPES, pH 7.0; 200 mM KCl; Glycerol 5 %, 3 x CMC β-DDM,). Standards from the high molecular weight Gel filtration calibration kit from Cytiva (Marlborough, MA, USA) was used to estimate the protein size. Fractions from size exclusion were pooled, concentrated, flash-frozen in liquid nitrogen and stored at -80 °C until use. A schematic overview of the purification process is given in Figure 2B.

Circular Dichroism Spectroscopy

A circular dichroism spectroscopy (CD) analysis was performed to determine the secondary structure of the purified protein. The purified protein was diluted in buffer (12.5 mM HEPES, pH 7.0; 200 mM KCl; 2.5 % Glycerol) to a final concentration of 0.2-0.24 mg/ml. Data were obtained using a Jasco1500 circular dichroism spectrophotometer at 20 °C, at 100 nm/min scan rate and 1 nm bandwidth. A cuvette with a 0.1 cm path length was applied. The resulting spectra represent 5 scans from 190-250 nm. Dichroweb was used to estimate secondary structure using the K2D method (50, 51). The protein sample used in CD-analysis were harvested following overnight production at room temperature. EfmRseP as purified as described above, except for using a ProteoSEC Dynamic 16/60 3-70 HR column (ProteinArk) for SEC-analysis.

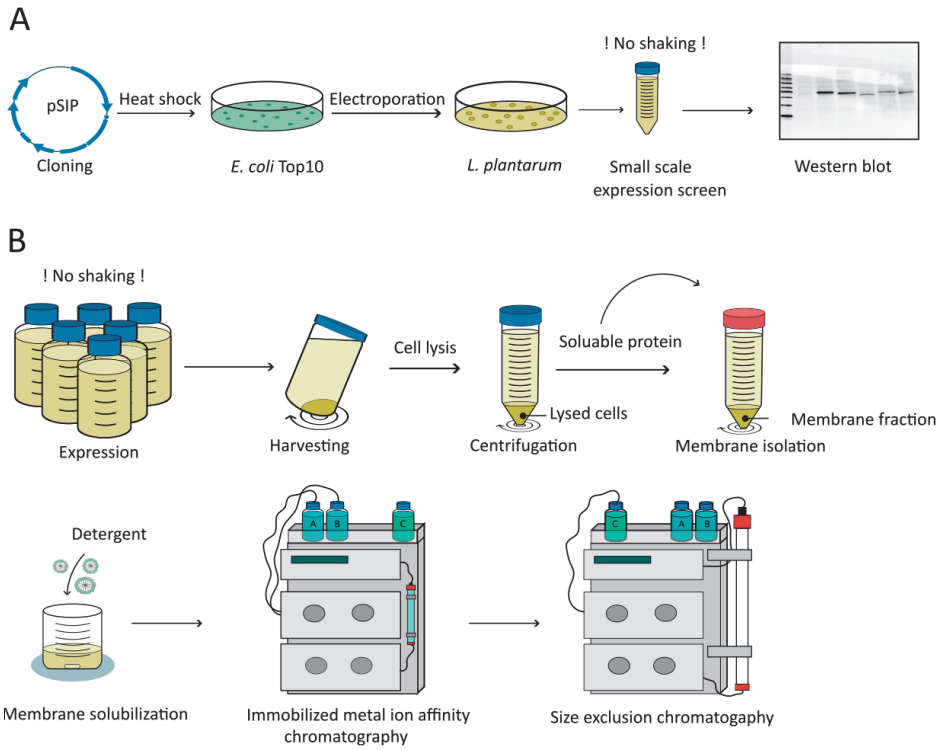

Figure 2 |A schematic overview of the established workflow employed for construction, expression, and purification of recombinant RseP using *L. plantarum* as a production host. A) Construction of the plasmid and small-scale expression screening. B) Scale-up of protein expression and two-step purification of recombinant RseP using immobilized metal affinity chromatography and size exclusion chromatography.

Statistics and bioinformatics

To evaluate the prevalence of Gram-positive bacteria as an expression host for IMPs, a custom tabular report was downloaded from the Protein data bank on 18.10.2022. All experimental entries annotated as transmembrane proteins (PDBTM) were selected and sorted based on the expression host. All unpublished entries and entries with no defined expression host were removed. NCBI taxonomy browser determines the taxonomy of the

expression organism. To validate the secondary structure determined using CD analysis, the EfmRseP structure was predicted using the protein fold recognition server Phyre 2 (52). The predicted AlphaFold2 structure of EfmRseP was used as an additional validation control (42).

Results

Identification of an RseP ortholog for expression and purification

Small changes in the amino acid sequence or length of heterologously expressed proteins may affect expression levels and solubility (47, 53, 54). Orthologue screening has proven to be a successful approach for identifying protein variants which can be produced with high yields. Thus, expression levels and functionality of five different RseP orthologs were evaluated using the pSIP-expression system. A C-terminal 6xHis-tag was included in all constructs to facilitate purification and detection of RseP. All orthologs screened, except for RseP from *L. plantarum* (LpRseP), act as a receptor for bacteriocins of the LsbB-family in their native organism (38-40). LpRseP was included in the expression screen as we hypothesized that the expression of a protein native to the expression host might ease the expression burden, thus resulting in higher protein production. As expected, all recombinant strains except *L. plantarum* expressing LpRseP, were sensitive to the LsbB family bacteriocin EntK1, suggesting that the RseP orthologs are functionally produced *in vivo* (Figure S1). Western blot analysis confirmed the production of all recombinant RseP orthologs in *L. plantarum* (Figure 3A). However, the expression levels varied considerably. Surprisingly, RseP derived from the host (LpRseP) and the closely related *L. lactis* (LlRseP) resulted in the lowest production levels, while RseP derived from *Enterococcus faecium* (EfmRseP) yielded the highest level. Thus, further optimization of protein production and purification was performed using the EfmRseP construct only.

Small-scale optimization of protein production in *L. plantarum*

To identify optimal conditions for RseP production in *L. plantarum*, 50 ml growth cultures were used to study the effects of various incubation temperatures, inducer concentrations, and harvesting time on the protein production. Initially, the production was analyzed at three different temperatures: 23°C, 30°C and 37°C, and harvested after 3, 6, 10 or 24 hours. Western blot analysis showed that the production level was largely temperature-dependent (Figure 3). A considerable level of EfmRseP was detected from 3 to 10 hours after induction at 30°C and 23°C, while the amount decreased significantly over the same period at 37 °C. Although the normalized protein production was comparable at 3- and 10 hours after induction at 30°C, the total protein yield was higher after 10 hours due to an increase in biomass (Figure 3B). A prolonged incubation past 10 hours resulted in less RseP regardless of the incubation temperature and is not ideal when the goal is to produce as much RseP as possible.

Induction of the protein expression significantly affected the cell growth of *L. plantarum* expressing EfmRseP at all temperatures (Figure 3C). Notably, the lack of protein expression after 10 hours at 37 °C correlates with the rapid increase in growth rate observed at the same time point (Figure 3B-C), suggesting that induction has ceased. Varying the inducer concentration (12.5-50 ng/ml) did not prolong RseP production time nor affect the growth rate (Figure S2).

L. plantarum is a facultative anaerobe organism, thus aeration is not recommended for optimal growth. However, enhanced flow of nutrients might be advantageous for prolonged incubations. Thus, growth and protein expression were monitored in cultures with minimal circulation (200 rpm). However, we did not observe any significant effect on neither growth rate nor protein production levels (data not shown).

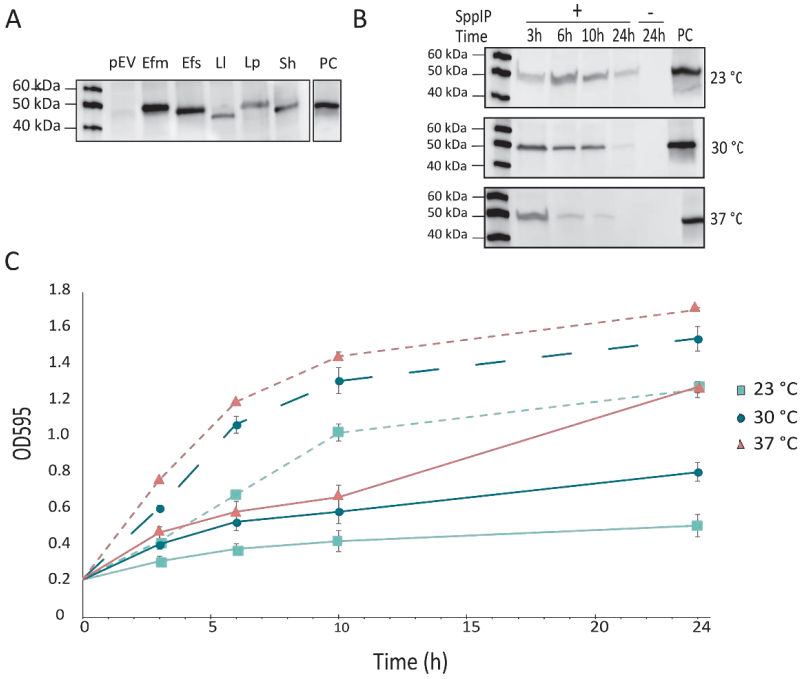

Figure 3 |Optimalization of RseP protein production. A) Heterologous production of RseP derived from five gram-positive bacteria was evaluated in *L. plantarum* WCFS1 using Western blot analysis: *E. faecium* (Efm), *E. faecalis* (Efs), *L. lactis* (Ll), *L. plantarum* (Lp) and *S. haemolyticus* (Sh). The production was evaluated at 37°C and induced with 25 ng/ml for 3 hours. The empty vector (pEV) was used as a negative control. Small-scale expression screening of EfmRseP was conducted in 50 ml cultures at three temperatures: 23 °C, 30 °C and 37 °C, and harvested at various time points after induction: 3h, 6h, 10h and 24h. All cultures were induced with 25 ng/ml SppIP at OD_{600} ~0.3, except a non-induced culture (-) harvested 24 h after induction was used as a negative control at each temperature. In the western blots (A, B), a purified 6xHis-protein was used as a positive control (PC). C) Growth curve of *L. plantarum* harboring pEfmRseP induced (25ng/ml SppIP; solid line) and non-induced samples (dashed line) at 23 °C, 30 °C and 37 °C. OD_{595} was measured at the time of induction (0h), and after 3h, 6h, 10h and 24h post induction. The experiment was performed using three biological replicates. Standard deviation is indicated at each data point.

Large-scale purification of recombinant EfmRseP from *L. plantarum*

The optimal conditions identified in the small-scale (50 ml) production screen were applied for large-scale (1 L) production and purification of EfmRseP (25 ng/ml SppIP, 30°C, 10 hours). A schematic overview of the workflow is summarized in Figure 2. EfmRseP was produced in 1 L tightly sealed Shott-Duran flasks, using a total of 6 L bacterial culture per round of purification. Following solubilization with β-DDM, EfmRseP was purified by immobilized metal ion affinity chromatography (IMAC) (Figure 2B). As seen in Figure 4, EfmRseP bound strongly to the NiNTA-resin, while most contaminants were found in flow-through and the wash fractions. EfmRseP was efficiently eluted using 50 % Buffer B, resulting in considerable protein levels at the expected size (46 kDa) in peak 1 (Figure 4A-B). However, several other bands were also visible in the same fraction, indicating contamination by other proteins. The EfmRseP containing fractions (peak1; Figure 4B) were pooled, concentrated, and applied to size-exclusion chromatography (SEC) to ensure the purity and homogeneity of the sample. SEC resulted in three distinct peaks at 68.64 ml, 78.46 ml, and 114.50 ml, respectively (Figure 4C). SDS-PAGE analysis of the fractions in peak S1 (Figure 4D) showed considerable levels of EfmRseP, while the protein contaminants observed following IMAC purification was eluted in peak S2. No bands were observed in peak S3. Fractions corresponding to Peak S1 were collected and concentrated resulting in a final yield of 0.35 mg RseP per gram wet cell pellet.

Comparison of the SEC elution profile with the elution profile of known protein standards allowed an estimation of the oligomeric state of EfmRseP. EfmRseP has an expected size of 46 kDa, however, the protein eluted at 68.64 ml, which is comparable to the retention volume of Aldolase (67.36 ml, 158 kDa) (Figure 4C-D, Figure S3). β-DDM forms relatively larger micelles (Mw ap. 65-70 kDa) (55, 56), indicating that EfmRseP may exist as a dimer.

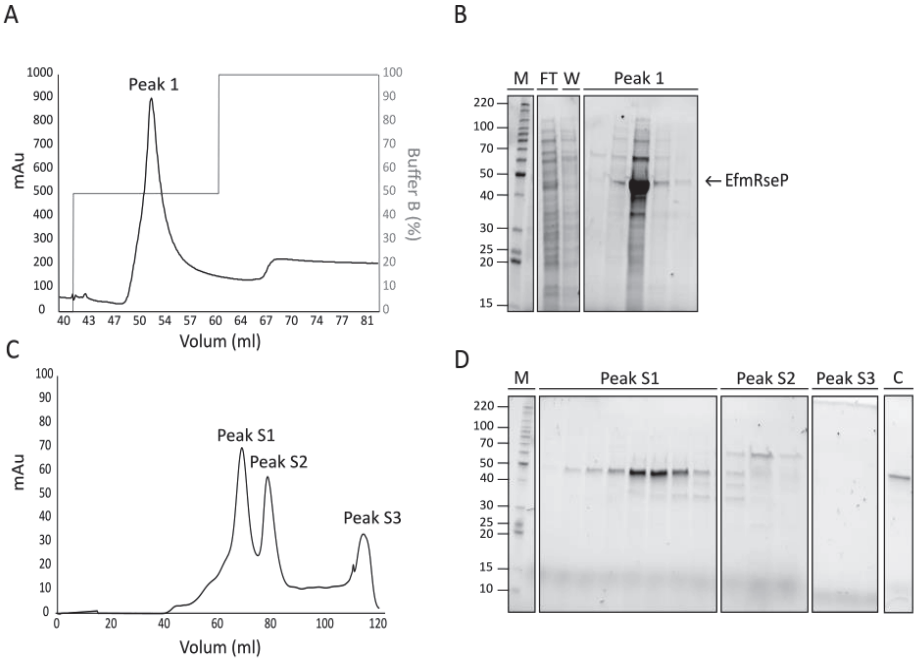

Figure 4|Overview of the two-step purification of EfmRseP using *L. plantarum* as host. A) A representative IMAC chromatogram profile showing the elution of EfmReP from the NiNTA resin. B) A 10 µl sample of the fractions from the flowthrough (FT), washing steps (W) and fractions corresponding to Peak 1 was analyzed using SDS-PAGE. Fractions containing EfmRseP (peak 1) were subsequently pooled and concentrated prior to being applied for SEC. C) A representative SEC chromatogram profile, indicated three size-exclusion peaks (S1, S2 and S3) D) A 10 µl sample from the fractions from each peak was analyzed using SDS-PAGE. To analyze the purity of EfmRseP a 1:10 dilution of the concentrated peak S1 was analyzed using SDS-PAGE (C). In both gels, EfmRseP runs at expected size of 46 kDa. M indicates molecular mass marker in kDa.

Secondary structure analysis of purified EfmRseP

To investigate the protein folding following the purification of EfmRseP, the secondary structure was determined using circular dichroism (CD) analysis. The CD spectrum was analyzed using the online tool DicroWeb (50, 51), which indicated that the secondary structure was a mixture of α-helices (35 %) and β-sheets (18%) (Figure 5). This is

comparable to the secondary structure data predicted by Phyre2 and AlphaFold2, suggesting that the purified protein is folded correctly and suitable for further analysis.

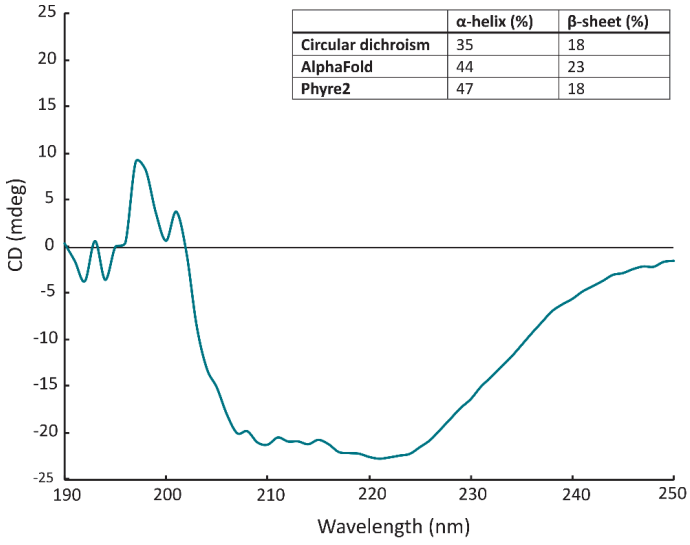

	α-helix (%)	β-sheet (%)
Circular dichroism	35	18
AlphaFold	44	23
Phyre2	47	18

Figure 5|Secondary structure analysis using circular dichroism (CD) spectroscopy. CD spectra of the purified EfmRseP. The table (inset) shows the percentage secondary structure of purified EfmRseP as estimated by Dichroweb and predicted by the structure prediction tools AlphaFold and Phyre2.

Large-scale purification of EfmRseP from *E. coli*

To evaluate *L. plantarum* as an expression and purification platform, EfmRseP expression and purification were attempted in the more traditional expression host *E. coli*. Using the standard IPTG inducible pET22b-vector, the detection of soluble EfmRseP failed in 2 of 3 tested *E. coli* strains (Figure S4). *E. coli* C43(DE3), a modified expression strain specifically developed for expression of toxic proteins, was the only strain that gave a detectable amount of soluble EfmRseP. The highest protein production levels were observed after incubation overnight at 23 °C (Figure S4). Purification of EfmRseP expressed in *E. coli* was attempted using the same purification scheme established for the purification of EfmRseP from *L. plantarum*. Figure 6A-B shows considerable levels of EfmRseP in Peak1 following

IMAC-purification from production in *E. coli*. However, similar to purification from *L. plantarum,* several contaminating proteins were observed in the first purification step. SEC analysis of the Peak 1 fractions from the IMAC resulted in two overlapping peaks at 59.01 and 63.92 ml, respectively (Figure 6C). One band at expected size of EfmRseP was observed in both peaks (46 kDa), together with an additional band between 80-90 kDa and a weaker band of ap. 100 kDa (Figure 6D). Since multiple bands were observed in fractions believed to contain EfmRseP, CD analysis was not performed.

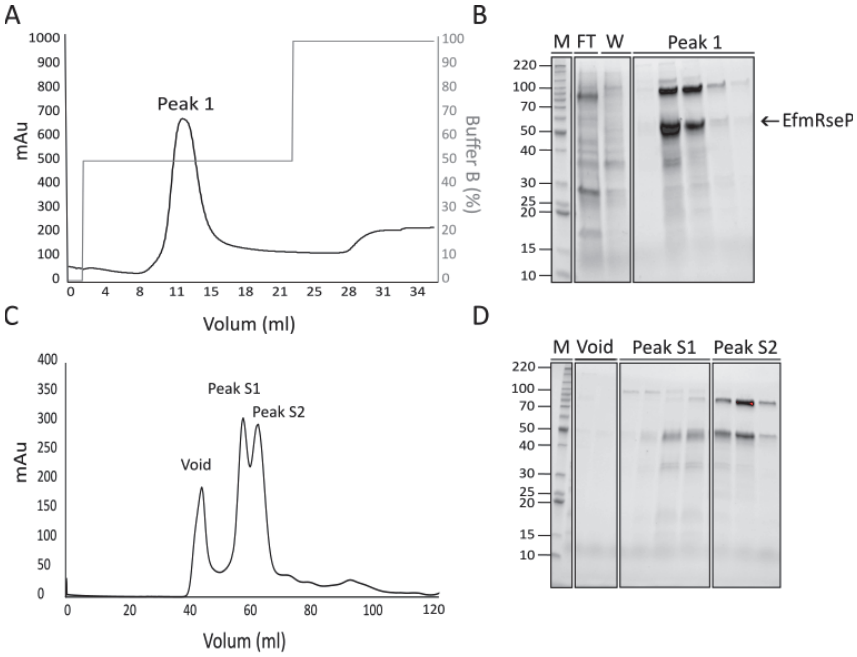

Figure 6| Overview of the two-step purification of EfmRseP expressed in *E. coli*. A) A representative IMAC chromatogram profile showing the elution of EfmReP from the NiNTA resin. B) A 10 ml sample of fractions from flowthrough (FT), the washing steps (W) and peak 1 was analyzed using SDS-page. Appreciable amounts of EfmRseP were found in fractions corresponding to Peak 1. Peak 1 was pooled and concentrated prior to SEC analysis. C) A representative SEC chromatogram. D) Fractions from the void, peak S1 and peak S2 were analyzed using SDS-PAGE. The arrow indicates the expected size of EfmRseP (46 kDa). M indicates molecular mass marker in kDa.

Discussion

Membrane proteins remain one of the most challenging targets to characterize, with the overproduction of soluble proteins being the major hurdle in this pipeline. *E. coli* is the most extensively used host for overproduction of recombinant membrane proteins (Figure 1), however, poor stability, toxicity, and formation of inclusion bodies of the target protein are common problems (5, 6). In recognition of these limitations, several tags (e.g., Mistic, MBP) and optimized expression strains (e.g., C41(DE3), C43(DE3), Lemo21) is used to improve protein expression and solubility (6). The membrane environment significantly impacts the stability of membrane proteins, while native cellular conditions and/or the presence of native chaperons may facilitate protein folding. Thus, screening different expression hosts can be an important strategy to achieve optimal production. In line with this notion, we evaluated both the Gram-positive *L. plantarum* and the more traditional expression host *E. coli* for expression and subsequent purification of the integral membrane protein RseP.

Five orthologs of RseP were successfully expressed in *L. plantarum,* with the RseP derived from *E. faecium* achieving the highest production levels at the conditions tested (Figure 3A). The small-scale optimization using *L. plantarum* harboring pEfmRseP indicated that incubation of 10 hours post-induction at 30°C was optimal (Figure 3B). EfmRseP was successfully purified using these conditions, yielding a total of 0.35 mg per gram wet cell pellet of highly pure protein (Figure 4). This is comparable with yields achieved for membrane proteins produced in *E. coli* (49).

Previous studies have indicated 2-6 hours post-induction as the optimal harvesting time for intracellular proteins using the pSIP system (26). However, it has not been evaluated at expression conditions below 30 °C. We demonstrated that protein production time is temperature dependent in *L. plantarum*, as induction is prolonged and protein degradation is reduced at lower temperatures (23 °C and 30 °C). It should be noted that although harvesting cells incubated at 30 °C 10 hours post-induction was suggested as optimal, the protein was also successfully obtained following incubation at room temperature overnight (0.24 mg pellet per gram wet cell pellet). The facultative anaerobic nature of *L. plantarum*,

and its ability to produce a large amount of protein at room temperature, suggests that this method could be suitable for industrial-scale production in bioreactors.

We also assessed the production of EfmRseP in three well-known production strains of *E. coli* (Figure S4). Surprisingly, the detection of soluble protein expression failed in two of the three strains tested. *E. coli* C43(DE3) produced considerable levels of EfmRseP; however, the same two-step purification as applied for EfmRseP using *L. plantarum,* did not effectively remove protein contaminants (Figure 6). Two strong protein bands were observed in peak S2 following SEC-analysis: one band at ap. 45 kDa (expected size of EfmRseP), and one band between 80 and 90 kDa. As the band of higher molecular weight correspond to an approximate doubling of the expected size of EfmRseP, it is tempting to speculate that EfmRseP exists in multiple oligomeric state following purification. While uncommon, dimerization following SDS-page analysis has been observed (57-59). It should be noted that *E. coli* previously have been successfully used to express and purify RseP orthologs from the thermophile archaea *Methanocaldococcus jannaschii* and *E. coli* (47, 54) . Interestingly, RseP from *E. coli* was found to exist in multiple oligomeric states following SEC-analysis, with a monodisperse RseP sample only being obtained following a second round of SEC-purification (54). Further investigations of the identity of the additional observed band in peak S2 and potentially further optimization of the *E. coli* purification scheme is beyond the scope of this paper.

To evaluate the folding of a recombinant protein, the biological activity of the purified protein is often tested. Previous studies have exploited the known substrates of RseP orthologs to perform a cleavage-based assay to confirm proper protein expression and folding (54, 60, 61). However, the RseP substrate in *E. faecium* is unknown. Moreover, lipids are known to influence the activity of purified membrane proteins, making activity assays challenging to establish for membrane proteases (62-64). To circumvent these difficulties, we investigated protein folding and functional expression of RseP using two different approaches. First, a spot-on-lawn assay was conducted on whole cells to confirm the proper expression and folding of all rseP orthologs *in vivo* (Figure S1). A key advantage of Gram-positive expression hosts is that it is monoderm, allowing direct evaluation of membrane protein targeting inhibitors or substrates, without the need to circumvent the outer

membrane of Gram-negative hosts. All RseP orthologs, with the anticipated exception of LpRseP, conveyed EntK1-senstivity to the EntK1-reistant host *L. plantarum*, suggesting the proteins were functionally expressed *in vivo* (Figure S1). Secondly, we investigated the secondary structure of the purified EfmRseP using CD analysis, a commonly used technique for the determination of secondary structure and folding properties of recombinantly expressed proteins. Using the Dichroweb analysis tool, purified EfmRseP was estimated to contain 35 % α-helices and 18 % β-sheets which is comparable to the estimated secondary structure predicted by Phyre2 and AlphaFold2, indicating that the protein is properly folded (Figure 5).

In summary, we present the pSIP expression system and *L. plantarum* as a novel platform for production of pure and soluble membrane proteins (Figure 2). Compared to *E. coli,* lactic acid bacteria offer some clear advantages, including low proteolytic pressure, small genome size and a monoderm cell envelope. In the specific case of EfmRseP, expression and purification of EfmRseP from *L. plantarum* was superior to expression and purification in *E. coli*.

Acknowledgements

This study was financed by the Research Council of Norway through project 275190. The funder had no role in study design, data collection and interpretation, or the decision to submit the work for publication.

References

1. Krogh A, Larsson B, Von Heijne G, Sonnhammer EL. 2001. Predicting transmembrane protein topology with a hidden Markov model: application to complete genomes. J Mol Biol 305:567-580.
2. Fagerberg L, Jonasson K, von Heijne G, Uhlén M, Berglund L. 2010. Prediction of the human membrane proteome. Proteomics 10:1141-1149.
3. Overington JP, Al-Lazikani B, Hopkins AL. 2006. How many drug targets are there? Nat Rev Drug Discov 5:993-996.
4. Bakheet TM, Doig AJ. 2009. Properties and identification of human protein drug targets. Bioinformatics 25:451-457.
5. Rogl H, Kosemund K, Kühlbrandt W, Collinson I. 1998. Refolding of *Escherichia coli* produced membrane protein inclusion bodies immobilised by nickel chelating chromatography. FEBS Lett 432:21-6.
6. Kaur J, Kumar A, Kaur J. 2018. Strategies for optimization of heterologous protein expression in *E. coli*: Roadblocks and reinforcements. Int J Biol Macromol 106:803-822.
7. Fernández FJ, Vega MC. 2013. Technologies to keep an eye on: alternative hosts for protein production in structural biology. Curr Opin Struct Biol 23:365-73.
8. Bernaudat F, Frelet-Barrand A, Pochon N, Dementin S, Hivin P, Boutigny S, Rioux JB, Salvi D, Seigneurin-Berny D, Richaud P, Joyard J, Pignol D, Sabaty M, Desnos T, Pebay-Peyroula E, Darrouzet E, Vernet T, Rolland N. 2011. Heterologous expression of membrane proteins: choosing the appropriate host. PLoS One 6:e29191.
9. Bashiri G, Baker EN. 2015. Production of recombinant proteins in *Mycobacterium smegmatis* for structural and functional studies. Protein Sci 24:1-10.
10. Goldstone RM, Moreland NJ, Bashiri G, Baker EN, Lott JS. 2008. A new Gateway® vector and expression protocol for fast and efficient recombinant protein expression in *Mycobacterium smegmatis*. Protein Expr Purif 57:81-87.
11. Kunji ER, Slotboom DJ, Poolman B. 2003. *Lactococcus lactis* as host for overproduction of functional membrane proteins. Biochim Biophys Acta 1610:97-108.
12. Harborne SP, Ruprecht JJ, Kunji ER. 2015. Calcium-induced conformational changes in the regulatory domain of the human mitochondrial ATP-Mg/Pi carrier. Biochim Biophys Acta 1847:1245-53.
13. Thangaratnarajah C, Ruprecht JJ, Kunji ER. 2014. Calcium-induced conformational changes of the regulatory domain of human mitochondrial aspartate/glutamate carriers. Nat Commun 5:5491.
14. Frelet-Barrand A. 2022. *Lactococcus lactis*, an Attractive Cell Factory for the Expression of Functional Membrane Proteins. Biomolecules 12:180.
15. Song AA, In LLA, Lim SHE, Rahim RA. 2017. A review on *Lactococcus lactis*: from food to factory. Microb Cell Fact 16:55.
16. Mierau I, Leij P, Van Swam I, Blommestein B, Floris E, Mond J, Smid EJ. 2005. Industrial-scale production and purification of a heterologous protein in *Lactococcus lactis* using the nisin-controlled gene expression system NICE: the case of lysostaphin. Microb Cell Fact 4:1-9.
17. Zhu D, Fu Y, Liu F, Xu H, Saris PE, Qiao M. 2017. Enhanced heterologous protein productivity by genome reduction in *Lactococcus lactis* NZ9000. Microb Cell Fact 16:1.

18. Bolotin A, Wincker P, Mauger S, Jaillon O, Malarme K, Weissenbach J, Ehrlich SD, Sorokin A. 2001. The complete genome sequence of the lactic acid bacterium *Lactococcus lactis* ssp. lactis IL1403. Genome Res 11:731-53.
19. Kleerebezem M, Beerthuyzen MM, Vaughan EE, de Vos WM, Kuipers OP. 1997. Controlled gene expression systems for lactic acid bacteria: transferable nisin-inducible expression cassettes for *Lactococcus, Leuconostoc,* and *Lactobacillus* spp. Appl Environ Microbiol 63:4581-4.
20. Sikkema HR, van den Noort M, Rheinberger J, de Boer M, Krepel ST, Schuurman-Wolters GK, Paulino C, Poolman B. 2020. Gating by ionic strength and safety check by cyclic-di-AMP in the ABC transporter OpuA. Sci Adv 6.
21. Berntsson RP, ter Beek J, Majsnerowska M, Duurkens RH, Puri P, Poolman B, Slotboom DJ. 2012. Structural divergence of paralogous S components from ECF-type ABC transporters. Proc Natl Acad Sci U S A 109:13990-5.
22. Swier LJ, Guskov A, Slotboom DJ. 2016. Structural insight in the toppling mechanism of an energy-coupling factor transporter. Nat Commun 7:11072.
23. Malinauskaite L, Quick M, Reinhard L, Lyons JA, Yano H, Javitch JA, Nissen P. 2014. A mechanism for intracellular release of Na+ by neurotransmitter/sodium symporters. Nat Struct Mol Biol 21:1006-12.
24. Erkens GB, Berntsson RP, Fulyani F, Majsnerowska M, Vujičić-Žagar A, Ter Beek J, Poolman B, Slotboom DJ. 2011. The structural basis of modularity in ECF-type ABC transporters. Nat Struct Mol Biol 18:755-60.
25. Straume D, Axelsson L, Nes IF, Diep DB. 2006. Improved expression and purification of the correctly folded response regulator PlnC from lactobacilli. J Microbiol Methods 67:193-201.
26. Mathiesen G, Axelsson L, Eijsink VGH. 2022. Heterologous Protein Production in *Lactobacillus (plantarum)* Using pSIP Vectors. Methods Mol Biol 2406:205-217.
27. Sørvig E, Grönqvist S, Naterstad K, Mathiesen G, Eijsink VGH, Axelsson L. 2003. Construction of vectors for inducible gene expression in *Lactobacillus sakei* and *L. plantarum*. FEMS Microbiol Lett 229:119-126.
28. Sørvig E, Mathiesen G, Naterstad K, Eijsink VGH, Axelsson L. 2005. High-level, inducible gene expression in *Lactobacillus sakei* and *Lactobacillus plantarum* using versatile expression vectors. Microbiology (Reading) 151:2439-2449.
29. Nguyen HA, Nguyen TH, Nguyen TT, Peterbauer CK, Mathiesen G, Haltrich D. 2012. Chitinase from Bacillus licheniformis DSM13: expression in *Lactobacillus plantarum* WCFS1 and biochemical characterisation. Protein Expr Purif 81:166-74.
30. Halbmayr E, Mathiesen G, Nguyen TH, Maischberger T, Peterbauer CK, Eijsink VG, Haltrich D. 2008. High-level expression of recombinant beta-galactosidases in *Lactobacillus plantarum* and *Lactobacillus sakei* using a Sakacin P-based expression system. J Agric Food Chem 56:4710-9.
31. Wiull K, Boysen P, Kuczkowska K, Moen LF, Carlsen H, Eijsink VGH, Mathiesen G. 2022. Comparison of the Immunogenic Properties of *Lactiplantibacillus plantarum* Carrying the Mycobacterial Ag85B-ESAT-6 Antigen at Various Cellular Localizations. Front Microbiol 13.
32. Makinoshima H, Glickman MS. 2005. Regulation of *Mycobacterium tuberculosis* cell envelope composition and virulence by intramembrane proteolysis. Nature 436:406-409.
33. Frank KL, Barnes AM, Grindle SM, Manias DA, Schlievert PM, Dunny GM. 2012. Use of recombinase-based in vivo expression technology to characterize *Enterococcus faecalis* gene expression during infection identifies in vivo-expressed antisense RNAs and implicates the protease Eep in pathogenesis. Infect Immun 80:539-549.

34. King-Lyons ND, Smith KF, Connell TD. 2007. Expression of hurP, a gene encoding a prospective site 2 protease, is essential for heme-dependent induction of bhuR in *Bordetella bronchiseptica*. J Bacteriol 189:6266-6275.
35. Yokoyama T, Niinae T, Tsumagari K, Imami K, Ishihama Y, Hizukuri Y, Akiyama Y. 2021. The *Escherichia coli* S2P intramembrane protease RseP regulates ferric citrate uptake by cleaving the sigma factor regulator FecR. J Biol Chem 296.
36. Kanehara K, Ito K, Akiyama Y. 2002. YaeL (EcfE) activates the sigma(E) pathway of stress response through a site-2 cleavage of anti-sigma(E), RseA. Genes Dev 16:2147-55.
37. Urban S. 2009. Making the cut: central roles of intramembrane proteolysis in pathogenic microorganisms. Nat Rev Microbiol 7:411-23.
38. Uzelac G, Kojic M, Lozo J, Aleksandrzak-Piekarczyk T, Gabrielsen C, Kristensen T, Nes IF, Diep DB, Topisirovic L. 2013. A Zn-dependent metallopeptidase is responsible for sensitivity to LsbB, a class II leaderless bacteriocin of *Lactococcus lactis* subsp. lactis BGMN1-5. J Bacteriol 195:5614-21.
39. Ovchinnikov KV, Kristiansen PE, Straume D, Jensen MS, Aleksandrzak-Piekarczyk T, Nes IF, Diep DB. 2017. The Leaderless Bacteriocin Enterocin K1 Is Highly Potent against *Enterococcus faecium*: A Study on Structure, Target Spectrum and Receptor. Front Microbiol 8:774.
40. Kranjec C, Kristensen SS, Bartkiewicz KT, Brønner M, Cavanagh JP, Srikantam A, Mathiesen G, Diep DB. 2021. A bacteriocin-based treatment option for *Staphylococcus haemolyticus* biofilms. Sci Rep 11:13909.
41. Ovchinnikov KV, Kristiansen PE, Uzelac G, Topisirovic L, Kojic M, Nissen-Meyer J, Nes IF, Diep DB. 2014. Defining the structure and receptor binding domain of the leaderless bacteriocin LsbB. J Biol Chem 289:23838-45.
42. Kristensen SS, Oftedal TF, Røhr Å K, Eijsink VGH, Mathiesen G, Diep DB. 2022. The extracellular domain of site-2-metalloprotease RseP is important for sensitivity to bacteriocin EntK1. J Biol Chem 298:102593.
43. Reinseth I, Tønnesen HH, Carlsen H, Diep DB. 2021. Exploring the Therapeutic Potenital of the Leaderless Enterocins K1 and EJ97 in the Treatment of Vancomycin-Resistant Enterococcal Infection. Front Microbiol 12:248.
44. Fredriksen L, Kleiveland CR, Hult LTO, Lea T, Nygaard CS, Eijsink VGH, Mathiesen G. 2012. Surface display of N-terminally anchored invasin by *Lactobacillus plantarum* activates NF-κB in monocytes. Appl Environ Microbiol 78:5864-5871.
45. Aukrust T, Blom H. 1992. Transformation of Lactobacillus strains used in meat and vegetable fermentations. Food Res Int 25:253-261.
46. Kleerebezem M, Boekhorst J, van Kranenburg R, Molenaar D, Kuipers OP, Leer R, Tarchini R, Peters SA, Sandbrink HM, Fiers MW, Stiekema RMKL, Bron PA, Hoffer SM, Grott MNN, Kerkhoven R, de Vires M, Ursing B, de Vos WM, Siezen RJ. 2003. Complete genome sequence of *Lactobacillus plantarum* WCFS1. Proc Natl Acad Sci U S A 100:1990-1995.
47. Feng L, Yan H, Wu Z, Yan N, Wang Z, Jeffrey PD, Shi Y. 2007. Structure of a site-2 protease family intramembrane metalloprotease. Science 318:1608-1612.
48. Schneider CA, Rasband WS, Eliceiri KW. 2012. NIH Image to ImageJ: 25 years of image analysis. Nature methods 9:671-675.
49. Subramani S, Morth JP. 2016. Heterologous expression and purification of the magnesium transporter A (MgtA) in *Escherichia coli*. Bio-protocol 6:e2001-e2001.
50. Andrade M, Chacon P, Merelo J, Morán F. 1993. Evaluation of secondary structure of proteins from UV circular dichroism spectra using an unsupervised learning neural network. Protein Engineering, Design and Selection 6:383-390.

51. Miles AJ, Ramalli SG, Wallace B. 2022. DichroWeb, a website for calculating protein secondary structure from circular dichroism spectroscopic data. Protein Sci 31:37-46.
52. Kelley LA, Mezulis S, Yates CM, Wass MN, Sternberg MJ. 2015. The Phyre2 web portal for protein modeling, prediction and analysis. Nat Protoc 10:845-858.
53. Savchenko A, Yee A, Khachatryan A, Skarina T, Evdokimova E, Pavlova M, Semesi A, Northey J, Beasley S, Lan N. 2003. Strategies for structural proteomics of prokaryotes: Quantifying the advantages of studying orthologous proteins and of using both NMR and X-ray crystallography approaches. Proteins 50:392-399.
54. Imaizumi Y, Takanuki K, Miyake T, Takemoto M, Hirata K, Hirose M, Oi R, Kobayashi T, Miyoshi K, Aruga R. 2022. Mechanistic insights into intramembrane proteolysis by *E. coli* site-2 protease homolog RseP. Sci Adv 34.
55. Slotboom DJ, Duurkens RH, Olieman K, Erkens GB. 2008. Static light scattering to characterize membrane proteins in detergent solution. Methods 46:73-82.
56. Strop P, Brunger AT. 2005. Refractive index-based determination of detergent concentration and its application to the study of membrane proteins. Protein Sci 14:2207-2211.
57. Lico DT, Lopes GS, Brusco J, Rosa JC, Gould RM, De Giorgis JA, Larson RE. 2015. A novel SDS-stable dimer of a heterogeneous nuclear ribonucleoprotein at presynaptic terminals of squid neurons. Neuroscience 300:381-92.
58. Kolodziejski PJ, Rashid MB, Eissa NT. 2003. Intracellular formation of "undisruptable" dimers of inducible nitric oxide synthase. Proc Natl Acad Sci U S A 100:14263-8.
59. Mei Y, Peng N, Zhao S, Hu Y, Wang H, Liang Y, She Q. 2012. Exceptional thermal stability and organic solvent tolerance of an esterase expressed from a thermophilic host. Appl Microbiol Biotechnol 93:1965-74.
60. Koide K, Ito K, Akiyama Y. 2008. Substrate recognition and binding by RseP, an *Escherichia coli* intramembrane protease. J Biol Chem 283:9562-9570.
61. Olenic S, Buchanan F, VanPortfliet J, Parrell D, Kroos L. 2022. Conserved proline residues of *Bacillus subtilis* intramembrane metalloprotease SpoIVFB are important for substrate interaction and cleavage. J Bacteriol 204:e0038621.
62. Subramani S, Perdreau-Dahl H, Morth JP. 2016. The magnesium transporter A is activated by cardiolipin and is highly sensitive to free magnesium *in vitro*. Elife 5:e11407.
63. Arias-Cartin R, Grimaldi S, Pommier J, Lanciano P, Schaefer C, Arnoux P, Giordano G, Guigliarelli B, Magalon A. 2011. Cardiolipin-based respiratory complex activation in bacteria. Proc Natl Acad Sci U S A 108:7781-6.
64. Osenkowski P, Ye W, Wang R, Wolfe MS, Selkoe DJ. 2008. Direct and potent regulation of gamma-secretase by its lipid microenvironment. J Biol Chem 283:22529-40.

Supplementary

Table S1| Primers used in this study

Primers	Sequence (5'-3')*	Ref.
EFs_V583_RseP_F	GGAGTATGATTCATATGAAAACAATTATCACATTCATTATT	This study
EFs_V583_Rsep_6HIS_R	TCGAACCCGGGGTACCTTAAT**GATGATGATGATGATGAT**GAAAGAAAAAG CGTTGAAT	This study
IL1403JRseP_F	GGAGTATGATTCATATGATAGAAACACTGATTACTTTTATT	This study
IL1403J_RseP6HIS_R	TCGAACCCGGGGTACCTTAAT**GATGATGATGATGATGAT**TTACAAAGGCTC GGAGAATATC	This study
SH_RseP_F	GGAGTATGATTCATATGAGCTATTTAATCACTATTGTCTCATTT	This study
SH_RseP6His_R	TCGAACCCGGGGTACCTTAAT**GATGATGATGATGATGAT**GCAAGAAATAA CGTTGTATATCGTTC	This study

* Introduction of the His-tag is marked in **bold**.

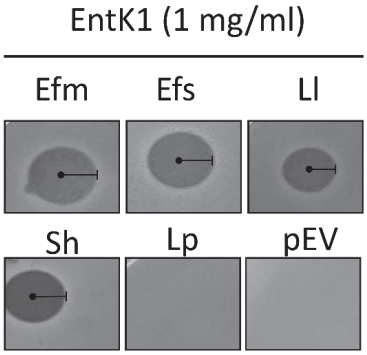

Figure S1| Inhibition zone of EntK1 in a spot-on-lawn assay. A 3 µl drop of EntK1 (1 mg/ml) was spotted on lawns of *L. plantarum* harboring different *rseP* orthologs. *L. plantarum* is naturally resistant towards EntK1, while *E. faecium* (Efm), *E. faecalis* (Efs), *L. lactis* (Ll) and some *S. haemolyticus* (Sh) strains are sensitive to EntK1. EntK1 depends on RseP as receptor for its antimicrobial activity, thus increased sensitivity towards EntK1 compared to the empty vector (pEV) indicates expression of a functional receptor protein. All strains, except for the strain harboring the empty vector (pEV) and the ortholog derived from the host itself (Lp), exhibit an inhibition zone. The approximate diameter of the inhibition zone is indicated.

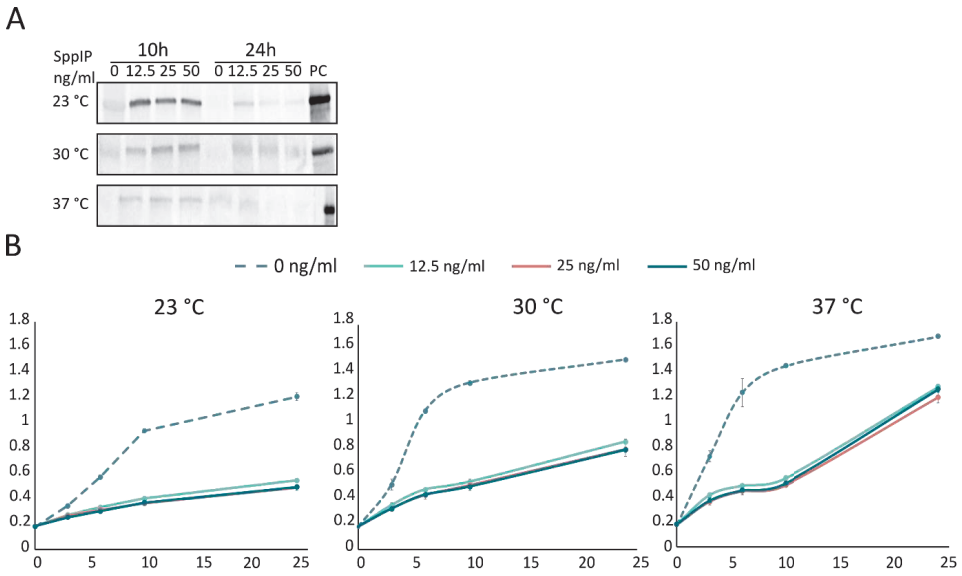

Figure S2| Effect of inducer concentration on protein production and growth. A) Western blot analysis showing the effect of inducer concentration on pro-longed protein expression (10h and 24h post induction) at 23 °C, 30 °C and 37 °C. Purified EfmRseP was used as a positive control (PC). B) Effect of increased inducer concentration on growth rate at 23 °C, 30 °C and 37 °C. Non-induced sample is indicated by a dashed line. OD_{595} was measured at induction (0h), as well as 3h, 6h, 10h and 24h post induction. The experiment was performed with three biological replicates. Standard deviation is indicated for each data point.

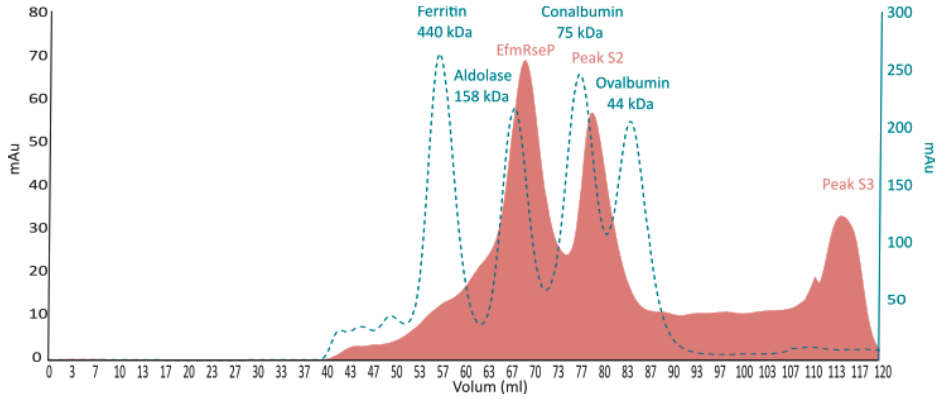

Figure S3|Chromatographic separation of standard proteins and EfmRseP on a HiLoad® 16/600 Superdex® 200 pg.

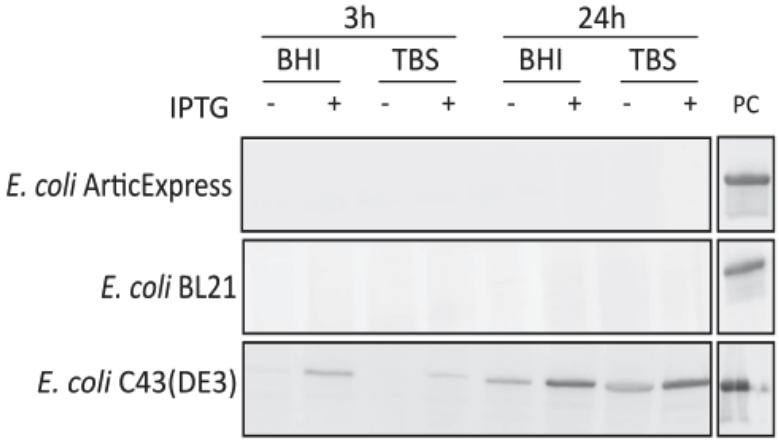

Figure S4 |Western Blot analysis of protein production in *E. coli* harboring pet22b-EFmRseP. The small-scale expression screen was performed using three strains: *E. coli* Artic Express, *E. coli* BL21, and *E. coli* C43(DE3). Expression was tested using two different media (BHI and TBS) and the cells were harvested 3 hours and 24 hours after induction. A 6xHis-tagged purified EfmRsep was used as a positive control (PC), while a non-induced sample (-) was used as a negative control for all conditions tested.

ISBN: 978-82-575-2052-6
ISSN: 1894-6402

Norwegian University
of Life Sciences

Postboks 5003
NO-1432 Ås, Norway
+47 67 23 00 00
www.nmbu.no

116270 / ANDVORDGRAFISK.NO